Engineered Fibronectin-based Hydrogels as Novel Three-Dimensional Microenvironments to Promote Microvasculature Growth

Ms. Sara Trujillo-Muñoz

BSc, MSc

Submitted in fulfilment of the requirements for the degree of

Doctor of Philosophy

School of Engineering

College of Science and Engineering

University of Glasgow

February 2019

Abstract

Hydrogel systems are of growing interest as extracellular matrix (ECM) mimetics due to their intrinsic and controllable properties (e.g. water content, stiffness and/or architecture) (Chaudhuri et al., 2016; Tse & Engler, 2010). Moreover, these systems can be further tailored with biologically active ligands (e.g. cell-adhesion motifs, protease-degradable peptides) and they can be used to instruct cell behaviour (DeVolder & Kong, 2012; Lutolf & Hubbell, 2005).

In order to sophisticate hydrogels as ECM mimetics, significant efforts have been made to incorporate proteins or protein fragments into a hydrogel backbone (Almany & Seliktar, 2005; Francisco et al., 2014; Mikaël M. Martino et al., 2011; Seidlits et al., 2011; Watarai et al., 2015). By incorporating full-length proteins, hydrogels could present binding domains for different molecules, which traditional peptide ligands lack. To this end, our work focuses on the formulation of hydrogels based on one of the major constituents of the ECM, fibronectin (FN).

Fibronectin is a glycoprotein that presents binding sites for heparin, collagen, other fibronectin molecules and growth factors, amongst others (Pankov, 2002). In addition, it has been shown that the exploitation of growth factor-fibronectin synergistic interactions can alter cell behaviour (e.g. improve cell migration, proliferation or differentiation) (Llopis-hernández et al., 2016; M. M. Martino & Hubbell, 2010).

In this work, we have developed and optimised two strategies to covalently link fibronectin to synthetic (polyethylene glycol, PEG) and natural (hyaluronic acid, HA) polymers to form three-dimensional microenvironments to promote vascularisation.

FNPEG hydrogels were formed using a Michael-type addition reaction that takes place at physiological pH and temperature. Using this approach, fibronectin was incorporated up to one $mg \cdot mL^{-1}$. The mechanical properties of this system were characterised together with the degradation profile when using protease-sensitive crosslinkers. Cytocompatibility was also studied using murine myoblasts and human endothelial cells. In addition, the interaction between vascular endothelial growth factor (VEGF) and fibronectin within FNPEG hydrogels was also explored, carrying out release and binding experiments. Fibronectin-VEGF interactions were investigated with endothelial cells, carrying out experiments of endothelial cell

sprouting (i.e. angiogenesis) and endothelial cell reorganisation into multicellular structures (i.e. vasculogenesis assays).

FNHA hydrogels were also fabricated, using a norbornene-modified HA and a ultraviolet (UV)-initiated thiol-ene chemistry. In this case, fibronectin was tethered to the HA backbone at different concentrations and up to two $mg \cdot mL^{-1}$. The mechanical properties of these hydrogels were characterised using different amounts of fibronectin. The morphology and yes associated protein (YAP) localisation of mesenchymal stem cells (MSCs) were studied using this system in two-dimensional (2D) cultures. Also, cytocompatibility of the hydrogels with MSCs was assessed in a three-dimensional (3D) culture system.

In conclusion, this thesis presents a new family of ECM mimetics that incorporate fibronectin covalently bound to the PEG or HA backbone for the 3D encapsulation of cells and molecules. Moreover, the interaction between fibronectin and VEGF was studied with the intention to use these fibronectin-based hydrogels as efficient 3D proangiogenic microenvironments.

Table of contents

List of tables

List of figures

List of equations

Acknowledgements

I've been wanting to write this section for four years. Because I am so thankful. To so many people. Here it comes.

First of all, I would like to thank the University of Glasgow and the School of Engineering, for funding three and a half years of my life.

I would like to thank my supervisors Manuel and Matt, especially Manuel, for believing in my skills (and somehow good scientific choices). Your sarcasm was my fuel to become better. Thank you.

Thanks to all the people from MiMe and CCE (former colleagues, new colleagues, all of them). I found a family that I wasn't expecting at all. Thank you.

I would like to thank as well all the people I met in Philadelphia. Thank you Jason, for letting me in. Thank you Sebastian, for guiding me. And the rest, for making three frightening months one of the best experiences of my life.

I would like to thank four Spaniards that have supported me since the beginning of my thesis: Pepe, Alex, Virginia and Cristina. Thank you for staying by my side, for encouraging me, for the advice, the conversations, the laughter, everything!

Also, I want to thank my Italian/quasi-Spaniard Marco (even when he thought I was Polish). You have been my colleague, my mentor, my friend, my brother. I needed every role you played in my life. Thank you!

I would like to thank as well all my friends from Spain. Thanks to my favourite biotechnologists María, Irene, Rosa, Hayk, Cristina, Julia, Alberto, Elena, Jose and Pablo, for supporting me. Always. For making me laugh every day. For your unconditional love. Thank you.

I would like to thank Pachi for helping me with one of the coolest assays of the thesis and for letting me know her a bit more. Thank you.

I want to thank Silvia. Mi great support, even from far away. Thank you.

I also want to thank my family, our awesome matriarchy. In particular my mom, because she has always done everything to secure I could take all the opportunities I've encountered; even when she didn't agree with them.

I hope I met all your expectations.

I hope I matched your love.

I hope I made you smile.

To all of you.

THANK YOU.

I would like to dedicate this thesis to my father.

You are always in my heart.

Finally, I would like to wrap up this section with a quote from Elisabeth Kübler-Ross, pioneer psychiatrist, who established the Kübler-Ross model or five stages of grief (denial, anger, bargaining, depression, and acceptance) in her book On death and dying.

“The most beautiful people we have known are those who have known defeat, known suffering, known struggle, known loss, and have found their way out of the depths. These persons have an appreciation, a sensitivity, and an understanding of life that fills them with compassion, gentleness, and a deep loving concern. **Beautiful people do not just happen**.”

Author's declaration

"I declare that, except where explicit reference is made to the contribution of others, this dissertation is the result of my own work and has not been submitted for any other degree at the University of Glasgow or any other institution."

Name: Sara Trujillo-Muñoz Date: 24-09-2018

Abbreviations

2D	two-dimensional
3D	three-dimensional
AFM	atomic force microscopy
BCA	bicinchonininc acid
BM	basement membrane
BME	ß-mercaptoethanol
BMP	bone morphogenetic protein
BOPS	benzotriazole-1-yl-oxy-tris-(dimethylamino)-phosphonium hexafluorophosphate
CAM	chorioallantoic membrane
CNT	carbon nanotube
DAPI	4',6-diamidino-2-phenylindole, dihydrochloride
DMEM	Dulbecco's modified Eagle's medium
DMSO	Dimethyl Sulfoxide
DPBS	Dulbecco's phosphate buffer
ECM	extracellular matrix
ELISA	enzyme-linked immunosorbent assay
FA	focal adhesion
FDA	food and drug administration
FGF	fibroblast growth factor
FMOC	9-fluorenylmethoxycarbonyl
FN	fibronectin
FNHA	fibronectin-based HA hydrogel
FNPEG	fibronectin-based PEG hydrogel
FS	force spectroscopy
GAG	glycosaminoglycan

GMA	glycidyl methacrylate
HA	hyaluronic acid
HAp	hydroxyapaptite
HDF	human dermal fibroblast
HLVE	Human large vessel endothelial medium
HUVEC	Human umbilical vein endothelial cells
IAA	iodoacetamide
IF	immunofluorescence
IL-1	interleukin-1
MAL	maleimide
MMP	matrix metalloproteinase
MSC	mesenchymal stem cell
NIR	near-infrared
Nor-amine	5-norbornene-2-methylamine
Nor-HA	norbornene-modified hyaluronic acid
NP	nanoparticle
O-NB	ortho-nitrobenzyl
PAGE	polyalcrylamide gel electrophoresis
PDGF	platelet derived growth factor
PDMS	polydimethylsiloxane
PEG	poly(ethylene glycol)
RGD	Arg-Gly-Asp
RH	relative humidity
RT	room temperature
rTIMP-3	recombinant tissue inhibitor of MMP-3
SMC	smooth muscle cell
TAZ	PDZ-binding motif
TCEP	Tris(2-carboxyethyl)phosphine hydrochloride

UV	ultraviolet
VEGF	vascular endothelial growth factor
YAP	yes associated protein

1 Chapter One: Introduction

This chapter will provide a general description of the cell microenvironment and its components. Furthermore, the role of biochemical and biophysical cues in the cell microenvironment will be discussed along with critical considerations on how to engineer biomaterials to recapitulate some aspects of the cell microenvironment with a focus on the blood vessel microenvironment.

1.1 The Cell Microenvironment

Cells are the basic structural, functional and biological units of all known living organisms; they reside within a highly dynamic, heterotypic and intricate collection of biochemical and biophysical cues - called the cell microenvironment (Figure 1.1).

The cell microenvironment is hierarchically organised to form the tissues in the body. There are many different tissues and so, there are many different organisations of cells and matrices; from tissues with mostly ECM and low amounts of cells (e.g. the connective tissue) to densely packed cell groups with a thin ECM membrane (e.g. epithelia).

Cell microenvironments are highly diverse, although the cell microenvironment of animals share some composition and function features. In general, there are three key components: (i) neighbouring cells, (ii) extracellular matrix (ECM) and (iii) soluble factors (Cipitria & Salmeron-Sanchez, 2017; Dalby, García, & Salmeron-Sanchez, 2018; Rice et al., 2013). All three components provide a myriad of biochemical and biophysical cues that act synergistically or antagonistically to regulate cell behaviour and consequently, cell function (i.e. migration, spreading, proliferation, differentiation, self-renewal and apoptosis). All three components will be discussed in the following sections, focusing on some important aspects for the understanding of this manuscript.

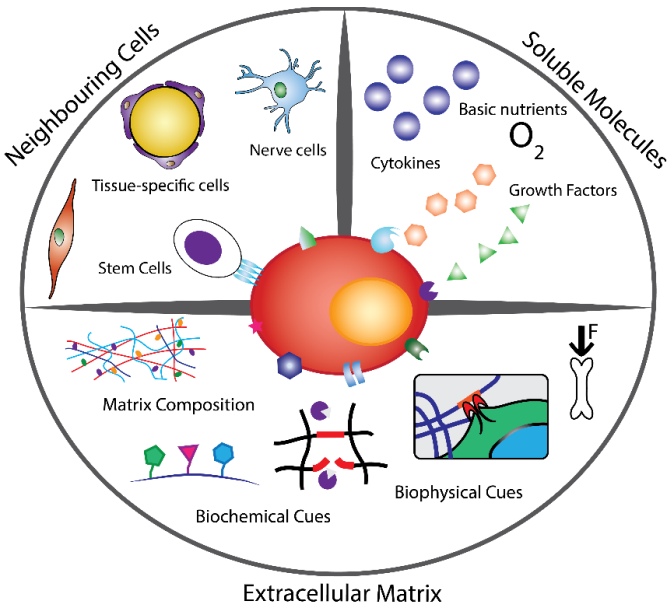

Figure 1.1 The cell microenvironment is the complex interplay of neighbouring cells, soluble molecules and the extracellular matrix.

Cells live within a dynamic and intricate assemblage of biochemical and biophysical cues. In general there are three key components of the cell microenvironment: neighbouring cells, soluble molecules and the ECM. All three components act together to regulate tissue homeostasis.

1.1.1 Neighbouring Cells

Cells in the body do not live isolated, they are gregarious entities capable of communication between similar and different types of cells. Cell-cell communication is a vital aspect of cell function over the cell lifecycle. It plays critical roles in tissue development and morphogenesis (Dejana, 2004).

A cell can communicate with its neighbours via direct (e.g. cell-cell contact) and/or indirect (e.g. mediated by soluble factors) interactions. This subsection will focus on direct cell-cell communication, while indirect cell-cell communication will be discussed later (in section 1.1.2).

Direct cell-cell communications include direct physical contact with the other cell through junctions or distant physical contact with other cells via mechanical communication through the fibrous portion of the ECM. There are three different types of cell junctions: tight junctions, anchoring junctions and gap junctions (Alberts et al., 2002).

Tight junctions are the closest cell-cell contacts and consist of a collection of proteins forming complexes that link together both cell membranes and

cytoskeletons of adjacent cells. This type of junction is typical of epithelial cells that are tightly packed together. Tight junctions hold cells together and obstruct the transportation of soluble molecules and water through the gaps between cells. In this manner, tight junctions separate tissues and cavities from their surroundings (Fanning et al., 1998; Utech, Bruwer, & Nustrat, 2006).

Anchoring junctions direct cell-cell and cell-ECM adhesions. There are three identified anchoring junctions: adherens junctions, desmosomes and hemidesmosomes. Adherens junctions and desmosomes are typically mediated by adhesion proteins such as cadherins and related proteins. These junctions are involved in the maintenance of tension and shape of tissues and cell-cell signalling (Leckband & de Rooij, 2014).

Gap junctions are mainly composed of connexin proteins arranged as channels or open pores that cross the cell membrane and through which ions and small molecules can pass at will (Hervé & Derangeon, 2013). As a consequence, gap junctions play crucial roles coupling metabolic activities of adjacent cells (e.g. synchronising contractions of cardiomyocytes (Haraguchi, Shimizu, Yamato, Kikuchi, & Okano, 2006)).

In addition to the abovementioned cell-cell interactions, it is worth mentioning that there is another type of direct cell contact mediated by the immunoglobulin and selectin superfamilies, which are involved in the immune response by the immune system and will not be discussed here.

Endothelial cells

Endothelial cells are one the major cell constituents of blood vessels (i.e. arteries, veins and capillaries). Endothelial and hematopoietic cells share a common precursor cell, the hemangioblast, which has mesodermal origin (Hirschi, 2012). Embryonic hemangioblasts can be identified by expression of two markers, the transcription factor Brachyury (Bry) and Flk-1, which is characteristic of endothelial cells (Huber, Kouskoff, Fehling, Palis, & Keller, 2004). Hemangioblasts are considered multipotent cells as Bry+ Flk-1+ cells can also generate vascular smooth muscle cells and Flk-1+ cells can form skeletal and cardiac muscle cells (Hirschi, 2012) (Figure 1.2).

VEGF signalling is essential for endothelial and hematopoietic cell generation as Flk-1 deficient mice resulted in absence of blood islands during embryonic ontogeny with deleterious effects (Shalaby et al., 1995). The formation of

hemangioblasts from the mesoderm is activated by bone morphogenetic protein 4 and mediated by Gata2 transcription factor, which initiates Flk-1 and stem cell leukaemia (Scl) expression (Lugus et al., 2007).

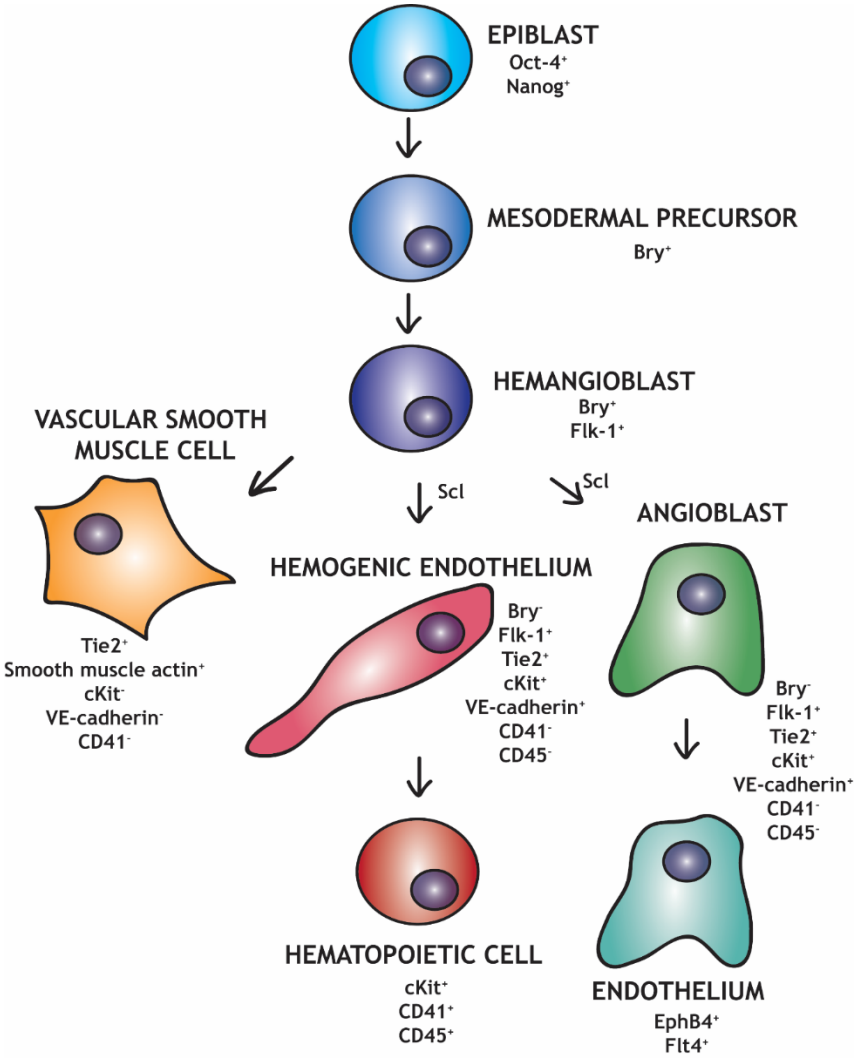

Figure 1.2 Endothelial cell origin and differentiation.

The epiblast gives rise to the three primary germ layers and thus, the mesoderm. From the mesodermal precursor derives the hemangioblast, which is the common ancestor of hematopoietic and endothelial cells. The hemangioblast is pluripotent as it can commit to several lineages such as the vascular smooth muscle cell. The precursor of the endothelial cell is the angioblast, which can give rise to aortic endothelial cells, vascular endothelial cells or lymphatic endothelial cells.

The endothelium is the inner cellular lining of the blood vessel and it is formed by a monolayer of endothelial cells. This continuous endothelial cell monolayer presents cells linked to each other by different cell junctions (Dejana, 2004). Tight junctions (mainly occludins) in endothelial cells help to seal the endothelial cell monolayer by the close juxtaposition of neighbouring cells' plasma membranes and, adherens junctions (primarily vascular endothelial cadherin, VE-cadherin) anchor their cytoplasmic part to a network of catenins, which are connected to

the actin cytoskeleton (Chavez, Smith, & Mehta, 2011; Dejana, 2004; Utech et al., 2006).

Endothelial cells have essential roles in the regulation of a myriad of properties such as vessel permeability, immune response or haemostasis. These key roles are due to their location (i.e. at the interface between the circulatory system and the tissue). The modulation of these processes highly depends on the activation or not of the endothelial cell. Quiescent endothelium has anticoagulant, vasodilatory and anti-adhesive functions with a moderate level of permeability, while activated endothelial cells have pro-coagulant, vasoconstricting and pro-adhesive functions with high transmigration of immune cells (Aird, 2008).

The most important property that is regulated by endothelial cells at the interface between blood and tissues is semi-permeability, which involves the transport in and out of the blood vessel of fluids, ions, macromolecules and cells (Claesson-Welsh, 2015).

During homeostatic conditions, a physiological flux takes place in capillaries, which are the major exchanging component of the circulatory system (Aird, 2007b; Chavez et al., 2011). Generally, fluids and small soluble molecules move passively between endothelial cells and this movement is regulated by endothelial junctions. Adherens junctions (i.e. cadherins and catenins) become phosphorylated-dephosphorylated in response of changes in Ca^{2+} levels, providing vessel permeability. Tight junctions (occludins and claudins) are responsible for maintaining the endothelial barrier and apical-basal polarity (Chavez et al., 2011; Claesson-Welsh, 2015). Consequently, the degree of permeability depends on the presence of junctions and transcytosis machinery. For example, VEGF stimulation regulates phosphorylation-dephosphorylation of junctions and thus, increases permeability. In a similar way, pro-inflammatory molecules like histamine or thrombin increase permeability by opening adherens junctions (Bates, 2010) (Figure 1.3).

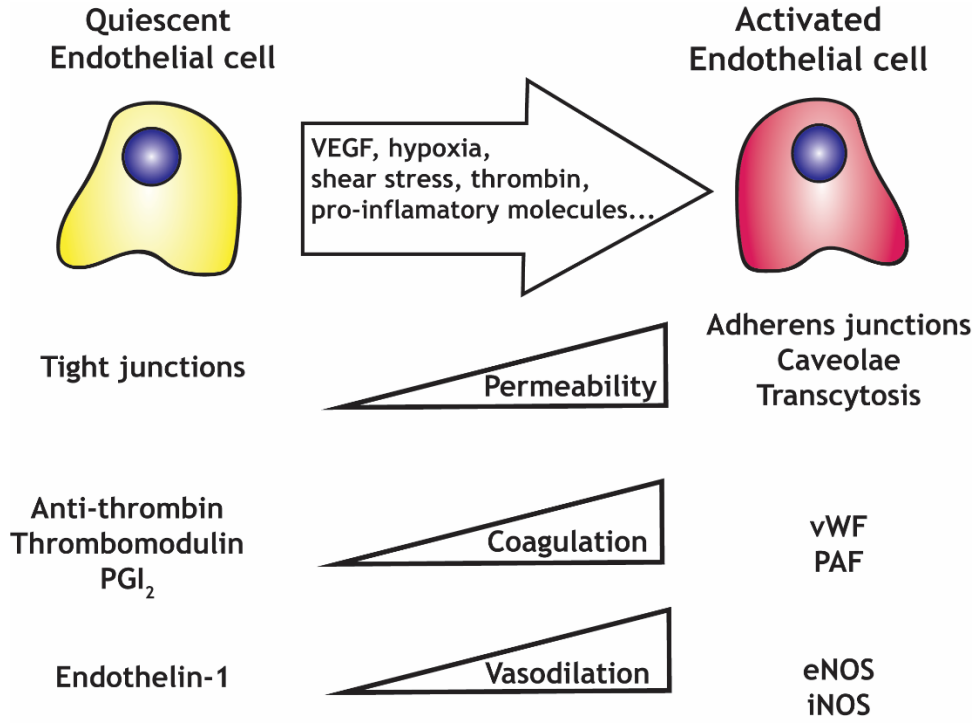

Figure 1.3 Different functions of endothelial cells upon activation.

Endothelial cells function differently when activated by different factors such as shear stress or hypoxia. Activated endothelial cells allow permeation of soluble molecules and macromolecules via adherens junctions, caveolae and transcytosis. Moreover, they secrete more Von Willebrand factor (vWF) that promotes coagulation by stabilisation with Factor VIII and the platelet activating factor (PAF). In basal conditions (quiescence), endothelial cells secrete prostacyclin (PGI_2) that inhibits platelet aggregation. NO is constitutively produced by activated endothelial cells (via nitric oxide synthase, eNOS and, the cytokine induced iNOS), which relaxes smooth muscle cells. In response to shear stress, thrombin or hypoxia, endothelial cells produce endothelin-1, which is a major vasoconstrictor.

Endothelial cells are attached to the basal lamina, and altogether constitute the intima. The basal lamina can be considered the scaffold of every blood vessel. The inside of this scaffold is lined with endothelial cells whereas the outer part is covered with smooth muscle cells (SMCs) or pericytes (Félétou, 2011). Endothelial cells are able to synthesise all the proteins that constitute the basal lamina and many relevant proteins for its remodelling like MMPs, which can degrade the basal lamina and therefore are key players in angiogenesis and the overall plasticity of blood vessels (Kiran, Viji, Kumar, Prabhakaran, & Sudhakaran, 2011) (see Figure 1.7 in "The ECM of the blood vessel" subsection for more information).

Endothelial cell morphology varies through the vascular hierarchy (i.e. capillaries, major and minor arteries and veins), however they are usually flat and to some extent elongated. Endothelial cells are found orientated along the axis of the blood vessel wall and so minimising shear stress forces exerted by the blood flow (Aird, 2007a; Félétou, 2011). There are several markers that are uniformly

expressed in the endothelium such as the platelet/endothelial cell adhesion molecule 1 (PECAM-1) or CD31, which is also expressed in monocytes; VE-cadherin, flk-1, Tie-2, Tie-1 and E-selectin (Garlanda & Dejana, 1997).

1.1.2 Soluble Molecules

In the body, cells come across numerous soluble molecules from their surrounding aqueous milieu. These molecules include basic nutrients (e.g. oxygen, glucose, amino acids) and signalling molecules (e.g. growth factors, cytokines, chemokines, hormones).

Amongst the basic nutrients, oxygen is not highly soluble in water and it is considered the easiest to be consumed in the media. The need of oxygen is a challenge when trying to engineer multicomponent and thick tissue constructs. Biomaterials capable to allow blood vessel penetration or the *de novo* formation of blood vessels are needed in order to overcome this challenge.

The concentration of oxygen – also referred as oxygen tension – has variable effects depending on the cell type or tissue affected. For example, low oxygen tension or hypoxia conditions has been shown to maintain stem cell pluripotency (Ezashi, Das, & Roberts, 2005; Forristal, Wright, Hanley, Oreffo, & Houghton, 2010), stimulate proliferation of cardiomyocytes (Nakada et al., 2017) or promote tumour angiogenesis (Dewhirst, Cao, & Moeller, 2008).

Cytokines are essential modulators of inflammation that participate in acute and chronic inflammation through an intricate set of interactions (Turner, Nedjai, Hurst, & Pennington, 2014). Key pro-inflammatory cytokines include interleukin-1 (IL-1), IL-6 and tumour necrosis factor alpha (TNFα). But cytokines not only participate in inflammatory processes. For instance, TNFα promotes proliferation of cells and induces cytolytic and cytostatic activities (Gupta, 2002). TNFα is also involved in lipid metabolism (X. Chen, Xun, Chen, & Wang, 2009) and insulin resistance (Borst, 2004). Moreover, other cytokines like IL-6 or IL-3 have shown activity promoting haematopoietic stem cell proliferation (Leary et al., 1988; Nitsche et al., 2003).

Chemokines (or chemotactic cytokines) are small proteins (1-12 kDa) produced mainly to recruit leukocytes in an injury or infected region. Chemokines induce integrin expression (e.g. lymphocyte-associated antigen 1 (LFA-1), a ß2 integrin). Although chemotaxis is the fundamental role of chemokines, they also exhibit

other activities such as the maintenance of homeostasis in haematopoiesis or the initiation of adaptive immune responses (Esche, Stellato, & Beck, 2005; Mendelson & Frenette, 2014).

Growth factors are the most widely studied soluble molecules for the engineering of the cell microenvironment. Each cell has its own growth factor microenvironment during tissue development, being secreted by the same cell (autocrine signalling), neighbouring cells (paracrine signalling), adjacent cells (juxtacrine signalling) and/or the circulatory system (endocrine signalling).

Many different growth factor families have been studied (Smith et al., 2014), but those widely studied in the context of 3D engineered biomimetic systems include bone morphogenetic proteins (BMPs) (Shekaran et al., 2014a), fibroblast growth factors (FGFs) (Tanihara, Suzuki, Yamamoto, Noguchi, & Mizushima, 2001), vascular endothelial growth factors (VEGFs) (Bao et al., 2017; Impellitteri, Toepke, Lan Levengood, & Murphy, 2012; E. A. Phelps, Landazuri, Thule, Taylor, & Garcia, 2010) or transforming growth factors (TGFs) (Jha et al., 2015). These growth factors can be found diffusing in the media or bound to the ECM (Dalby et al., 2018).

Growth factors play key roles in many cell processes by regulating their spatial supply, timing and bioactivity. For instance, VEGF has demonstrated to promote endothelial cell proliferation (S. Wang et al., 2008) but also, gradients of VEGF concentration have been shown to drive blood vessel growth in hypoxia conditions (Ferrara, Gerber, & LeCouter, 2003). Growth factors often have crosstalk effect to further regulate cell function (Cao et al., 2003; Kano, 2005). Taking into account the important roles that growth factors exert, the controlled release, delivery and secretion of these molecules is an area of intense research when engineering the cell microenvironment.

Vascular Endothelial Growth Factor (VEGF)

VEGF is a glycoprotein composed of two identical subunits. This homodimer of approximately 40-45 kDa can bind to heparin. The human *VEGFA* gene presents eight exons separated by seven introns. Alternative splicing of this gene generates different isoforms: $VEGF_{121}$, $VEGF_{165}$, $VEGF_{189}$ and $VEGF_{206}$; each isoform contains 121, 165, 189 and 206 amino acids, respectively. For example, $VEGF_{165}$ lacks amino acids encoded in exon six, whereas $VEGF_{121}$ lacks residues set in exons six and seven.

$VEGF_{121}$ is highly acidic and cannot bind to heparin. This isoform is found freely diffusing through the ECM. VEGF isoforms 189 and 206 are highly basic and present high affinity towards heparin. These isoforms are found completely sequestered within the ECM. $VEGF_{165}$ present intermediate properties, it is found both bound to the ECM and also in soluble form (Ferrara et al., 2003). The loss of the heparin-binding property results in a significant decrease in VEGF's mitogenic activity (Keyt & Berleau, 1996).

VEGF can also bind other proteins of the ECM such as fibronectin via its $FNIII_{12-14}$ domain, which has been reported as a promiscuous growth factor binding site (M. M. Martino & Hubbell, 2010; Moulisová et al., 2017).

The regulation of VEGF gene expression is governed by oxygen tension, growth factors and oncogenes. VEGF is produced in hypoxia conditions to favour angiogenesis in that region by activating endothelial cells that will migrate towards the VEGF gradient produced (C. Lin, McGough, Aswad, Block, & Terek, 2004). Different growth factors such as TGFs or FGFs – among others - regulate the expression of VEGF, which suggest autocrine or paracrine signalling that collaborates with the low oxygen tension to increase VEGF release (Ferrara et al., 2003; Ferrara & Kerbel, 2005). Oncogenic mutations and amplification of Ras promote VEGF production, which consequently leads to tumour progression (S. H. Lee, Jeong, Han, & Baek, 2015) (Figure 1.4).

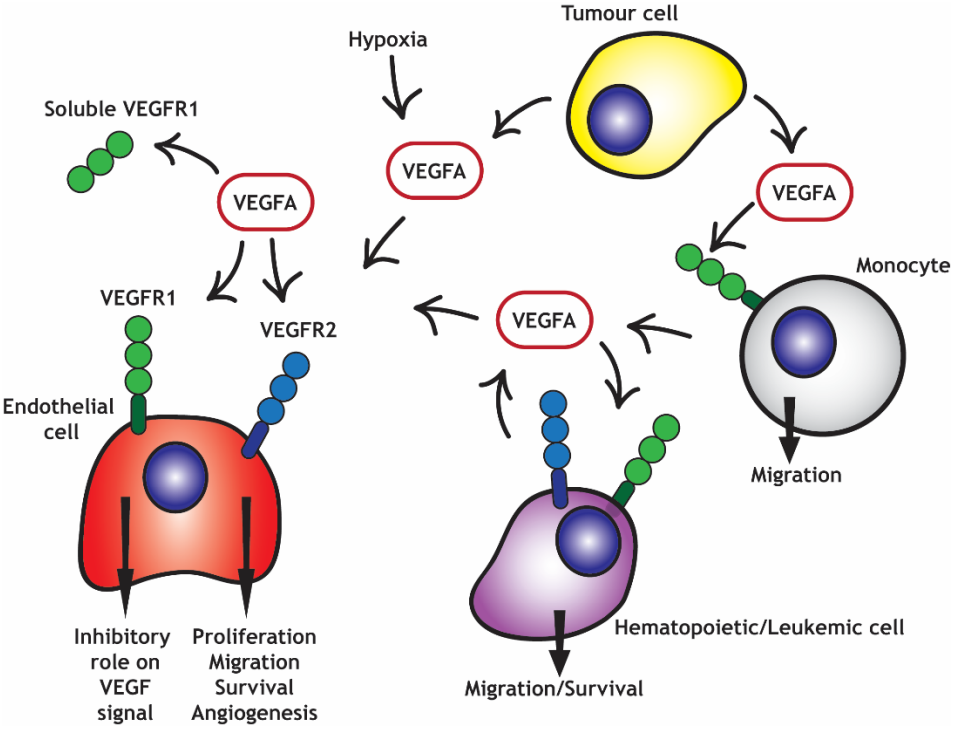

Figure 1.4 Role of VEGFA signals on different cell types.

VEGF receptors 1 and 2 (VEGFR1, VEGFR2) are expressed in the cell surface of most endothelial cells and VEGFA binds both. VEGFR2 is the master mediator of endothelial cell proliferation, survival, angiogenesis and vascular permeability. In opposition, VEGFR1 (both membrane bound and soluble) performs an inhibitory role by sequestering VEGF and preventing its binding to VEGFR2. However, VEGFR1 plays a role in mediating monocyte migration. In addition, in hematopoietic stem cells and leukemic cells, VEGFR1 and VEGFR2 mediate migration and survival. Other cells like tumour cells and cancer associated fibroblasts together with hypoxia conditions promote the production of VEGFA.

VEGF exhibits a myriad of activities (Ferrara et al., 2003). It is well known that VEGF promotes growth of endothelial cells and, it is also key in the survival of endothelial cells both *in vitro* – by preventing apoptosis - and *in vivo*, where VEGF inhibition results in an increase in apoptosis in neonatal but not adult mice (Gerber et al., 1999). VEGF induces vessel leakage and endothelial fenestration (Roberts & Palade, 1995). Among others, VEGF induces vasodilation *in vitro* due to the production of nitric oxide by the endothelial cell (Ku, Zaleski, Liu, & Brock, 1993). VEGF also affects non-endothelial cells and there are studies suggesting that VEGF has a neuroprotective role (Storkebaum & Carmeliet, 2004).

1.1.3 The Extracellular Matrix

The ECM is usually defined as all secreted molecules that are immobilised outside of a cell, which includes growth factors, cytokines and cell adhesion molecules. Actually, it is a dynamic 3D mesh-like structure that provides not only physical support to cells but, actively regulates cell behaviour and tissue homeostasis

(Frantz, Stewart, & Weaver, 2010). Some of its functions are: (i) to confer a well-defined architecture separating one tissue from another, (ii) to maintain an appropriate level of hydration and the local pH of the surroundings; (iii) to provide diffusion of nutrients and waste, along with soluble signals - like growth factors or chemokines; (iv) to make available receptors for cells and other molecules (e.g. other proteins); (v) to degrade, on demand, during tissue development and remodelling (e.g. after damage) (Mouw, Ou, & Weaver, 2014).

A matured ECM can dynamically respond to surrounding stimuli like applied force, injury or even physiological stresses such as disease. All these diverse functions are attained through its sophisticated composition and architecture, which are furthermore tissue-specific. Every tissue presents its unique ECM signature to enable the exact requirements of the tissue. For instance, the ECM in bones and teeth is mostly constituted by an inorganic part (e.g. calcium deposits) that confers strength to them; other tissues like cartilage are more elastic and lubricated – and mainly composed of proteoglycans.

The composition and roles of the ECM exist within a dynamic state regulated by cells. ECM homeostasis is widely accepted to be crucial for the maintenance of tissue functions and cell behaviour (Bowers, Banerjee, & Baudino, 2010). All these aspects of the ECM are described below.

Composition of the ECM

In a broad sense, the ECM components can be categorised into proteins and glycosaminoglycans (GAGs). ECM proteins include collagen, elastin, laminin and fibronectin (FN), among others (Figure 1.5).

Collagen is the most abundant protein in mammals, representing 25% of our total protein mass (Hynes, 2009). Primarily found in skin and bone, there are twenty-eight different collagen molecules. The structure of collagen is a triple-stranded helix formed by three polypeptide chains, called α-chains. Procollagen is the term used to describe the triple helix formed in collagen, which allows for a tightly packed structure that helps during its self-assembly. Once secreted, proteolytic enzymes modify procollagen to allow it to form longer fibrils. Then, these fibrils (tens of nanometres in diameter) aggregate to form collagen fibres (hundreds to thousands of nanometres in diameter), which are further organised to improve the tensile strength of the ECM (Brinckmann, 2005).

Collagens are organised in classes according to their properties. In this manner, *fibrillar* collagens (types I, II, III, V and XI) are the majoritarian, covering 90% of body collagens (Frantz et al., 2010; Mouw et al., 2014). Classical examples of fibrillar collagens are those forming tendons and ligaments. *Fibril-associated* or FACIT collagens (types IX, XII, XIV, XVI and XIX) do not form fibrils but they are involved in the assembly of collagen fibrils. *Network-forming* collagens (types IV, VII, VIII and X) form mesh-like structures involved in the formation of sheet-like structures; like the one formed in basement membranes (BMs). *Multiplexins* are another class of collagens (types XV and XVIII) that play a critical role in neovascularisation. Multiplexins are a special group of collagens because they have GAGs attached, and so they can also be classified as proteoglycans. *Membrane-associated* or MACIT collagens (types XIII, XVII, XXIII) are cell surface molecules with extracellular and intracellular domains (Mouw et al., 2014).

Laminins are a family of glycoproteins consisting of sixteen heterotrimeric isoforms (Aumailley, 2013; Rhodes & Simons, 2007). Laminins present five α-chains, four ß-chains and three ϒ-chains; one of each type assemble to form one large coiled-coil trimer with typically three short arms and one large arm (cross-shaped structure, although there are laminins presenting Y-shape (three arms) or rod-shape (single arm) structures) (Colognato & Yurchenco, 2000). Laminins are basically found in basement membranes and have shown to have adhesive and signalling functions. They mainly act as bridges between molecules, although Laminin-111 self-assemble into aggregates (Mouw et al., 2014; Rhodes & Simons, 2007).

Elastins are hydrophobic proteins present in tissues like skin or blood vessels because they confer the ability to momentarily stretch (Eble & Niland, 2009). Tropoelastin is the precursor molecule of elastins, which is secreted into the extracellular space where tropoelastins crosslink to each other to form networks of elastin sheets and fibres (Mithieux & Weiss, 2006). Elastins are composed of two types of segments that alternate along their polypeptide chain; one is a α-helix rich in alanine and lysine residues – where the crosslinks are formed; the other is a hydrophobic segment responsible for the elastic properties of the molecule (Mithieux & Weiss, 2006). The random coil structure of elastin molecules crosslinked into a network is thought to be responsible for their ability to stretch like rubber. Elastin is the most abundant ECM protein in arteries, constituting 50% of the dry weight in major arteries (Karnik, 2003).

Glycosaminoglycans (GAGs) are long, linear carbohydrate chains formed by two repeating disaccharide units: N-acetylglucosamine (GlcNAc) or N-acetylgalactosamine (GalNAc) and glucuronic or iduronic acid. GAGs form a highly hydrated mesh or gel-like structure, in which the fibrous proteins are embedded. The polysaccharide chains of GAGs are too stiff to fold into compact structures like polypeptides typically form, so they tend to adopt extended conformations occupying large relative volumes. They are highly negatively charged and can attract cations (such as Na^+), which confers osmotic pressure to the matrix; this swelling pressure, due to the entry of water, enables the matrix to stand compressive forces (Mouw et al., 2014).

Hyaluronan is the simplest GAG, being a linear polysaccharide and composed of GlcNAc β1-3 GlcA β1-4 repeating bonds. It is not sulphated nor associated with a core protein. Hyaluronan is mainly found in skin, skeletal tissues and synovial fluid. One of the most important functions of HA in the body is its ability to immobilise large amounts of water and hence, change ECM's volume and compressibility. In cartilage for instance, HA functions as an aggregation centre for aggrecan, embedded within a collagenous network (Esko, Kimata, & Lindahl, 2009). In synovial fluid, HA provides lubrication to the joint, serving as a shock absorber and reducing friction while allowing bone movement (Kogan, Šoltés, Stern, & Gemeiner, 2007).

HA is not only an inert molecular filling of the connective tissue, it mediates many other activities and plays important roles in embryogenesis, cell motility and signal transduction (Hascall & Esko, 2017). HA is also associated with cancer invasiveness and metastasis (Hirose et al., 2012). Moreover, depending on the size of the molecule HA can play very different roles. Large HA molecules are anti-angiogenic and immunosuppressive, while intermediate size HA molecules (25-50 repeating units) are inflammatory and immunostimulatory and highly angiogenic; small HA molecules are antiapoptotic and promote the production of heat shock proteins (Kogan et al., 2007; Stern, Asari, & Sugahara, 2006).

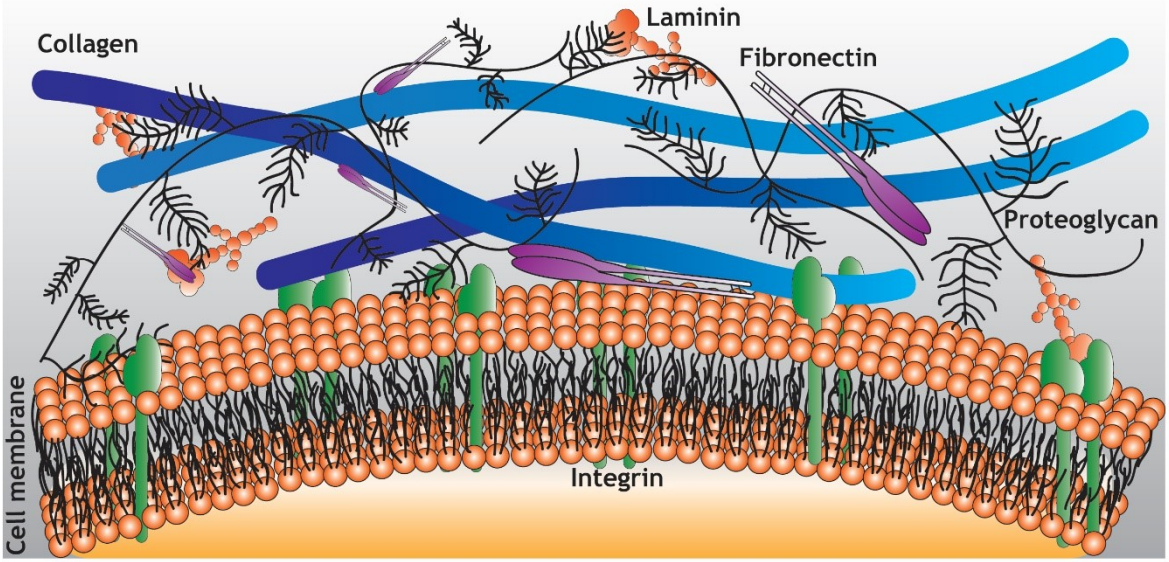

Figure 1.5 The extracellular matrix composition.

The ECM is a dynamic and complex structure that brings together collagens, laminins, fibronectins, proteoglycans, soluble molecules and cell surface receptors like integrins, among others.

The rest of GAGs are covalently linked to proteins to form proteoglycans. The main functions of proteoglycans come from the biochemical and hydrodynamic features of GAGs, which provide hydration and compressive resistance by binding water (Esko et al., 2009; Mouw et al., 2014). Some of the most important proteoglycans include heparan sulphate, chondroitin sulphate, dermatan sulphate, hyaluronan and keratin sulphate. Heparan sulphate proteoglycans are a major constituent of basement membranes; they can be cell surface-bound (e.g. syndecans), glycophosphatidylinositol-linked (e.g. glypicans), or secreted molecules (e.g. perlecans, collagen XVIII or agrin). Chondroitin sulphate proteoglycans are components of the neural ECM and cartilage. Lecticans are the most common chondroitin sulphate proteoglycans, consisting of aggrecan, veriscan, neurocan and brevican. Lecticans have binding domains for hyaluronic acid, lectins and growth factors (Esko et al., 2009).

The function of proteoglycans and GAGs is not limited to provide a hydrated space around cells, their polysaccharide chains can vary the pore size and charge density of the network and thus, regulate the diffusion of molecules, i.e. they can act as molecular filters such as perlecan in the basal lamina of the kidney glomerulus (Morita, 2005).

Proteoglycans have a role in chemical signalling, binding various secreted signal molecules such as certain growth factors. Besides binding, proteoglycans can also

regulate the activity of other secreted proteins by: (i) immobilising the protein close to where it was produced and restricting its action; (ii) sterically blocking the activity of the protein; (iii) providing a reservoir of the protein to postpone its release; (iv) protecting the protein from proteolysis and thus, prolonging its action; (v) concentrating the protein to enhance its presentation to cell-surface receptors. Chemotaxis is an example of this last function, where heparin sulphate proteoglycans can immobilise different chemokines at an inflammatory site to stimulate white blood cells to migrate into the inflamed tissue (Esko et al., 2009; Frantz et al., 2010; Mouw et al., 2014).

Note that not all proteoglycans are excreted components of the ECM, some of them are constituents of the cell membrane, with the core protein inserted into the lipid bilayer, such as syndecans. Syndecans can serve as receptors for different matrix proteins; they can be found in focal adhesions, where they modulate integrin function by interacting with fibronectin on the cell surface (Afratis et al., 2017). Syndecans can also bind some growth factors and present them to their respective receptors (Chung, Multhaupt, Oh, & Couchman, 2016).

Fibronectin

Fibronectin is also a protein component of the ECM. As this protein has a central role in this thesis, it will be described in more detail in this section.

Fibronectin is a glycoprotein consisting of two subunits (each subunit of approximately 240 KDa) that form a homodimer linked via two disulphide bonds at the C-termini. Each monomer is formed by the repetition of three different modules (types I, II and III) (Figure 1.6). Fibronectin contains twelve type I, two type II and fifteen to seventeen type III domains. All type I and type II modules present two intramolecular disulphide bonds that stabilise the tertiary structure of the protein. Type III domains are formed by seven ß-barrel strands that lack disulphide bonds. All forms of fibronectin are encoded by a single gene, which contains around 50 exons; alternative splicing produce the different isoforms of fibronectin (Pankov, 2002). Cellular fibronectin presents two extra type III modules called EDA and EDB, which are not found in plasma fibronectin (Zollinger & Smith, 2017).

Fibronectin is essential in embryogenesis and wound healing. The inactivation of the *FN* gene in mice is deleterious at early stages as demonstrated by George et

al. more than twenty years ago (George, Georges-Labouesse, Patel-King, Rayburn, & Hynes, 1993).

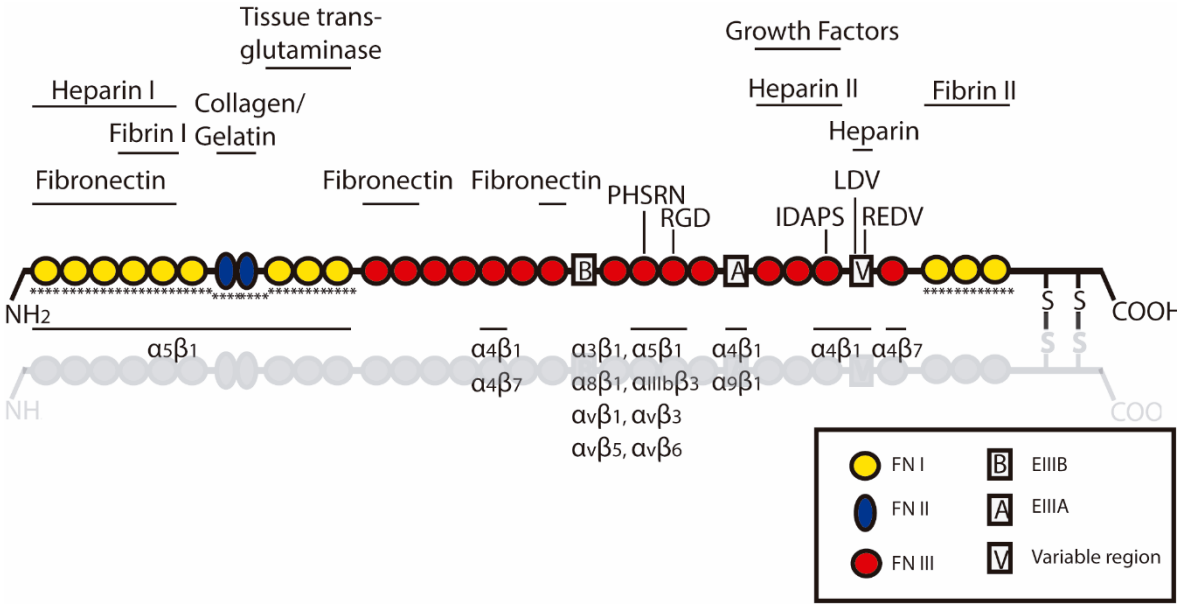

Figure 1.6 Fibronectin interacts with many different molecules.

Sketch of the fibronectin modular configuration with some of the molecules that can interact with fibronectin. FN type I domains are depicted in yellow, FN type II domains in blue and FN type III modules in red. Asterisks (*) mark the presence of cysteine residues. Adapted from (Pankov, 2002)**.**

Fibronectin exists in soluble and fibrillar forms. Plasma fibronectin is soluble and circulates in the bloodstream to enhance blood clotting and, subsequently, wound healing and phagocytosis. Fibronectin's dimeric structure plays a key role in fibronectin fibril assembly, whilst the monomer alone is not able to form fibrils.

The FNI_{1-5} repeats together with the $FNIII_1$ module are essential for fibronectin self-association (Schwarzbauer, 1991). Fibrillogenesis is also mediated by cells via interactions between integrins (mainly $\alpha_5\beta_1$ integrin) and the RGD (Arg-Gly-Asp) cell attachment domain, which is located at the $FNIII_{9-10}$ modules (Leiss, Beckmann, Girós, Costell, & Fässler, 2008; Pankov, 2002). Integrins that bind to the RGD site on fibronectin can bind to fibronectin even when the synergy site – PHSRN motif (Pro-His-Ser-Arg-Asn), located in the $FNIII_9$ repeat- is not present but, the synergy site is required to initiate fibril assembly (Benito-Jardón et al., 2017; Singh, Carraher, & Schwarzbauer, 2010). Through focal adhesions, cells are able to exert forces on fibronectin and these cell contractile forces can lead to conformational changes on fibronectin that can expose cryptic domains (Gee, Ingber, & Stultz, 2008; Ingham, Brew, Huff, & Litvinovich, 1997).

Fibronectin is important during the process of collagen matrix deposition. Collagens can interact with fibronectin at the FNI_6, $FNII_{1-2}$ and FNI_{7-9} (these domains are called the collagen binding site) (Kadler, Hill, & Canty-Laird, 2008). Collagen matrix is not deposited in the absence of fibronectin, although once a collagen matrix has been deposited it provides a structure that limits the capability of fibronectin to stretch (Sottile, 2002).

Apart from collagen, fibronectin also binds fibrin, gelatin, tenascin and heparan sulphate (Pankov, 2002). Fibronectin can bind bacteria such as *Staphylococcus aureus* (Hoffmann, Ohlsen, & Hauck, 2011).

Fibronectin plays an important role as a provisional matrix that promotes or allows other matrices structures during matrix formation or remodelling due to its ability to bind many other ECM components (Singh et al., 2010). This characteristic of fibronectin is important in wound healing and diseases such as cancer (K. Wang, Seo, Fischbach, & Gourdon, 2016).

Fibronectin is a substrate for cell adhesion as mentioned above. The importance of the RGD sequence that fibronectin shares with other ECM components like vitronectin is mainly due to the discovery of integrins (Serini, Valdembri, & Bussolino, 2006). The RDG loop of fibronectin can be found in the $FNIII_{10}$, which is a promiscuous binding site for integrins such as $\alpha_5\beta_1$, $\alpha_3\beta_1$, $\alpha_8\beta_1$ and $\alpha_v\beta_3$ (Pankov, 2002).

Integrin binding to fibronectin is conformation dependent and, there are integrins that can bind only the RGD sequence and integrins that bind both the RGD and the PHSRN synergistic motif. If fibronectin is undeformed, the synergy site is approximately 32 Å near the RGD sequence. This allows the binding of integrin $\alpha_5\beta_1$. When fibronectin stretches, it can acquire a state where both PHSRN and RGD are undeformed but the distance between them increases to 55 Å. It is in this state where the binding of integrin $\alpha_5\beta_1$ is reduced but other integrins like $\alpha_v\beta_3$ – that do not require the PHSRN motif to engage with fibronectin – can still bind (André Krammer, Craig, Thomas, Schulten, & Vogel, 2002). García's group demonstrated that, by altering the conformation of the $FNIII_{9-10}$ modules, $\alpha_5\beta_1$ versus $\alpha_v\beta_3$ integrin binding could be controlled. This conformational switch was shown to affect important cellular pathways leading to proliferation or differentiation (Keselowsky, Collard, & García, 2003, 2005). In addition, Barker's group engineered fibronectin fragments that support specific integrin engagement

(α_5 versus α_v). By using this approach, they showed that spontaneous epithelial to mesenchymal transition could be prevented (Markowski, Brown, & Barker, 2012). More recently, Segura's group showed that engineering fibronectin fragments with specific binding to either $\alpha_3/\alpha_5\beta_1$ or $\alpha_v\beta_3$ was enough to control vessel formation and vascular permeability (S. Li et al., 2017).

Fibronectin can mediate cell signalling by presenting growth factors to adherent cells. Fibronectin specifically binds growth factors in the $FNIII_{12-14}$ repeats and, it has been shown that this is a promiscuous binding site. Fibronectin is capable to bind most growth factors from the platelet-derived growth factor, vascular endothelial growth factor and fibroblast growth factor superfamilies. Moreover, fibronectin is able to bind some growth factors form the transforming growth factor-ß and neurotrophin families (M. M. Martino & Hubbell, 2010; Mikaël M Martino et al., 2011).

Fibronectin presents two VEGF binding sites. One is constitutively active and the other is regulated by heparin (Mitsi, Hong, Costello, & Nugent, 2006). Enhanced activity of growth factors has been shown when these are bound to fibronectin in the ECM compared to growth factors in their soluble form. Sobel's group showed that the biological activity of VEGF increases when it is bound to fibronectin. In addition, they showed that VEGF bound to fibronectin also increased migration and differentiation of endothelial progenitor cells (Wijelath et al., 2002, 2004, 2006).

Biochemical roles of the ECM

One important biochemical role of the ECM is to provide adhesion ligands to bind cell surface receptors (e.g. integrins) to form focal adhesions or hemidesmosomes. These ECM-cell interactions are essential for the transduction of microenvironmental cues from the ECM or mediated by the ECM and, play important roles in cell spreading (Caliari, Vega, Kwon, Soulas, & Burdick, 2016), migration (Hakkinen, Harunaga, Doyle, & Yamada, 2011) or differentiation (Trappmann et al., 2012). Most of the ECM components present adhesion ligands including collagen, laminin, fibronectin and GAGs. The absence of cell adhesion cues could lead to loss of cells or unwanted cell behaviours in different cell types. Many studies have demonstrated the importance of cell adhesion sites in the regulation – in space and time - of cell morphology, migration and differentiation (Cosgrove et al., 2016; Hahn, Miller, & West, 2006; Khetan & Burdick, 2010; S. Li et al., 2017; Schultz, Kyburz, & Anseth, 2015; Wade, Bassin, Gramlich, & Burdick, 2015).

Another important biochemical role of the ECM is to act as a reservoir for soluble molecules (e.g. growth factors) by sequestering and storing them (Brizzi, Tarone, & Defilippi, 2012). In this manner, the ECM is able to spatially distribute these signalling molecules and regulate their bioactivity and stability (Hynes, 2009). The sequestration of soluble molecules by the ECM is usually facilitated by non-covalent interactions (e.g. electrostatic or hydrogen bonds) (Jha et al., 2015). Examples of these interactions include TGF-β1 and BMP-2 to collagen II, VEGFs and platelet derived growth factors (PDGFs) to fibronectin or VEGFs, FGFs and PDGFs to heparin (M. M. Martino & Hubbell, 2010; Sawicka, Seeliger, Musaev, Macri, & Clark, 2015; Wijelath et al., 2006; Jia Zhu & Clark, 2014a).

Biophysical roles of the ECM

From a biophysical point of view, the ECM provides structural presentation of macromolecules, mechanical stiffness and variations of these in space and time.

Some components of the ECM can assemble into fibres. Fibres within the ECM are hierarchically organised forming anisotropic structures, although this organisation differs from tissue to tissue (Mouw et al., 2014). Structural variations in the ECM across a broad range of length scales can lead to changes in cell and tissue function. For instance, fibre organisation is an important characteristic of collagen I fibres and, their orientation and alignment guide cells through the organisation of their ligands, directing cell migration and polarity (Chaubaroux et al., 2015; Riching et al., 2015). Another important physical characteristic of the ECM is the presence of pores. The density and size of the pores within the ECM will define the available space where the cells are confined and can determine cell growth (Jana, Cooper, & Zhang, 2013).

Tissues in the body have mechanical properties within different order of magnitude, from compliant or “soft” tissues like brain or fat – with elastic moduli ≤ 1 kPa - to stiff or “hard” tissues like bone – with elastic moduli in the range of the GPa.

Many studies have shown that, the stiffness of a two dimensional (2D) substratum can regulate almost every aspect of cell behaviour; from migration (Pelham & Wang, 1997) or proliferation (Goldshmid & Seliktar, 2017; Her et al., 2013) to cell differentiation. Subsequently, a material with stiffness closer to bone will drive mesenchymal stem cell (MSC) differentiation towards the osteocyte lineage (A. J. Engler, Sen, Sweeney, & Discher, 2006).

Mechanical fields should be distinguished from mechanical properties. Cells experiment a huge range of stress and strain forces *in vivo* and, these forces are regulated by the mechanical properties of their local microenvironment. For instance in the vasculature, blood cells withstand shear forces from the flowing blood. Heart and lungs experiment cycles of tensile stress and strain and, cartilage and bone experience compressive forces during movement. The study of the effects of mechanical fields on cell behaviour have shown that mechanotransduction is relevant for tissue development and regeneration (Humphrey, Dufresne, & Schwartz, 2014; N. Wang, Tytell, & Ingber, 2009).

In vitro studies have demonstrated that shear stress modulates endothelial cell adhesion and smooth muscle cell-endothelial cell interactions (Hur et al., 2012; Qi et al., 2011). Shear stress also promotes cancer cell migration (H. J. Lee et al., 2017). Tensile forces have shown to promote maturation of cardiomyocytes (Tallawi, Rai, Boccaccini, & Aifantis, 2015), myotube differentiation from myoblasts (Ahmed et al., 2010) and MSC commitment to the SMC lineage (Rothdiener et al., 2016). Compressive stress have been also shown to promote muscle regeneration (Cezar et al., 2016).

Likewise, electrical fields have shown to regulate cell function. Electrical fields have demonstrated their efficacy in the maturation of cardiac, musculoskeletal (Park et al., 2008) and neural tissues (J.-F. Feng et al., 2012). Being particularly important in the communication, synchronisation and beating of cardiomyocytes (Tandon et al., 2009).

The ECM of the blood vessel

Generally, blood vessels are composed of three concentric layers, which are the tunica intima, the tunica media and the tunica adventitia (Figure 1.7). These layers are separated by two membranes, the membrane limitans interna and the membrane limitans externa. A monolayer of endothelial cells forms the tunica intima, where endothelial cells can be found lining the internal surface of the vessel. The tunica media accommodates the mural cells that basically, are smooth muscle cells in larger blood vessels and pericytes in capillaries. Usually, the tunica media is thicker in arteries than in veins (Eble & Niland, 2009).

The tunica adventitia links the vessel tube to its surroundings (e.g. connective tissue) and it is generally thicker in veins than arteries. This general structure changes depending on the type of blood vessel to ensure that they fulfil their own tasks properly. For example, the endothelial cell lining of capillaries is continuous in most tissues; however, the capillaries of endocrine and exocrine glands are

often fenestrated and, capillaries in liver, spleen and bone marrow are even discontinuous. These changes increase the exchange rate of hormones and metabolites (Eble & Niland, 2009; Rhodes & Simons, 2007).

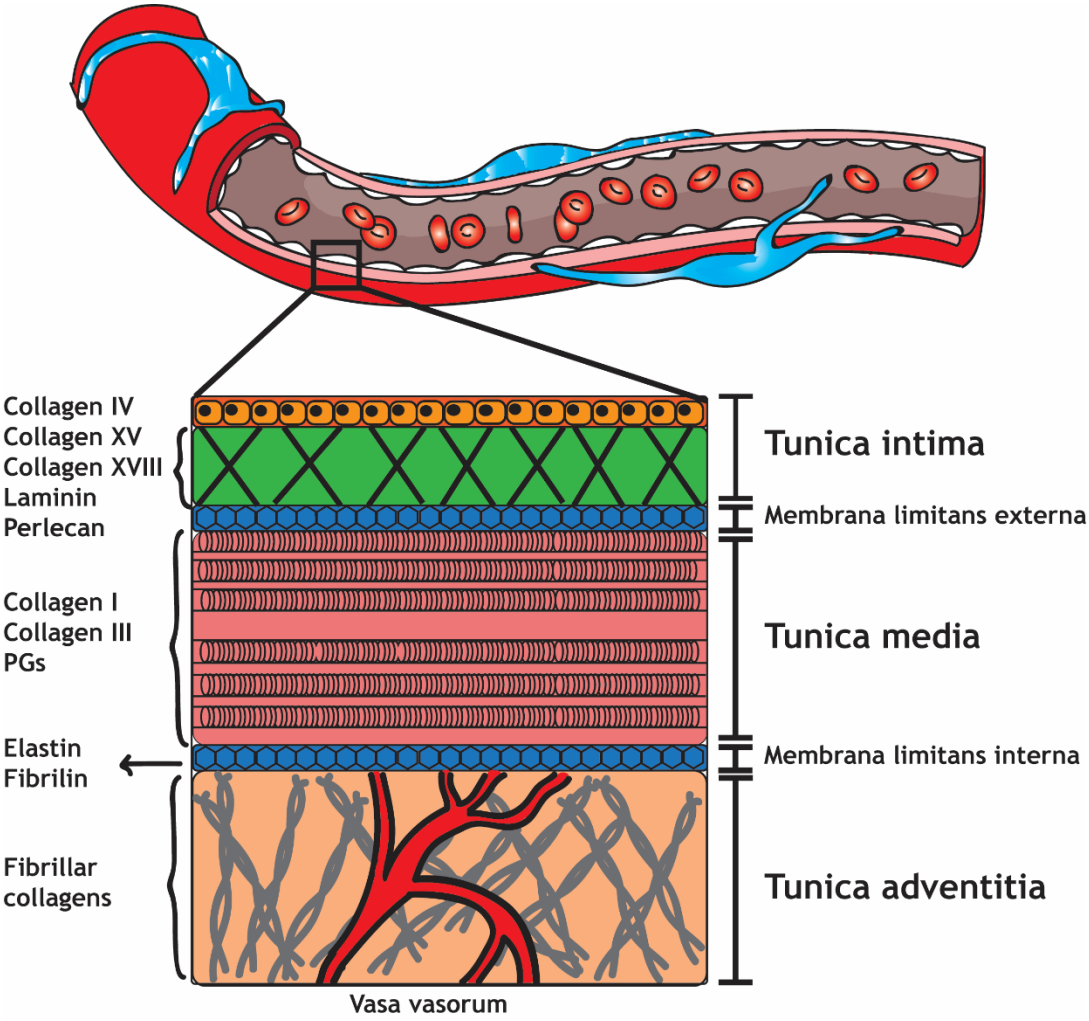

Figure 1.7 The ECM of the blood vessel.

This sketch shows the general composition of a vessel section with its three main layers: tunica intima, tunica media and tunica adventitia. The structure and thickness of these layers vary depending on the type of vessel (capillary, vein or artery). On the top sketch, coloured in blue, there are pericytes supporting the blood vessel. Vascular smooth muscle cells (depicted as striated structures) are found in the tunica media. Endothelial cells are found forming a monolayer at the tunica intima.

The tunica intima consists of a single sheet of endothelial cells that are attached to a basement membrane. Underneath this basement membrane there is a thin layer of endothelial connective tissue together with the inner limiting membrane. The basement membrane serves as foundation for endothelial cells to anchor and

as tissue border between the endothelium and the vascular connective tissue (Eble & Niland, 2009; Folkman & D'Amore, 1996).

The word "endothelium" was first used in 1865 by the anatomist Wilhem His (Aird, 2007a); since then and up to the early 70s this layer was considered a mere passive membrane separating blood cells form the vascular ECM (ECM). Now, the endothelium is known for playing major roles in vascular homeostasis such as the control of blood fluidity (e.g. thrombosis, fibrinolysis) and the aggregation of platelets, the regulation of vascular tone and also is an important regulator of inflammation, angiogenesis or immunology (endothelial cells are also present in lymphatic vessels) (Félétou, 2011).

The ECM components of blood vessels are: collagen, laminin, fibronectin, elastin, nidogen, GAGs, perlecan and syndecans (Rhodes & Simons, 2007), which have been described above (section 1.1.3).

1.2 Engineering Biomimetic Materials

Having stated the challenges in understanding the cell microenvironment, this section will focus on describing the state of the art in engineering biomimetic materials to study and comprehend the cell microenvironment. These biomatrices are not only designed to recapitulate the properties of the *in vivo* ECM but also to create new synthetic constructs not available in nature, to be able to deconstruct the cell microenvironment and perform fundamental studies on cell behaviour.

Many studies in the last decade have focused on the development of biomaterials to study how biochemical cues (e.g. chemical functional groups, adhesion ligands or soluble factor immobilisation) affect cell behaviour and also, how biophysical cues (e.g. architecture, topography, mechanical properties or degradability) influence cell function (Murphy, McDevitt, & Engler, 2014).

1.2.1 Classification of biomimetic materials

Biomimetic materials could be defined as those with architecture, composition, properties and/or functions similar to native materials (Caliari & Burdick, 2016). From a material's perspective, biomimetic materials can be classified as metallic, ceramic or polymeric materials. Traditionally, metallic and ceramic materials (e.g. titanium, bioactive glasses) have been used to mimic hard tissues like bone (El-Rashidy, Roether, Harhaus, Kneser, & Boccaccini, 2017; Pobloth et al., 2018), while polymeric materials (e.g. 3D polymeric scaffolds or hydrogels) have been

also used to engineer soft tissues (Berkovitch, Yelin, & Seliktar, 2015; Qian et al., 2018; Rose et al., 2017).

Again, from a material's point of view, the ECM is a gel-like scaffold, full of water. Because of that, hydrogels have been extensively used to engineer the 3D cell microenvironment (Caliari & Burdick, 2016; Khetan & Burdick, 2009a). Hydrogels are water-swollen 3D polymeric network materials (H. Gulrez, Al-Assaf, & O, 2011) with many advantages to be used to engineer the cell microenvironment; including their high water content, their structural similarity with the natural ECM, their biocompatibility, easy handling and shaping and their potential biochemical and biophysical tunability (Khetan & Burdick, 2009b; Kyburz & Anseth, 2015).

Hydrogels can be classified as: physically or chemically crosslinked (according to their crosslinking strategy); anionic, cationic or neutral (according to their electrical properties), electrically conductive, magnetically responsive, or photosensitive (according to their physical characteristics) and, naturally or synthetically derived (according to their origin) (H. Gulrez et al., 2011). The latter classification will be used to describe some relevant hydrogels.

Naturally derived hydrogels

Naturally derived hydrogels are materials extracted from natural sources and, both animal and plant sources can be used. A typical mammalian source for hydrogels is decellularized ECM, which is obtained by removing antigens and cells from the tissues using primarily detergents. Decellularized ECM can maintain some properties of the original tissue or organ such as composition – i.e. containing the same proteins, adhesion ligands and some soluble molecules - or architecture, e.g. keeping the natural organ's vascular network (Yu, Alkhawaji, Ding, & Mei, 2016).

Many organs and tissues have been used to obtain decellularized ECM such as heart, liver, cartilage or dermis (Yu et al., 2016). For instance, Taylor and colleagues repopulated a whole decellularized rat heart with neonatal cardiac cells and endothelial cells by perfusion and, observed native-like organisation with macroscopic contractions and primitive pumping functions (Ott et al., 2008). Similar studies have been shown similar results for other decellularized tissues, e.g. blood vessel (Quint et al., 2011) or diaphragm (Gubareva et al., 2016).

Despite the many encouraging results obtained from decellularized matrices *in vitro*, these studies rarely surpass preclinical characterisation. This is due to batch-to-batch variability, which is donor dependent and is not completely

understood. Therefore, there is a difficulty trying to identify the relevant components that make those matrices effective.

In contrast, purified components from natural tissues are more relievable, have better defined composition and can be better controlled in comparison to decellularized matrices. These types of hydrogels can be further categorized into protein-based or polysaccharide-based hydrogels. Protein-based hydrogels are matrices formed by an individual protein such as collagen, gelatin, elastin and fibrin, or mixtures of proteins (Koike et al., 2004; Mason, Starchenko, Williams, Bonassar, & Reinhart-King, 2013; Nakatsu et al., 2003; Stratesteffen et al., 2017). These hydrogels are usually fabricated by self-assembly or cross-linking through amino acid sequences under physiological conditions. They are widely used as biomimetic materials due to their biocompatibility, fibrous nature and thus, architecture and topography. They also provide inherent cell adhesion ligands and can be enzymatically degraded, allowing matrix remodelling and cell migration. However, there is batch-to-batch variability and degradation within this type of hydrogels is poorly controlled.

Polysaccharide-based hydrogels such as alginate, chitosan or hyaluronic acid (HA), are formed using mild conditions and are also biocompatible (Jana et al., 2013; Jha et al., 2016; Rowley & Mooney, 2002). Moreover, they are usually less immunogenic than protein-based hydrogels and their mechanical properties can be better controlled. Many widely used polysaccharide-based hydrogels (e.g. chitosan, alginate) do not present adhesion ligands and are not biodegradable. As a consequence, they need to be modified to incorporate such features (Q. Feng, Zhu, Wei, & Bian, 2014; Jha et al., 2016; Lam, Truong, & Segura, 2014; Rowley & Mooney, 2002; W. Wang et al., 2015).

Normally, polysaccharide-based hydrogels are chemically cross-linked using genipin or glutaraldehyde to toughen them, since their physically cross-linking via temperature or pH can be mechanically insufficient for 3D cell culture (Shankar et al., 2017).

Some approaches to strengthen these hydrogels include the incorporation of functional groups such as acrylates, thiols or maleimides (Caliari & Burdick, 2016; Khetan et al., 2013a). These functionally derived macromers allow the fabrication of polysaccharide-based hydrogels with more refined physicochemical properties.

Synthetic hydrogels

Synthetic hydrogels are those fabricated by crosslinking bioinert monomers or macromers through synthetic chemical reactions. Synthetic hydrogels present their own advantages compared to naturally derived hydrogels. For instance, the composition of these hydrogels can be finely controlled and the chemistries used to fabricate them can be used to custom-design different physicochemical properties of the hydrogels. This improves reproducibility during fabrication. Even though synthetic hydrogels are bioinert and non-degradable, they can be tailored to incorporate bioactivity ligands such as adhesion cues or degradable peptides (Guvendiren & Burdick, 2013; Kyburz & Anseth, 2015; Lutolf & Hubbell, 2005; Raeber, Lutolf, & Hubbell, 2005).

Many synthetic polymers have been used to study cell fate like poly(ethylene glycol) (PEG) (Cruz-Acuña et al., 2017), poly(acrylamide) (PA) (Tse & Engler, 2010), poly(vinyl alcohol) (PVA) (Nuttelman, Mortisen, Henry, & Anseth, 2001) or poly(N-isopropyl acrylamide) (PNIPAAm) (Jha, Jackson, & Healy, 2014) and derivatives.

PA has been widely used to study cell behaviour in 2D cultures since it can be finely controlled and it is possible to crosslink proteins on top. While PA systems have been very useful to elucidate how stiffness affects cell behaviour on 2D substrates (Denisin & Pruitt, 2016; Elosegui-Artola et al., 2016), PEG hydrogels are commonly used as 3D environments to study cell behaviour (Lutolf & Hubbell, 2005; Raeber et al., 2005). In addition, PEG can be crosslinked to form hydrogels via several cytocompatible chemistries such as Michael-type addition reaction or thiol-ene reaction (Junmin Zhu, 2010).

Supramolecular hydrogels – i.e. rationally designed, custom made and peptide/protein based hydrogels - are another important group of synthetic hydrogels. They can be engineered to be stimuli-responsive, that can be remodelled by cells and, create dynamic cell microenvironments (Alakpa et al., 2016; M. Zhou et al., 2009). Controlling the self-assembling process of supramolecular hydrogels can lead to materials with properties that are difficult to obtain using traditional synthetic hydrogels (Inostroza-Brito et al., 2015). These supramolecular hydrogels can recapitulate the hierarchical organisation and disposition of biological cues (e.g. biodegradability, adhesion, growth factor immobilisation) of native tissues – from the nano to the macro scale. Among its

limitations, supramolecular hydrogels present weak mechanical properties and, at present they are not cost-effective.

Poly(ethylene) Glycol

Amongst synthetic hydrogels, PEG hydrogels have been widely used in literature. PEG hydrogels are biocompatible, nontoxic and bioinert, which means that they are resistant to unspecific cell adhesion or protein adsorption (Krsko & Libera, 2005). In addition, PEG hydrogels can be crosslinked under mild or physiological conditions, so cells can be encapsulated *in situ* without important loss of viability. PEG has been approved by the Food and Drug administration (FDA) and the European medicine agency (EMA) for oral and topical applications and it can be found in cosmetics, soaps and drug formulations.

PEG's monomer, ethylene glycol, presents a simple structure ($C_{2n}H_{4n+2}O_{n+1}$). This structure matches the structure of poly(ethylene oxide) (PEO). Although the name PEG is typically used when referring to polymers with molecular weights less than or equal to 20 kDa, PEG and PEO are often used interchangeably. PEG is also an amphoteric compound (i.e. can act as either a base or an acid, depending on the medium). It is soluble in many organic solvents and also in aqueous media. Plus, PEG's hydrophilic feature is one of the main reasons for its use in biomedical applications, including drug delivery and tissue engineering. The hydrophilic character of PEG confers similar structural and physicochemical properties of the ECM (Krsko & Libera, 2005). PEG polydispersity index is relatively low, between 1.01 and 1.1, which offers high control over its physicochemical properties compared to other polymers (Pfister & Morbidelli, 2014).

PEG hydrogels have been fabricated using many different functional groups at the end of the macromer, including acrylate, maleimide, norbornene, thiol or amine, among many others. Therefore, there is an extensively developed chemistry for the gelation of PEG chains. While different gelation methods exist such as ionic, physical or covalent; the chemically covalent-bonded hydrogel presents a relatively stable structure with tuneable properties (Pfister & Morbidelli, 2014).

There are three main categories of covalent PEG polymerization: the free-radical or chain-growth photopolymerization, the step-growth and the mixed-mode polymerizations. The first one is based on the photocleavage of initiator molecules in the presence of UV light to form free radical species capable to react with acrylate or vinyl groups on PEG molecules. The crosslink is formed quickly so it is suitable for cell encapsulation (Junmin Zhu, Tang, Kottke-Marchant, & Marchant, 2009).

The second occurs when at least two functional macromers contain mutually or complementary reactive groups that could be added in a balance or imbalance molar ratios. This reaction could be performed at physiological moieties and it permits more control over the density of the network than the photopolymerization approach. Indeed there is no need for using an initiator, which are usually cytotoxic. The Michael-type addition reaction is a type of step-growth polymerization broadly used in PEG-hydrogels and it can be performed at physiological conditions (Fu & Kao, 2011); but compared with the free-radical photopolymerization, takes longer to achieve a gelation. Another kind of step-growth polymerization technique is the click chemistry. This methodology creates well-defined architectures and better swelling capacities. The reaction occurs between an azide and alkyne groups that are "clicked" in the presence of a catalyst. This type of chemistry required a copper catalyst which is cytotoxic and consequently, was not suitable for cell encapsulation. Nevertheless, Bertozzi and colleagues developed a copper-free click chemistry that allowed cell encapsulation (Baskin et al., 2007).

Finally the mixed-mode polymerization was developed by Anseth and colleagues using a thiol-acrylate photopolymerization and no use of initiator is required (Salinas & Anseth, 2008).

These approaches have been used to create a large amount of PEG hydrogels with the incorporation of different bioactive molecules. Hubbell and co-workers developed a series of PEG hydrogels crosslinked by Michael-type addition reaction using a vinyl sulfone-PEG polymer and a PEG-dithiol with cell-adhesive sequences and degradable peptides; they showed tuneable capacities of the gels in terms of elastic moduli or swelling ratio and also they studied their biological functions *in vitro* and *in vivo* (Elbert, Pratt, Lutolf, Halstenberg, & Hubbell, 2001; Simon C. Rizzi et al., 2006; Simone C. Rizzi & Hubbell, 2005). In addition, García and colleagues used a Michael-type addition reaction with maleimide-functionalized PEG as a specific reaction for thiol groups in a fast and physiological pH conditions in comparison to PEG-acrylate or PEG-vinyl macromers (Edward A. Phelps et al., 2012). This group have also demonstrated the ability of these maleimide-thiol PEG hydrogels to release bioactive molecules such as VEGF, showing an improvement of vessel growth formation in studies *in vivo* (Edward A. Phelps, Templeman, Thulé, & García, 2015).

Seliktar and coworkers have shown the capacity to crosslink a whole protein to the PEG backbone (Almany & Seliktar, 2005). They performed a photopolymerization reaction between PEG-diacrylate and the cysteines of a previously denatured fibrinogen to accomplish a 3D scaffold. With the addition of the entire protein, they added an ample number of bioactive sites for cell culture studies (Dikovsky, Bianco-Peled, & Seliktar, 2006). In a similar way, Zhou et al. designed a genetically modified protein with terminal cysteines to bind it covalently with a PEG-maleimide monomer showing its suitability for cell culture studies (Du et al., 2014).

In conclusion, the use of PEG hydrogels in Tissue Engineering has a well-developed chemistry with a large amount of possibilities. The addition of different bioactive molecules to the PEG backbone is an important field for study cell-matrix interactions.

1.2.2 PEGylation

PEGylation, i.e. the incorporation of PEG molecules to a certain compound, is a versatile technique due to the variety of chemistries that can be used. PEGylation is a common strategy in drug delivery due to the improvements in pharmacokinetics properties that PEG confers. Covalent linkage of PEG is shown to increase the half-life circulation of therapeutic proteins *in vivo* (F M Veronese & Mero, 2009). This could point toward a prolongation of the therapeutic effects and a dosage reduction of the PEGylated drug. At present, there are several PEGylated drugs on the market (e.g. Adagen® (approved in 1990), Puricase1® (approved in 2010)) (W. Li, Zhan, De Clercq, Lou, & Liu, 2013).

There are three main strategies to PEGylate molecules: non-specific, site-specific and non-covalent PEGylation Figure 1.8. Because of their relevance, this section will focus on non-specific and site-specific PEGylation strategies.

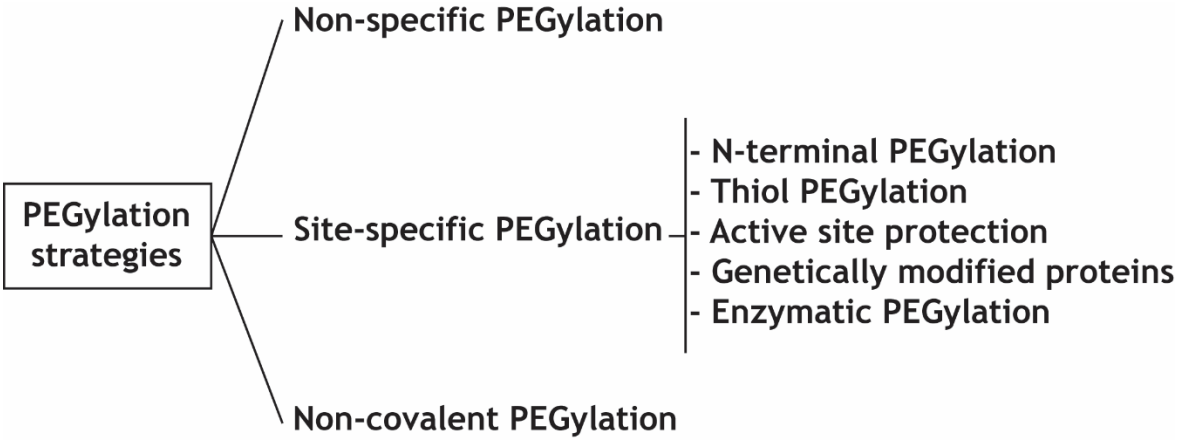

Figure 1.8 Schematic of the different PEGylation strategies.

Non-specific PEGylation takes advantage of the affinity of active esters towards primary amines; site-specific PEGylation presents a more selective chemistry, targeting specific groups on proteins and, non-covalent PEGylation offers a more labile strategy of PEGylation.

Non-specific PEGylation was one of the first strategies developed. Active esters were obtained by reacting PEG-carboxylic acid with N-hydroxysuccinimide (NHS) to achieve succinimidyl esters. These active esters can react with primary amines in mild conditions and form amide bonds. Lysine residues are very common in protein amino acid sequences and, therefore PEGylation through the amine group leads to complex mixtures of proteins with different degrees of PEGylation. However, this strategy has shown success by bringing the first PEGylated drug to the market (Adagen®).

Site-specific PEGylation was developed later and there are five main strategies: N-terminal PEGylation, thiol PEGylation, active site protection, genetically modified proteins and enzymatic PEGylation (Hermanson, 2013a; F M Veronese & Mero, 2009; Francesco M. Veronese, 2001).

N-terminal PEGylation was developed to have a more selective chemistry towards the amino group (Hermanson, 2013b). As there only is one amino terminal group, the PEGylation sites considerably decrease compared to the non-specific PEGylation at amino groups.

Thiol PEGylation exhibits good selectivity, although there is rarely a single free cysteine residue available through the amino acid sequence to react. Cysteine residues are usually paired with another cysteine to form disulphide bridges (Shaunak et al., 2006). PEG-maleimide is the most widely used PEG for site-specific thiol PEGylation (Fontaine, Reid, Robinson, Ashley, & Santi, 2015; Fu &

Kao, 2011). The double bond of the maleimide group and the thiol group react by Michael's addition to form a thioether bond. Some strategies in literature have tried to open the disulphide bridge to expose the thiol group and thus, tackle the problem of cysteine residues' scarcity. The main drawback of disulphide bridge opening is the modification of the secondary structure that can potentially terminate some functional aspects of the protein (C. Zhang, Hekmatfar, Ramanathan, & Karuri, 2013).

The active site protection strategy selectively blocks the undesired sites from being PEGylated. One of the most widely used protection groups is 9-fluorenylmethoxycarbonyl (FMOC) (Miller, 2015). FMOC deprotection is usually achieved by the addition of piperidine.

Genetically modified proteins present a different approach for PEGylation, where you can potentially add free cysteine residues (Yang et al., 2003) or delete lysine residues (Yamamoto et al., 2003) to increase PEGylation selectivity. A more generic approach for the PEGylation of recombinant proteins is the addition of a histidine tag sequence at either the C-terminal or N-terminal ends of the protein.

Enzymatic PEGylation is a highly specific strategy because enzymes are selective catalysts. One of the most used enzymes for PEGylation is transglutaminase, which can catalyse the addition of PEG-amine to glutamine residues (Fontana, Spolaore, Mero, & Veronese, 2008). Glyco-PEGylation, i.e. PEGylation at glycosylation sites, is of growing interest because the linkage of glycans to proteins is well studied (Pasut & Veronese, 2012).

1.2.3 Biochemically Engineered Constructs

The biological/biochemical properties of biomimetic materials greatly influence cell response and so, they need to be carefully incorporated (Cosgrove et al., 2016; Petrie, Capadona, Reyes, & García, 2006; Rao, Peterson, Ceccarelli, Putnam, & Stegemann, 2012). There are numerous approaches to engineer biomaterials that mimic certain biochemical cues of the cell microenvironment but, due to the scope of this text only adhesion ligands and growth factor immobilisation will be discussed.

Adhesion Ligands

Most of cells within their microenvironment rely on adhesion as one of the primary steps to maintain cell activity and their biological functions. Because of that, adhesion is a major aspect that needs to be counted in when designing biomimetic constructs (Hersel, Dahmen, & Kessler, 2003).

Biologically active peptides are widely used as an easy way to incorporate adhesion cues into non-adhesive hydrogels (e.g. PEG-based systems (Edward A. Phelps et al., 2012; Raeber et al., 2005) or alginate hydrogels (Rowley & Mooney, 2002; W. Wang et al., 2015)). Peptides consisting of a number of selected amino acids can often mimic some functional units of full-length proteins. The use of short sequences also reduces complexity and makes synthesis and purification simpler in comparison to full-length proteins. In addition, biologically active peptides are custom-designed and can be engineered in a controlled manner. Many types of adhesive peptides have been used in literature including: Arg-Gly-Asp (RGD), Gly-Phe-Hyp-Gly-Glu-Arg (GFOGER), Ile-Lys-Val-Ala-Val (IKVAV) , Arg-Glu-Asp-Val (REDV) or Tyr-Ile-Gly-Ser-Arg (YIGSR) (Assal, Mie, & Kobatake, 2013; Petrie et al., 2006; Shekaran et al., 2014a; Taubenberger et al., 2016; Tocchio et al., 2015; W. Wang et al., 2015).

Numerous studies have shown that the type, concentration and spatial disposition of the adhesive ligand can affect adhesion, spreading, migration, proliferation and differentiation of cells (Fischer-Cripps, 2011; Kuen et al., 2004; Maheshwari, Brown, Lauffenburger, Wells, & Griffith, 2000; Xuan Wang et al., 2013; Ye et al., 2015).

3D bulk hydrogels have been modified to incorporate adhesive cues. These peptides are usually mixed with the polymer to be integrated during gelation, resulting in a homogeneous distribution of the ligand through the hydrogel. One of the most common approaches to incorporate biochemical cues within 3D hydrogel constructs is thiol-based chemistries such as thiol-acrylate photopolymerisation, thiol-maleimide Michael-type addition reaction or thiol-norbornene step-growth photopolymerisation. Advances in photopolymerisation chemistries such as the one developed by Anseth's group, where a copper-free photo cross-linking process was used to improve cytocompatibility, have allowed 3D cell encapsulation using traditional click chemistries (Deforest, Polizzotti, & Anseth, 2009).

Not only cell-ECM adhesive motifs are used in biomimetic constructs, cell-cell interactions are also studied by using, for example, N-cadherin peptide mimetics, which have shown to promote chondrogenesis in HA hydrogel systems (Kwon et al., 2018).

More sophisticated systems incorporate protein fragments to study more complex interactions, such as the incorporation of the synergy site of fibronectin, the incorporation of adhesive fragments to study the effect of specific integrins or the integration of heparin-binding sites (Jha et al., 2015; M. M. Martino & Hubbell, 2010; Mikaël M. Martino et al., 2011; Petrie et al., 2006; Roy, Wilke-Mounts, & Hocking, 2011).

Moreover, many efforts are being taken to incorporate full-length ECM proteins in order to obtain systems that recapitulate better complex interactions within the ECM in a highly controllable manner. For instance, fibrinogen was covalently linked to a PEG network for cardiac repair (Almany & Seliktar, 2005; Kerscher et al., 2016), fibronectin has been incorporated to a HA system (Seidlits et al., 2011) and laminin has been also incorporated into a PEG backbone (Francisco et al., 2014). Yet, these examples are relatively rare in the literature, in part because it is easier to use biologically active peptides. Subsequently, there is a need for more comprehensive studies of cell behaviour within this type of matrices, where there is a high control over the physicochemical properties of the material but recapitulates more complex biological interactions.

Growth Factor Immobilisation

Growth factors, as explained in previous sections, have important roles in cell function, being specially critical in cell fate determination. For instance, BMP-2 promotes osteogenesis (Shekaran et al., 2014b) and VEGF promotes angiogenesis (Zisch, 2003). The ECM is able to regulate the distribution and activation of growth factors by either sequestration or diffusion of the molecules (Figure 1.9).

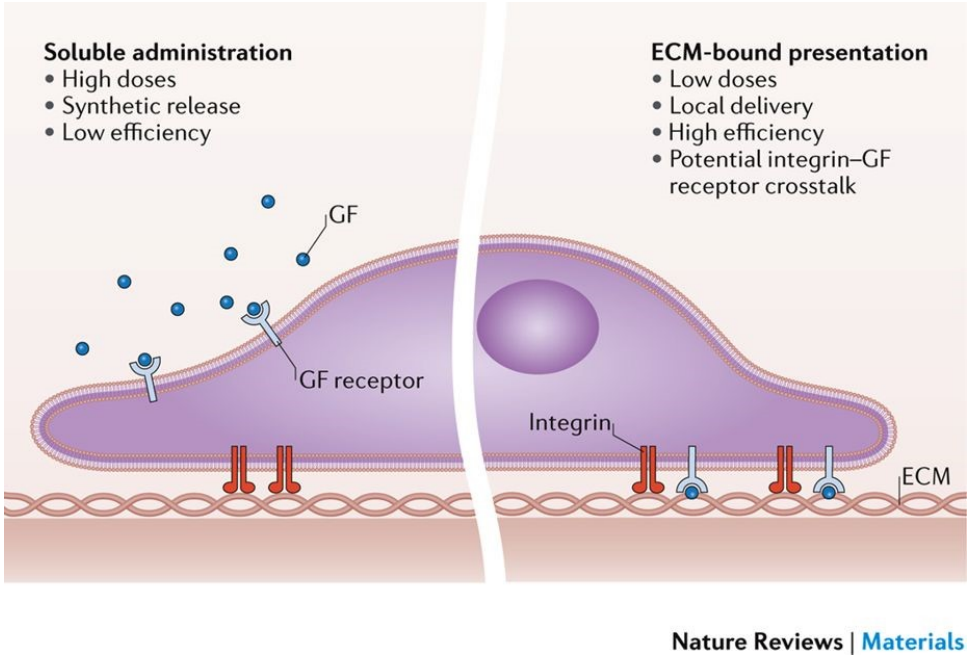

Figure 1.9 Soluble versus matrix-bound growth factor delivery.

Soluble growth factor supplementation generally requires high doses and exhibits low efficiency when compared to matrix-bound growth factor delivery. When the growth factor is bound to the ECM, the crosstalk between integrins and growth factors is possible (taken from (Dalby et al., 2018)**).**

The free diffusion of growth factors plays important roles in tissue homeostasis. For example, soluble growth factors create gradients that can guide tissue repair (Roam et al., 2015). Many examples in literature can be found about free diffusion of growth factors through hydrogels used as systems for their release (Mellott, Searcy, & Pishko, 2001; Tanihara et al., 2001). However, this section aims to focus on growth factor immobilisation that mimic ECM sequestration capabilities.

The immobilisation of growth factors presents several advantages, including the prolongation of growth factor presentation and the prevention of its enzymatic degradation (Cipitria & Salmeron-Sanchez, 2017; Dalby et al., 2018). Growth factors can be immobilised physically through hydrophobic or electrostatic interactions, chemically by covalent bonding or using molecules with high affinity towards them like proteins (e.g. fibronectin, collagen, GAGs or synthetic materials such as custom-designed peptides) (Anjum et al., 2016; Impellitteri et al., 2012; Leslie-barbick, Moon, & West, 2009; M. M. Martino & Hubbell, 2010; Mikaël M. Martino, Briquez, Maruyama, & Hubbell, 2015; Nie, Baldwin, Yamaguchi, & Kiick, 2007; Watarai et al., 2015; Jia Zhu & Clark, 2014b) (Figure 1.10).

Among the limitations of these immobilisation approaches are: the presentation/release of growth factors cannot be spatiotemporally controlled and the need of high amounts of growth factor that is required to fabricate these systems.

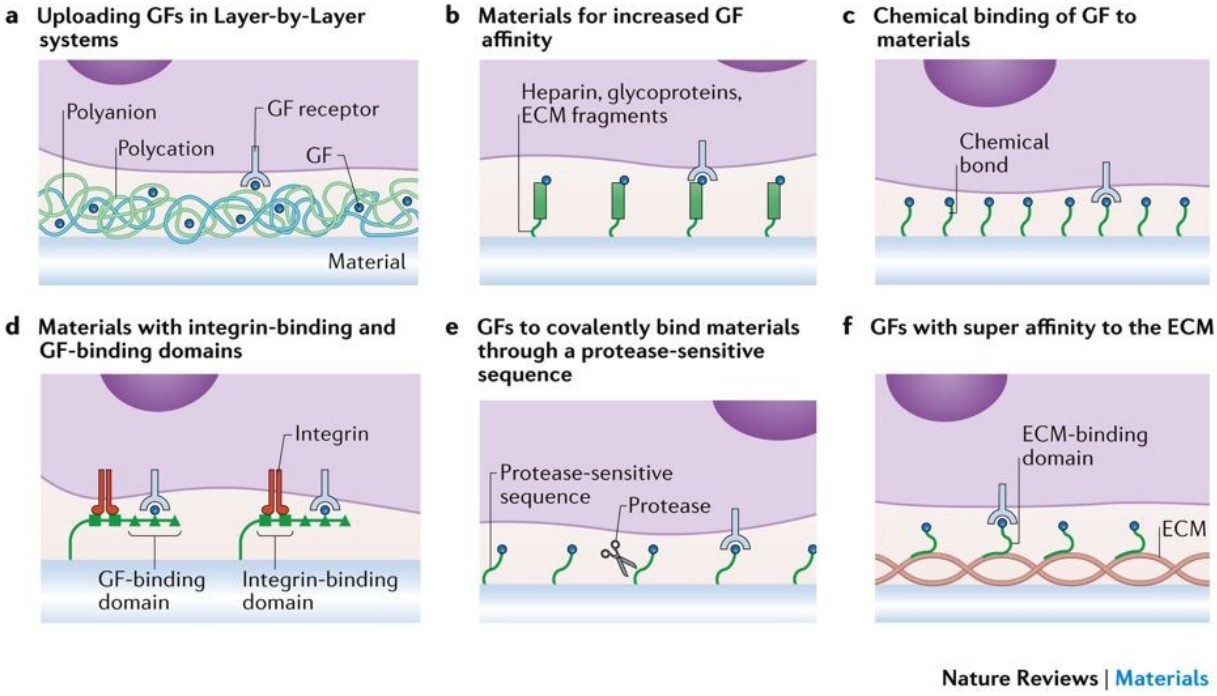

Figure 1.10 Strategies for growth factor presentation.

Systems can be engineered to load growth factors and control their delivery and presentation. Using layer-by-layer (a) growth factors can be entrapped and released in a tuneable manner; (b) materials can incorporate molecules that naturally bind growth factors like heparin or heparin-binding domains. (c) Growth factors can be immobilised via chemical linkage, (d) materials can also incorporate protein fragments that contain both growth factor binding affinities and integrin binding motifs; (e) materials can covalently immobilise growth factors but incorporate degradable sequences to control their release through MMP secretion. (f) Growth factors can be engineered to exhibit increased affinity for its usual binding domain. Taken from (Dalby et al., 2018).

In order to increase the efficiency of growth factors, material systems have been engineered to contain integrin binding motifs as well as growth factors. For instance, when VEGF is presented with the RGD motif in a hydrogel system, vascularisation is promoted more efficiently (E. A. Phelps et al., 2010). Also, specific integrin binding can modulate endothelial cell response in hydrogels loaded with VEGF (S. Li et al., 2017). When VEGF is bound to collagen presents long-term activation of the VEGF receptor 2 of endothelial cells in comparison to soluble VEGF (T. T. Chen et al., 2010). These examples show how strategies based on materials can be utilised to improve the efficiency or activity of growth factors.

1.2.4 Biophysically Engineered Constructs

Biochemical and biophysical cues overlap powerfully in the cell microenvironment and it is difficult to distinguish to which degree one affects the other and vice versa. Because of that, the design of constructs with specific biophysical features have demonstrated to be critical to control cell fate. This subsection will describe some biophysical features that can be controlled with an emphasis in mechanical properties and degradability.

As mentioned before, cells are able to sense structural and topographical features (Dalby, Gadegaard, & Oreffo, 2014). One related parameter incorporated to engineered biomimetic constructs is microporosity. The ECM is a highly porous mesh-like structure filled with water, where soluble molecules freely diffuse through the spaces. This porosity provides a large surface area for cells to interact and thus, influencing cell behaviour. Some important parameters in porous design include pore size, interconnectivity and percentage of porosity, all of which have demonstrated to modulate cell behaviour (Annabi et al., 2010; Q. Zhang, Lu, Kawazoe, & Chen, 2014). As a general rule, an increase in porosity, pore size or interconnectivity leads to enhanced tissue ingrowth, cell infiltration and diffusion of molecules; although this could change depending on the application (Engelmayr et al., 2008). There are many approaches for the engineering of porous hydrogel structures such as solvent casting, particle leaching or freeze-drying. In addition, with the emergent printable approaches for biomimetic hydrogel materials, there is a potential for the fabrication of well-defined porous tissue-like structures (Loh & Choong, 2013).

Another advantage of fabricating porous structures is to improve transport – e.g. nutrients and waste. Native tissues are usually surrounded by capillaries that facilitate oxygen transport and nutrients/waste diffusion. Vascularisation of tissue constructs is a critical parameter in tissue regeneration due to the many pathological outcomes of ischemia. Because of that, there is a preference for interconnected and highly porous structures in tissue engineering.

Mechanical Properties

As mentioned in section 1.1.3, many studies have confirmed the influence of mechanical properties in cell behaviour, mainly using 2D materials with well-defined stiffness (Discher, 2005; A. J. Engler et al., 2006).

3D systems have been also used as more relevant models than 2D substrata to study the role of mechanical cues in cell behaviour. To that end, 3D cell microenvironments with precisely controlled mechanical properties have been used until now. This include the use of hydrogels with linear elasticity (Huebsch et al., 2010), viscoelasticity (Bennett et al., 2018; Chaudhuri et al., 2015, 2016; Gong et al., 2018) and spatiotemporally controlled mechanical properties (Doyle, Carvajal, Jin, Matsumoto, & Yamada, 2015) – e.g. stiffness gradients, material stiffening, material softening.

Elasticity represents the ability of a material to resist deformation (when a force is applied) and return to its original state after this force is removed. Elasticity is usually described by stress-strain curves and typically characterised by stiffness or Young's modulus.

Stiffness of hydrogels can be controlled by modulating polymer concentration, density of crosslinking or molecular weight of polymers. Hydrogels with stiffness ranging between Pa to MPa have been reported using either naturally derived or synthetic hydrogels (Huebsch et al., 2010). When cells are cultured within these hydrogels respond to fluctuations in stiffness with changes in morphology, spreading, migration and differentiation (Boontheekul, Hill, Kong, & Mooney, 2007; Charras & Sahai, 2014; Her et al., 2013; Pek, Wan, & Ying, 2010).

For example, alginate hydrogels were fabricated within a wide range of stiffness (2.5 to 110 kPa) and MSCs encapsulated showed adipogenic-like phenotype when culturing them within 2.5-5 kPa hydrogels, whereas osteogenesis was observed using 11-30 kPa (Huebsch et al., 2010). Similar results have been obtained using other 3D hydrogel systems like RGD-functionalised PEG hydrogels (Parekh et al., 2011).

In addition, hMSCs cultured in stiff HA hydrogels showed low cell spreading and nuclear translocation of the yes associated protein (YAP) and the transcriptional coactivator with PDZ-binding motif (TAZ), conflicting the results obtained in 2D (Caliari et al., 2016).

Stiffness plays important roles in cell function, as stated before. However, soft tissues and most hydrogels are viscoelastic. Viscoelastic materials show both elastic (characterised by stiffness or storage modulus) and viscous (characterised by viscosity or loss modulus) properties. Viscoelastic hydrogels exhibit stress relaxation or creep behaviours. Stress relaxation is observed when stress decreases in response to the same amount of strain applied, whereas creep

behaviour is detected when materials deform permanently under the same mechanical stress.

The viscoelastic properties of a hydrogel can be modulated by controlling its composition, concentration, molecular weight or crosslinking type/density. Many studies have demonstrated the importance of the viscoelastic properties in cell behaviour including cell spreading, cell proliferation and cell differentiation. For instance, Mooney and colleagues developed an alginate hydrogel system in which the stress relaxation was controlled independently of stiffness, adhesion ligand density or degradability. In this work, they showed how spreading and proliferation of fibroblasts was greater in hydrogels with faster relaxation times. Moreover, encapsulated MSCs showed osteoblastic commitment within hydrogels with faster relaxation (Chaudhuri et al., 2015, 2016).

Degradability

Degradation is a crucial parameter in tissue homeostasis. The ECM is a dynamic entity that is being remodelled in a spatiotemporal manner. Many of the macromolecules that compose the ECM are enzyme-sensitive, especially to cell-secreted proteases such as MMPs. Proteases are capable of cleaving proteins within an specific site and, the secretion of these enzymes allows a cell-mediated degradation of the ECM. By degradation, cells can control their local microenvironment and receive instantaneous feedback from it. Degradation is in this sense involved in cell behaviour (e.g. spreading, migration and differentiation) (Khetan et al., 2013b; Silva et al., 2016). ECM remodelling is critical in tissue homeostasis and tissue repair (Page-McCaw, Ewald, & Werb, 2007). Subsequently, uncontrolled degradation could lead to disease.

Engineering the degradability of biomaterials is important to be able to control cell motility, soluble molecules immobilisation or material properties. Two important challenges when engineering degradable materials are the degradation by-products and degradation kinetics. Degradation by-products must be compatible with cell viability and the degradation kinetics needs to match the one of native tissues.

Degradation by-products not only need to be cytocompatible, they can carry instructive cues that modulate cell behaviour. The latter type of by-products are also called matrikines and matricryptins (Ricard-Blum & Salza, 2014). For example, calcium and phosphate ions are released upon mineralised matrix

degradation, promoting osteogenesis (Alford, Kozloff, & Hankenson, 2015). In addition, endostatin (one of the degradation products of collagen) has shown antifibrotic activity in both dermal and pulmonary fibrosis (Yamaguchi et al., 2012).

The degradation profile depends on the hydrogel type, crosslinking method and environmental conditions. Several methodologies have been developed to control the degradability of engineered hydrogels, such as enzymatic degradation, hydrolytic degradation or photolytic degradation (Ozcelik, 2015).

Several studies incorporate enzyme-sensitive peptides as enzymatically degradable crosslinkers. For example, PEG-based hydrogels have been crosslinked with MMP-degradable peptides by several methods (L. Lin, Marchant, Zhu, & Kottke-Marchant, 2014; Edward A. Phelps et al., 2012; Watarai et al., 2015). Degradation is strongly linked with the type of MMP-sensitive peptide used (J. Patterson & Hubbell, 2010) and, when used in combination with RGD-ligands and VEGF, MMP-degradable hydrogels promoted the sustained release of VEGF for two weeks and enhanced vascularisation *in vivo* (J. Patterson & Hubbell, 2010). In addition, other degradable peptides have been used to control degradability like peptides sensitive to plasmin or elastase (Aimetti et al., 2009; Roam et al., 2015).

The spatial control of degradable peptides plays an important role in cell behaviour. Burdick and colleagues used a partially crosslinked acrylate-HA with MMP-degradable peptides. After cell encapsulation, sequential crosslinking of the remaining acrylate groups inhibited MSC spreading even in the presence of adhesive ligands (Khetan, Katz, & Burdick, 2009). This strategy was also used to produced HA hydrogels with patterning of MMP-sensitive peptides that controlled MSC spreading and differentiation (Khetan & Burdick, 2010).

Hydrogels have been also engineered to release molecules (e.g. drugs) or cells upon degradation. These systems are designed to respond to high levels of proteases, which typically occur in cancer and other diseases. However, the activity of the proteolytic enzymes and thus the effectivity of the release are very much influenced by the local environment. Using this strategy, Purcell et al. modified HA hydrogels with dextran sulphate to sequester recombinant tissue inhibitor of MMP-3 (rTIMP-3). These gels were used in a porcine myocardial infarction model. When injected, the rTIMP-3 was released as a response of the high MMP levels in the surroundings and inhibited the action of MMPs, which

contributed to attenuate adverse post-myocardial infarction remodelling (Purcell et al., 2014).

Hydrolytically degradable hydrogels are those containing hydrolysable linkages such as ester or hydrazone. Hydrolytic degradation can occur in relatively mild conditions and does not involve catalytic molecules (Zustiak & Leach, 2010).

For example, HA hydrogels have been modified with glycidyl methacrylate (GMA) in order to obtain hydrolytically degradable hydrogels. The degradation rate in this system can be controlled by varying the ratio of high molecular weight and low molecular weight GMA-HA molecules (Jennifer Patterson et al., 2010). The use of hydrolytically degradable hydrogels is an effective method to control bulk degradation of hydrogels. However, it can be affected by multiple factors such as the local pH of the environment.

Photolytic degradation offers good control over the spatial and temporal degradability properties of hydrogel materials. Anseth and colleagues conjugated a photodegradable acrylic monomer with nitrobenzyl ether-derived (ortho-nitrobenzyl, o-NB) groups into a PEG macromer. Then, using *in situ* photodegradation they were able to create channels that allowed encapsulated fibrosarcoma cells to migrate through them (Kloxin, Kasko, Salinas, & Anseth, 2009).

Kasko and co-workers used a series of o-NB molecules to immobilise several therapeutic agents into PEG hydrogels with different photodegradation sensitivities. The release profile of the therapeutic agents was controlled by varying the exposure time or wavelength and intensity of light and thus, achieving complex release profiles (Griffin & Kasko, 2012). However, the nitrobenzene moieties used in the abovementioned examples can absorb light and therefore, limit its penetration. This can cause a lost in degradation depth. To overcome this limitation, near-infrared (NIR) light has been used to engineer materials with controlled degradability upon exposure to NIR light (Peng et al., 2011; Qin, Wang, Rottmar, Nelson, & Maniura-Weber, 2018). NIR light presents a better applicability *in vivo* due to its good tissue penetrability and causing less cellular photodamage. Yet, the thermal effects of NIR need to be further studied.

Dimensionality

Most of our knowledge about the cell microenvironment comes from studies onto 2D surfaces where cells grow in monolayer. 2D systems offer an over-simplistic

model to study cell behaviour, far away from what is occurring *in vivo* – an actual 3D microenvironment.

Cells cultured on 2D surfaces can only interact with the substrate through their ventral side, whereas in 3D systems all sides of the cells are in contact with the material. On 2D, cells acquire an apical-basal polarity that is unnatural. In addition, cells on 2D systems can spread and migrate freely while within 3D systems have spatial constraints – by the surrounding matrix - and cells need to fit through the existing pores or to degrade the existing matrix to migrate. As a consequence, cell migration speed is extremely different and the response to stiffness changes comparing 2D versus 3D. Furthermore, soluble factors can diffuse freely in a 2D cell culture system, whereas in 3D the diffusion of soluble molecules is governed by immobilisation from matrix components and, physical barriers (Baker & Chen, 2012).

Accordingly, cells in 3D matrices display behaviours more similar to what happens *in vivo* compared to 2D substrates and thus, these systems represent a more relevant model for the study of cell function. Classical examples show that dedifferentiated chondrocytes can recover their phenotype in 3D matrices (Benya & Shaffer, 1982) or that human breast epithelial cells, which exhibit a tumorigenic phenotype cultured in 2D surfaces, recover their normal phenotype in 3D systems (Petersen, Ronnov-Jessen, Howlett, & Bissell, 1992; Weaver et al., 1997). In addition, many examples in literature have demonstrated that tumour models work better in 3D environments (Fischbach et al., 2009; Roudsari, Jeffs, Witt, Gill, & West, 2016; Song, Park, & Gerecht, 2014; Stock et al., 2016; Taubenberger et al., 2016).

Numerous efforts have been done to recapitulate the 3D cell microenvironment using biomimetic materials, which are typically hydrogels. But the cell microenvironment changes over time, leading to a continuous and dynamic variation of the ECM properties. In cases such as modelling the tumour microenvironment or drug screening, it could be desirable to be able to track the 4D evolution of cell behaviour and thus, is important to engineer biomatrices that can be controlled in 4D (i.e. systems with time-modulated features) (Brown & Anseth, 2017).

1.3 Engineering pro-angiogenic microenvironments

Angiogenesis is a complex, multicellular process throughout which new blood vessels are formed from pre-existing ones. The product of angiogenesis is a new vascular network that supports tissue's demand of oxygen and nutrients (Rhodes & Simons, 2007). The ultimate goal of therapeutic angiogenesis is restoring blood flow in ischemic tissues (i.e. where endogenous tissue is insufficiently perfused) by promoting the formation of new vessels (Briquez, Clegg, Martino, Gabhann, & Hubbell, 2016; Carmeliet, 2003; Rufaihah & Seliktar, 2016).

The process of angiogenesis is regulated by an intricate collection of biochemical and biophysical cues and it happens within a 3D and dynamic setting, the ECM.

During angiogenesis, the growth of healthy and functional vessels relies on the highly synchronised interplay of different cell types and growth factors. In this scenario, endothelial cells are activated upon certain signals (e.g. hypoxia, growth factors). These activated endothelial cells can assemble into new tube-like structures (vessel morphogenesis) and then, associate with mural cells (e.g. pericytes) during vessel maturation. Pericytes produce a myriad of regulatory signals; some of them involve the TGF-b1/TGF-R, Angiopoietin/Tie2 and EphrinB2/EphB4 pathways, which guide endothelial cells to quiescence during vessel stabilisation (Patan, 2000; Ribatti, Nico, & Crivellato, 2011).

Vascular endothelial growth factor (VEGF) is a master regulator of physiological angiogenesis (e.g. reproductive angiogenesis) and also pathological angiogenesis (e.g. tumour-related angiogenesis). VEGF itself is able to start the complex cascade of events that leads to vascular growth. Furthermore, the formation of VEGF gradients within the matrix leads to sprouting of new capillaries (Ferrara et al., 2003; L. Li, 2003). The endothelial cells that are activated by VEGF become tip cells (or leader cells), which are capable of sensing the VEGF concentration gradient within the matrix through thin filopodial extensions, migrating towards it. This process is regulated by Notch signalling. Tip cells upregulate the Notch ligand Delta-like-4 (Dll4), which activates Notch1 in contiguous cells, guiding them to function as stalk cells (or follower cells). Stalk cells then start proliferating to form the main trunk of the new vessel, right behind the tip cell (Eilken et al., 2017; Gerhardt, 2008).

Cells are capable of secreting proteases that degrade the BM (i.e. collagen IV and laminin-1) and expose the endothelial cells that are sprouting (tip cells) to the interstitial ECM (mainly composed of collagen I and elastin) (Eble & Niland, 2009). By doing so, tip cells are able to migrate and stalk cells proliferate, forming the new vessel. Adhesive proteins like fibronectin and vitronectin link collagen I to cell-surface integrins that are essential for vascular development. Integrins are transmembrane receptors involved in cell adhesion. Integrins are capable of transducing mechanical forces coming from the ECM to the cytoskeleton (i.e. mechanotransduction), leading to changes in cell signalling (Serini et al., 2006). The cytoplasmic domains of integrins interact with signalling molecules such as the focal adhesion kinase (FAK) and Src, which are critical for the crosstalk between integrin and growth factor receptors signalling. Normally, of the integrins that are expressed on endothelial cells, $\alpha_5\beta_1$ binds to fibronectin (Wijelath et al., 2006) while $\alpha_1\beta_1$ and α2β1 bind to collagen, $\alpha_3\beta_1$, $\alpha_6\beta_1$ and $\alpha_6\beta_4$ to laminin, and αvβ3 to several ECM substrates (including fibronectin). This lets endothelial cells to sense a number of changes in their local microenvironment and adjust their behaviour accordingly.

The ECM naturally regulates the distribution and activity of growth factors through changes in their local concentration, availability and therefore, signalling. In order to recapitulate this feature of the ECM, biomaterials have been functionalised with specific growth factor binding sites (Jha et al., 2014; M. M. Martino, Briquez, Ranga, Lutolf, & Hubbell, 2013; M. M. Martino & Hubbell, 2010; Mikaël M Martino et al., 2011; Rice et al., 2013).

Most of the angiogenic growth factors (e.g. VEGF, PDGF or FGF) have the capability to bind certain sites on the ECM and they usually interact first with the ECM before finding a cell surface receptor.

$VEGF_{165}$, FGF-2 and PDGF-BB have affinity to heparan sulphate proteoglycans and these growth factors and several others have been shown to bind fibronectin (Llopis-hernández et al., 2016; M. M. Martino & Hubbell, 2010; Moulisová et al., 2017), vitronectin (Byzova et al., 2000), fibrinogen (M. M. Martino et al., 2013) or tenascin C (Laporte, Rice, Tortelli, & Hubbell, 2013). Once bound, the release of growth factors depends on the action of proteases that can specifically cleave certain sites of ECM proteins . This allows the spatiotemporal regulation of growth factor delivery in a very tight manner.

In order to mimic these exquisite ECM-growth factor interactions, biomaterials have been decorated with heparin or heparin sulphate-like molecules (Tae et al.,

2007), which possess the natural ECM's ability to sequester certain growth factors and control their delivery. For example, Peattie's group fabricated a HA hydrogel tethered with increasing amounts of heparin and were able to accomplish sustained release of VEGF and FGF-2 (Pike et al., 2006). Similarly, Nie et al. prepared a crosslinked heparin hydrogel showing controlled release of bFGF (Nie et al., 2007). Tanihara et al. also showed the ability of a bFGF loaded heparin-alginate hydrogel to improve angiogenesis *in vivo* (Tanihara et al., 2001).

These examples show how the integration of natural growth factor binding domains (either by the incorporation of promiscuous heparin binding domains, heparan sulphate or growth factor-binding peptides (Impellitteri et al., 2012)) within biomaterial matrices permits the efficient release of low amounts of growth factors.

Apart from the control of growth factor availability, ECMs can also modulate growth factor signalling via the interaction among ECM proteins, growth factors, cell-adhesion proteins, cell-adhesion receptors and growth factor receptors. It has been shown that VEGF binds to fibronectin forming molecular complexes, which induce the formation of clusters between integrins and VEGF receptors (VEGFR) (Mikaël M. Martino et al., 2011; Wijelath et al., 2006).

Growth factor receptors and integrins share some of the molecules involved in their respective signalling pathways; therefore, the clusters formed between integrins and growth factor receptors substantially enhance signalling (Comoglio, Boccaccio, & Trusolino, 2003; Yamada & Even-Ram, 2002). This synergistic signalling has been exploited to lower the dosage of growth factors used in biomaterials. For example, Hubbell's group engineered hydrogel matrices incorporating the heparin-II binding domain of fibronectin showing that this promiscuous growth factor-binding fragment works better when tethered next to the cell-adhesion fragment of fibronectin (FN type III 9-10th repeats) and showing wound healing and bone repair *in vivo* (Mikaël M. Martino et al., 2011).

In conclusion, in order to develop efficient pro-angiogenic microenvironments, it is necessary to understand how growth factors are presented by the natural ECM during physiological angiogenesis. In particular, microenvironments capable of mimicking growth factor-ECM's interactions in a simple way will be highly relevant in future for clinical translation.

1.4 Full-length proteins of the ECM to recapitulate native microenvironments

During decades collagen type I has been the protein of choice for the fabrication of scaffolds to simulate the natural microenvironment provided by the ECM and to study cell behaviour *in vitro*. Collagen I can form hydrogels by a change of pH. This strategy can be used to fabricate collagen sponges and to encapsulate cells *in situ* (Shekaran et al., 2014a). Another example is fibrinogen, which can be converted to fibrin by using the enzyme thrombin (which is the basis of fibrin-based blood clots). Fibrinogen has been used to study critical processes such as wound healing and angiogenesis. Moreover, fibrin hydrogel's formation allows the encapsulation of cells. (Kniazeva & Putnam, 2009; Nakatsu et al., 2003) Polymerisation of other ECM proteins such as fibronectin (reviewed in (Llopis-Hernández, Cantini, González-García, & Salmerón-Sánchez, 2015) or laminin (Hochman-Mendez, Lacerda de Menezes, Sholl-Franco, & Coelho-Sampaio, 2014; Menezes, Ricardo Lacerda de Menezes, Assis Nascimento, de Siqueira Santos, & Coelho-Sampaio, 2010) have been described but, these examples refer to protein mats (flat, 2D sheets of proteins) that cannot be used as 3D environments for cell encapsulation studies.

As described in section 1.1.3, fibronectin is a key protein of the ECM. Its cell-adhesion motif – RGD – has been extensively used as the archetype of cell adhesion. Consequently, several systems have used the RGD peptide as a way to incorporate fibronectin (or vitronectin) into both 2D and 3D matrices (Bayless, Salazar, & Davis, 2000; Ferreira et al., 2007; Peyton, Raub, Keschrumrus, & Putnam, 2006; C. Zhang, Hekmatfer, & Karuri, 2014). By using this approach - although it has provided considerable amount of data about cell adhesion mechanisms – the full fibronectin molecule is reduced to just three amino acids.

The cell-binding domain of fibronectin is located at the $FNIII_{9-10}$ domains. This domain also contains the synergy site of cell adhesion (PHSRN motif), which enhances some cellular activities. For instance, Petrie and colleagues showed that the recombinant fragment $FNIII_{7-10}$ of fibronectin – which contains both the RGD and PHSRN motifs in the native structural form – exhibited increased adhesion strength, cell proliferation, focal adhesion kinase (FAK) activation and specificity for $\alpha_5\beta_1$ integrin compared to both RGD and RGD-linker-PHSRN peptides (that showed specificity for $\alpha_v\beta_3$ integrin) (Petrie et al., 2006).

Fibronectin also contains in its structure two heparin-binding domains. The heparin-binding II domain, which is located in the $FNIII_{12-14}$, has been reported to bind several growth factors (M. M. Martino & Hubbell, 2010). Martino and colleagues demonstrated that the recombinant fragments of fibronectin including both the cell-adhesion domain and the heparin-binding II domain promoted wound healing and bone regeneration more efficiently than each fragment alone (using fibrin hydrogels) (Mikaël M. Martino et al., 2011).

Fibronectin also contains a collagen-binding domain, which is located in the $FNI_6FNII_{1-2}FNI_{7-9}$ domain. *In vivo,* fibronectin is one of the first proteins to be secreted when a tissue is developing or regenerating (acting as a transient primitive ECM). Moreover, collagen cannot assemble *in vivo* if there is not fibronectin deposited first (reviewed in (Zollinger & Smith, 2017)).

Fibronectin also contains fibronectin-binding sites, which allow the assemblage of this protein into networks (Pankov, 2002; Singh et al., 2010). Moreover, fibronectin also contains cryptic domains that are exposed under certain conditions (Ingham et al., 1997; Roy et al., 2011).

As a consequence, the incorporation of full-length proteins in general and fibronectin in particular is of critical importance. There is a need for new matrices that incorporates the complexity of full-length proteins but within controllable microenvironments.

Seliktar's group worked on the incorporation of full-length fibrinogen into synthetic PEG matrices instead of working with fibrin hydrogels (Almany & Seliktar, 2005; Dikovsky et al., 2006); laminin was incorporated into PEG hydrogels as well (Francisco et al., 2014) and, fibronectin has also been incorporated into a hyaluronic acid hydrogel (Seidlits et al., 2011). Although there are a few examples in literature, the incorporation of full proteins is not trivial and more work needs to be carried out to achieve better matrices with controllable properties for the study of cell behaviour.

1.5 Hypothesis and aims

The cell-material interface is an intricate and dynamic microenvironment where both material and cell mutually dictate one another's fate. The material through its physicochemical properties (e.g. degradability, stiffness, adhesion, architecture or porosity) and the cell by modifying its surroundings (e.g. degradation, secretion of molecules).

During the last decade, there has been a lot of effort trying to reproduce the physicochemical properties of the ECM and consequently, materials (mostly hydrogels) have appeared as three-dimensional environments that can be finely engineered to recapitulate many properties of the ECM. Additionally, the incorporation of biological molecules such as peptides derived from ECM proteins (e.g. RGD, IKVAV, GFOGER) has led to an improvement in material's chemical properties, acting as better ECM mimetics for the interaction with cells. Furthermore, these new microenvironments can be loaded with soluble molecules and also control their release.

Despite all the advances achieved, materials still lack certain complexity, and they are not able to reproduce some central features of the ECM such as the interaction between proteins and soluble molecules or some specific cell-protein interactions. For instance, many groups use the RGD peptide as a cell-adhesion mimetic of the fibronectin protein; however, the cell attachment domain of fibronectin ($FNIII_{9-10}$) contains the synergy site (PHSRN motif), which has been shown to increase cell spreading and fibril assembly. Additionally, the full-length fibronectin molecule contains many other binding sites and even splicing variants that cannot be recapitulated using a peptidomimetic.

In order to comprehend better tissue homeostasis, tissue repair and disease, there is a need for 3D microenvironments that can mimic better some of the more complex cell-ECM interactions that occur naturally. This will be extremely useful not only to improve our understanding of these interactions but to be able to use them as therapeutic strategies to tackle disease and tissue repair.

The main goal of this work is to engineer a new family of highly tuneable hydrogel materials that incorporate full-length fibronectin. Fibronectin is an important protein from the ECM that – due to its structure - can bind growth factors in close proximity to integrin binding and thus, this system can be used as a tool to synergistically enhance growth factor's activity in 3D.

The specific aims of this work are:

- Design a strategy to covalently link fibronectin to a hydrogel polymeric network.
- Engineer the system to control physicochemical properties such as stiffness and degradability.
- To present VEGF in synergy with integrins via fibronectin binding of growth factor in close proximity to integrins.
- Explore the effect of the VEGF-fibronectin interaction in angiogenic and vasculogenic *in vitro* models.
- Explore the effect of the VEGF-fibronectin interaction in an *in vivo* model.

2 Chapter two: Materials and methods

2.1. Materials

All the materials used during this thesis are listed in the following tables:

Table 2.1 List of polymers used.

Reagent	Product	Provider	Notes
4-arm-PEG-Maleimide	4arm-PEG-MAL-20K-5g	LaysanBio	PEG-MAL, 20 kDa
SH-PEG-SH	PSB-613	Creative PEGworks	PEGdiSH, 2 kDa
Sodium hyaluronate	HA60K	Lifecore Bimomedical	75 kDa as per CoA

Table 2.2 List of cells and cell culture reagents used.

Reagent	Product	Provider	Notes
C2C12s	91031101	Sigma	Murine
Dermal fibroblasts	HDFp	Caltag Medsystems	Human, pooled donor
Human umbilical vein endothelial cells (HUVECs)	ZHC-2301	Caltag Medsystems	Human, pooled donor
MSCs	PT-2501	Lonza	Human, single donor
Dulbecco's modified Eagle's medium	41965-039	Gibco	DMEM
α-MEM	12561056	Gibco	
Human large vessel endothelial medium	ZHP-2353	Caltag Medsystems	HLVE
Penicillin/Streptomycin	15140-122	Gibco	P/S
Foetal Bovine Serum	10500-064	Gibco	FBS

Table 2.3 List of kits used.

Reagent	Product	Provider	Notes
DyLight™ 488 NHS Ester	46402	ThermoFisher	
ELISA kit Reagent Diluent	DY995	R&D Systems	
ELISA kit Substrate	DY999	R&D Systems	
ELISA kit Stop Solution	DY994	R&D Systems	
LIVE/DEAD® kit Calcein-AM	C3099	ThermoFisher	
LIVE/DEAD® kit Ethidium homodimer-1	E1169	ThermoFisher	
Micro BCA™ assay kit	23235	ThermoFisher	

Table 2.4 List of antibodies and other reagents used for immunodetection.

Reagent	Product	Provider	Notes
4',6-diamidino-2-phenylindole, dihydrochloride	62247	ThermoFisher	DAPI, Dilution 1:5000
Mouse-anti-FN (cell adhesion site, monoclonal)	HFN7.1-s	Developmental Studies Hybridoma Bank	Dilution 1:330,
Mouse-anti-FN (gelatin binding site, monoclonal)	MAB1892	Millipore	Dilution 1:1000,
Mouse-anti-FN (heparin binding site II, monoclonal)	P5F3	Santa Cruz Biotechnology	Dilution 1:2000,
Rabbit-anti-FN (polyclonal)	F3648-.2ML	Sigma	Dilution (1:400, IF) (1:1000, ELISA),
Goat-anti-mouse-Alexa Fluor 488	A-11001	ThermoFisher	Dilution 1:200
Rabbit-anti-mouse-Cy3	315-165-003	Jackson Immunoresearch	Dilution 1:200
Goat-anti-rabbit-Cy3	111-165-003	Jackson Immunoresearch	Dilution 1:200
Goat-anti-mouse-HRP	626520	Invitrogen	Dilution 1:10000
Goat-anti-rabbit-HRP	31460	Invitrogen	Dilution 1:10000
Mouse-anti-Vinculin (monoclonal)	V9131-.2ML	Sigma	Dilution 1:400
Rabbit-anti-YAP (polyclonal)	H-125	Santa Cruz Biotechnology	Dilution 1:200
NucBlue	R37605	ThermoFisher	
Phalloidin	A12379	ThermoFisher	Dilution 1:300
Rhodamine	R415	ThermoFisher	Dilution 1:200
Triton-X100	T8787	Sigma	
Tween 20	P2287	Sigma	
Vectashield	H1000	Vectorlabs	

Table 2.5 List of proteins and peptides used.

Reagent	Product	Provider	Notes
α-chymotrypsin	C4129	Sigma	Bovine
Bovine Serum Albumin	A7979	Sigma	BSA
Collagenase I	17100-017	Gibco	
Fibronectin	663	YoProteins	Human, from plasma
VEGF-A	293-VE-050/CF	R&D Systems	Isoform 165
VPM peptide	Custom synthesised	GensScript	GCRDVPMSMRGGDRCG

Table 2.6 List of other materials and reagents used.

Reagent	Product	Provider	Notes
1,4-dithiothreitol	R0861	ThermoFisher	DTT
2-Hydroxy-4′-(2-hydroxyethoxy)-2-methylpropiophenone	410896-10G	Sigma	Irgacure-2959
5-norbornene-2-carboxylic acid	446440	Sigma	
Anhydrous Dimethyl Sulfoxide	276855	Sigma	DMSO
Benzotriazole-1-yl-oxy-tris-(dimethylamino)-phosphonium hexafluorophosphate	8510040025	Sigma	BOPS
Cytodex-3 microcarriers	C3275	Sigma	
D_2O	191701	Sigma	
Dowex® resin 50Wx8	44514-100G-F	Sigma	
Dulbecco's phosphate buffer solution	14190-094	Gibco	DPBS
Iodoacetamide	I1149-5G	Sigma	IAA
L-Cysteine	44889	ThermoFisher	
NaCl	S/3160/53	Fisher	
NaOH	S/4920/53	Fisher	
Optimal cutting temperature compound	361603E	VWR	OCT
Rain-X	80199200	Rain-X	
Tetrabutylammonium	86854	Sigma	TBA
Tris(2-carboxyethyl)phosphine hydrochloride	75259-5G	Sigma	TCEP
Trypan blue	T8154	Sigma	
Trypsin-EDTA	T4049-100ML	Sigma	0.25%
Urea	U5378	Sigma	

2.2 Methods

2.2.1 Fibronectin PEGylation

Fibronectin (YoProteins, 3 mg/mL) was PEGylated by modifying a procedure from Seliktar's group (Almany & Seliktar, 2005) (Figure 2.1). Fibronectin was denatured in denaturing buffer (5 mM TCEP, 8 M urea, pH 7.4) for 15 min at room temperature (RT). Then 4-arm-PEG-Maleimide (PEGMAL, 20kDa, LaysanBio) was incubated for 30 min and RT at a molar ratio FN:PEGMAL 1:4. The PEGylation was stopped using 1 M NaOH (pH 8.5). After PEGylation, remaining non-reacted cysteine residues were blocked by alkylation using 14 mM iodoacetamide (IAA,

Sigma). The product of the reaction was dialysed using (Mini-A-Lyzer, MWCO 10 KDa, ThermoFisher) against DPBS for one hour at RT. Then, the protein solution was precipitated using cold ethanol. Briefly, nine volumes of cold absolute ethanol were added to the protein solution and mixed using a vortex mixer. The mixture was then incubated at -20°C overnight and centrifuged at 15000 g and 4°C for 15 min. The supernatant was discarded and the protein pellet was further washed with 90% cold ethanol and centrifuged again at 15000 g and 4°C for 5 min. Pellets were dried and solubilised using 8 M urea at a final protein concentration of 2.5 mg/mL. Once the protein was dissolved, the solution was dialysed against DPBS and stored in the freezer or immediately used.

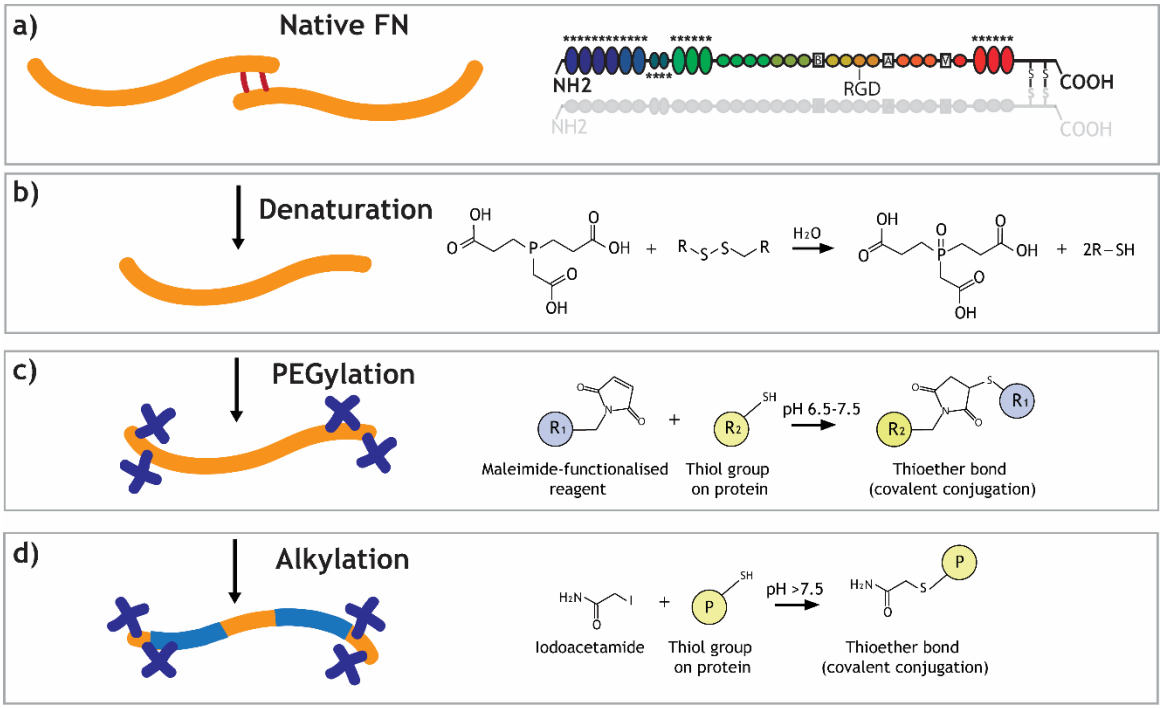

Figure 2.1 Schematic illustration of the fibronectin PEGylation work-flow.

(a) Native fibronectin was used to conjugate with PEG molecules because it contains two disulphide bonds (four cysteine residues) in each fibronectin module types I and II as marked with asterisks on the right image. (b) To expose thiols, TCEP was used as a denaturant as it can catalyse the rupture of a disulphide bond in water. (c) PEGylation was carried out using Michael-type addition reaction between maleimide groups of 4-arm-PEG-maleimide macromers and thiol groups on fibronectin. (d) Alkylation reaction was assessed in order to block the thiol groups that did not react during the PEGylation step.

2.2.2 Cell culture

C2C12 cells (Sigma) between passages 4 and 7 were used for early adhesion studies and viability for PEG hydrogels. C2C12s were grown in DMEM high glucose without pyruvate and 20% FBS.

HUVEC cells (Caltag Medsystems) between passages 1 and 5 were used for viability and angiogenesis/vascularisation *in vitro* assays. HUVECs were grown in growth media (HLVC media).

HDFs (Caltag Medsystems) between passages 1 and 6 were used for angiogenesis studies. Cells were grown in DMEM high glucose without pyruvate and 10% FBS until seeding. Once seeded, HLVC media was used.

hMSCs (Lonza) between passages 4 and 7 were grown in 10 mm petri dishes using α-MEM and 10% FBS.

All media used were supplemented with 1% penicillin/streptomycin.

2.2.3 Cell adhesion assay on PEGylated fibronectin

PEGylated and fibronectin was adsorbed onto glass coverslips at 20 µg/mL for one hour at RT. Native fibronectin was adsorbed at the same concentration and time as a control. After adsorption, samples were washed twice with DPBS and kept in the incubator (37ºC, 5% CO_2) until seeding. C2C12 cells were seeded onto the glass coverslips at 10,000 cells/cm^2 using FBS free media. Cells were let to attach for three hours (37ºC and 5% CO2). After that time, cells were fixed with 4% paraformaldehyde for 30 min at RT and kept at 4ºC. Conditions were tested in triplicate, twice.

2.2.4 Enzyme-linked immunosorbent assay

Enzyme-linked immunosorbent assay (ELISA) plates were coated with the capture antibody rabbit-polyclonal-anti-FN (Sigma) overnight at RT. Then, the capture antibody was washed three times with washing buffer (0.05% Tween 20 in DPBS). After washing, the plate was blocked using 1% BSA for one hour at RT. After blocking, the plate was washed three times using washing buffer. Then, samples (PEGylated fibronectin or native fibronectin) were added to the plate for one hour at RT. After sample incubation the plate was washed three times with washing buffer. Then, the primary antibodies (either HFN7.1 (1:330), P5F3 (1:2000) or MAB1892 (1:1000)) were added for one hour at RT. After incubation, samples were washed three times using washing buffer. Then, secondary antibody (goat-anti-mouse-HRP (1:10000)) was added for one hour at RT and was washed three times with washing buffer. After that, substrate solution (1:1 V/V Reagent A:Reagent B, R&D Systems) was added for 20 min. The reaction was stopped using 4 N sulphuric

acid (Stop solution, R&D Systems). The ELISA plate was read at 450 nm and 540 nm using a plate reader (BIOTEK).

2.2.5 Atomic force microscopy (AFM) imaging

Proteins (either PEGylated fibronectin or native fibronectin) were adsorb onto PEA spin coated glass coverslips for 10 min at 20 µg/mL and RT as described (Salmerón-Sánchez et al., 2011). AFM in AC mode (Nanowizard-3, JPK) was used to obtain phase and height images of the fibronectin-coated PEA samples. A pyramidal tip (silicon nitride, MPP-21220, f_0 =59-69 Hz, Bruker) was used. Images were processed using the JPKSPM data processing software.

2.2.6 PEG Hydrogel formation

PEG hydrogels were formed using Michael-type addition reaction under physiological pH and temperature. Briefly, a final concentration of 1 mg/mL of PEGylated fibronectin was added to different amounts of PEGMAL (3%, 5% or 10% (w/V), Table 2.7). The crosslinker was added always at the end at a molar ratio 1:1 maleimide:thiol to ensure full crosslinking. Crosslinkers used were either PEG-dithiol (PEGSH, 2 KDa, Creative PEGWorks) or mixtures of PEGSH and protease-degradable peptide flanked by two cysteine residues (VPM peptide, GCRDVPMSMRGGDRCG, purity 96.9%, Mw 1696.96 Da, GenScript) (Table 2.8). Cells and/or soluble molecules such as growth factors were always mixed with the protein and PEGMAL before adding the crosslinker. Once the crosslinker was added, samples were incubated for 30 min at 37°C to allow gelation. PEG only hydrogels were produced as well without the addition of the PEGylated fibronectin. The final volume of the hydrogels prepared was always 50 µL unless otherwise noticed.

Table 2.7 Hydrogels used according to the amount of PEGMAL.

FNPEG hydrogels	3% FNPEG	5% FNPEG	10% FNPEG
Fibronectin (mg/mL)	1	1	1
PEGMAL (mg/mL)	30	50	100
PEG hydrogels	**3% PEG**	**5% PEG**	**10% PEG**
Fibronectin (mg/mL)	-	-	-
PEGMAL (mg/mL)	30	50	100

Table 2.8 Percentages of crosslinker used for FNPEG and PEG hydrogels.

Percentage of crosslinker (from total amount of crosslinker needed)	VPM (%)	PEGSH (%)
0VPM	0	100
0.1VPM	10	90
0.2VPM	20	80
0.3VPM	30	70
0.5VPM	50	50

2.2.7 Water sorption

Hydrogels were formed and immersed in MilliQ water up to a week using filtered Eppendorf tubes. Empty baskets were weighed before starting the experiment and then, for every timepoint samples were centrifuged at 6500 rpm for 5 min to remove the supernatant from the basket so only the hydrogel sample would remain into the basket holder. Then, sample and basket were weighed. The amount of water absorbed was calculated as follows:

Equation 2.1 Percentage of water absorbed after hydrogel formation.

$$\boldsymbol{Water\ Sorption}\ (\%) = \frac{\boldsymbol{m_t - m_0}}{\boldsymbol{m_0}} * \mathbf{100}$$

Being m_t the weight of the hydrogel at a certain time and m_0 the weight of the hydrogel after formation.

2.2.8 Protein quantification

Protein from supernatants (in solution) was collected and quantified using bicinchoininc acid. Micro bicinchoninic acid protein assay kit (Micro BCA™, Thermo Fisher Scientific) was used following manufacturer's instructions. Briefly, standard and samples were loaded onto a 96-well microplate and were mixed with the same volume of working reagent (25:24:1 (V:V:V) of Reagents A:B:C from the kit). Then, the microplate was sealed and incubated for two hours at 37°C. After incubation, the microplate was let to cool down for 20 min at RT, protected from light. The absorbance at 562 nm was measured using a plate reader (BIOTEK). Bovine serum albumin (BSA, 2mg/mL) was use to prepare the standard curve. Conditions were prepared in triplicate and samples were measured in triplicate.

2.2.9 Polyacrylamide gel electrophoresis

The polyacrylamide gel electrophoresis (PAGE) was run using 0.1% SDS in a Trys-Glycine running buffer (Bio-Rad). Samples were loaded using a reducing loading buffer prepared by mixing Laemmli buffer (4X, Bio-Rad) and ß-mercaptoethanol (350 mM, Bio-Rad), following manufacturer's instructions (three parts of sample and one part of loading buffer). Fifteen microliters of each sample (sample + loading buffer) were loaded and 5 µL of the marker (colour prestained protein ladder, broad range (11-245 kDa, New England Biolabs P7712S) were used. A gradient precast gel (BioRad, 4-20% TGX-PAGE) was used to run the samples. The running conditions were 100 V, 1800 min. Gels were incubated in fixing solution (45% methanol, 45% water, and 10% glacial acetic acid (V/V/V)) during 30 min at RT. Then, gels were stained with 0.025% Coomassie Blue G250 (Bio-Rad) in 10% acetic acid overnight at RT using an orbital shaker. Finally, each gel was destained twice in 10% acetic acid (30 min and 60 min, respectively) and transferred to water. Images of the gel were taken using the scanner of a canon image runner advance C5235i multifunctional laser printer. Each condition was run in triplicate in the same gel except for the protein ladder, which was run twice in the same gel.

2.2.10 Preparation of cryo-sections

Hydrogels were embedded in OCT (optimal cutting temperature compound, VWR) and flash frozen by immersion in liquid nitrogen to preserve the structure of the gel. Samples were stored at -80°C until use. A cryostat (Leica, -20°C) was used to cut the samples. Sections of 40 and 100 µm of thickness were prepared on microscope slides (Superfrost® slides, ThermoFisher).

2.2.11 Immunofluorescence

Fibronectin was detected via immunofluorescence (IF) in hydrogel samples. Hydrogel samples or hydrogel sections were blocked with blocking buffer (1% BSA) for 30 min at RT. Then, primary antibody rabbit polyclonal-anti-FN (Sigma) was added and incubated for one hour at RT. After the addition of the primary antibody, samples were washed three times using washing buffer (0.5% Tween 20 in DPBS). Then, secondary antibody goat-anti-rabbit-Cy3 was incubated for one hour at RT (protected from light). After that, samples were washed three times using washing buffer. Images were taken at 10X, 20X and 40X using a ZEISS AxioObserver Z.1.

In order to study cell adhesion, C2C12s were stained for vinculin, actin and nuclei using a standard immunostaining procedure. Briefly, samples were permeabilised for 5 min using 0.1% Triton-X100, washed twice with DPBS and blocked with blocking buffer for 30 min at RT. After blocking, samples were incubated with primary antibody anti-vinculin (1:400) for one hour at RT and washed three times with washing buffer (0.5% Tween 20 in DPBS). Then secondary antibody Cy3-anti-mouse (1:200) and AlexaFluor-488 Phalloidin (1:200) were added to the samples for 1h at RT protected from light. After that, samples were washed three times using washing buffer and mounted using VECTASHIELD mounting media with DAPI. Images were taken at 63X magnification using an epifluorescence microscope.

IF to detect YAP was performed as follows. First, cells were permeabilised with 0.1% Triton-X100 for 5 min and blocked with 3% BSA for 45 min. After blocking, the primary antibody rabbit-anti-YAP was added and incubated overnight at 4ºC (dilution 1:200). Then, the primary antibody was washed with washing buffer three times. After washing, a secondary antibody goat-anti-rabbit-Alexa Fluor 488 was added for two hours at RT (dilution 1:200). Three washes with washing buffer follow the antibody incubation. Then, rhodamine phalloidin was added for 20 min (dilution 1:200) and DAPI staining for 10 min (dilution 1: 5000). Images were taken using an epifluorescence microscope at 20X magnification.

2.2.12 AFM nanoindentation

Nanoindentation was assessed using atomic force microscopy in force spectroscopy mode (AFM/FS, Nanowizard-3, JPK). Cantilevers (Arrow-TL1-50, spring constant ~ 0.03 N/m, Nano World innovative technologies) were functionalised manually with silicon oxide microbeads (20 mg/mL, size 20 µm, monodisperse, Corpuscular Inc.). The actual stiffness of the cantilever was estimated using the thermal calibration method. Samples tested were 100 µm sections of the hydrogels fully swollen in milliQ water. Measurements were carried out in immersion. Indentation of at least 500 nm were assessed using constant force. The area of the sample was mapped defining squared areas (2500 μm^2, 25 measurements). Five maps per replicate were measured and at least three replicates per sample were tested, unless otherwise noticed. The analysis (JPKSPM processing software) was performed using the Hertz model for a spherical indenter to fit the curves obtained.

2.2.13 Enzymatic degradation

Hydrogels were formed and swollen in DPBS for three days to ensure hydrogels were fully swollen before starting the enzymatic degradation. All samples were weighed before starting the degradation. Then, samples were covered with protease (collagenase type I (Gibco) or α-chymotrypsin (from bovine pancreas, Sigma), 50 U/mL in DPBS, 37°C). For every timepoint all supernatants were removed by centrifugation at 6500 rpm for 5 min and samples were weighed. To continue the experiment fresh protease solution was added. The degradation rate was calculated as follows:

Equation 2.2 Percentage of mass lost during degradation.

$$M_{loss}\ (\%) = \frac{M_i - M_t}{M_i} * 100$$

Being M_{loss} the percentage of mass lost during degradation, M_i the mass after 72 hours swelling in milliQ water (initial mass) and M_t, the mass at the different timepoints after the addition of the protease solution.

2.2.14 Growth factor labelling

In order to study growth factor binding and release, VEGF (carrier free, R&D Systems) was fluorescently labelled with an amino reactive dye (DyLight® NHS Ester, Thermo Fisher Scientific) following manufacturer's instructions. Briefly, VEGF was prepared for buffer exchange using dialysis membrane tubes (Mini-A-Lyzer, COMW 10 kDa, ThermoFisher) against 0.05 M Sodium borate buffer at pH 8.5 for two hours at RT. Then, the appropriate amount of dye was added (as calculated by manufacturer's guidelines) to the VEGF solution. The dye and the growth factor were let to react for one hour at RT, protected from light. Then, the non-reacted dye was removed by dialysis against DPBS for three hours, adding fresh DPBS every hour. The labelled VEGF was aliquoted and stored at -20°C until use. The labelled VEGF will be named VEGF-488 from hereafter.

2.2.15 Growth factor binding isotherms

Hydrogels were prepared as explained in section 2.2.6 with a final hydrogel volume of 50 µL. Hydrogels were immersed in 10 mM L-cysteine solution for two hours to make sure all the maleimide groups from the hydrogels were reacted. After that, samples were washed three times in DPBS and immersed in VEGF-488 solutions of different concentrations (5, 10 and 15 µg/mL). Once immersed, samples were incubated for 20 hours at 37°C protected from light. Then, the supernatant was taken and read using a plate reader (Ex/Em 493/518 nm). All

conditions were prepared in quadruplicate and all samples were measured twice. The initial solutions were also measured and used as standard curve to be able to correlate fluorescence intensity with concentration of VEGF-488. The fluorescence intensity of hydrogels immersed in DPBS (without VEGF-488) was measured to normalise the data.

The percentage of VEGF-488 bound was calculated as follows:

Equation 2.3 Amount of VEGF-488 retained in hydrogels.

$$m_{VEGFbound} = m_{VEGFi} - m_{VEGFs}$$

Where $m_{VEGFbound}$ is the final mass of VEGF-488 retained in the hydrogels, m_{VEGFi} is the initial total mass of VEGF-488 added to the samples in solution and m_{VEGFs} is the total mass of VEGF-488 measured in the supernatant after incubation.

Once calculated the amount of VEGF-488 retained in the samples, the percentage of VEGF-488 bound to hydrogels was calculated as follows:

Equation 2.4 Percentage of VEGF-488 bound to hydrogels.

$$\boldsymbol{VEGF_{bound}}\ (\%) = \mathbf{100} - \boldsymbol{VEGF_{soluble}}\ (\%)$$

Where $VEGF_{bound}$ is the percentage of VEGF retained in the hydrogel and $VEGF_{soluble}$ is the percentage of VEGF measured from the supernatants after the incubation of the VEGF with the hydrogel.

2.2.16 Growth factor release assays

Hydrogels were prepared as explained in section 2.2.6 incorporating VEGF-488 to the mixture before adding the crosslinker. The final concentration of VEGF-488 loaded was 10 µg/mL and hydrogels were made with a final volume of 50 µL. Then, samples were immersed in DPBS and incubated at 37°C protected from light. At every timepoint all the DPBS solution was taken and used to measure the fluorescence (Ex/Em 493/518 nm). Fresh DPBS was added after each timepoint. A standard curve using VEGF-488 was prepared and empty (not loaded with growth factor) hydrogels were used as controls. All conditions were prepared in triplicate and each sample was measured three times.

The cumulative release was calculated as follows:

Equation 2.5 Percentage of VEGF released from hydrogels.

$$\boldsymbol{VEGF_{released}}(\%) = (\boldsymbol{m_{VEGFs}} * \mathbf{100})/\boldsymbol{m_{VEGFi}}$$

Where $VEGF_{released}$ is the percentage of VEGF-488 released from hydrogels, m_{VEGFs} is the amount of VEGF-488 measured in the supernatant and m_{VEGFi} is the amount of VEGF-488 initially loaded.

2.2.17 Cell viability

Cytocompatibility of hydrogels with C2C12s was tested using Live/Dead® assay (ThermoFisher) following manufacturer's instructions. Briefly, C2C12 cells were encapsulated at $8{\cdot}10^6$ cells/mL according to Garcia *et al.* (Salimath & García, 2016) and incubated within the hydrogels at different timepoints. For every timepoint cells were stained using a Live/Dead® assay kit (ThermoFisher). Briefly, samples were washed twice in DPBS and then immersed in 2 µM Calcein-AM and 4 µM Ethidium homodimer-1 and incubated for 15 min. Samples were washed twice before imaging with epifluorescence microscope.

Cytocompatibility of hydrogels with HUVECs was also tested using a cell density of 10^6 cells/mL at different timepoints. To assess viability a Live/Dead® assay was performed as explained above. Samples were washed twice using DPBS before imaging with a confocal microscope (ZEISS CLSM 880) at 10X magnification.

Cytocompatibility of hydrogels with hMSCs was tested in HA hydrogels using a cell density of 106 cells/mL at different timepoints. To test viability a Live/Dead® assay was performed as explained above. Samples were imaged using a confocal microscope (Leica) at 10X and 20X magnification.

2.2.18 Angiogenesis assays

Angiogenesis is a multistep process that involves endothelial cell activation and sprouting from the parent vessel. This is followed by migration, proliferation, reorganisation and alignment. Finally, tube formation (lumen formation) and anastomosis (vessel fusion) with other vessels. Endothelial cell sprouting is, therefore, one of the first steps that occurs in the angiogenic process.

To test whether or not endothelial cells can be activated and form sprouts in 3D, usually cells are seeded on top of beads and encapsulated within different matrices, this creates a confluent endothelial cell monolayer on the outer part of the bead, simulating the parent vessel. From that monolayer, endothelial cells are able to receive different signals (e.g. a VEGF gradient) and migrate towards it forming many different sprouts (Juliar, Keating, Kong, Botvinick, & Putnam, 2018;

Nakatsu et al., 2003; Rioja, Tiruvannamalai Annamalai, Paris, Putnam, & Stegemann, 2016).

Angiogenic sprouting was assessed using bead microcarriers. Briefly, HUVECs were mixed with dextran-coated Cytodex 3 microcarriers (Sigma) at a final concentration of 400 cells per bead in one millilitre of growth medium. Cells and beads were mixed gently every 20 min for four hours at 37°C. Then, cells and beads were transferred to a 25 cm^2 tissue culture flask with growth medium and left overnight in the incubator (37°C and 5% CO_2). Before encapsulation, cell-coated beads were washed three times with growth medium. Finally, cell-coated beads were loaded into hydrogels at a final concentration of 400 beads/mL. Once the hydrogels were prepared, twenty thousand human dermal fibroblasts were seeded on top. Growth media supplemented with different concentrations of VEGF (0, 50, 500 ng/mL, R&D Systems) was changed every other day. The assay was monitored every day for four days. Samples were fixed using 4% para-formaldehyde for 30 min at RT and stained for actin (AlexaFluor-488 Phalloidin dilution 1:300) and nucleus (NucBlue, LifeTechnologies) for one hour. Samples were washed three times with 0.5% Tween20 in DPBS and mounted onto bottom glass petri dishes using VECTASHIELD mounting medium (VectorLabs). Samples were imaged using confocal microscopy (ZEISS LSM 880) at 10X magnification.

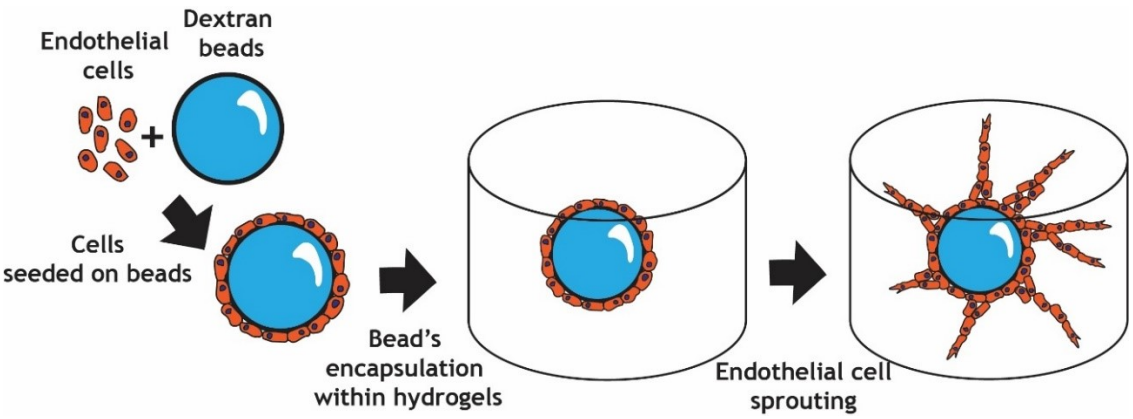

Figure 2.2 Sketch of the 3D angiogenesis assay.

Endothelial cells were seeded on top of dextran-coated beads to form a monolayer on the outer layer of the bead. Endothelial cell-coated beads were encapsulated then within hydrogels and VEGF was supplemented in the cell culture media. After 4 days, cell sprouting was assessed using fluorescence images.

2.2.19 Vascularisation assays

For vascularisation studies, HUVECs were encapsulated ($5 \cdot 10^6$ cells/mL) *in situ* within hydrogels loaded with 200 pmol/mL VEGF-A_{165} (R&D Systems) or unloaded

hydrogels (without growth factor). Samples at days one, two and three were fixed with 4% paraformaldehyde for 30 min at RT and stained for actin and nucleus as explained in section 2.2.18 (on page 84). Samples were imaged using confocal microscopy (ZEISS LSM 880) at 10X magnification.

2.2.20 Chorioallantoic membrane assay

Among various animal model systems designed to study the mechanisms underlying angiogenesis, the chick embryo has been a useful model for the analysis of the angiogenic potential of soluble factors, cells and biomaterials. The chorioallantoic membrane (CAM) allows gas exchange between the chick embryo and the atmosphere that surrounds the egg (and effectively working as a lung for the developing embryo). The CAM consists of three germ layers (ectoderm, mesoderm and endoderm). The ectoderm faces the shell membrane and is underlined by the capillary plexus, which starts to form between days 5-6 of embryonic development (E5-6) by both angiogenesis and vasculogenesis. Consequently, due to the fast developing vascular system present within the CAM, the chick embryo is a commonly used host to perform pro-angiogenic and anti-angiogenic assays (Deryugina & Quigley, 2008; Moreno-Jimenez, Kanczler, Hulsart-Billstrom, Inglis, & Oreffo, 2017).

Fertilised eggs were received at day eight post-fertilisation (E8). Eggs were kept in an incubator (37.5 ºC, 50-60% relative humidity (RH)). To perform the CAM assay, eggs were candled to detect and mark the air sac of the embryo and then, the egg shell was cut on top of the air sac to expose the CAM. Once the membrane was exposed, each sample was laid carefully on top of the membrane Figure 2.3. The samples used were: 5% PEG 0.5VPM, 5%PEG 0.5VPM with 2.5 µg/mL $VEGF_{165}$, 5% FNPEG 0.5VPM, 5% FNPEG 0.5VPM with 2.5 µg/mL $VEGF_{165}$ and an empty condition, where the CAMs were exposed but no material was placed on top. After that, the exposed area of the egg with the sample was sealed and labelled. All eggs were incubated (37.5 ºC, 50-60% RH) for four days (E12), when the membranes were imaged using a stereomicroscope (Leica MZ APO) using X8 and X16 magnifications. Six replicates per condition were used; two pictures per replicate at each magnification used were taken (trying to cover as much area of the CAM as possible and imaging under the hydrogel and far away from the hydrogel).

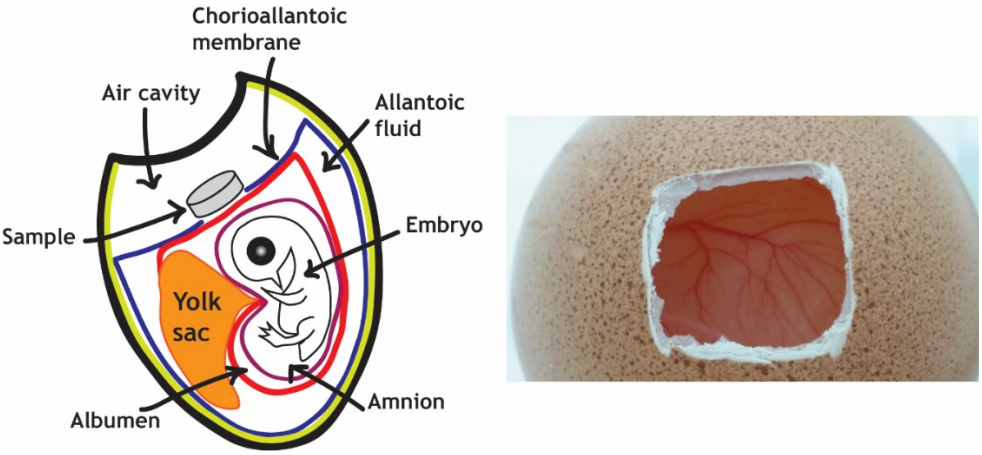

Figure 2.3 Sketch of the chick chorioallantoic membrane assay.

Left image shows the structure of the chick embryo. At day 7-8 post-fertilisation, the egg shell is cut on top of the air cavity to expose the CAM, where the hydrogel sample is deposited carefully. Right picture shows the CAM of the chick embryo, which is a well vascularised membrane.

2.2.21 Norbornene-modified hyaluronic acid (NorHA) synthesis

Prior to NorHA synthesis, HA was modified using tetrabutylammonium salt (HA-TBA) in order to solubilise HA in DMSO for the reaction. Briefly, sodium hyaluronate (Na-HA, Lifecore Biomedical, ~75 kDa) was dissolved in deionised (DI) water at a concentration around 20-50 mg/mL. Once dissolved, Dowex resin (50Wx8, Sigma) was added to the solution at a ratio 3:1 (w/w) resin to Na-HA for two hours while stirring at RT. Then, the mixture HA/resin was filtered using a kitasatos flask (whatman paper #2, vacuum). After that, a solution of TBA in DI water was prepared (1:1 V/V, for 1 g HA typically 12 mL TBA diluted solution). Neutralisation of the HA solution was performed using TBA solution, until pH 7.02-7.05. Once neutral, the solution was partitioned into 50 mL tubes, frozen (-80°C, overnight) and lyophilised (four days, < 130E-03 mBar, -80°C). The product of lyophilisation was stored at -20°C until use. ^{1}H-NMR spectrum of HA-TBA was performed dissolving 5 mg of HA-TBA in 700 µL of D_2O; the spectrum obtained was used to confirm the degree of modification.

Norbornene-modified hyaluronic acid (Nor-HA) was synthesised mixing HA-TBA with 5-norbornene-2-methylamine (Nor-amine) and anhydrous DMSO (~5 mL per 0.1 g HA-TBA, via cannulation) in a round bottom flask under inert atmosphere. Once HA was fully dissolved a benzotriazole-1-yl-oxy-tris-(dimethylamino)-phosphonium hexafluorophosphate (BOP, in DMSO) solution was added via cannulation to the HA/Nor-amine solution and it was reacted for two hours at RT.

After reaction, the solution was quenched with cold DI water and transferred to a pre-soaked dialysis tube (MWCO 6-8 kDa). Dialysis was performed for five days in DI water (adding ~5 g NaCl in the dialysis water, changing water twice daily). Then, the dialysed product was filtered using a kitasatos flask (whatman paper #2, vacuum). The filtrated product was dialysed again in DI water for three to five days. The dialysed product was partitioned into 50 mL tubes, frozen overnight and lyophilised in four days.

2.2.22 HA hydrogel photopolymerisation

Solutions containing NorHA (2 wt.%), DTT, Irgacure-2959 (0.05 wt.%) and DPBS were prepared using different formulations (Table 2.9). Once dissolved, 70 µL of the solution were placed on a polydimethylsiloxane (PDMS) mould and the samples were covered with a glass coverslip treated with Rain-X. Then, samples were photopolymerised (Excellitas Omnicure S1500, filter 320-390nm, 10 min, 10 mW/cm^2).

For fibronectin-HA hydrogels, fibronectin was denatured using 20 mM TCEP (15 min, RT, shaking). Then, the denatured fibronectin was mixed with the HA solution for 10 min and hydrogels were formed by photopolymerisation (10 min, 10 mW/cm^2).

Table 2.9 HA hydrogels formulations used.

* Fibronectin was used at different concentrations. Unless otherwise noted, fibronectin was used at 50 µg/mL. **SH groups coming from the crosslinker, either DTT or VPM were used.

HA hydrogels	FNHA 0VPM	FNHA VPM
Nor-HA (mg/mL)	20	20
FN* (µg/mL)	50	50
SH**:Norbornene ratio	0.6:1	0.6:1

For cell encapsulation experiments, cells were trypsinised and resuspended in HA polymer solution at a final density of $5{\cdot}10^5$ cells/mL. The solution with cells was added to a 6 mm cylindrical mould and irradiated for 10 min at 10 mW/cm^2. The newly formed gels were immediately transferred to a 24-well plate with growth medium.

2.2.23 Dynamic mechanical analysis (DMA) tests

Mechanical tests were performed using a TA instruments DMA Q800 in compression mode. Briefly, a force ramp of 0.5 N/min was applied up to 15 N of force were

reached . The compressive modulus (E) was obtained from stress-strain curves and calculated as the slope between 10-20% strain using TA instruments software. Conditions were prepared in triplicate. Each sample was measured twice.

2.2.24 Cell adhesion assay on NorHA hydrogels

For cell adhesion experiments, hMSCs were grown in 10 mm petri dishes using growth medium (α-MEM and 10% FBS). All hydrogels were polymerised and maintained in DPBS until seeding. Cells were seeded on top of the hydrogels at a density of 5,000 cells/cm^2 for three or twenty-four hours in medium without serum. Glass controls were seeded at the same cell density using growth medium.

2.2.25 Image analysis

Cell morphology analysis

Cell shape descriptors were measured using ImageJ 1.51v (National Institutes of Health, US). Briefly, actin cytoskeleton images were binarized using a threshold function. Then, the wand tracing tool was used to select the outline of the cell and the measure function was used to calculate parameters such as cell area, aspect ratio and roundness. The aspect ratio is defined as the ratio between the major and minor axis of the shape selected and the roundness was calculated as follows:

Equation 2.6 Roundness calculation.

$$Roundness = (4 * area)/(\pi * (major\ axis)^2)$$

FA analysis

Vinculin images were used for the FA analysis. They were uploaded to the Focal Adhesion Analysis Server (Berginski & Gomez, 2013) along with the corresponding actin cytoskeleton image to use as a cell mask. The results obtained include a binarized image of the FAs and measurements for several parameters, from which the FA number per cell, the FA area and size were used.

Viability from Live/Dead® staining

The percentage of viability was calculated from the images taken using ImageJ. For single images (taken with epifluorescence microscope), each channel was filtered using a gaussian blur filter with a sigma ball radius of two and then, the find maxima process was utilised to count cells.

When analysing stacks of images, for each channel the maximum intensity Z-projection images were obtained using ImageJ. Then, a Gaussian blur filter was

passed (sigma ball radius of two) and the number of cells in each channel was counted using the find maxima process.

In both cases the total number of cells was calculated using Equation 2.7.

Equation 2.7 Calculation of total number of cells for Live/Dead® staining.

$$N_{total} = live_{cells} + dead_{cells}$$

Being $live_{cells}$ the total number of cells quantified using the live channel stack and $dead_{cells}$ the total number of cells quantified using the dead channel.

Then, the percentage of cell viability was calculated as per Equation 2.8.

Equation 2.8 Calculation of viability (%) for Live/Dead® staining.

$$Viability\ (\%) = (live_{cells}/N_{total}) * 100$$

Cell morphology analysis (vasculogenesis assay)

Stacks obtained from confocal imaging were analysed using ImageJ 1.51v. Briefly, actin cytoskeleton stacks were opened and segmented using the *trainable weka segmentation 3D* plugin. Once the stacks were converted to 8-bit segmented stacks, the segmented objects were quantified using the *3D objects counter* tool with the following parameters: volume (V, μm^3), number of voxels/object, surface (S, μm2), number of voxels/surface and centroids. Prior to the quantification a size exclusion filter was applied, so objects smaller than 500 voxels were not counted (i.e. to avoid quantification of segmented background noise). The sphericity (Ψ) of the objects was calculated as follows:

Equation 2.9 Sphericity calculation.

$$\Psi = [\pi^{1/3} \cdot (6 \cdot V)^{2/3}]/S$$

Capillary formation analysis (CAM assay)

Images obtained from the stereomicroscope at X16 magnification were used for the quantification. Images (RGB colour format) were split into the three RGB (red, green and blue) channels. The green channel was chosen for the segmentation as it was the one with best contrast to detect the capillaries. Segmentation was assessed manually, tracing a black line on top of each capillary. The result of the segmentation was used to quantify the number of branches, the number of junctions and the number of triple points per image via the *skeletonize* tool on ImageJ.

YAP localisation

For YAP localisation experiments, hMSCs were grown in 10 mm petri dishes using growth medium. All hydrogels were polymerised and maintained in DPBS until

seeding. Cells were seeded on top of the hydrogels at a density of 5,000 cells/cm^2 for three hours in medium without serum.

The quantification of YAP was assessed from the fluorescence images using ImageJ. The nuclear/cytoplasm ratio was defined using Equation 2.10:

Equation 2.10 YAP's integrated density fluorescence nucleus/cytoplasm ratio.

$$YAP_{nuc/cyt}\ ratio = [(YAP_{nuc}/A_{nuc})/(YAP_{cyt}/A_{cyt})]$$

Being YAP_{nuc} the integrated density of YAP in the nucleus, A_{nuc} the area of the nucleus; YAP_{cyt} the integrated density of YAP in the cytoplasm (defined as per Equation 2.11) and A_{cyt} the area of the cell cytoplasm (defined as per Equation 2.12).

Equation 2.11 YAP's integrated density fluorescence in the cytoplasm.

$$YAP_{cyt} = YAP_{cell} - YAP_{nuc}$$

Being YAP_{cell} the integrated density of YAP in the entire cell.

Equation 2.12 Definition of cytoplasmic area.

$$A_{cyt} = A_{cell} - A_{nuc}$$

Being A_{cell} the area of the entire cell.

2.2.26 Statistical analysis

The statistical analysis was performed using GraphPad Prism 6.01 software. All experiments were carried out in triplicate unless otherwise noticed. All graphs represent mean ± standard deviation (SD) unless otherwise noted. The goodness of fit of all data-sets was assessed via D'Agostino-Pearson Normality test. When comparing three or more groups: normal distributed populations (homoscedastic data) were analysed via analysis of variance test (ANOVA test) performing a Tukey's *post hoc* test to correct for multiple comparisons; when populations were heteroscedastic (i.e. not distributed normally), a Kruskal-Wallis test was used with a Dunn's *post hoc* test to correct for multiple comparisons. When comparing only two groups, parametric (normal distributed population, t-test) or non-parametric (Mann-Whitney test) tests were performed. Differences among groups are stated as follows: for p-values <0.05 (*), when p-values <0.01 (**), for p-values < 0.005 (***), for p-values < 0.001 (****), when differences between groups are not statistically significant (n.s).

3 Chapter Three: Engineering Fibronectin-based PEG Hydrogels

3.1 Introduction

Scaffolds for Tissue Engineering are usually fabricated from either synthetic polymers or biological components. On the one hand, synthetic materials offer controllable physicochemical properties but lack biological functionalities for cell instruction. On the other hand, biological materials present many interesting biological capabilities; however, they offer physicochemical features that vary from batch to batch, making it difficult to predict outcomes (more information in section 1.2).

In this sense, biosynthetic hydrogels present the advantages of both natural and synthetic materials. Biosynthetic hydrogels are generally fabricated by using the backbone of a synthetic polymer, which are then decorated with biologically active ligands (Almany & Seliktar, 2005; Cruz-Acuña et al., 2017; Shekaran et al., 2014a). Here, we focus on the stable incorporation of the full-length fibronectin protein into a PEG hydrogel network. Fibronectin is an abundant glycoprotein from the ECM and its generally studied as a paradigm protein for cell adhesion due to its RGD and PHSRN motifs (Hersel et al., 2003; Petrie et al., 2006; Salinas & Anseth, 2008). Moreover, fibronectin contains other binding sites such as the heparin-binding site that has been shown to promiscuously bind growth factors (M. M. Martino & Hubbell, 2010). The use of fibronectin to present growth factors in synergy with integrins has been used in literature (Llopis-hernández et al., 2016; Mikaël M. Martino et al., 2011; Moulisová et al., 2017).

This chapter focuses on the incorporation of fibronectin into a PEG hydrogel system using a thiol based Michael-type addition reaction that takes place at physiological pH and temperature (Edward A. Phelps et al., 2012). This hydrogel system aims to provide a highly tuneable platform for cell encapsulation with the distinct advantage that, due to the presence of fibronectin, can bind growth factors in synergy with integrins.

To be able to covalently link the protein, we first functionalised it in a PEGylation step to subsequently homogenise it within the PEG solution to achieve gelation. The PEGylated fibronectin was tested to study biological activity using ELISAs, AFM

and studying cell adhesion. Then, fibronectin-based PEG hydrogels were characterised to test their mechanical performance, degradability features and their ability to allow *in situ* encapsulation of cells.

3.2 Materials and methods

The materials and methods used for the work discussed in this chapter are described in Chapter 2; more specifically fibronectin PEGylation is described in section 2.2.1, cell culture in section 2.2.2, cell adhesion assays in section 2.2.3, ELISA assays in section 2.2.4, AFM imaging in section 2.2.5, hydrogel formation in section 2.2.6, water sorption tests in section 2.2.7, BCA assay in section 2.2.8, SDS-PAGE in section 2.2.9, preparation of cryo-sections in section 2.2.10, IF assays in section 2.2.11, nanoindentation measurements in section 2.2.12, degradation experiments in section 2.2.13, viability assays in section 2.2.17, image analysis in section 2.2.25 and statistical analysis in section 2.2.26.

3.3 Results

3.3.1 Fibronectin PEGylation and hydrogel formation

Fibronectin-PEG Hydrogel fabrication

Fibronectin-based PEG hydrogels are made from PEGylated fibronectin monomers that are subsequently crosslinked to a PEG network utilising Michael-type addition reaction at physiological pH and temperature. Figure 3.1shows the series of steps followed to covalently link PEG molecules to the fibronectin monomer and hydrogel formation. Fibronectin was initially denatured (at ~pH 7.4) using TCEP as denaturant and urea as chaotropic agent. This chemical denaturation allows the exposure of thiol groups present in the fibronectin structure. After denaturation, the PEGylation step was carried out forming thioether bonds between the maleimide groups present on PEG molecules and the previously exposed thiol groups on fibronectin. As a final step, all the non-reacted thiol groups were blocked via alkylation using iodoacetamide Figure 2.1.

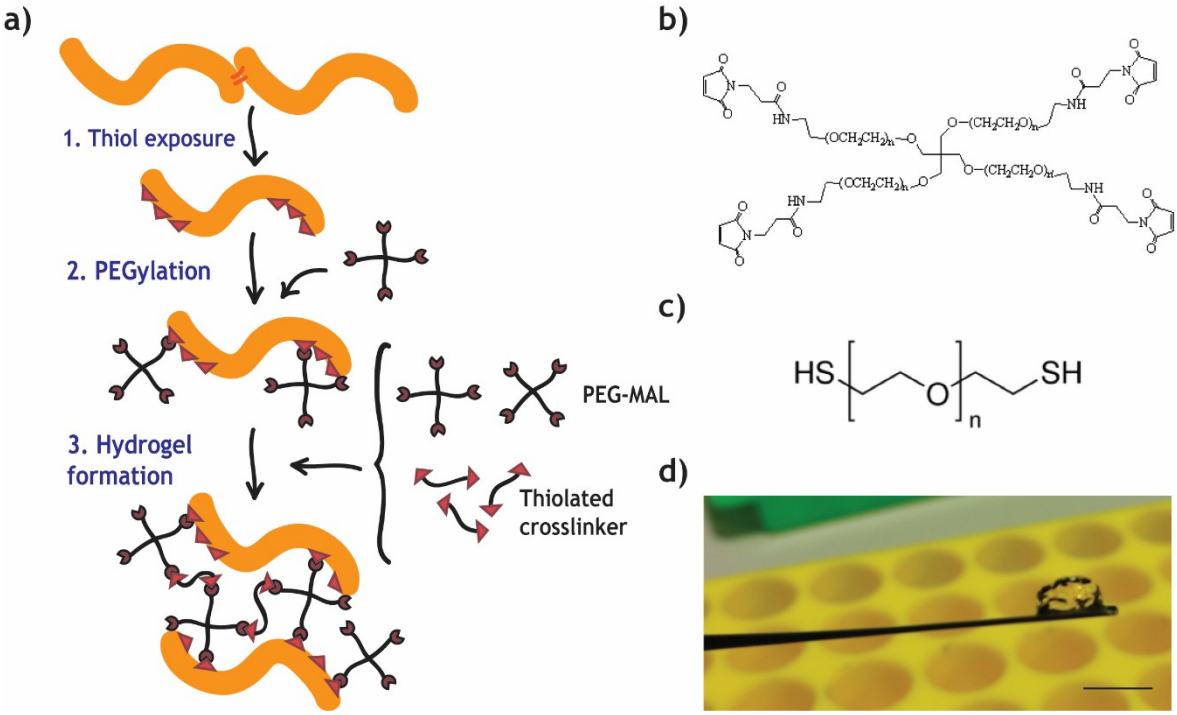

Figure 3.1 Fibronectin-PEG hydrogel formation process.

(a) The fabrication of fibronectin-PEG hydrogels needs of the exposure of thiol groups on fibronectin prior to the PEGylation of the molecule. Then, PEGylated fibronectin is incorporated to a PEG network formed by 4-arm-PEG-maleimide and a thiolated crosslinker (PEG-dithiol or protease-degradable peptide flanked by two cysteine residues). (b) Structure of the 4-arm-PEG-maleimide, (c) structure of the PEG-dithiol and (d) macroscopic picture of a fibronectin-PEG hydrogel. Scale bar: 5 mm.

Exposure of binding sites on PEGylated fibronectin

The biological activity of the PEGylated fibronectin was tested via ELISA to study the availability of certain domains of fibronectin (Figure 3.2). In addition, C2C12 cells were seeded on top of PEGylated fibronectin coated glass to test cell morphology and adhesion (Figure 3.3 and Figure 3.4). Finally, the capability of PEGylated fibronectin to form networks was also tested using poly(ethyl) acrylate (PEA). PEA has shown to spontaneously organise fibronectin molecules into fibrillar networks, whereas when fibronectin is adsorbed on other surfaces it retains its globular conformation (Ballester-Beltrán et al., 2012; Salmerón-Sánchez et al., 2011). The fibrils observed on PEA are similar as those formed *in vivo* where fibronectin fibrillogenesis occurs. This phenomenon called material-driven fibronectin fibrillogenesis has been used as a strategy to make the growth factor binding site of fibronectin more available compared to fibronectin's globular conformation. The conformation of fibronectin on this surface has demonstrated to enhance BMP-2 and VEGF activities *in vivo* (Llopis-hernández et al., 2016; Moulisová et al., 2017). (Figure 3.5).

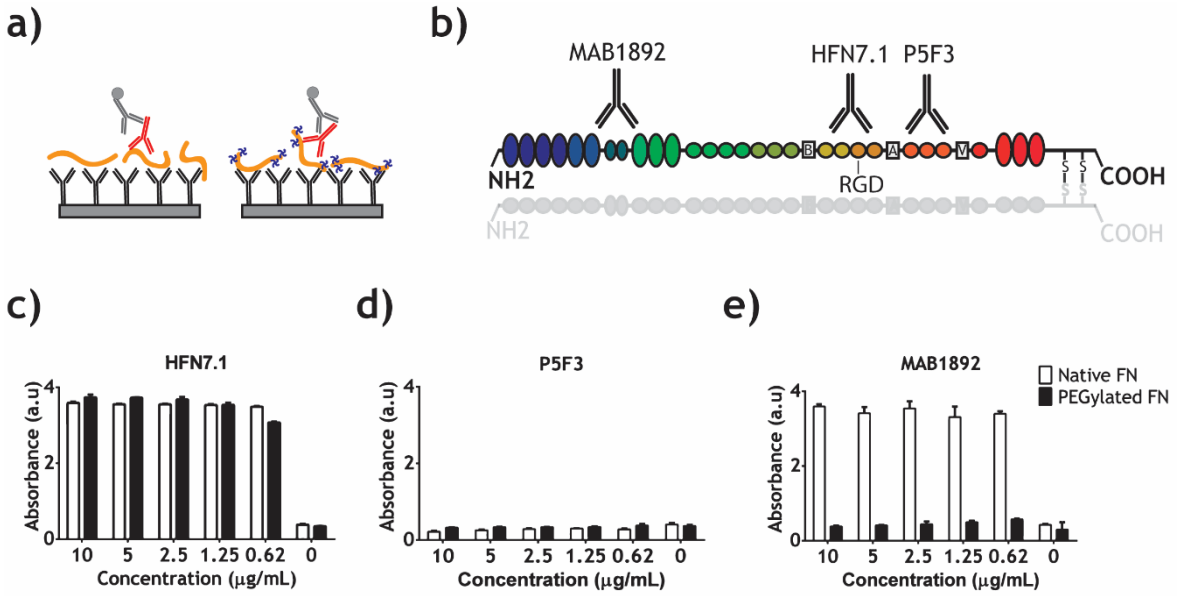

Figure 3.2 Native and PEGylated fibronectin present similar domain exposure in solution.

(a) Sketch of the ELISA procedure, were native or PEGylated fibronectin in solution were captured using a polyclonal antibody anti-FN (in black) and different monoclonal antibodies anti-FN (in red) were used to study the availability of different domains. The detection was assessed via a secondary antibody with a horse radish peroxidase enzyme bound (in grey); (b) scheme of the affinity for the three different antibodies anti-FN used. (c) Absorbance (in arbitrary units, a.u.) of the ELISA with HFN7.1 antibody, (d) absorbance of the ELISA using P5F3 antibody and (e) absorbance values of the ELISA with MAB1892 antibody. Graphs (c-e) show mean ± SD (n=3).

As can be seen in Figure 3.2, native and PEGylated fibronectin were compared using three different monoclonal antibodies that recognise three different areas on fibronectin. HFN7.1 antibody recognises the cell-adhesion domain, P5F3 antibody recognises the heparin-II binding domain and MAB1892 antibody recognises the gelatin binding domain. When studying the availability of the cell adhesion domain, both native and PEGylated fibronectin present high accessibility, with absorbance values close to saturation at all concentrations tested. In addition, although the absorbance measurements were low and close to blank at all concentrations tested, both native and PEGylated fibronectin showed similar values for the availability of the heparin-II binding domain. When testing the accessibility of the gelatin binding domain, differences were observed between native and PEGylated fibronectin. Native fibronectin showed high absorbance values, close to saturation at all concentrations tested, whereas PEGylated fibronectin presented low absorbance values close to blank values.

Figure 3.3 shows the comparison of C2C12 cell morphology when seeded on top of either native fibronectin or PEGylated fibronectin coated glass. Cells seeded on both surfaces presented similar actin and vinculin staining, with developed actin fibres and formation of focal adhesions. Cell area, cell size (via aspect ratio) and roundness were quantified from the images taken, not revealing any statistical differences between native and PEGylated fibronectin. Furthermore, by using the vinculin staining, FAs were segmented and several parameters were studied such as the number of FAs and the area and size distribution of FAs (Figure 3.4).

From the segmented vinculin images it was possible to assess that FAs formed in the native or PEGylated fibronectin conditions were distributed similarly, with clear FA complexes forming at the edges of the cell. When comparing the number of FAs formed per cell tested, in both cases the number of FAs was similar and ranging between 300 and 500 per cell. The distribution of the FA areas and sizes were also similar when comparing native and PEGylated fibronectin conditions, showing a relatively high frequency of mature FAs (with areas and sizes larger than 2.0 μm^2 and 2.0 μm, respectively).

Fibronectin fibrillogenesis capability was assessed by using a polymer-based method previously published (Salmerón-Sánchez et al., 2011). Briefly, PEA polymer coatings have shown to trigger spontaneous fibronectin fibrillogenesis, which has been shown to expose the growth factor binding site of this protein. (Llopis-hernández et al., 2016; Moulisová et al., 2017). Figure 3.5 shows phase images obtained via tapping mode using AFM. These pictures show that both native and PEGylated fibronectin are able to form fibrillar networks when adsorbed onto PEA polymer coatings.

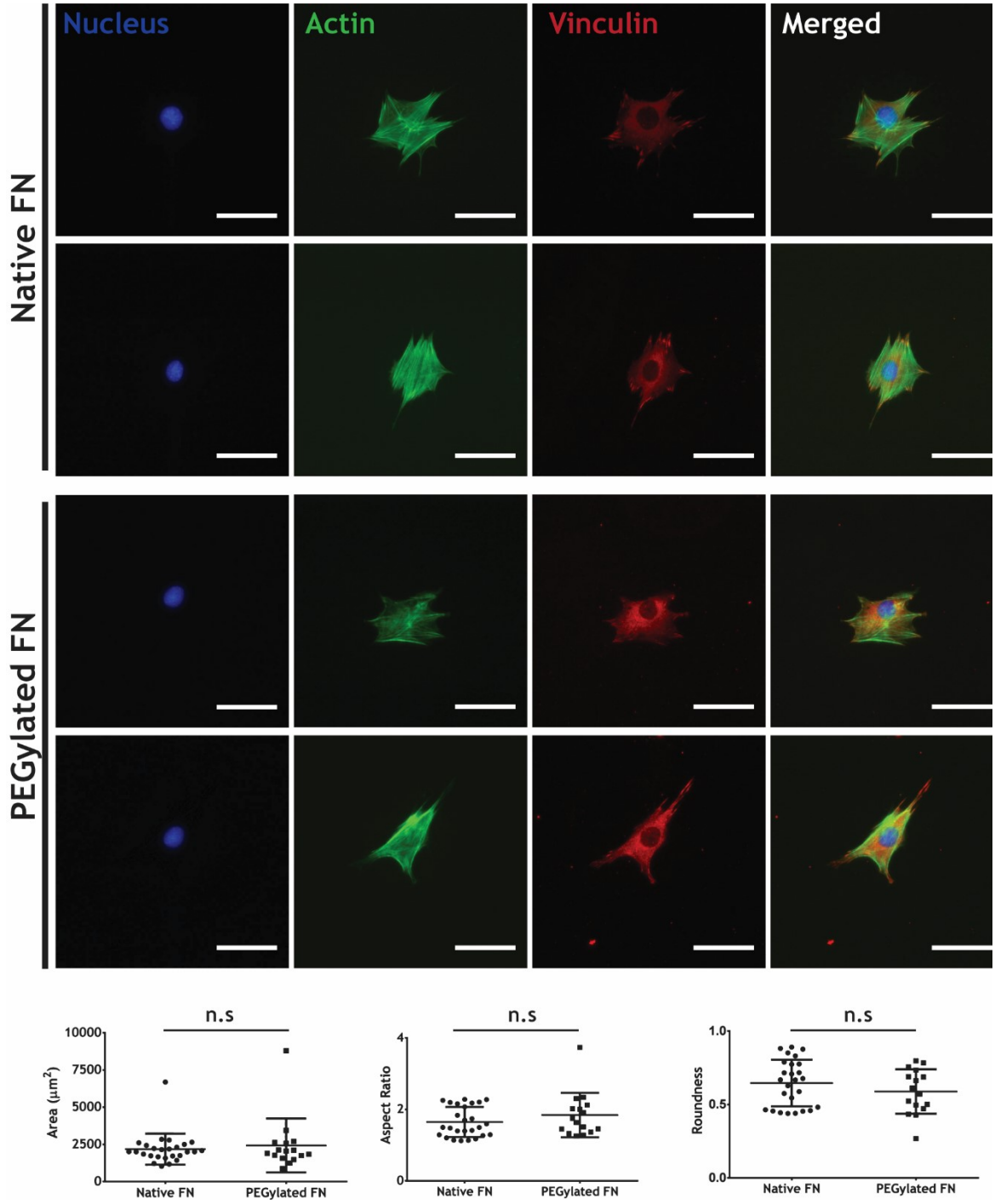

Figure 3.3 Similar cell morphologies shown using either native or PEGylated fibronectin.

C2C12 cells seeded on top of glass coverslips coated with either native or PEGylated fibronectin at 20 µg/mL for one hour. Then, C2C12 cells were seeded on top for three hours to study cell morphology. Two representative fluorescent images per condition tested are shown; from left to right: DAPI (blue), actin cytoskeleton (green), vinculin (red) and merged (all three channels). From the pictures cell area, aspect ratio and roundness were quantified. Scale bar: 50 µm. Graphs show mean ± SD of n ≥ 10. Statistics show results from a parametric t-test, where n.s shows no differences between groups.

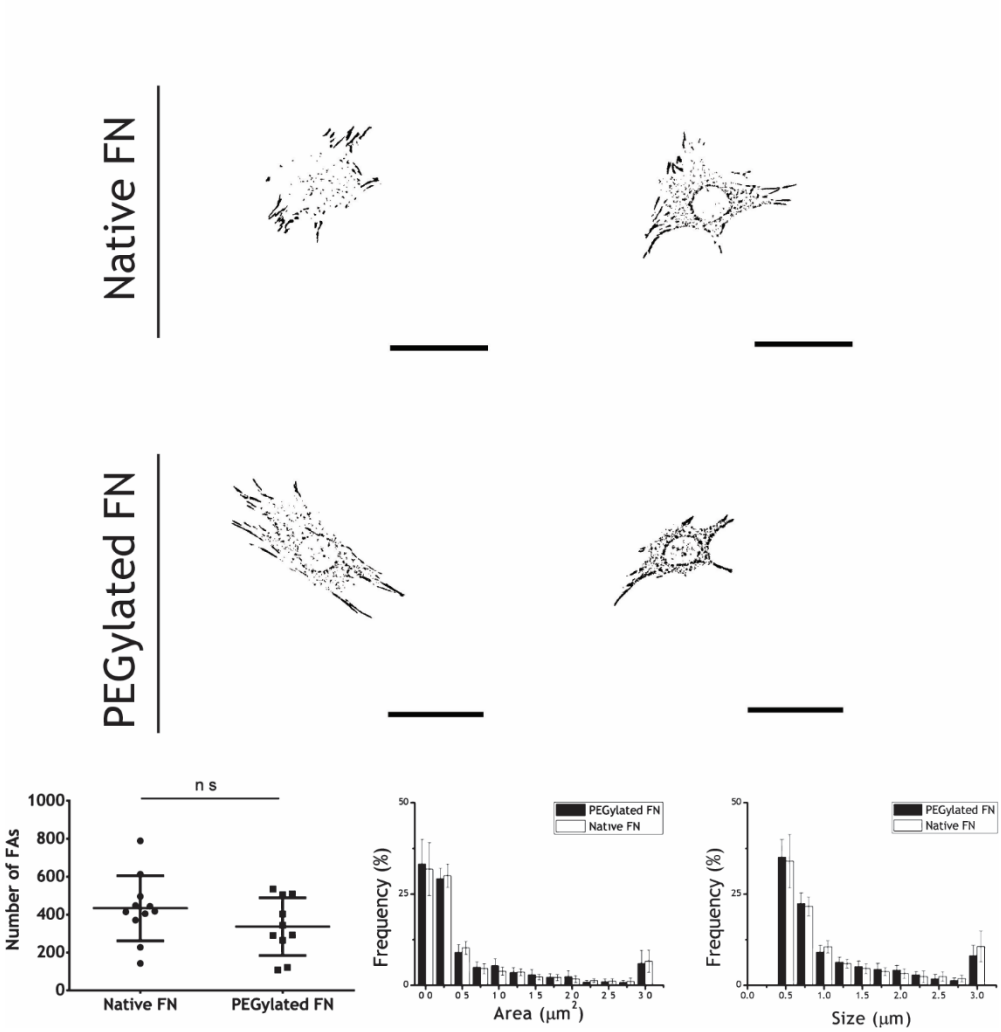

Figure 3.4 No differences shown in focal adhesion (FA) formation comparing native and PEGylated fibronectin.

Images show two representative cells of either native FN or PEGylated FN with binarized FAs obtained from analysis of the vinculin staining. Scale bar: 50 μm. Graphs (mean ± SD) show the average number of FAs, the frequency distribution of the focal adhesion area and size per cell analysed (n ≥ 10) (left to right, respectively). Differences were analysed via parametric t-test.

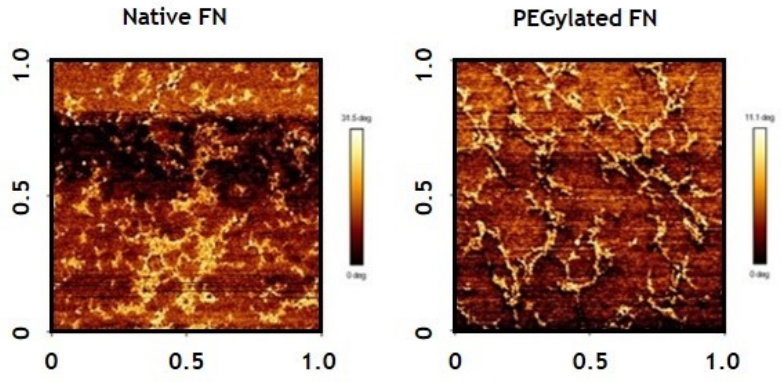

Figure 3.5 PEGylated fibronectin forms networks like native fibronectin on PEA surfaces.

Native and PEGylated fibronectin were adsorbed on top of a PEA spin coated surface and the morphology of the coating was assessed. From left to right images show the phase signal in tapping mode AFM of native fibronectin and PEGylated fibronectin. Scale: 1 µm x 1 µm.

3.3.2 Fibronectin-based PEG hydrogels characterisation

Fibronectin is covalently bound to the hydrogel network

Once the biological activity of PEGylated fibronectin was characterised, fibronectin PEG hydrogels were synthesised using 4-arm-PEG-maleimide, PEGylated fibronectin and PEG-diSH to form the hydrogel network, following protocol described in section 2.2.6.

Figure 3.6 shows an immunostaining for fibronectin (in red) on cryo-sectioned hydrogels of different PEG percentages. These images showed the presence of fibronectin once the hydrogels are formed and also the distribution of fibronectin throughout the matrix is relatively homogeneous. Fibronectin was found to cover all the cryo-sections stained. Only PEG hydrogels (without fibronectin) did not show any staining.

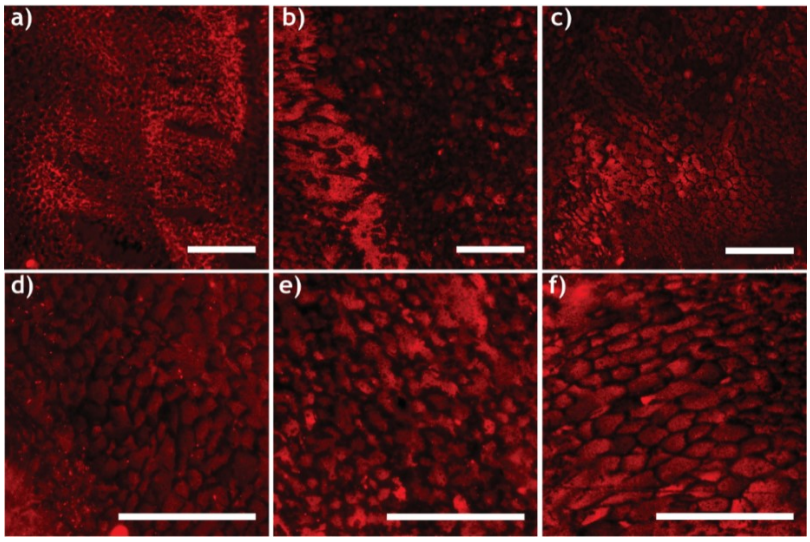

Figure 3.6 Detection of fibronectin on fibronectin-PEG hydrogel cryo-sections.

Fluorescent images showing the presence of fibronectin within hydrogel cryo-sections. (a, d) 3% FNPEG, (b, e) 5% FNPEG and (c, f) 10% FNPEG hydrogels. Scale bar: 100 µm.

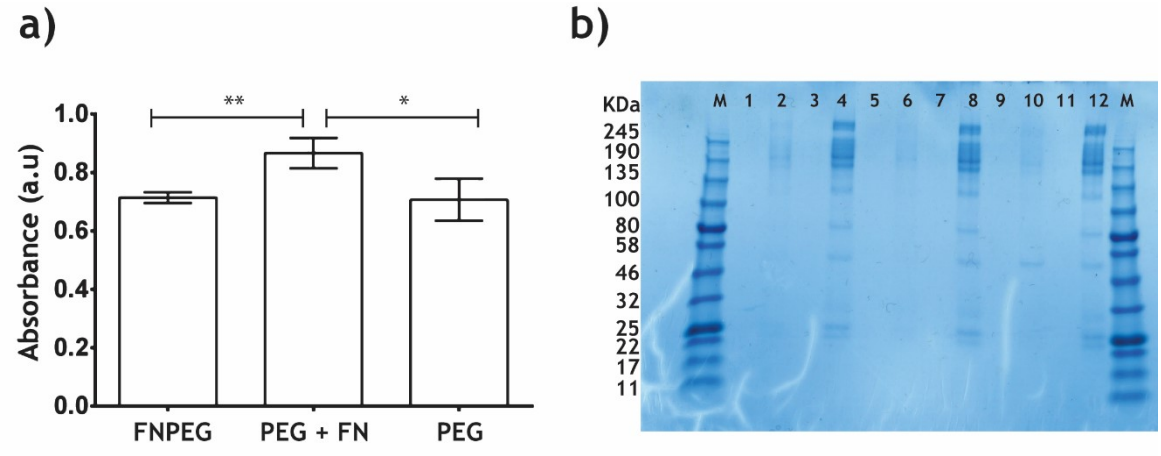

Figure 3.7 Release of fibronectin shown only when fibronectin is not covalently bound to the PEG network.

(a) Protein content in supernatants of immersed hydrogels at 24 h was measured via BCA assay. Conditions tested are: FNPEG (using PEGylated fibronectin), PEG + FN (PEG only hydrogel with native fibronectin physically trapped) and PEG (PEG only hydrogel). Graph shows mean ± SD (n=3), groups were compared via Kruskal-Wallis test and Dunn's test; (b) supernatants were used to run a SDS-PAGE and were stained with Coomassie Blue. The Mw of the protein ladder is shown on the left. Samples are named: protein ladder (lanes M), FNPEG (lanes 1,5 and 9), PEG + FN (lanes 2,6 and 10), PEG (3,7 and 11) and positive control (native FN, lanes 4,8 and 12).

Figure 3.7 shows the release of fibronectin after 24 hours in immersion. In order to prove that fibronectin was covalently bound to the hydrogel network, three different hydrogel conditions were fabricated: an only PEG hydrogel (PEG, without

fibronectin), a FNPEG hydrogel (using PEGylated fibronectin and thus, covalently bound to the PEG network) and a PEG hydrogel with fibronectin trapped into the mesh (PEG + FN, using native fibronectin, not covalently bound to PEG). These hydrogels were immersed in DPBS for 24 hours and the supernatants were tested for protein release (note that the only protein source in this experiment is fibronectin). BCA assay tested the amount of protein released and Figure 3.7a shows the absorbance values obtained during BCA. The PEG only condition presented absorbance values around 0.6, similar to the FNPEG condition. For the condition with trapped fibronectin (PEG+FN), the absorbance values obtained were relatively higher and around 0.8. These results were statistically significant, showing that the FNPEG hydrogels were not releasing fibronectin. These results were furthermore confirmed via SDS-PAGE (Figure 3.7b), where the supernatants were run and stained using a Coomassie blue staining. Only positive controls (where pure fibronectin was loaded) and the PEG+FN condition (with physically trapped fibronectin) showed presence of protein.

Fibronectin-based PEG hydrogels physicochemical properties

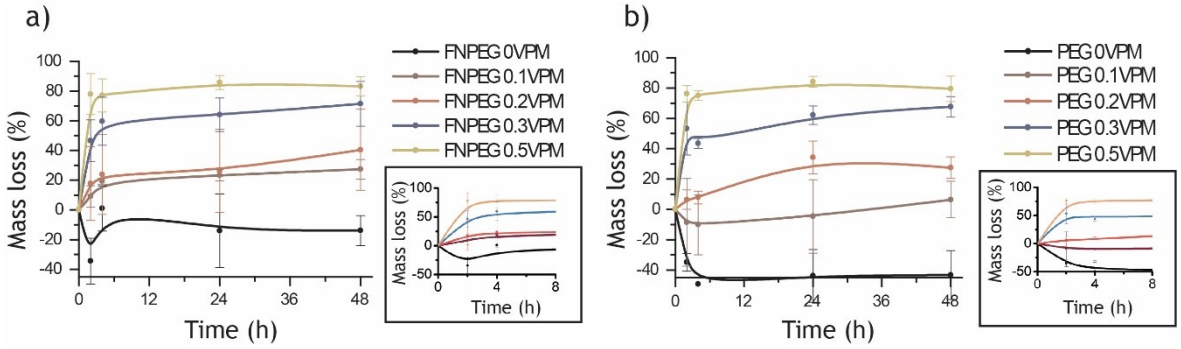

Figure 3.8 Degradation is governed by VPM peptide using collagenase type I that cannot cleave fibronectin.

Degradation was carried with gels swollen at equilibrium in DPBS. Then 50 U/mL of collagenase I were added to each hydrogel (mean ± SD, n = 3). Comparison between (a) 5% FNPEG hydrogels with different ratios of degradable crosslinker (VPM) and (b) 5% PEG hydrogels with the same crosslinker ratios were studied. Insets show in more detail the first timepoints of the degradation curve for all conditions tested.

Degradability profiles were also studied (Figure 3.8 and Figure 3.9). Different ratios of degradable and non-degradable crosslinkers (i.e. VPM peptide and PEG-diSH) were used. Collagenase type I was used as this enzyme can recognise the cleavage site on VPM peptide but cannot cleave fibronectin and, α-chymotrypsin was used as it can degrade both VPM peptide and fibronectin. Figure 3.8 shows the degradation profile obtained for hydrogels fabricated with different amounts

of VPM peptide as a crosslinker. In both PEG only and FNPEG hydrogels, the degradability of the hydrogels increased monotonically with the increase in VPM peptide ratio. Hydrogels gelled with 100% non-degradable crosslinker did not lose mass at the time points tested - note that a negative mass loss in this case means that the hydrogels increased mass (i.e. absorbed water). However, hydrogels fabricated using 10% of VPM peptide (0.1 VPM conditions, Table 2.8) lost around 10-20% of the initial mass. When 20% VPM peptide (0.2 VPM conditions, Table 2.8) was incorporated into the system, around 30% mass was lost throughout the assay. At higher ratios, using 30 and 50% degradable crosslinker, degradability reached 60 and 80%, respectively. Similar degradation profiles were obtained when using PEG and FNPEG hydrogels, meaning that the degradation profile in this case, using collagenase I, is governed by the amount of VPM crosslinker added.

Figure 3.9 shows the comparison between using collagenase type I and α-chymotrypsin. These two proteases were selected because of their differential ability to cleave fibronectin (i.e. collagenase I does not cleave fibronectin and α-chymotrypsin cleaves fibronectin). Similar degradation rates were obtained in all conditions tested except for FNPEG 0VPM, where collagenase type I did not show degradation and α-chymotrypsin showed some degradation, with a percentage of mass loss around 40%. This experiment shows that the presence of full-length fibronectin also provides degradability to the hydrogel system.

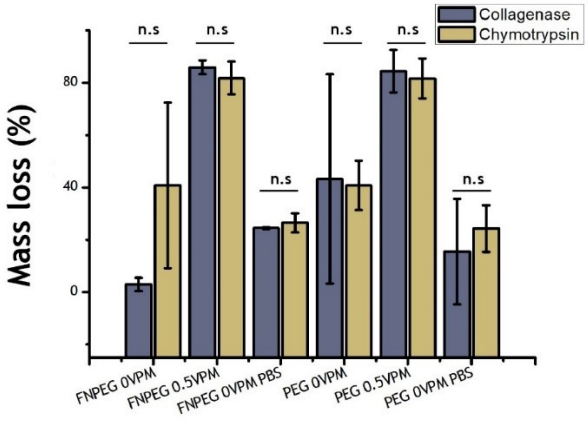

Figure 3.9 Fibronectin can be degraded in the system as shown by α-chymotrypsin degradation.

Degradation was assessed using either collagenase I (cleaves only VPM peptide) or α-chymotrypsin (cleaves both VPM peptide and fibronectin) for seven days (50 U/mL). Comparison between 5% FNPEG or 5% PEG with or without VPM crosslinker was studied. Samples 'FNPEG 0VPM PBS' and 'PEG 0VPM PBS' were incubated without protease solution as controls. Graphs show mean ± SD (n = 3), no

statistically significant differences between enzymes were found in a parametric t-test.

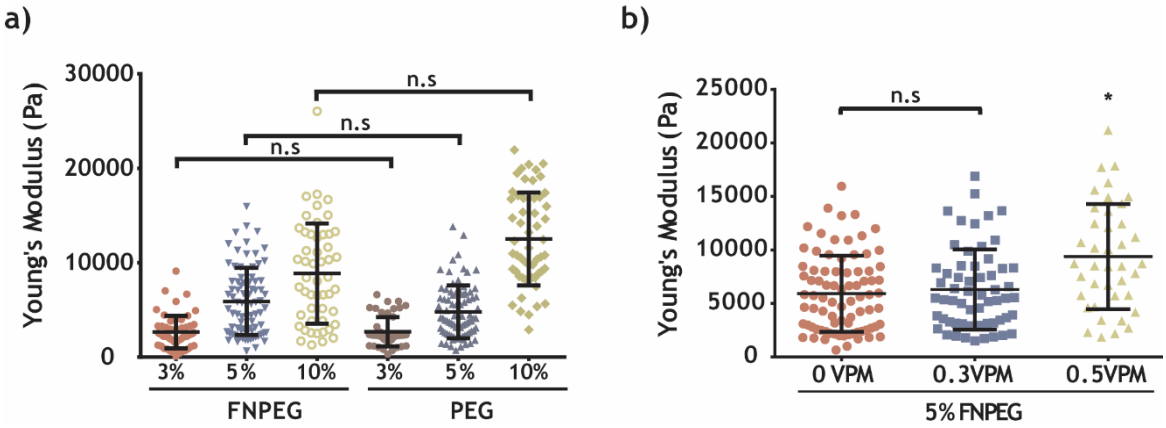

Figure 3.10 Mechanical properties can be controlled independently of the presence of fibronectin.

Sections of 100 µm were swollen in milliQ water and used for indentation with the AFM. Cantilevers (k ~ 0.03 N/m) with a bead of 20 µm diameter were used to indent at least 500 nm. The Young's modulus was obtained after fitting the force-indentation curves according to the Hertz model using the JPK processing software. Mean ± SD (n > 100 curves). Significant differences were analysed by Kruskal-Wallis test followed by a Dunn's *post hoc* test.

The mechanical properties of the hydrogels were also characterised by using AFM as a nano-indenter (Figure 3.10). Hydrogels with different amounts of PEG were fabricated and cryo-sections of the hydrogels were obtained for mechanical testing (Figure 3.10a). Increasing the amount of PEG within the hydrogel system increases the Young's modulus, independently of the presence of fibronectin. Hydrogels obtained using 3% PEG show an elastic modulus of around 2 kPa, hydrogels fabricated with 5% PEG present a Young's modulus of approximately 6 kPa and hydrogels prepared using 10% PEG polymer result in elastic modulus of 10-12 kPa.

How the incorporation of degradable crosslinker affects the mechanical properties of the hydrogel system was also studied (Figure 3.10b). In this case, hydrogels of 5% PEG polymer were prepared and the amount of VPM peptide was varied from 0 to 50%. Incorporation of VPM peptide up to 30% did not show any statistical differences compared to the non-degradable version of the hydrogel. An addition of 50% VPM peptide in the system slightly increased the Young's modulus of the hydrogel from around 6 kPa (obtained for 0VPM and 0.3VPM conditions) to 8 kPa.

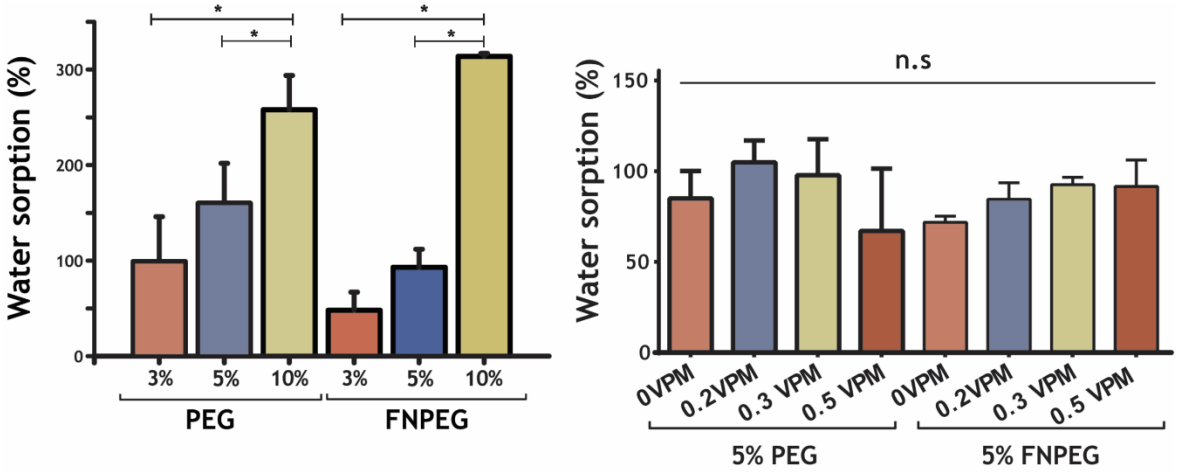

Figure 3.11 Water sorption increases with the percentage of PEG at 24 hours.

Water absorption capacity (Equation 2.1Equation 2.1 Percentage of water absorbed after hydrogel formation.) was measured at 24 h for different percentages of PEG (3%, 5% and 10%, both with and without fibronectin) and for 5% hydrogels it was measured presenting different ratios of degradable: non-degradable crosslinkers. Graphs show mean ± SD (n = 3), (*) p-value< 0.05 in an ANOVA test followed by a Tukey's *post hoc* test.

Water sorption of the hydrogels was also measured. The uptake of water was studied for hydrogels prepared with increasing amounts of PEG and also with different ratios of degradable:non-degradable crosslinkers. As can be seen in Figure 3.11, the percentage of water absorbed increased monotonically with the amount of PEG in the system, independently of the presence of fibronectin. This result is counterintuitive; less water absorption was expected when increasing the percentage of PEG in the system, because the modulus is increasing with the amount of PEG as seen in Figure 3.10. However, this result could be due to the use of a hydrophilic crosslinker (PEG-dithiol polymer) instead of a short, hydrophobic crosslinker. The addition of increasing amounts of VPM peptide in the system seems not to have a significant effect in the water uptake at 24 hours, independently of the presence of fibronectin.

Fibronectin-based PEG hydrogels allow in situ encapsulation of C2C12s

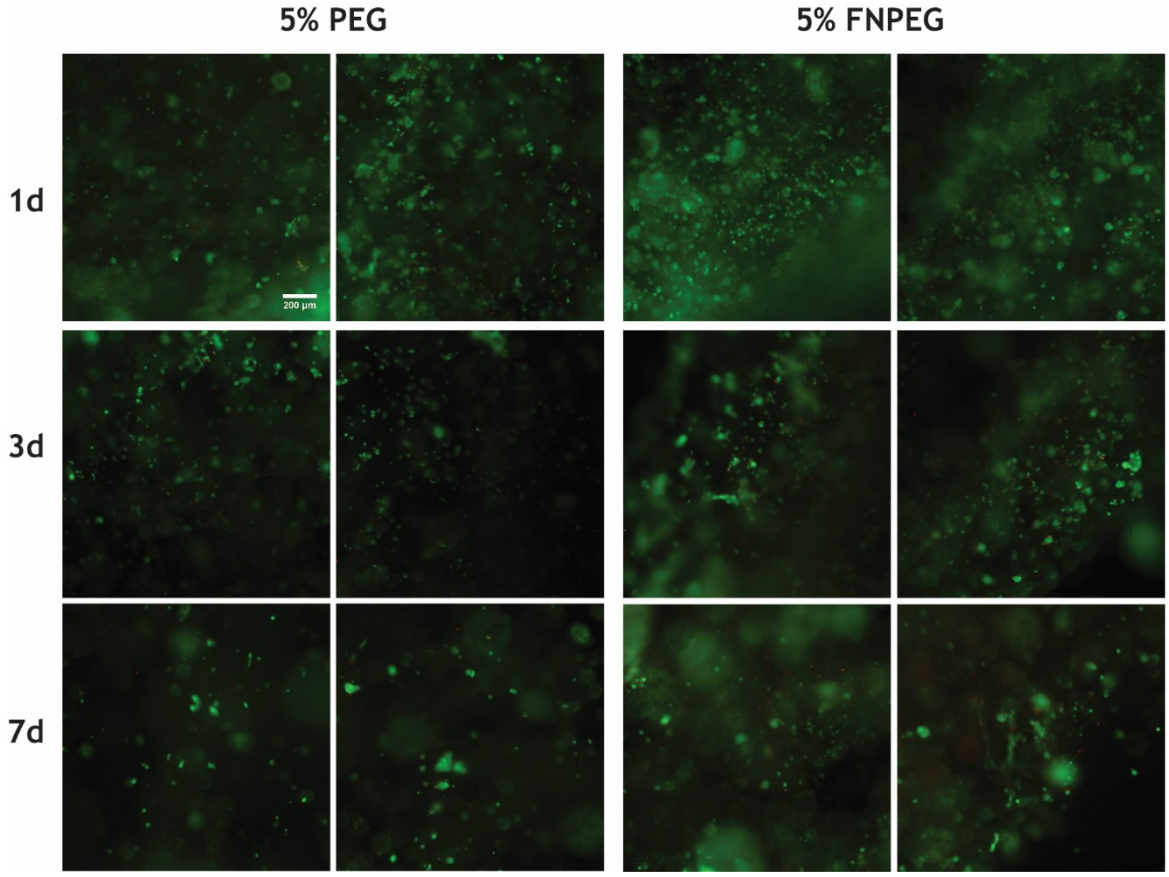

Figure 3.12 Hydrogels allow *in situ* encapsulation of C2C12 cells with high viability.

C2C12 cells were encapsulated within either 5% PEG 0VPM or 5% FNPEG 0VPM hydrogels at a final density of $8{\cdot}10^6$ cell/mL for seven days (in triplicates). Representative images of the Live/Dead® staining are shown where green represents living cells and red shows dead cells for days one, three and seven after encapsulation. Scale bar: 200 µm.

After the physicochemical characterisation of the hydrogels, C2C12 cells were used to test cytocompatibility. The encapsulation procedure and gelation time could affect cell viability. In order to study this effect murine myoblasts were encapsulated within 5% hydrogels with and without fibronectin for seven days and Live/Dead® staining was carried out to quantify the percentage of viable cells. As can be seen in Figure 3.12, cells appear to be mostly viable (as seen by the green staining compared to the red staining). Figure 3.13 shows the percentage of viability obtained. After 24 hours, cells are approximately 90% viable and, after 3 and 7 days the viability decreases slightly, always greater than 70%.

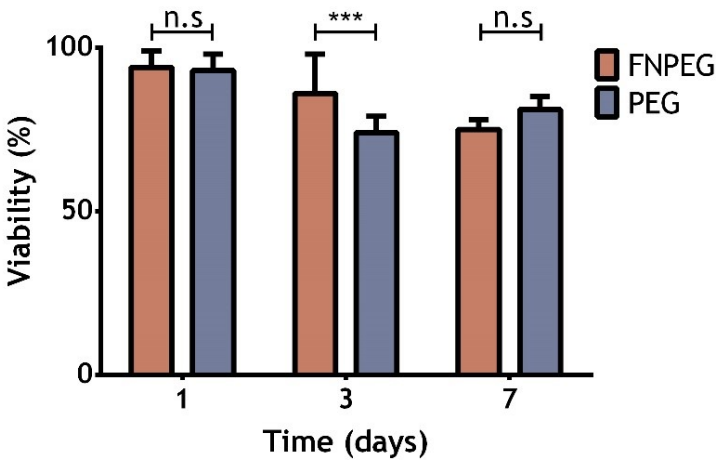

Figure 3.13 C2C12 cells were encapsulated with high viability.

Images obtained from Live/Dead® staining of C2C12 cells encapsulated within hydrogels were used to quantify the percentage of viability. Mean ± SD (n ≥ 10 images). Statistical differences shown via two-way ANOVA followed by a Tukey's *post hoc* test.

3.4 Discussion

The design of protein-tethered synthetic hydrogels is a robust approach to engineer new hydrogel materials as they are able to promote cell adhesion and proliferation, present proteolytic sites and the potential ability for growth factor immobilisation, among other biological activities. All of this while providing mechanical and other physicochemical properties that are controlled based on their synthetic polymer composition.

Fibronectin-based PEG hydrogels were fabricated following Almany et al. and Phelps et al. methods with some modifications (Almany & Seliktar, 2005; Edward A. Phelps et al., 2012). Fibronectin was covalently linked to a synthetic PEG backbone via Michael-type addition reaction between maleimide and thiol groups. Prior to gel formation, fibronectin was PEGylated. The PEGylation of proteins is a tool to improve the half-life of the protein but also to incorporate new functional sites to be able to perform different chemistries while maintaining the biological activity of the protein (see section 1.2.2).

The PEGylation of fibronectin was previously reported by Karuri's group, where they described two methods to link PEG to the fibronectin molecule: one using lysine residues and the other using cysteine residues (C. Zhang, Desai, Perez-Luna, & Karuri, 2014; C. Zhang et al., 2013). Both strategies resulted in biologically active fibronectin (e.g. cell adhesion, fibronectin fibril assembly) with some proteolytic stability. For the incorporation of PEG-diacrylate to fibronectin,

Karuri's team used ß-mercaptoethanol (BME) as reductant, whereas Seliktar's team used TCEP for the denaturation of fibrinogen (Almany & Seliktar, 2005; C. Zhang et al., 2013). TCEP was selected as denaturing agent due to its proven efficacy and the fact that it does not present thiol groups in its structure (compared to BME or DTT) that could interfere with the Michael-type addition reaction. Furthermore, TCEP is stable at larger ranges of pH (Getz, Xiao, Chakrabarty, Cooke, & Selvin, 1999; Han & Han, 1994).

Fibronectin has also the capability of refolding after denaturation. Patel et al. characterised the differences between native fibronectin and refolded fibronectin (i.e. fibronectin after a denaturing-renaturing cycle) (Patel, Chaffotte, Amana, Goubard, & Pauthe, 2006; Patel, Chaffotte, Goubard, & Pauthe, 2004). Some of their findings were that: (i) there were not differences in the content of secondary structure, (ii) the affinity for gelatin was conserved, (iii) the unfolding was reversible, (iv) the refolded fibronectin can multimerise and (v) there was evidence of higher affinity of refolded fibronectin for heparin (explained by exposure of a third heparin binding domain called Hep III, which is hidden in the native Hep II domain).

These findings suggest that the fibronectin structure can change during denaturation/PEGylation steps but still be able to maintain several biological activities. The selection of cysteine residues as target amino acid for the PEGylation step confers good selectivity as cysteine residues are localised within the fibronectin molecule. By using thiol-PEGylation we are targeting specific regions on fibronectin (all FNI and FNII domains contain two disulphide bonds, whereas FNIII do not contain any disulphide bond (Pankov, 2002)). Our ELISAs (Figure 3.2) confirm that the PEGylation occurred mainly at the FNI and FNII domains (e.g. when using MAB1892 there is a difference in antibody affinity comparing native and PEGylated fibronectin, while antibodies HFN7.1 and P5F3 that target FNIII domains show similar affinity between native and PEGylated fibronectin). Although there were not differences observed when using P5F3 antibody (which targets the growth factor binding domain) between native and PEGylated fibronectins, it is worth mentioning that the blank condition showed comparable absorbance values, which could point to a low affinity of the antibody to the targeted region. Moreover, when native fibronectin is in solution this domain is usually hidden due to the globular conformation that fibronectin presents in its soluble form and thus, PEGylated fibronectin was not expected to show higher availability of this domain in solution.

The biological activity of the cell adhesion domain was further tested (Figure 3.3 and Figure 3.4), demonstrating that C2C12 cells are able to attach and form FAs on top of PEGylated fibronectin similarly as when they are on top of adsorbed native fibronectin. This could be due to the fact that the RGD sequence in its native conformation is part of a loop, without any secondary structure. There are some studies showing that the affinity for integrin $\alpha_5\beta_1$ is mainly the one that decreases caused by an increase in the distance between the RGD sequence and the PHSRN synergy site (A. Krammer, Lu, Isralewitz, Schulten, & Vogel, 1999; Patel et al., 2006).

Also, molecular imaging using AFM shows that our PEGylated fibronectin is able to assemble in a similar way as the natural fibronectin assembles when adsorbed on top of PEA coatings (Llopis-hernández et al., 2016). This suggests that there might be some self-assembling domains available (fibronectin-binding domains are located mainly near the amino terminal) but also, it could be due to fibronectin multimerization during the denaturation-renaturation process throughout PEGylation, as discussed by Patel and co-workers (Patel et al., 2006, 2004). Another possibility could be that, during the PEGylation step some fibronectin monomers could be linked via one PEG-MAL molecule, although the ratio used to PEGylate was 4:1 (meaning four molecules of PEG-MAL per fibronectin monomer), as this is a stochastic process, some fibronectin monomers could be linked via PEG-MAL molecules.

Fibronectin and some of its fragments have been previously used to fabricate hydrogels (S. Li et al., 2017; Mikaël M. Martino et al., 2011; Seidlits et al., 2011). To our knowledge, fibronectin has not been incorporated to a synthetic hydrogel with controlled properties before. We used maleimide-thiol reaction as maleimides have higher affinity towards thiols and shorter gelation times at physiological pH than hydrogels fabricated using acrylates (Edward A. Phelps et al., 2012). Figure 3.6 shows the presence of fibronectin in the hydrogels prepared and Figure 3.7 shows the release of fibronectin in covalently bound fibronectin-based PEG hydrogels compared to physically trapped fibronectin within a PEG only network, proving that fibronectin was covalently incorporated into the PEG backbone.

Our fibronectin-based PEG hydrogel system was further engineered to incorporate increasing amounts of a protease-degradable crosslinker, VPM. By doing this, the

system can be designed to be cell-degradable at different rates as can be seen in Figure 3.8. Stevens et al. and Jones et al. showed that, using the same degradable crosslinker (GPQ peptide) within a PEG hydrogel system but with different amounts is enough to modify the degradability from a few days to a few hours, respectively (Jones, Marchant, Von Recum, Gupta, & Kottke-Marchant, 2015; Stevens, Miller, Blakely, Chen, & Bhatia, 2015). Furthermore, the addition of fibronectin to the system incorporates another degradable signal. Figure 3.9 shows that, fibronectin can be degraded in the presence of the appropriate enzymes. Cells are also able to respond to the type of protease-degradable peptide used, being capable of secreting different MMPs as demonstrated by Jha et al. when comparing three different protease-degradable crosslinkers (Jha et al., 2016). Protease-induced matrix degradation also regulates cell traction, which is enough for MSCs to commit to different lineages (Khetan et al., 2013b). In addition, enzyme-mediated matrix degradation has demonstrated to have a role on the release of soluble molecules such as VEGF (Jha et al., 2016; Yao et al., 2006).

The control over the mechanical properties of the hydrogel is key when mimicking a microenvironment (see section 1.2.4). Figure 3.10 shows that the Young's modulus of this hydrogel system changes when varying the amount of PEG and independently of the presence of fibronectin. These results are in agreement with results obtained by other groups using PEG hydrogel systems where Young's modulus of a few kPa were reported (Bott et al., 2010; Jones et al., 2015; Lutolf & Hubbell, 2003; Edward A. Phelps et al., 2012).

Substrate mechanics (and ligand density) are important when trying to mimic the blood vessel microenvironment. For instance, Califano and Reinhart-King showed that endothelial cell network assembly was promoted on compliant materials (0.2 and 1 kPa) in the presence of high amounts of collagen but there was not assembly on stiffer substrates (2.5, 5 and 10 kPa). However, they were able to induce endothelial cell assembly on stiff substrates just by lowering the amount of collagen incorporated (Califano & Reinhart-King, 2008). Also, soft (i.e. of approximately 2 kPa), degradable PEG hydrogels have shown to improve vascularisation *in vivo* compared to stiff (~18 kPa), degradable PEG hydrogels (Schweller, Wu, Klitzman, & West, 2017).

All hydrogels tested appeared to be cytocompatible showing high cell viability at the timepoints tested (Figure 3.12 and Figure 3.13), even though the hydrogels were not formulated with degradable crosslinker.

3.5 Conclusions

Overall, we describe a new procedure to incorporate fibronectin into a PEG synthetic matrix showing that the PEGylated protein retains several of the native capabilities of fibronectin such as the availability of the cell-attachment domain or the capability to assemble in fibres. By using PEGylated fibronectin, we were able to covalently link the protein to a synthetic PEG network. This PEG backbone was used as a versatile "blank slate" to control relevant physicochemical properties such as the mechanical properties or the degradability profile. Finally, this system has shown its suitability to encapsulate viable cells and thus, to serve as a potential 3D bio-functional microenvironment for endothelial cell encapsulation and assembly, which will be discussed in chapter 4.

4 Chapter Four: fibronectin-based PEG hydrogels for the promotion of angiogenesis

4.1 Introduction

The development of a microvasculature in engineered biomaterials is essential when fabricating thick scaffolds. Cells *in vivo* are normally in the vicinity of a blood vessel (within approximately 100 μm); therefore, a microvasculature is crucial for tissues thicker than 200 μm (Jain, Au, Tam, Duda, & Fukumura, 2005). This allows better nutrient and oxygen diffusion, which prevents cell necrosis. Hence, the capability of the bioengineered microenvironment to allow capillary growth should be considered before implantation.

In general, there are two pathways from which capillaries are formed: vasculogenesis and angiogenesis. Vasculogenesis is usually defined as the *de novo* formation of blood vessels, whereas angiogenesis is defined as the formation of a new blood vessel that sprouts from an established one. During vasculogenesis, endothelial cell precursors coalesce forming what are called blood islands. Then, cells from each blood island start to migrate towards the periphery forming a hollow structure that will grow to form a tube-like construct (Ishak, Djuansjah, Kadir, & Sukmana, 2014; Ucuzian, Gassman, East, & Greisler, 2010). In later stages, mural cells migrate to help stabilise the newly formed capillary. In angiogenesis, endothelial cells respond to angiogenic signals (i.e. biochemical signals) such as VEGF or hypoxia (Gerhardt, 2008; Ribatti et al., 2011). During the process of angiogenesis the tip cell migrates in the direction of the angiogenic signal. Then, stalk cells start to actively proliferate and rearrange themselves to form a hollow tube right behind the tip cell. Later, mural cells help to stabilise the structure as in vasculogenesis (Carmeliet & Jain, 2011; Coultas, Chawengsaksophak, & Rossant, 2005; Ferrara & Kerbel, 2005; Jain et al., 2005; Silvestre, Lévy, & Tedgui, 2008; Ucuzian et al., 2010).

VEGF is a crucial regulator of physiological and pathological angiogenesis (Ferrara et al., 2003; Storkebaum & Carmeliet, 2004). VEGF is generally considered the rate-limiting step of the angiogenic pathway, meaning that it is usually the slowest step - in a metabolic pathway - that causes the overall rate of the other reactions in the pathway (Ferrara et al., 2003; Ferrara & Kerbel, 2005). The sequestration and presentation of VEGF in a 3D biochemically engineered construct has been

shown to promote endothelial cell activation and subsequently, formation of tube-like structures via either vasculogenic or angiogenic pathways (Kano, 2005; E. A. Phelps et al., 2010; Edward A. Phelps et al., 2015).

Here, we hypothesise that it could be valuable to exploit the known fibronectin-VEGF affinity as a more biologically relevant way of sequestering VEGF compared to the mere covalent immobilisation. By sequestering VEGF using a natural ECM's sequestering protein, could be possible to enhance endothelial cell response towards VEGF due to its presentation together with integrins, promoting synergistic signalling. This approach to exploit the activity of different growth factors using fibronectin has been shown successful in bone repair and also in wound healing (Llopis-hernández et al., 2016; M. M. Martino & Hubbell, 2010; Mikaël M. Martino et al., 2011; Moulisová et al., 2017).

This chapter focuses on the interaction between fibronectin and VEGF, and their role in promoting angiogenesis/vascularisation. To that end, the release and binding of VEGF in fibronectin-based PEG hydrogels was studied, endothelial cells were also encapsulated and the promotion of angiogenesis and vascularisation was tested in vitro. Finally, the ability of this system to enhance angiogenesis *in vivo* – via CAM assay – was tested.

4.2 Materials and methods

The materials and methods used for the work discussed in this chapter are described in Chapter 2; more specifically VEGF labelling is described in section 2.2.14, VEGF binding experiments in section 2.2.15, VEGF release experiments in section 2.2.16, cell culture in section 2.2.2, cell viability in section 2.2.17, fibronectin PEGylation in section 2.2.1, PEG hydrogel formation in section 2.2.6, vascularisation assays in section 2.2.19, angiogenesis experiments in section 2.2.18, CAM assay in section 2.2.20, image analysis in section 2.2.25 and statistical analysis in section 2.2.26.

4.3 Results

4.3.1 Fibronectin-VEGF interactions

Release of VEGF from fibronectin-based PEG hydrogels

Fibronectin-based PEG hydrogels have been previously described as suitable microenvironments for 3D cell culture (see chapter 3). Fibronectin-based PEG hydrogels were studied as potential sequestering environments of growth factors, in particular VEGF for the study of angiogenesis and vasculogenesis *in vitro*.

Figure 4.1 shows the VEGF-488 release profile from different hydrogel formulations. As can be seen in Figure 4.1b, there is a difference in the amount of VEGF-488 released by only PEG hydrogels compared to FNPEG hydrogels. PEG hydrogels were able to release all the VEGF-488 loaded at the timepoints tested, whereas FNPEG hydrogels released around 50% of the initial amount of VEGF encapsulated. This could mean that FNPEG hydrogels are capable to retain up to half the amount added at the beginning. We also studied the effect on the release of VEGF with the addition of different amounts of degradable crosslinker. Figure 4.1c shows the release profile for VEGF loaded FNPEG hydrogels. All the formulations tested presented a similar release profile of around 40-50% of VEGF-488 released within the time frame studied. As can be seen in Figure 4.1d, the VEGF release profile for PEG hydrogels with different amounts of VPM peptide is also similar, with no significant differences. All PEG hydrogels formulations released around 75-100% of the VEGF-488 initially loaded.

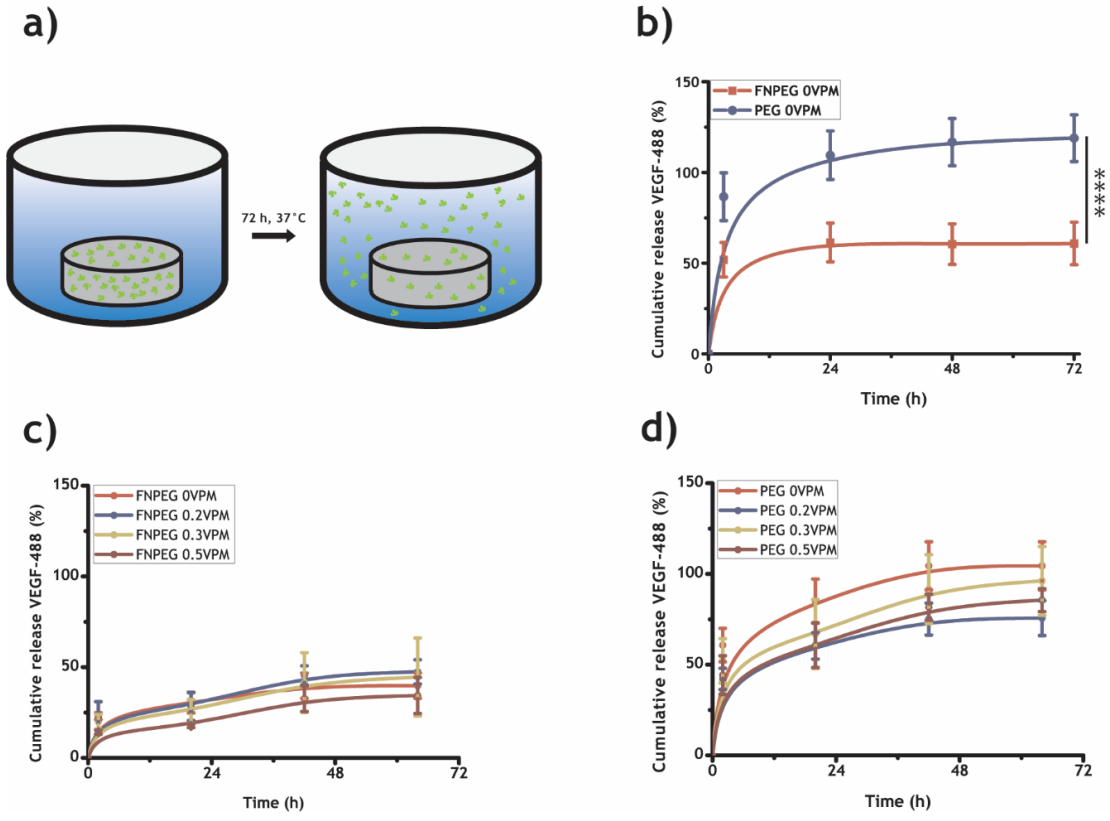

Figure 4.1 FNPEG hydrogels release less VEGF compared to PEG hydrogels.

The release of VEGF from hydrogels previously loaded with the fluorescently labelled VEGF (VEGF-488) was studied as explained in sections 2.2.14 and 2.2.16. (a) Cumulative release of VEGF-488 from either FNPEG 0VPM or PEG 0VPM hydrogels (mean ± SD, n = 6); (b) Cumulative release of VEGF-488 from FNPEG hydrogels with different VPM crosslinker ratios (mean ± SD, n = 3); (c) cumulative release of VEGF-488 from PEG hydrogels with different amounts of VPM (mean ± SD, n = 3). Each replicate was measured twice. Significant differences shown (****) in a t-test.

Fibronectin-based PEG hydrogels uptake VEGF

We also studied the ability of these hydrogels to uptake VEGF when immersed in VEGF solution. Figure 4.2 shows the results obtained for the uptake studies. As can be observed in Figure 4.2b, FNPEG hydrogels were able to uptake VEGF-488 at higher percentages compared to their counterparts without fibronectin. This result was found consistent at all VEGF concentrations tested. Consequently, as Figure 4.2c shows, the amount of VEGF bound per hydrogel assayed was higher in FNPEG hydrogels. All these differences were found statistically significant.

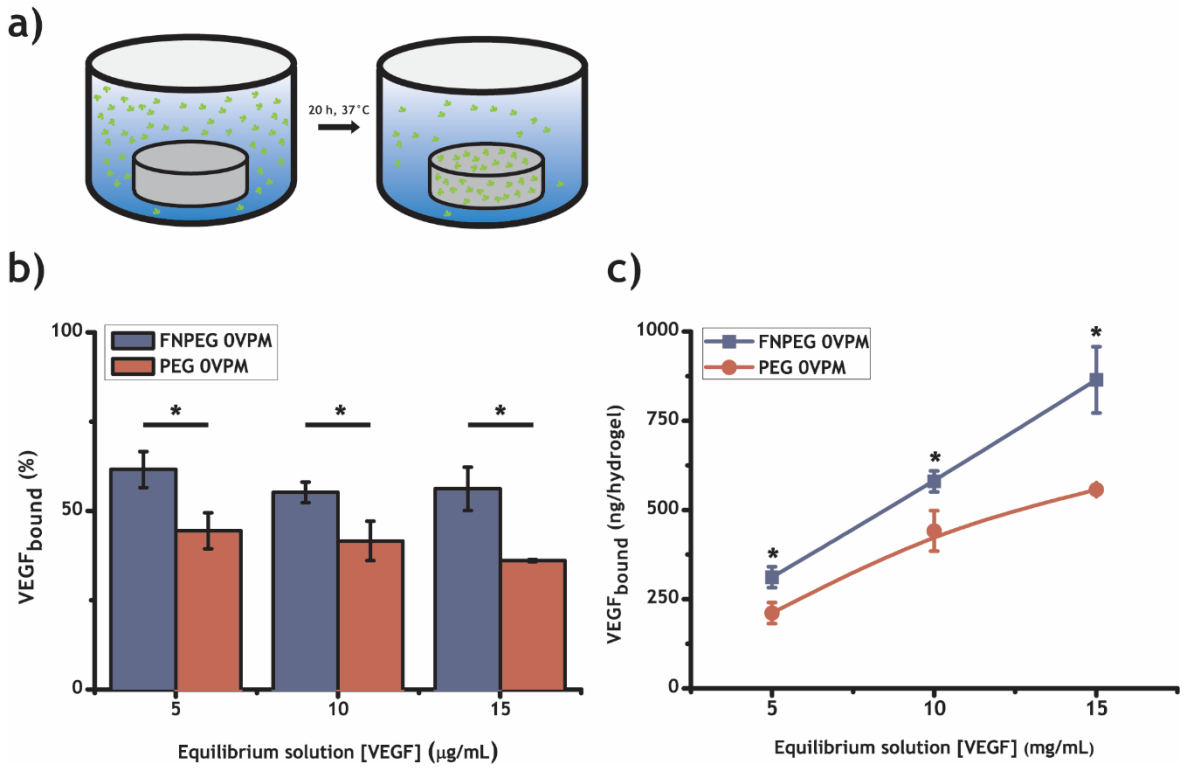

Figure 4.2 FNPEG hydrogels uptake more VEGF compared to PEG.

The binding capacity of VEGF to either FNPEG 0VPM or PEG 0VPM was tested as explained in section 2.2.15. (a) Outline of the assay, where hydrogels were incubated within VEGF solutions of different concentrations and after 20 h the remaining soluble VEGF was measured. From that it was calculated (b) the percentage of VEGF bound (mean ± SD, n = 3) and (c) the amount of VEGF bound per sample (mean ± SD, n = 3). Significant differences were assessed by means of t-tests comparing FNPEG 0VPM and PEG 0VPM results at each concentration of VEGF used.

4.3.2 Endothelial cell-loaded in fibronectin-based PEG hydrogels

Endothelial cell viability

With the purpose of testing endothelial cell viability, HUVECs were encapsulated within PEG and FNPEG hydrogels containing 0.5VPM. Live/Dead® staining was carried out at different timepoints. Figure 4.3 shows the results obtained. HUVECs were viable at all timepoints studied, obtaining viabilities of approximately 80%.

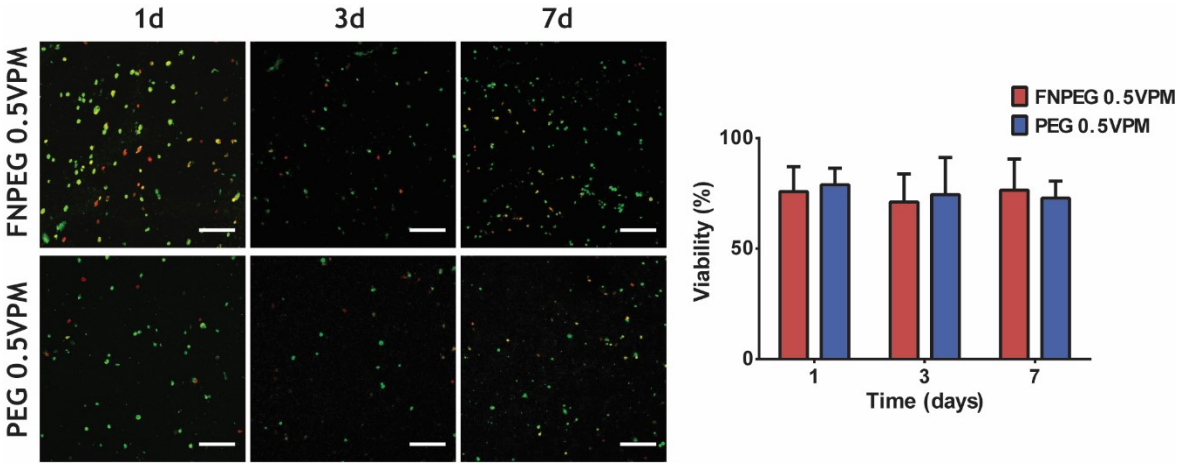

Figure 4.3 HUVECs encapsulated within hydrogels with high viability.

Representative maximum Z-axis projection images from stacks of images showing in green alive cells and in red dead cells. Percentage of viability calculated from the images taken (mean ± SD, n = 9 images, conditions in triplicate).

Endothelial cell reorganisation

In order to study endothelial cell reorganisation in 3D, HUVECs were encapsulated *in situ* within different hydrogels with or without VEGF. Figure 4.4 shows representative images at day one post-encapsulation. As can be seen in this figure, HUVECs were well distributed throughout the stack (insets), with some differences. When looking at Matrigel conditions cells were predominantly isolated, i.e. single cells, relatively not interacting with each other. PEG only hydrogels presented some cell-cell interactions, but cells were found mainly isolated. FNPEG hydrogels presented many cell-cell interactions, forming groups of cells. These clusters of cells were more noticeable in the condition with VEGF.

Figure 4.5 shows representative images of endothelial cells encapsulated at day two. Similar results were observed at day two in comparison with day one for the Matrigel and PEG only conditions. FNPEG samples presented more endothelial cell reorganisation (i.e. clusters of cells forming elongated structures) that was more visible in the condition with VEGF. Figure 4.6 shows the 3D reconstruction of cells within Matrigel condition versus FNPEG condition at day two to stress differences.

Figure 4.7 shows images of encapsulated endothelial cells at day three. At this stage, cells cultured within FNPEG hydrogels did not show the same degree of reorganisation found at days one and two. Matrigel and PEG only conditions did not show many differences compared to previous days. However, Matrigel samples with VEGF presented an increase in cell-to-cell contacts and groups of approximately 2-4 cells.

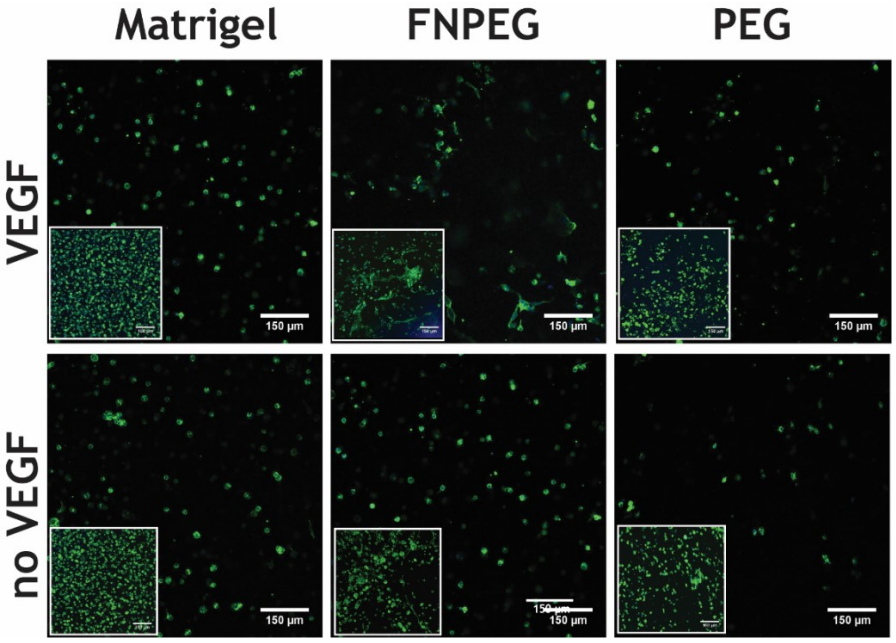

Figure 4.4 Study of endothelial cell rearrangement within hydrogels (day one).

Representative images (from a stack imaged) of either Matrigel, 5% FNPEG 0.5VPM or 5% PEG 0.5VPM, with or without VEGF at day one. Insets show the maximum intensity Z-axis projection of a stack. Images show in green the actin cytoskeleton and in blue the nucleus. Scale bar: 150 µm. Scale bar inset: 150 µm.

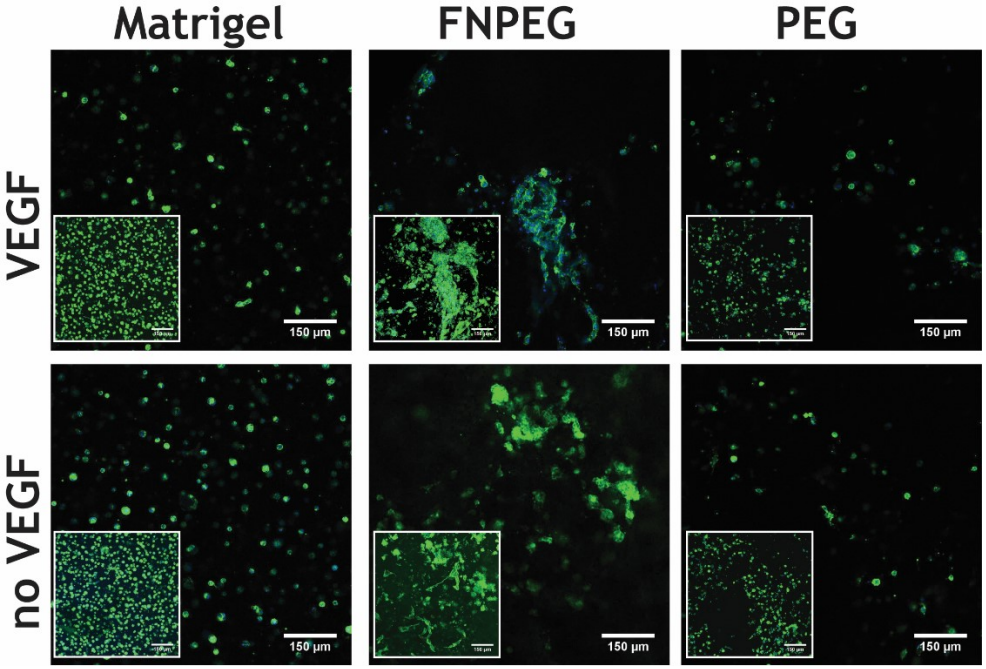

Figure 4.5 Study of endothelial cell rearrangement within hydrogels (day two).

Representative images (from a stack imaged) of either Matrigel, 5% FNPEG 0.5VPM or 5% PEG 0.5VPM, with or without VEGF at day two. Insets show the maximum intensity Z-axis projection of a stack. Images show in green the actin cytoskeleton and in blue the nucleus. Scale bar: 150 µm. Scale bar inset: 150 µm.

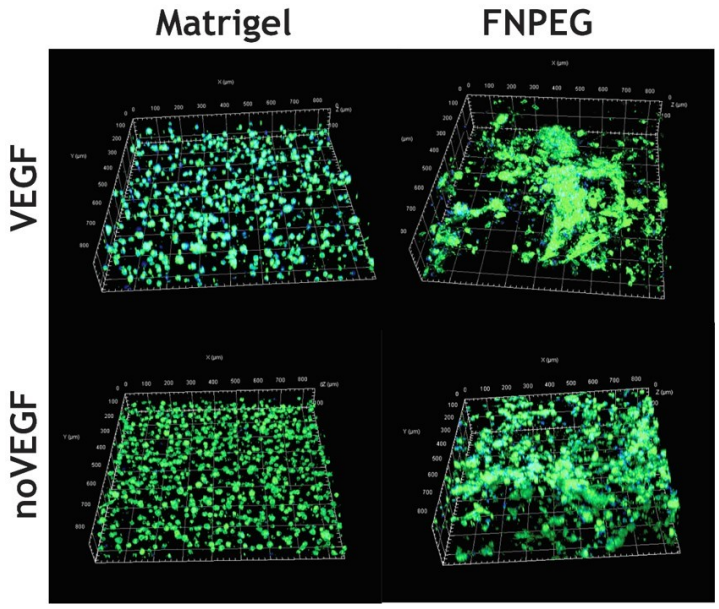

Figure 4.6 3D reconstruction of representative stack from day two.

Comparison of 3D cell organisation between Matrigel versus FNPEG at day 2, with and without VEGF. Scale bar: 800 x 800 x 200 µm.

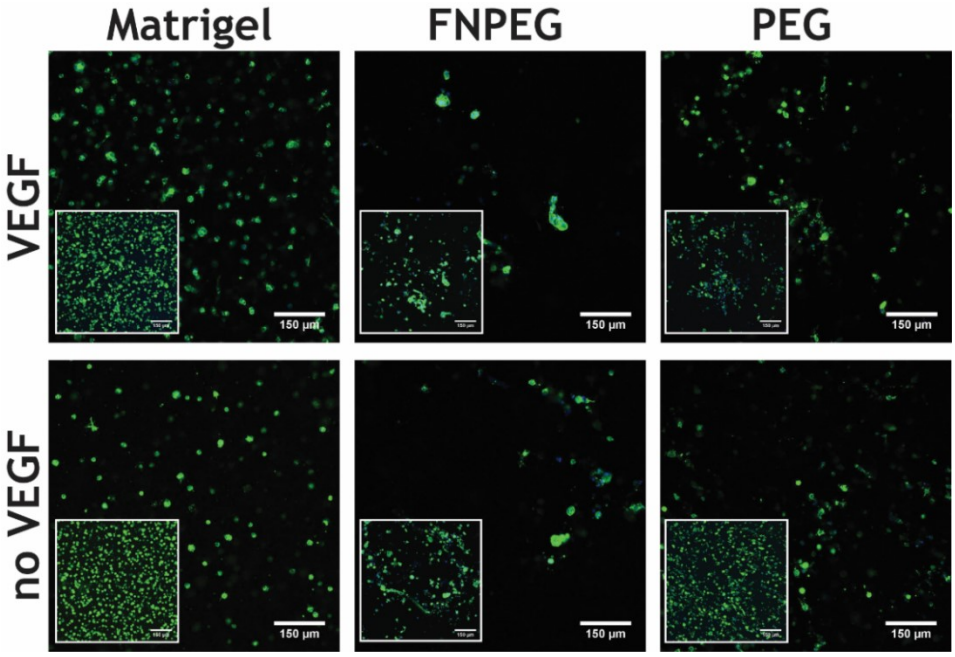

Figure 4.7 Study of endothelial cell rearrangement within hydrogels (day three).

Representative images (from a stack imaged) of either Matrigel, 5% FNPEG 0.5VPM or 5% PEG 0.5VPM, with or without VEGF at day three. Insets show the maximum intensity Z-axis projection of a stack. Images show in green the actin cytoskeleton and in blue the nucleus. Scale bar: 150 µm. Scale bar inset: 150 µm.

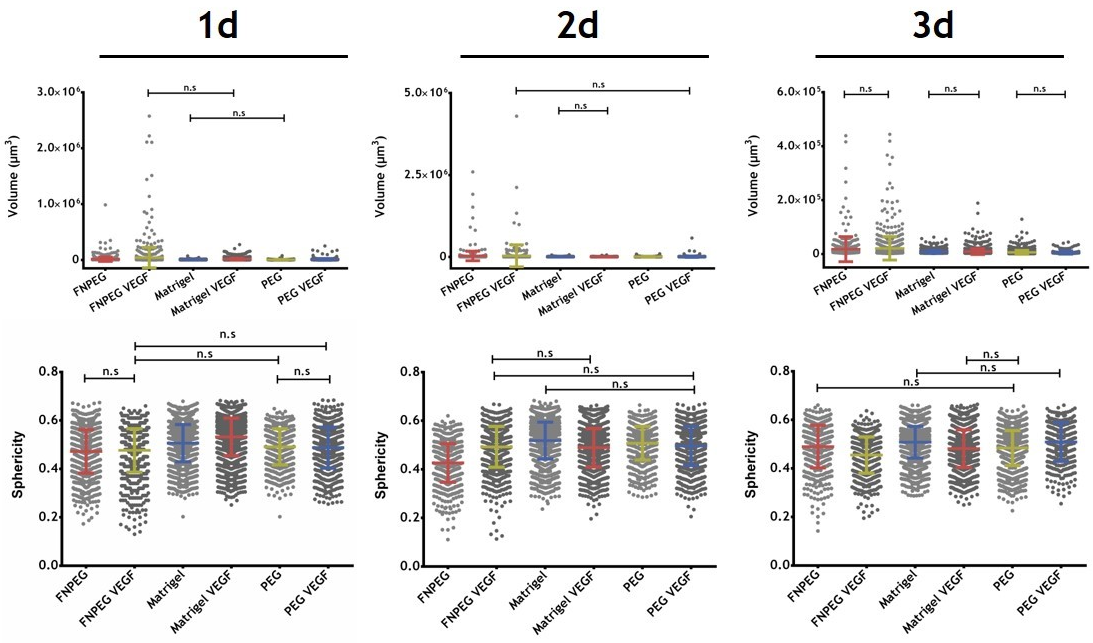

Figure 4.8 Shape descriptors calculated from vascularisation experiments.

Top row show the calculated volumes (µm^3) for all objects imaged at days 1-3. Bottom row represents the calculated sphericity (Ψ) for all object imaged at days 1-3. Graphs show mean ± SD (datapoints in grey). For simplicity only non-statistically significant (n.s) differences are shown.

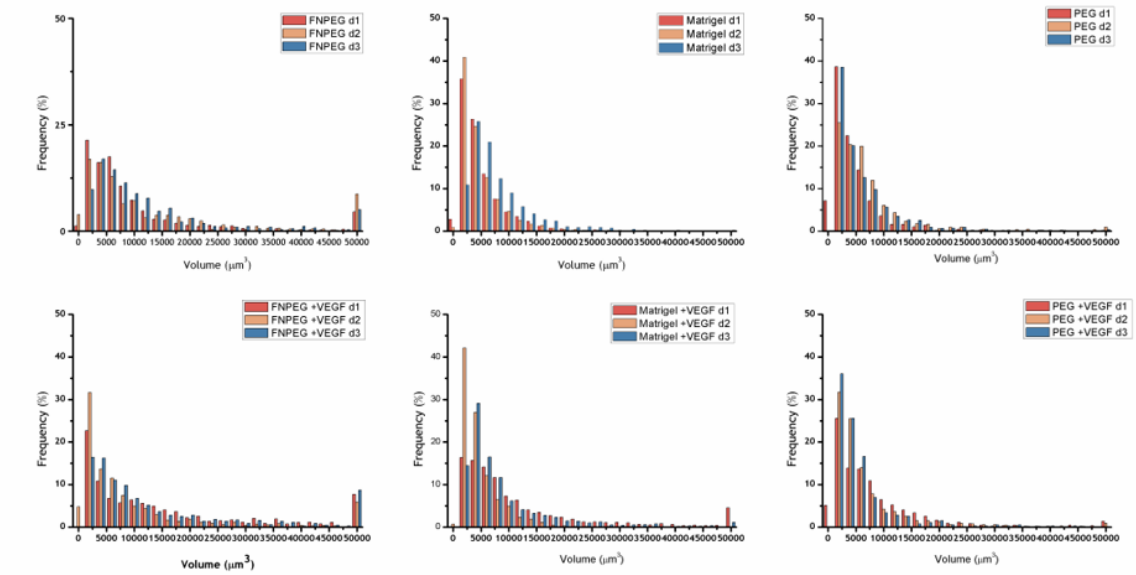

Figure 4.9 Volume distribution obtained from vascularisation experiments.

Graphs show the distribution of volumes (µm^3) for FNPEG, PEG and Matrigel (with and without VEGF) at days 1-3. Volumes equal or larger than 50000 µm^3 were categorised under the "50000" bin centre.

From the quantification assessed (Figure 4.8 and Figure 4.9), the total volume of all objects found and the sphericity of these objects were studied. As can be seen in Figure 4.8, the largest volumes were found within FNPEG conditions at all timepoints tested. It is also worth noting that Matrigel condition showed a

noticeable increase in object's volume at day three. When looking at the volume distribution (Figure 4.9), there can be found extremely large objects (≥ 50000 μm^3) in FNPEG samples.

Sphericity calculations (Figure 4.8) show that FNPEG conditions present higher amount of cells with low sphericity, which could indicate more cell spreading or higher cell reorganisation into more elongated structures.

Endothelial cell sprouting

Endothelial cell angiogenic sprouting was also evaluated (Figure 4.10). To assess this, endothelial cells were seeded on top of collagen-coated dextran beads and then, these endothelial cell-coated beads were encapsulated within either FNPEG hydrogels or Matrigel, with or without VEGF. Results show that in the absence of VEGF, endothelial cells are not able to sprout even in the Matrigel condition. When using relatively low amounts of VEGF (50 ng/mL supplemented with the media), endothelial cells were capable of forming a few sprouts, being more noticeable in the Matrigel condition. The use of relatively high amounts of VEGF allowed endothelial cells to form many sprouts.

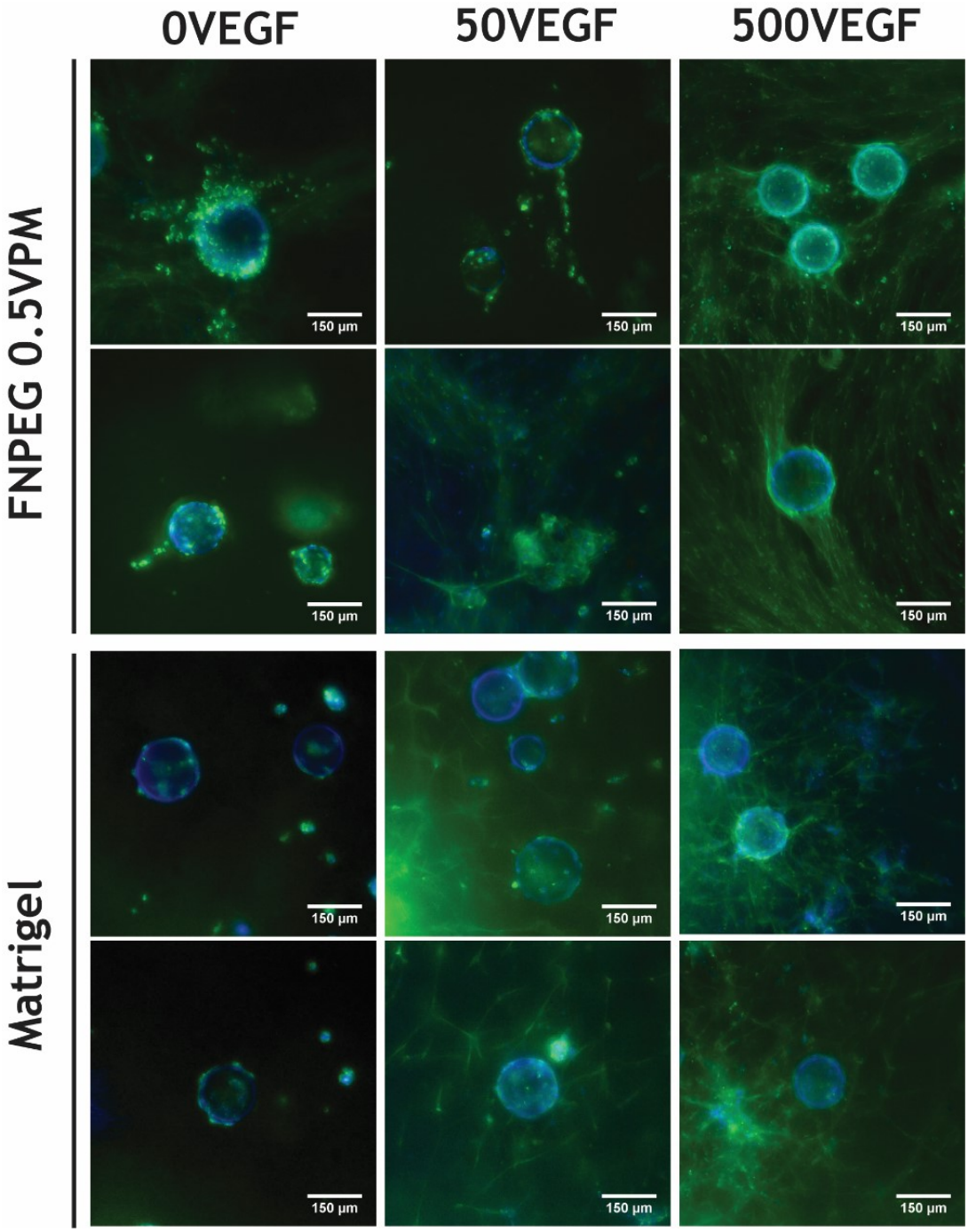

Figure 4.10 FNPEG allow endothelial cell sprouting in 3D via encapsulated cell-coated beads.

Representative maximum intensity Z-axis projection images from manually taken stacks, showing in green the actin cytoskeleton and in blue the nuclei of HUVECs. Cultures were kept for 7 days. Different amounts of VEGF were added to growth media: 0VEGF (0 ng/mL of VEGF), 50VEGF (50 ng/mL of VEGF) and 500VEGF (500 ng/mL of VEGF). Scale bar: 150 µm.

Chorioallantoic membrane assay

The angiogenic potential of these hydrogels was also assessed using the chicken chorioallantoic membrane assay, which is a classical model to study neovascularisation. The results obtained from this experiment can be found in Figure 4.11. Membranes were imaged and quantified manually.

Our results show that PEG only hydrogels did not affect the normal development of the membrane, presenting similar values as the empty condition (i.e. without material). PEG VEGF samples showed a slightly increase in the amount of branching as can be seen in the number of junctions observed. However, this was not enough to obtain a significant increase in the formation of new capillaries. However, the FNPEG condition (without VEGF) presents an average increase in capillary formation compared to PEG with VEGF; as can be seen in the average number of branches formed per image as well as in the number of junctions. The latter could be an indicator of the connectivity of the capillary plexus analysed. This result is encouraging although it is not statistically significant. FNPEG condition with VEGF was the best condition in terms of performance, presenting the highest average number of branches. Also, the highest number of junctions were found for this condition. In addition, FNPEG with VEGF performed better than PEG with VEGF but, when comparing FNPEG with and without VEGF there were not statistically significant differences.

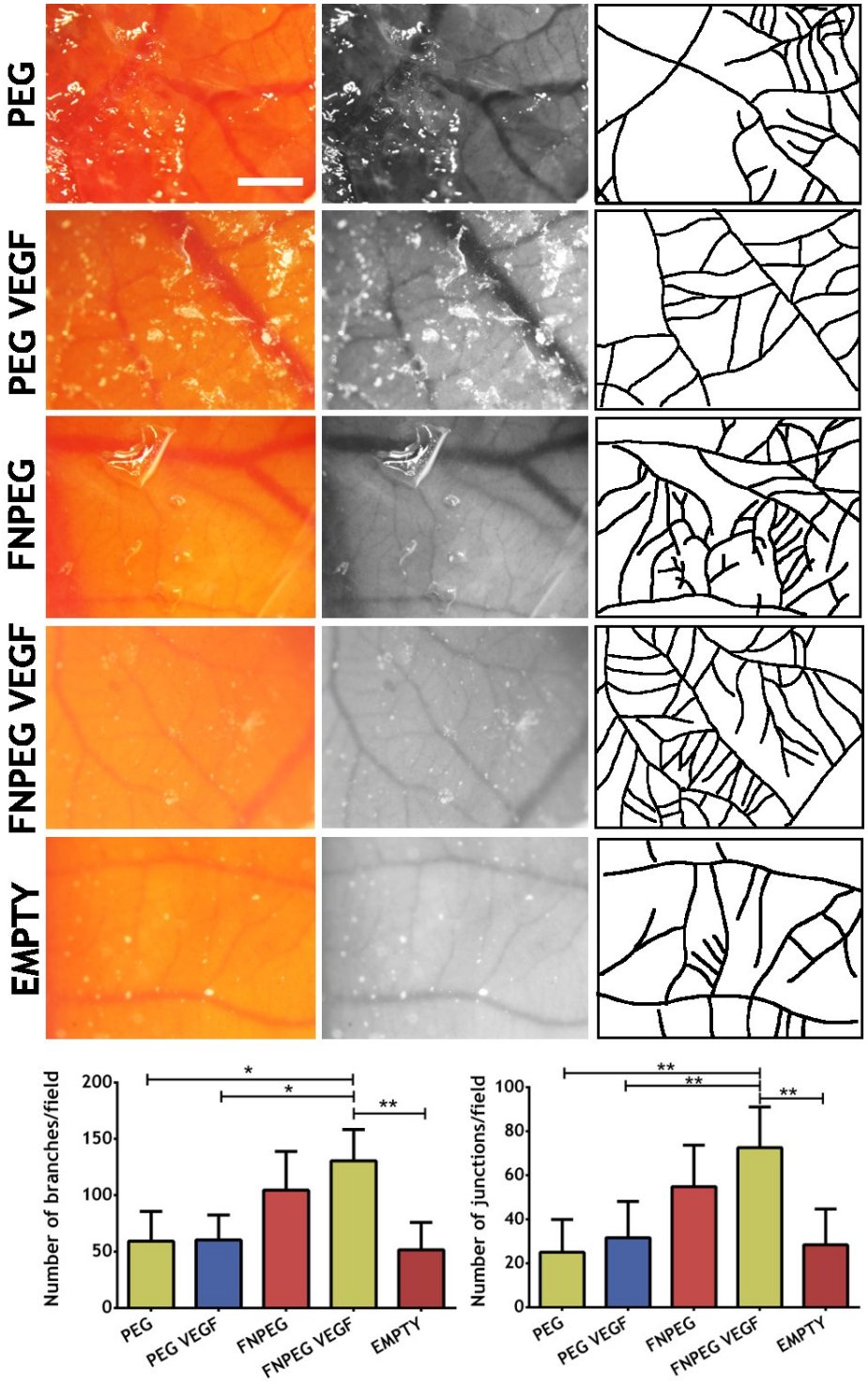

Figure 4.11 FNPEG hydrogels promote angiogenesis *in vivo* shown by CAM assay.

Membranes were exposed and imaged. Conditions tested were: PEG (5% PEG 0.5VPM), PEG VEGF (5% PEG 0.5VPM loaded with 2.5 µg/mL of VEGF), FNPEG (5% FNPEG 0.5VPM), FNPEG VEGF (5% FNPEG 0.5VPM loaded with 2.5 µg/mL of VEGF) and EMPTY (where the CAM was exposed but no material was used during the experiment). Left column shows colour images (RGB images) obtained from the microscope; middle column shows the green channel obtained from RGB images that was used for capillary segmentation and the right column shows the result from the skeletonise tool. Scale bar: 1 mm. Graphs show (from left to right): the number of branches per image and the number of junctions per image (mean ± SD, n= 6 replicates). Significant differences shown as (*) p-value < 0.5, (**) p-value < 0.1 in an ANOVA test.

4.4 Discussion

FNPEG hydrogels have shown their suitability as new 3D microenvironments for cell culture (see chapter 3). This chapter explores the idea of using fibronectin's natural ability to sequester growth factors for the promotion of microvasculature growth. First, we tested the efficiency of VEGF sequestration by studying VEGF release and binding (Figure 4.1 and Figure 4.2). FNPEG hydrogels present relatively high ability to sequester VEGF, being able to retain up to 50% of the initial VEGF loaded. In our case VEGF is not covalently bound to the PEG network (VEGF presents free cysteine residues in its structure, (Edward A. Phelps et al., 2015)) as PEG only formulations released all VEGF loaded. This could be due to the fast reactivity of the maleimide group and also, in our system we do not previously incubate VEGF with the PEGMAL polymer, so we do not encourage this binding. From the binding assays, we also found that FNPEG hydrogels were able to sequester soluble VEGF; this is important because when implanted *in vivo*, FNPEG hydrogels could be able to sequester many growth factors, as fibronectin's heparin-II binding domain is a promiscuous growth factor binding site (M. M. Martino & Hubbell, 2010).

The study of the pro-angiogenic activity of this system *in vitro* was assessed using HUVECs; which are a widely studied cell-model system (Hasenberg et al., 2015; Hendriks, Riesle, & Blitterswijk, 2010; Kiran et al., 2011; Saik, Gould, Keswani, Dickinson, & West, 2011). Vasculogenic experiments (Figure 4.4 to Figure 4.9) showed that endothelial cells were able to rearrange themselves within FNPEG hydrogels but not in Matrigel or PEG only hydrogels. The structures found within FNPEG hydrogels were even larger in the condition with VEGF. These results are in agreement with results shown by West's group, where they covalently immobilized VEGF into a PEG network showing HUVEC reorganisation between days one and two (Leslie-Barbick, Moon, & West, 2009). These structures regressed by day three, where these large structures were no longer found. These results are in agreement with literature, where it is reported that endothelial cells need mural cells to stabilise these type structures. For instance, Peters et al., studied HUVECs in co-culture with mural cells, being able to study tubulogenesis at longer timepoints (i.e. seven and fourteen days) (Peters, Christoforou, Leong, Truskey, & West, 2016).

The ability of HUVECs to sprout within our system was also tested using different VEGF concentrations in the media (Figure 4.10). The highest sprouting was found with the highest amount of VEGF in the media (500 ng/mL). This is not in accordance with literature, where usually it is found that high amounts of VEGF are detrimental for endothelial cell sprouting and, lower amounts of VEGF (in the range of 1 to 10 ng/mL) enhances sprouting significantly (S. Li et al., 2017; Nakatsu et al., 2003). That said, these examples use other hydrogel systems such as fibrin, which has been reported to also sequester growth factors (M. M. Martino et al., 2013). Generally, fibrin matrices contain higher amounts of fibrinogen compared to the amount of fibronectin incorporated in our system, so it is conceivable that the amount of growth factor readily sequestered within fibrin matrices could be higher compared to our system. Consequently, comparisons have to be taken carefully.

The performance of FNPEG hydrogels was also tested in a more *in vivo* scenario (Figure 4.11) by using the chick CAM assay. The CAM is an extraembryonic membrane that facilitates gas diffusion and nutrient exchange until hatching. This membrane has a dense capillary network that is generally used to study angiogenesis and anti-angiogenesis *in vivo*. Among the most commonly tested things can be found: tissues, cells, drugs, soluble factors or biomaterials (Ribatti, 2008, 2016).

Our results from this experiment show that FNPEG with VEGF samples were able to promote the formation of a higher number of capillaries compared to PEG only with VEGF. This result could be due to a rapid release of VEGF from the PEG only condition, not being able to build the necessary VEGF gradient that is required for angiogenic sprouting. In addition, this result also suggests that the presence of fibronectin and subsequently binding of VEGF could enhance the effects of the latter via integrin recruitment near the growth factor bound to the fibronectin molecule.

Our release studies showed that PEG samples release all VEGF loaded after 24 h, whereas FNPEG samples only released approximately 50% of the VEGF loaded at 72 h (Figure 4.1) and these materials were incubated *in ovo* for four days.

These results could indicate that a more sustainable release of VEGF, creating a biochemical gradient, could promote more neovessel formation.

The need for a sustainable release of VEGF has been reported in literature. For instance, Li et al. fabricated gelatin hydrogels with heparin and showed that

gelatin-heparin hydrogels could sequester up to 40% of the VEGF initially used. When testing this via CAM assay, they found that gelatin-heparin with VEGF showed the highest number of vessel formation, compared to gelatin gels with VEGF (without the sequestering molecule heparin). Despite they do not show the quantification for the gelatin-heparin without VEGF to compare, they do show the results of an *in vivo* subcutaneous implantation; with similar results (Z. Li et al., 2015).

Koch et al. also studied the effect of VEGF immobilisation in collagen matrices via CAM assay. They found that the percentage of increase in capillary number compared to the empty control was higher in collagen matrices with VEGF covalently bound than in collagen samples with non-immobilised VEGF (Koch et al., 2006). Similarly, Zisch et al. studied the effect of covalently binding VEGF to a PEG network (Zisch, 2003). They found that VEGF covalently bound promoted more angiogenesis at the site where the hydrogel was placed compared to soluble VEGF where they found sprouting at the periphery of the hydrogel. The latter example could explain why we did not observe the expectable increase in capillary formation using PEG with VEGF; probably, a more vascularised capillary plexus was formed at the surroundings of the implanted hydrogels, that could not be well quantified as we took images covering under the hydrogel setting and far away from the hydrogel. Despite this, all these examples corroborate the need for a sustainable release of VEGF.

4.5 Conclusions

To conclude, we present a hydrogel system that can sequester VEGF using the natural capacity of fibronectin to bind promiscuously different growth factors. This system has shown to allow endothelial cell reorganisation in 3D at early timepoints without the addition of mural cells – although mural cells are needed for a more stable capillary formation at longer timepoints. Moreover, FNPEG hydrogels have shown that can promote endothelial cell sprouting both *in vitro* using endothelial cell-coated beads and *in vivo* via CAM assay. All these results suggest that the intrinsic ability of fibronectin to present VEGF promotes microvasculature growth. The results obtained are in accordance with results shown for fibronectin's presentation of growth factors in synergy with integrins (Mikaël M. Martino et al., 2011; Moulisová et al., 2017).

5 Chapter Five: engineering fibronectin-based HA hydrogels

Note: Part of the results presented in this chapter were carried out during an internship (September-December, 2016) in the Polymeric Biomaterials Laboratory within the Bioengineering Department of the University of Pennsylvania (Philadelphia, US) supervised by Prof. Jason Burdick.

5.1 Introduction

HA is a non-sulphated, nonimmunogenic glycosaminoglycan, found throughout the body in many tissues, from cartilage to the vitreous of the eye (more information in section 1.1.3). HA is also an important element of the ECM, in which its structural and biological properties have a role in cellular signalling, wound repair, tissue morphogenesis, and matrix organization (W. Y. J. Chen & Abatangelo, 1999; Kogan et al., 2007). Hyaluronidase is an enzyme found in the body that can rapidly degrade HA (Stern et al., 2006). HA and its derivatives have been clinically used as medical products for decades. For instance, dermal fillers such as Restylane® was approved in 2003 (Ballin, Cazzaniga, & Brandt, 2013) and SYNOJOINT™ (Teva Pharmaceuticals, USA), which is an injectable form of hyaluronic acid meant for its use in the treatment of pain in osteoarthritis and it was approved in 2018 .

Recently, HA has become an important building block for the fabrication of new biomaterials that can be used in tissue engineering. In addition, HA can be modified in numerous ways, altering the properties of the resulting biomaterials, including their physicochemical features and biological activities. In this sense, HA can be crosslinked into a hydrogel to form a stable scaffold by different chemistries such as aldehyde (Cai, López-Ruiz, Wengel, Creemers, & Howard, 2017), divinyl sulfone (Lai, 2014) or photo-crosslinking (Gramlich, Kim, & Burdick, 2013).

The use of radically induced thiol-norbornene click reactions lessens the problems of non-specific reactions due to the high reactivity of thiols to norbornenes and the low norbornene-norbornene reactivity (Hoyle & Bowman, 2010). The use of thiol-ene UV initiated polymerisation strategies have demonstrated to be a facile approach to encapsulate molecules and cells maintaining their bioactivity (Fairbanks et al., 2009; McCall & Anseth, 2012).

In this chapter we demonstrate that full proteins such as fibronectin can be covalently linked into a HA hydrogel network by using a thiol-ene UV-polymerisation, maintaining key properties of the fibronectin molecule such as the availability of the adhesion motif while being able to tune some physicochemical aspects of the hydrogel system like the mechanical properties. Moreover, both fibronectin and HA can bind growth factors, which adds higher versatility to this system as it can potentially sequester higher amounts of growth factors. This system aims to be used as a pro-angiogenic material, providing a more physiological-like microenvironment for wound healing purposes.

5.2 Materials and methods

The materials and methods used for the work discussed in this chapter are described in Chapter 2; more specifically the synthesis of norbornene-modified HA is described in section 2.2.21, the procedure to fabricate HA hydrogels via photo-polymerisation is described in section 2.2.22, mechanical tests performed are described in section 2.2.23, cell adhesion experiments are described in section 2.2.24, cell culture is described in section 2.2.2, cell viability tests are described in section 2.2.17, image analysis in section 2.2.25 and statistical analysis in section 2.2.26.

5.3 Results

5.3.1 Fibronectin-based hyaluronic acid hydrogel characterisation

Fibronectin-based HA formation via thiol-ene reaction

HA was modified with norbornene groups following published protocol (Caliari et al., 2016; Gramlich et al., 2013). The synthesised NorHA (Figure 5.1a) can be reacted with thiolated compounds via ultraviolet light mediated thiol-ene addition reactions (Figure 5.1c) and form hydrogels (Figure 5.1d). By using this chemistry fibronectin can be incorporated throughout its cysteine residues that can be exposed via protein chemical unfolding.

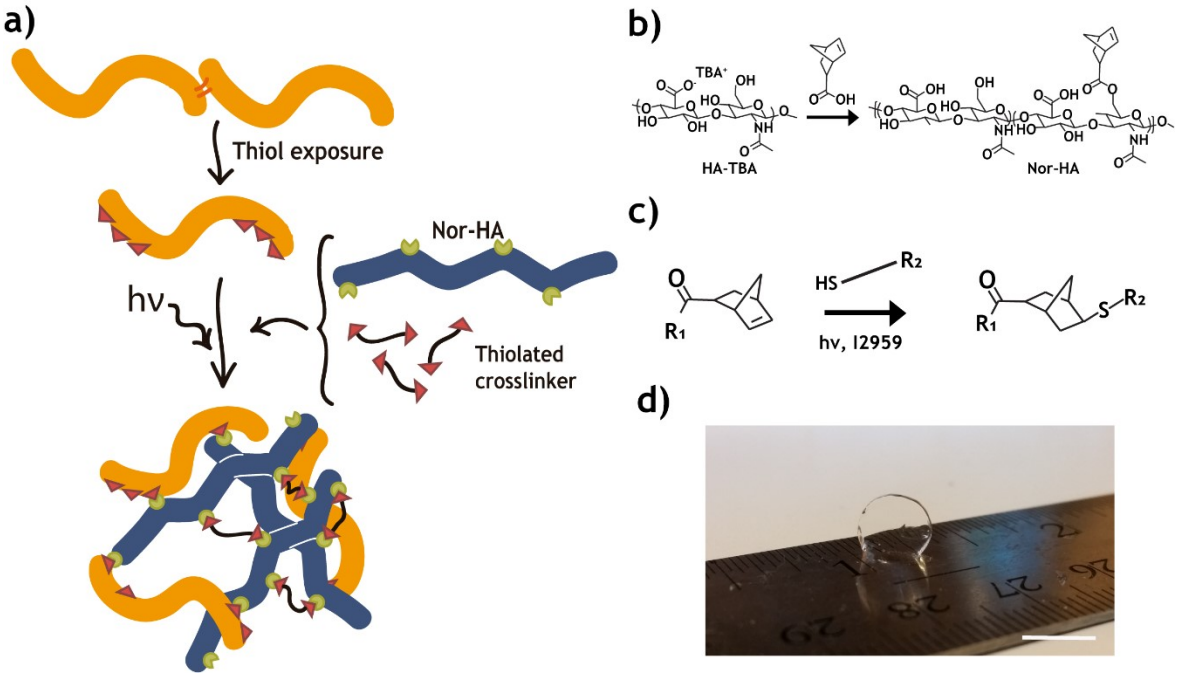

Figure 5.1 Nor-HA synthesis and thiol-ene hydrogel polymerisation.

(a) Fibronectin-based HA hydrogel formation procedure. (b) Nor-HA was synthesised as explained in section 2.2.21; (c) scheme of the thiol-ene UV-polymerisation reaction. (d) Macroscopic image of a FNHA hydrogel (scale bar: 6 mm).

Fibronectin is covalently bound to hyaluronic acid

Figure 5.2 shows the presence of fibronectin after fibronectin-HA hydrogels were fabricated. As can be seen in Figure 5.2a-d, fibronectin was detected in all fibronectin-HA hydrogels while it was not detected in HA only hydrogels (Figure 5.2e). Furthermore, in order to test the fibronectin covalent bonding to the NorHA backbone, HA hydrogels were prepared encapsulating native fibronectin (i.e. with no cysteine residues exposed and thus, with no capability to bind NorHA) and, after several washes, fibronectin was stained via immunofluorescence. Figure 5.2f shows that there were no traces of fibronectin within the hydrogels after all the washes, meaning that fibronectin was not covalently bound to the hydrogel.

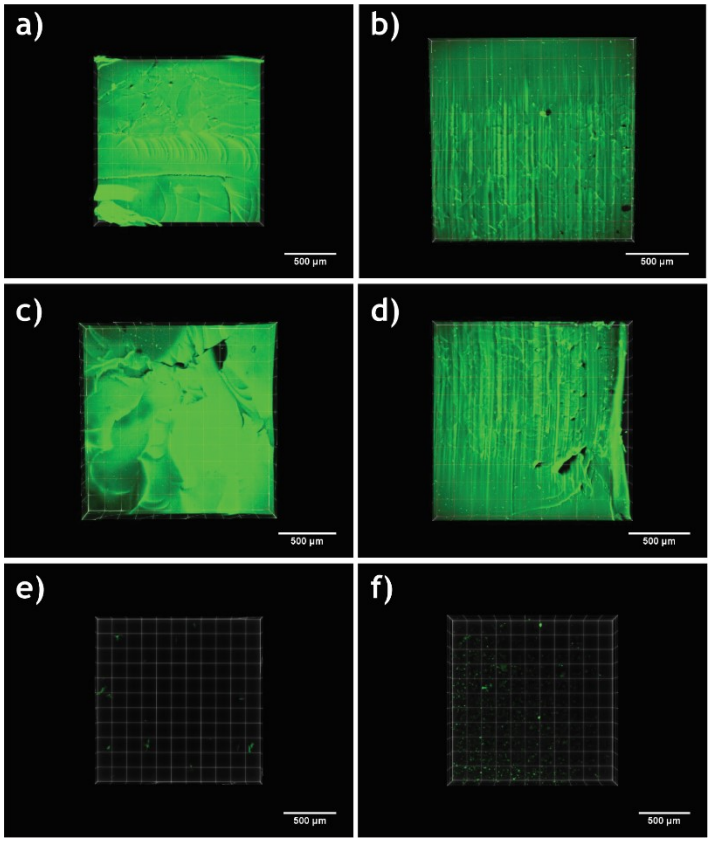

Figure 5.2 Fibronectin is bound to HA hydrogels.

(a, c) FNHA 0VPM surface and cross-section; (b, d) FNHA VPM surface and cross-section; (e) HA only and (f) HA with non-crosslinked fibronectin. Scale bar: 500 µm.

Mechanical properties of Fibronectin-based HA hydrogels can be controlled

The mechanical properties of these hydrogels were tested using DMA in compression mode. As shown in Figure 5.3, the elastic modulus increases monotonically with the increase in crosslinking density up to 1. The crosslinking density was defined by the ratio between thiol and norbornene groups so, when the system reaches maximum crosslinking density (i.e. there are equal number of norbornene groups and thiol groups and all have reacted, ratio 1:1 thiol:norbornene). Once the maximum crosslinking density is reached, the mechanical properties decrease, as there are more thiol groups than norbornene groups, not all crosslinkers are fully reacted. This result is in agreement with literature (Gramlich et al., 2013). Crosslinking ratio of 0.6 was selected to fabricate fibronectin-HA hydrogels, which were mechanically tested as well (Figure 5.3b). As can be observed in Figure 5.3b, all HA hydrogels presented similar elastic modulus (no significant differences), independently of the final concentration of fibronectin used.

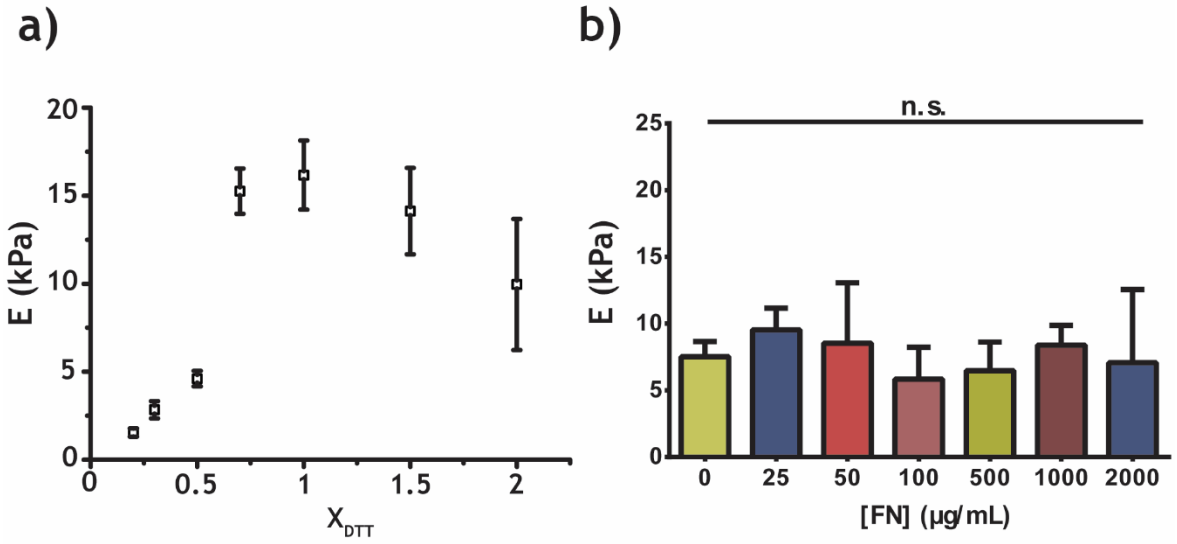

Figure 5.3 The elastic modulus can be controlled independently of the amount of fibronectin used.

Hydrogels with different amounts of fibronectin crosslinked were fabricated and used to measure their mechanical properties using DMA in compression mode. (a) Elastic modulus of HA hydrogels (without fibronectin) using different crosslinking densities (X_{DTT} is the ratio SH from DTT to Norbornene from HA). (b) Elastic modulus of fibronectin-HA hydrogels using different concentrations of fibronectin. Graphs show mean ± SD (n=3, measured twice); n.s, not statistically different via ANOVA test and Tukey's *post hoc* test.

5.3.2 Mesenchymal stem cells and fibronectin-based HA hydrogels

Mesenchymal stem cells seeded on fibronectin-based HA hydrogels

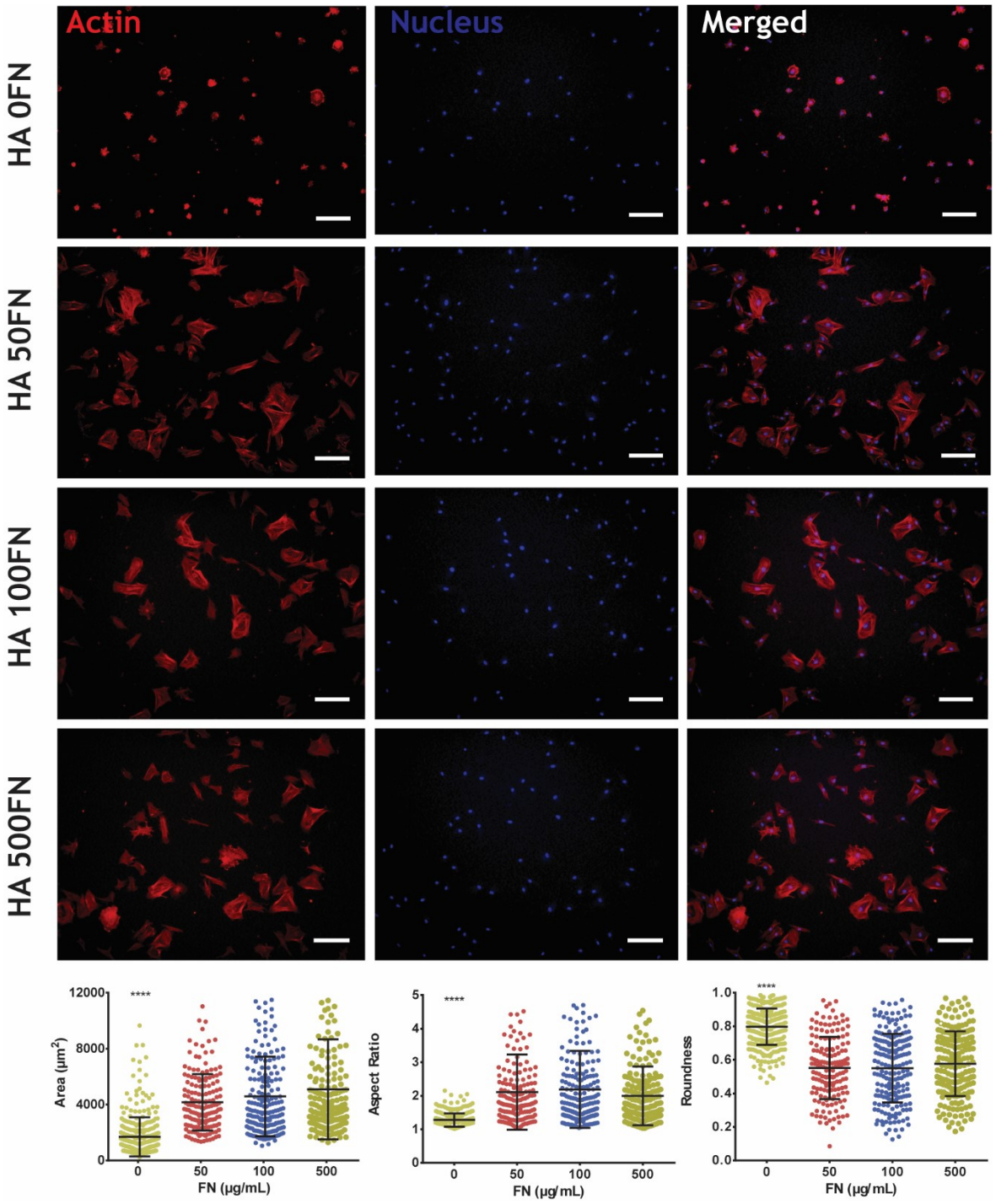

Figure 5.4 MSCs attach to FNHA hydrogels in 2D.

hMSCs were seeded on top of FNHA 0VPM hydrogels with different amounts of fibronectin (depicted as XFN where X is the total amount of fibronectin in μg/mL) for three hours. Representative images of cells for every condition tested and graphs show the mean ± SD of cell area (μm^2), aspect ratio and roundness, respectively (n > 100 cells, conditions in triplicate). Statistical differences studied by Kruskal-Wallis test followed by Dunn's *post* hoc test to correct for multiple comparisons. Scale bar: 200 μm.

Human MSCs were seeded on top of fibronectin-HA hydrogels with different amounts of fibronectin (Figure 5.4). MSCs seeded on top of fibronectin-HA hydrogels were found to spread similarly on all fibronectin concentrations tested as quantified by the total cell area, the aspect ratio and roundness. These cells were able to develop well-defined actin filaments, with presence of stress fibres. Still, cells seeded on top of HA only hydrogels did not spread, showing a rounded conformation with diffuse actin staining.

Yes associated protein localisation

YAP staining of MSCs seeded on top of HA hydrogels was studied and quantified (Figure 5.5 and Figure 5.6). Similar morphologies (in terms of average cell area, aspect ratios and roundness) were found agreeing with previous adhesion experiments (Figure 5.4). When looking at YAP localisation, cells seeded on top of HA 0FN hydrogels present a diffuse staining mainly localised in the cytoplasm, cells seeded on top of HA 25FN hydrogels presented YAP staining in both cytoplasm and nucleus. Cells from both HA 50FN and HA 500FN hydrogels show a clear localisation of YAP in the nucleus. These events were further confirmed after quantification of the $YAP_{nuc/cyt}$ ratio (Figure 5.6d), where there is a trend in the localisation of YAP that correlates with increasing amounts of fibronectin in the gels, although the elastic modulus tested was similar in all formulations used.

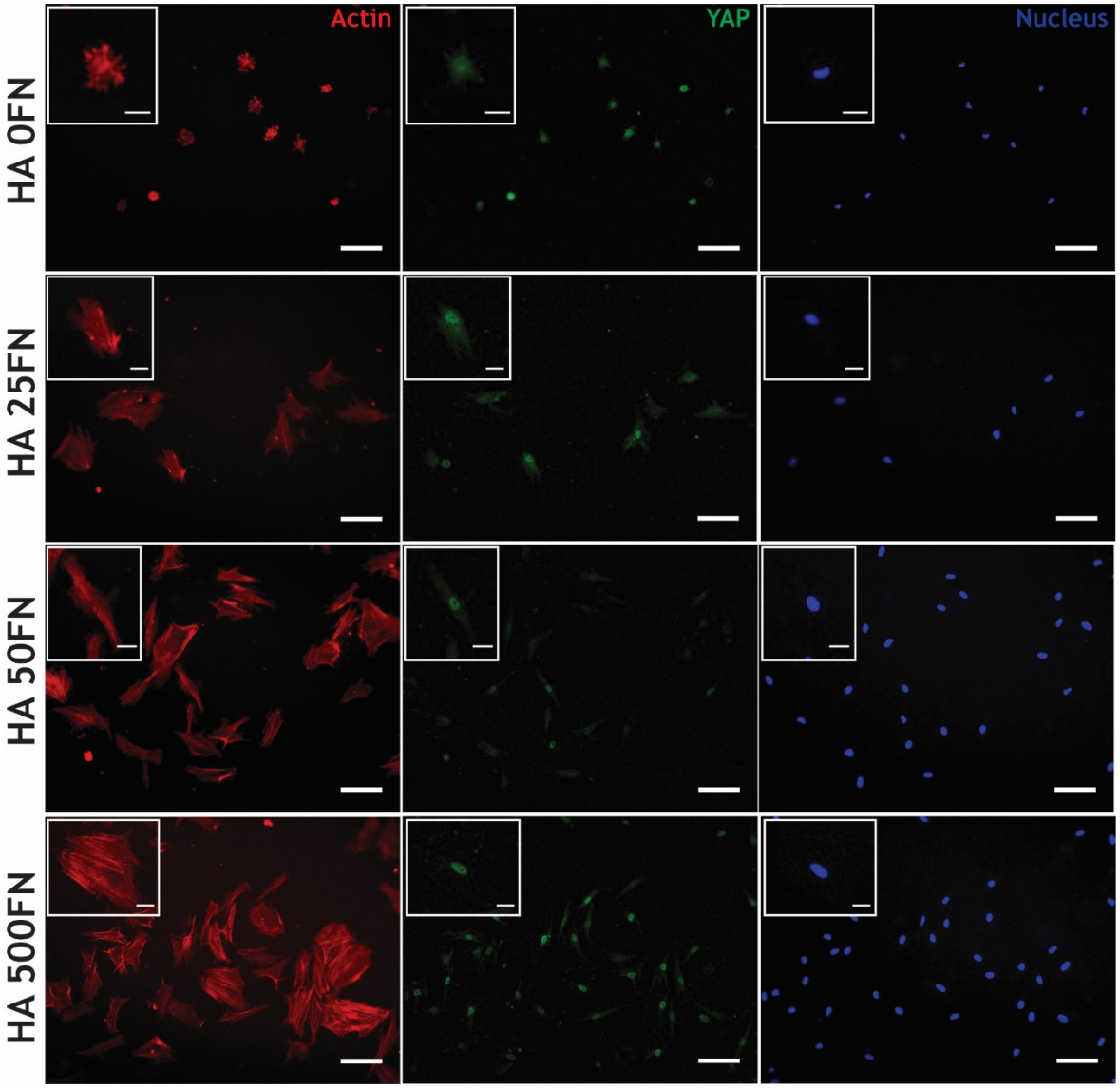

Figure 5.5 YAP staining of hMSCs seeded onto fibronectin-HA hydrogels.

hMSCs were seeded on top of FNHA 0VPM hydrogels with different amounts of fibronectin (depicted as XFN where X is the total amount of fibronectin in µg/mL) for three hours. Representative images of cells for every condition tested (scale bar: 200 µm) and representative single cell images of each condition are shown in insets (scale bar inset: 50 µm), where red depicts actin, green YAP and blue nuclei, respectively.

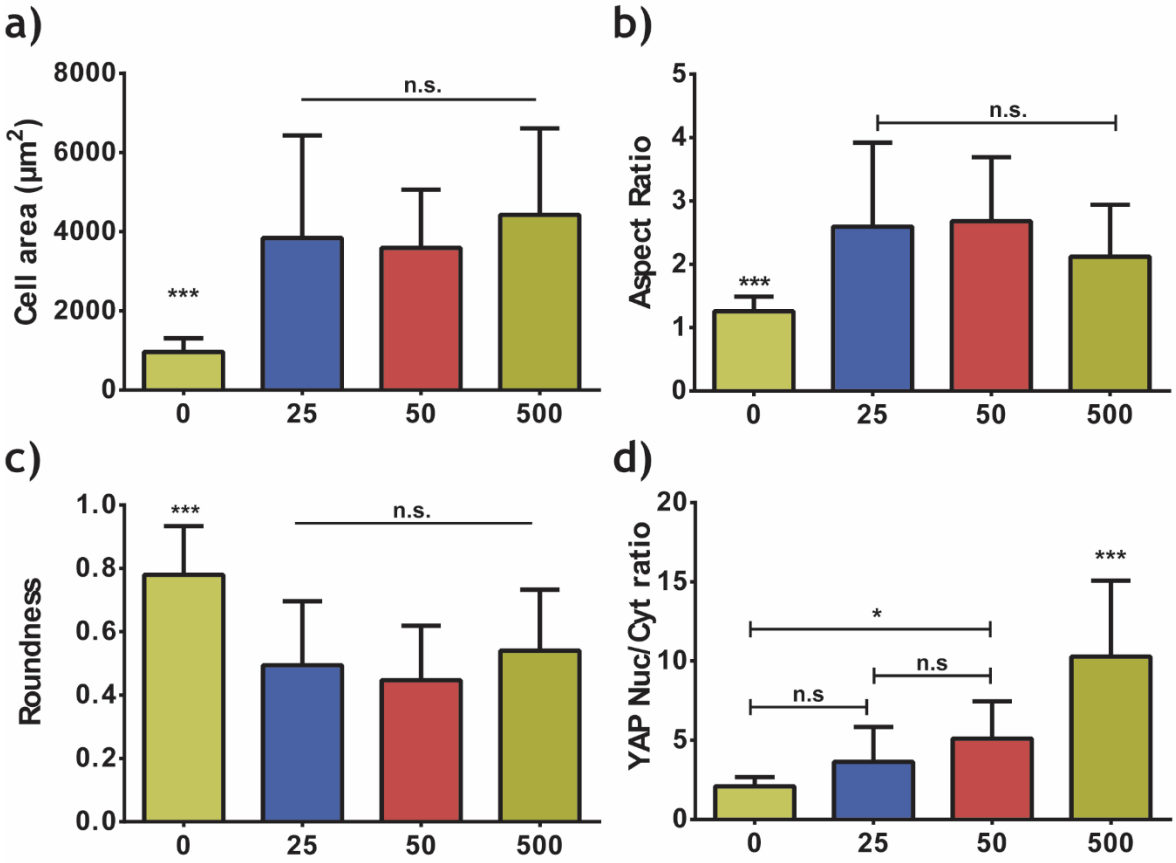

Figure 5.6 Cell shape and YAP localisation quantification.

hMSCs were seeded on top of FNHA 0VPM hydrogels with different amounts of fibronectin for three hours. Graphs show mean ± SD (n ≥ 15 cells, conditions in triplicate) of (a) cell area (μm^2), aspect ratio, roundness and the YAP$_{nuc/cyt}$ ratio versus the amount of fibronectin used within the gels (0, 25, 50 or 500 μg/mL). Significant differences were tested by means of ANOVA test followed by Tukey's multiple comparison test.

Mesenchymal stem cells viability after encapsulation

After the initial characterisation of this new hydrogel system, we tested whether or not MSCs were capable to survive encapsulation. Figure 5.7 shows the results for a Live/Dead® staining at three and seven days. The percentage of viability for the gels tested was equal or greater than 80%, which shows high cytocompatibility. This result confirms the suitability of ultraviolet light triggered thiol-ene reactions for 3D cell culture as well as when fibronectin is crosslinked.

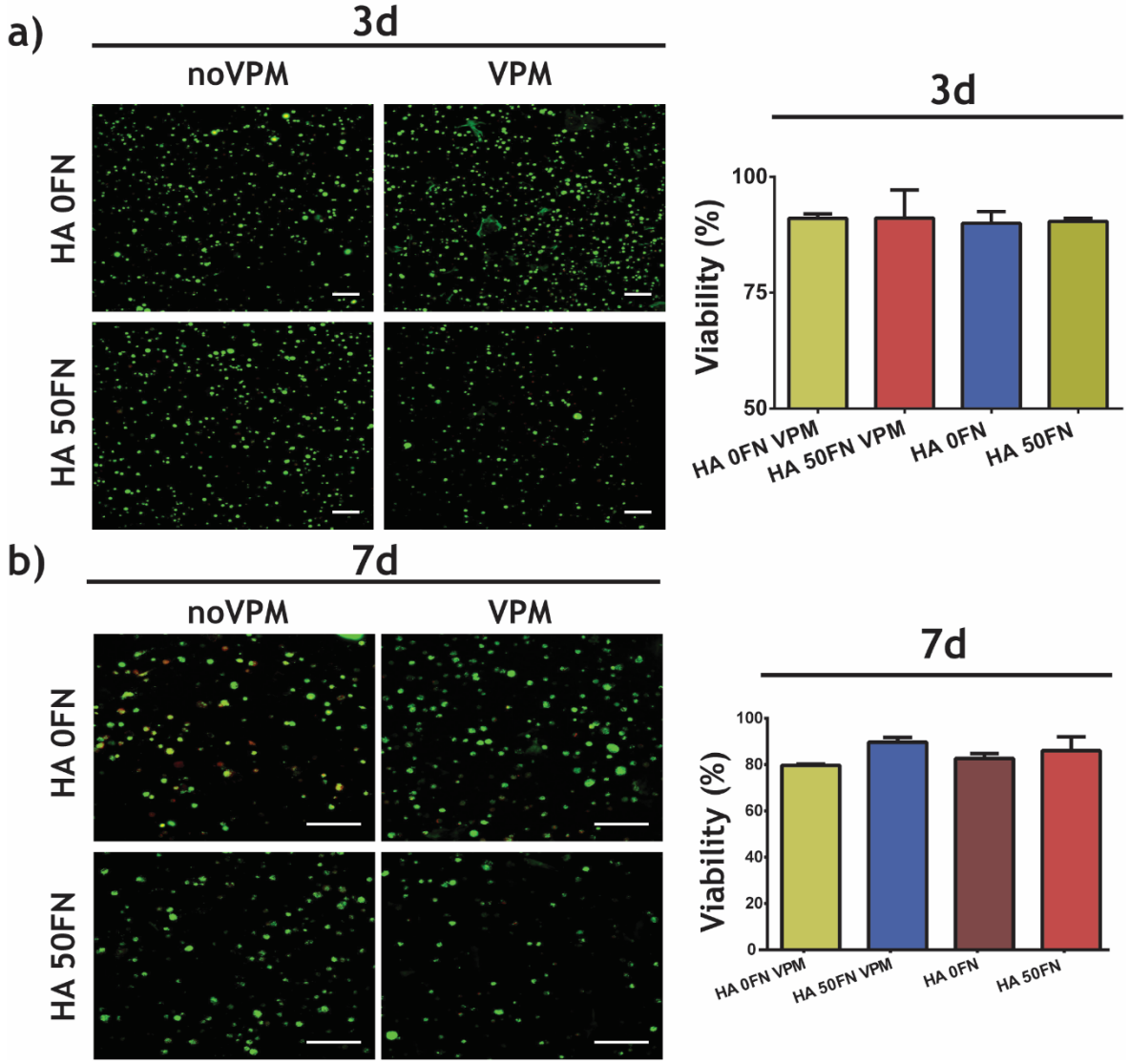

Figure 5.7 hMSCs encapsulated within fibronectin-HA hydrogels show high viability.

hMSCs were encapsulated within fibronectin-HA hydrogels with and without VPM (0VPM and VPM conditions) and with and without fibronectin (0FN and 50FN, 0 and 50 µg/mL, respectively) for seven days and their viability was tested by Live/Dead® staining at three and seven days. (a) Maximum Z-axis projection of a stack of images from the Live/Dead® staining of different fibronectin-HA hydrogels where green represents live cells and red dead cells (scale bar: 200 µm) and, graph (mean ± SD, n = 3, samples in triplicate) for three days of culture. (b) Maximum Z-axis projection images and graph showing viability at seven days of culture (scale bar 200 µm, n = 3, triplicates).

5.4 Discussion

The use of functionalised HA as a natural backbone for the fabrication of hydrogels is a relevant approach due to its nature (i.e. HA is a naturally found polysaccharide present in the ECM), plus the functionalisation offers great control over many physicochemical properties (e.g. mechanical properties, crosslinking) that are not usually well-defined when formulating biomaterials based on natural polymers.

Fibronectin-HA hydrogels were fabricated following Gramlich et al. procedure (Gramlich et al., 2013). Fibronectin was covalently linked to the NorHA backbone as demonstrated in Figure 5.2. Fibronectin has been previously crosslinked to a HA hydrogel for the 3D culture of endothelial cells (Seidlits et al., 2011). Seidlits et al. used also photopolymerisation via acrylate groups incorporated to fibronectin through a functionalised PEG that reacted with the amino groups present in the lysine residues. By doing this they were able to incorporate fibronectin up to 500 µg/mL, whereas we prepared hydrogels with increasing amounts of fibronectin and up to 2 mg/mL. Furthermore, they showed that the viability of endothelial cells when using their photoplolymerisation strategy was around 40-50% except for the conditions with more fibronectin incorporated that reached 90% viability. In our case, the viability of HA 0FN was as high as conditions with fibronectin, showing that the methodology of encapsulation is cytocompatible. This is in agreement with results in literature, where only HA hydrogels are highly cytocompatible (Kwon et al., 2018).

When tuning the mechanical properties, NorHA based hydrogels fabricated showed a high range of stiffness (Figure 5.3), meaning that the range of stiffness observed went from a less than one kPa to 15 kPa, for that percentage of HA used. This range could be further tuned if using different percentages of HA in the system or HA with a higher percentage of norbornene modification. The results obtained in Figure 5.3a are in agreement with previous results shown in literature (Gramlich et al., 2013). The incorporation of fibronectin at the amounts tested did not show any significant differences in elastic modulus. This could indicate that the crosslinking added by the incorporation of fibronectin is not enough to increase or decrease the mechanical properties of the material. It could be tested whether or not the viscoelasticity of the system varies with the amount of fibronectin incorporated.

Human MSCs were able to attach to the different formulations of fibronectin-HA hydrogels when seeded on top (Figure 5.4). Cells were adhered as could be observed by cell morphology, where cells seeded on top of fibronectin-HA hydrogels presented a well spread shape, with actin fibres well-developed. Cells seeded on top of only HA hydrogels presented a more rounded morphology with a diffuse actin staining. There were not significant differences in terms of morphology when comparing HA 50FN, HA 100FN and HA 500FN, meaning that probably the amount of adhesion domains available on the surface of the material

was already saturated at 50 μg/mL of fibronectin and, as the mechanical properties are similar, cells did not reflect any differences in spreading.

To further investigate this, MSCs were seeded on top of HA 0FN, HA 25FN, HA 50FN and HA 500FN (Figure 5.5 and Figure 5.6). The addition of HA 25FN aimed to test whether or not cells attach and spread similarly to the rest of the fibronectin-based conditions. Results showed that there were not differences in terms of cell morphology among the fibronectin-HA hydrogels tested. However, YAP staining revealed some differences. Figure 5.6 shows that there is a linear increase of nuclear YAP that correlates with the increase in fibronectin, while the elastic modulus remains similar. YAP/TAZ are considered master regulators of mechanotransduction, being of critical importance translating external mechanical signals (e.g. ECM stiffness) to the nucleus, initiating downstream signalling through the Hippo pathway. Piccolo's team showed that in 2D substrates there is a correlation between elevated substrate stiffness and nuclear translocation of YAP (Dupont et al., 2011). The same group showed that cell spreading also regulates YAP/TAZ translocation independently of the available adhesion area – by using micropillars (Dupont et al., 2011). In addition, it has been recently shown that the nuclear translocation of YAP depends on not only the stiffness of the material but on other parameters such as dimensionality and degradability (Caliari et al., 2016).

YAP/TAZ has also been correlated with angiogenesis. Wang et al. showed that the activity of YAP/TAZ is controlled/activated by VEGF throughout angiogenesis and that endothelial cells' expression of YAP/TAZ is key for vasculogenesis (Xiaohong Wang et al., 2017).

Our data suggest that, that the amount of fibronectin incorporated plays a role in YAP's translocation to the nucleus. Engler et al. reported that smooth muscle cell spreading on soft and stiff gels was unresponsive to ligand density (A. Engler et al., 2004). Elostegui-Artola et al. reported that the overall cell forces measured decreased when cells were seeded on top of substrates with lower fibronectin density, which in their study was 100 μg/mL (Elosegui-Artola et al., 2014). Topography has also been shown to affect YAP translocation to the nucleus in HUVECs (Mascharak et al., 2017).

More fundamental studies have been done using RGD peptide tethering in relation to ligand density and cell behaviour. Cell adhesion generally shows a sigmoidal increase as a function of RGD concentration (Kantlehner et al., 2000). This means that there is critical minimum ligand density for cell response. Massia and Hubbell

found that cells need a minimum of 1 fmol of RGD/cm^2 to achieve spreading and 10 fmol RGD/cm^2 to form focal adhesions and stress fibres (Massia & Hubbell, 1991). Similar results have been shown by Rowley and Mooney using alginate-RGD gels (Rowley & Mooney, 2002). Taken together, the fibronectin density readily available on the surface of the fibronectin-HA hydrogels needs to be measured to see whether or not the range of concentrations tested can trigger cell adhesion responses. In addition, other parameters such as changes in topography or conformation of fibronectin at the surface of the hydrogels could be investigated.

It could also be relevant to further investigate this phenomenon by studying the viscoelastic properties of these materials and track changes (if any) in the degradability profile of these hydrogels. Moreover, it could be also studied the localisation of YAP/TAZ after treatment with an actin polymerisation inhibitor such as Cytochalasin D, as it has been shown that the actin cytoskeleton is required to maintain nuclear YAP in MSCs (Caliari et al., 2016; Dupont et al., 2011).

Besides this, it could be also valuable to test how VEGF affects YAP on these materials and whether or not this trend observed is consistent when increasing the dimensionality of the culture (i.e. from 2D to 3D).

Finally, MSCs viability (Figure 5.7) after encapsulation via thiol-ene UV-initiated polymerisation shows that this system allows the *in situ* encapsulation of cells, proving its suitability as a 3D microenvironment (McCall & Anseth, 2012).

5.5 Conclusions

Overall, this chapter shows a new strategy to incorporate full-length fibronectin into a natural HA network by synthesising a norbornene-functionalised hyaluronic acid and using it to covalently bind fibronectin via UV-triggered thiol-ene chemistry. These hydrogels were fabricated to incorporate different amounts of fibronectin. The mechanical properties were controlled independently of the amount of fibronectin tested. These hydrogels also supported 3D encapsulation of hMSCs. In addition, we observed a trend on YAP localisation in 2D culture that should be further investigated.

6 Chapter Six: General discussion

The need for vascularisation strategies

As stated throughout this thesis, there is a need for strategies that promote angiogenesis and/or vascularisation as capillaries are key structures for tissue oxygenation and nutrient distribution. The growth of capillaries is extremely important for tissue regeneration purposes. There is a huge size limitation when designing a tissue construct, which is due to diffusion restrictions in thick engineered scaffolds. For instance, cells will only survive in the vicinity of a capillary (within 100-200 μm of the nearest capillary) (Jain et al., 2005; K. Lee et al., 2009).

Moreover, the integration with the host vasculature *in vivo* is also a critical factor. A correct integration will help to avoid tissue graft necrosis that usually occurs when oxygen and nutrients supply becomes limited by diffusion. Graft incorrect innervation could be deleterious in some cases and, there is also correlation between vascularisation and nerve growth (Auger, Gibot, & Lacroix, 2013).

There are many applications for vascularisation strategies such as tissue repair (e.g. wound healing of chronic wounds) (Mikaël M. Martino et al., 2011; Roy, Mooney, Raeman, Dalecki, & Hocking, 2013), thrombosis (to address problems like inflammation and clotting) (Quint et al., 2011), drug screening of pro-angiogenic and anti-angiogenic molecules (to fight cancer and several ischaemic/inflammatory diseases) and also, to study different blood and lymphatic processes (Briquez et al., 2016).

Engineering pro-angiogenic scaffolds

Engineered scaffolds provide a 3D context to cells that allow them to attach, migrate, proliferate and/or differentiate, among other things. Generally, there are two main types of scaffolds: synthetically or naturally derived scaffolds (Guvendiren & Burdick, 2013; Kyburz & Anseth, 2015).

Apart from the nature of the scaffold, there are several parameters that have to be taken into account when designing pro-angiogenic materials. The material must be biomimetic. This means that the material needs to be cell-friendly - i.e. biocompatible - and not to trigger any immunogenic response from the host body (Briquez et al., 2016). Furthermore, the material has to match several features of the targeted tissue such as stiffness, viscoelasticity or porosity (Chaudhuri et al.,

2016; Huebsch et al., 2010; Q. Zhang et al., 2014). These features will be different for bone compared to skin or cardiac tissues.

In addition, materials should be able to promote angiogenesis and so, able to deliver angiogenic factors. Generally, it would be ideal to find the minimum number of angiogenic factors that can trigger functional angiogenesis. To this end, one of the major goals when engineering the ideal pro-angiogenic material is the sustainable release of growth factors. This is achieved via sequestration of the growth factor and subsequent delivery of it (Cipitria & Salmeron-Sanchez, 2017; Dalby et al., 2018).

Other things to take into consideration when engineering pro-angiogenic biomaterials is the crosstalk among material, cells and growth factors (Salmerón-Sánchez & Dalby, 2016). There is a complex and powerful net of interactions that could be finely controlled to greatly enhance angiogenesis if taken into account (Mikaël M. Martino et al., 2011; Moulisová et al., 2017). Moreover, thoughts on how to translate the biomaterial strategy into clinic have to be always present.

Engineered matrices are increasingly becoming more and more efficient in mimicking and exploiting ECM's natural capabilities. Peptides, protein fragments, recombinant proteins, full-length proteins and other several strategies have been used so far, with good results (M. M. Martino et al., 2013; Mikaël M. Martino et al., 2011, 2015; Edward A. Phelps & García, 2010; Pike et al., 2006; Seidlits et al., 2011). However, there is still a need for matrices that can better mimic ECM's features to release low doses of growth factors to be used in clinical applications.

Fibronectin naturally presents growth factors in synergy with integrins

The main objective of this thesis was to engineer a hydrogel system that could sequester and deliver growth factors – VEGF in this case - in close proximity to integrins, so the efficiency of VEGF could be enhanced. To do that, we covalently tethered full-length fibronectin to both synthetic and natural polymers (PEG and HA). This new family of hydrogels can be further controlled and so we showed that mechanical properties and degradability could be tuned independently of the presence of fibronectin.

By using fibronectin, we hypothesised that we could have a system that can act as a reservoir for growth factors in addition to release growth factors as it naturally happens *in vivo*. Moreover, aside from regulating growth factors availability, fibronectin is capable of the modulation of growth factor signalling

through the interaction with cell-adhesion domains/integrins and growth factor receptors as stated throughout this thesis.

When VEGF (or other growth factors) binds to fibronectin, induces the formation of clusters between VEGF receptors and integrins (due to the close spatial proximity between the cell-adhesion domain and the heparin-binding domain II of fibronectin) (M. M. Martino & Hubbell, 2010; Moulisová et al., 2017; Wijelath et al., 2004). As growth factor receptors and integrins share certain molecules of their respective signalling pathways, the clusters formed boost their respective signalling. This synergistic signalling has been exploited in several strategies to substantially lower the dosage of growth factors used in clinical applications (Salmerón-Sánchez & Dalby, 2016). However, when fibronectin is in its soluble form, the growth factor binding site is not exposed due to fibronectin's globular conformation. For this domain to become available, fibronectin needs to unfold. This unfolding occurs naturally when fibronectin molecules interact with each other to form networks, also known as fibronectin fibrillogenesis (Leiss et al., 2008; Schwarzbauer, 1991; Singh et al., 2010; X. Zhou et al., 2008).

What has this work achieved?

We were able to incorporate high amounts of fibronectin within our matrices (between 1-2 mg/mL, i.e. between 0.02 to 0.1 (w/w of the hydrogel)). This was twice the amount of fibronectin incorporated compared to other groups working with full-length fibronectin (Seidlits et al., 2011)). Seidlits et al. functionalised fibronectin with acrylate groups and incorporated it into a hyaluronic acid hydrogel via photopolymerisation. The maximum amount of fibronectin incorporated by this group was 500 µg/mL, although they did not show the presence of the molecule in the system, neither characterised important parameters such as stiffness or exploited the ability of fibronectin to bind other molecules. They did show that their system was cytocompatible using HUVECs. Compared to this previous work with fibronectin hydrogels, this thesis has characterised more extensively the system, showing directly the presence of fibronectin into the gels by immunofluorescence, characterising mechanical properties, cell adhesion capabilities and studying VEGF-fibronectin interactions with HUVECs.

We hypothesised that this system could significantly increase the synergistic signalling between integrins (such as $\alpha_v\beta_3$) and VEGF. This should let us decrease the amount of growth factor loaded within the hydrogels while still having an

effect in angiogenesis. This was motivated by previous work done by Hubbell and colleagues, were they exploited the synergistic signalling of fibronectin using fibronectin fragments covering both adhesion and heparin-II binding domains. By incorporating these fragments into fibrin hydrogels they showed increase in angiogenesis *in vivo* using a wound healing model in diabetic mice (Mikaël M. Martino et al., 2011).

Other groups have had success working with full-length fibrinogen in synthetic hydrogels for cardiac repair (Almany & Seliktar, 2005; Dikovsky et al., 2006; Kerscher et al., 2016). Moreover, proteins such as laminins, which are extremely important in basement membranes and the neural ECM have been incorporated in PEG hydrogel systems for neural repair (Francisco et al., 2014; Roam et al., 2015). In this sense, Roam et al. tethered laminin and heparin in PEG microspheres to form growth factor gradients (Roam et al., 2015).

These examples show the importance of the incorporation of full-length proteins in controllable systems.

So far we have demonstrated that we can covalently incorporate fibronectin to both synthetic and natural hydrogels, PEG and HA. This did not affect the ability of the system to be further engineered to control mechanical properties and degradability rates. These systems also proved to be cytocompatible, which is a pre-requisite for biomaterials.

We have also shown that our matrices are able to bind VEGF as hypothesised and keep a sustainable release of it. We have also tested the capabilities of these hydrogels to promote angiogenesis and vasculogenesis *in vitro* using HUVECs. We also tested the performance of the system in a *in vivo* scenario using the chick chorioallantoic membrane assay, where we showed that the fibronectin-based hydrogels are able to promote angiogenesis in a more complex environment. This results are extremely positive and have encouraged us to continue developing these hydrogels towards a more translational system.

What's next?

At present, we are working on lowering the dosage of VEGF loaded within these hydrogels and also studying the central role of integrins-VEGF-fibronectin interactions in the system.

This system has the potential to be used in many different applications, due to the promiscuous nature of the growth factor binding site on fibronectin and the major roles that fibronectin plays in the ECM. As a starting point, we will work on

the incorporation of BMP-2 and this will be tested using *in vivo* models for bone repair. For translational approaches, fibronectin-based hydrogels will be optimised for their fabrication using microfluidics and 3D printing. These two techniques will allow us to prepare fibronectin-based hydrogels as an injectable material (using microfluidics, for example) or fabricate hydrogels in well-defined geometries for different purposes (using 3D printing).

7 Chapter Seven: Conclusions

The need for biomaterial systems that promote angiogenesis/vascularisation is still an important clinical hurdle. However, major efforts have been done in the field as discussed throughout this thesis.

The principal objective of this work was to formulate a new biosynthetic hydrogel system based on the protein fibronectin, to be able to present growth factors in synergy with integrins, as has been discussed.

- This work has been able to incorporate fibronectin in two different hydrogel systems, a PEG synthetic polymer and a natural HA polymer.
- Fibronectin was covalently bound to both PEG and HA polymer networks, providing a stable linkage of the molecule.
- The amount of fibronectin incorporated is the highest reported in literature for a hydrogel system containing full-length protein that does not form gels by itself.
- Fibronectin hydrogels were further engineered and, we achieved control over the mechanical properties and degradability rates independently of the presence of fibronectin.
- We used two thiol-based chemistries for the formulation of these hydrogels: a Michael-type addition reaction using maleimide functional groups; because they spontaneously react with thiol groups at physiological pH and, UV-initiated click chemistry using norbornene functional groups. Both chemistries demonstrated their suitability to encapsulate cells *in situ*, which is essential for 3D cell culture systems.
- Fibronectin-PEG hydrogels showed that they can uptake and retain VEGF due to the presence of fibronectin. These hydrogels showed a sustainable release of VEGF, which is a key feature in the angiogenic process.
- Fibronectin-PEG hydrogels were able to promote *in vitro* sprouting of endothelial cells when VEGF was present.
- Fibronectin-PEG hydrogels promoted the rapidly 3D reorganisation of endothelial cells into multicellular structures when VEGF was presented.

- Moreover, fibronectin-PEG hydrogels showed their ability to promote angiogenesis *in vivo* using the chick choriallantoic membrane assay and demonstrating higher performance when VEGF was presented by fibronectin compared to VEGF within PEG only controls.

Even though this thesis has achieved very encouraging results, there is still work to do in order to improve the system for translational purposes.

More efforts are necessary to elucidate the mechanisms behind the presentation of VEGF in this particular system (and maybe the presentation of two or more growth factors). Work has to be done on lowering the dosage of VEGF while retaining the enhanced efficiency of the fibronectin-VEGF presentation. This is one of the major challenges when thinking of the translation of this system to the clinic. In addition, other fabrication methods should be implemented such as microfluidics or 3D printing to be able to scale-up the production of this material for the clinic.

8 Chapter Eight: References

Afratis, N. A., Nikitovic, D., Multhaupt, H. A. B., Theocharis, A. D., Couchman, J. R., & Karamanos, N. K. (2017). Syndecans - key regulators of cell signaling and biological functions. *The FEBS Journal*, *284*(1), 27–41. https://doi.org/10.1111/febs.13940

Ahmed, W. W., Wolfram, T., Goldyn, A. M., Bruellhoff, K., Rioja, B. A., Möller, M., … Kemkemer, R. (2010). Myoblast morphology and organization on biochemically micro-patterned hydrogel coatings under cyclic mechanical strain. *Biomaterials*, *31*(2), 250–258. https://doi.org/10.1016/j.biomaterials.2009.09.047

Aimetti, A. A., Tibbitt, M. W., Anseth, K. S., Aimetti, A. A., Tibbitt, M. W., & Anseth, K. S. (2009). Human neutrophil elastase responsive delivery from poly(ethylene glycol) hydrogels. *Biomacromolecules*, *10*(6), 1484–1489. https://doi.org/10.1021/bm9000926

Aird, W. C. (2007a). Phenotypic heterogeneity of the endothelium: I. Structure, function, and mechanisms. *Circulation Research*. https://doi.org/10.1161/01.RES.0000255691.76142.4a

Aird, W. C. (2007b). Phenotypic heterogeneity of the endothelium: II. Representative vascular beds. *Circulation Research*. https://doi.org/10.1161/01.RES.0000255690.03436.ae

Aird, W. C. (2008). Endothelium in health and disease. In *Pharmacological Reports*. https://doi.org/10.1055/s-2007-1002703

Alakpa, E. V., Jayawarna, V., Lampel, A., Burgess, K. V., West, C. C., Bakker, S. C. J., … Dalby, M. J. (2016). Tunable Supramolecular Hydrogels for Selection of Lineage-Guiding Metabolites in Stem Cell Cultures. *Chem*, *1*(3), 512. https://doi.org/10.1016/j.chempr.2016.08.001

Alberts, B., Johnson, A., Lewis, J., Raff, M., Roberts, K., & Walter, P. (2002). *Molecular Biology of the Cell, 4th edition*. *Garland Science*. https://doi.org/10.3389/fimmu.2015.00171

Alford, A. I., Kozloff, K. M., & Hankenson, K. D. (2015). Extracellular matrix networks in bone remodeling. *International Journal of Biochemistry and Cell*

Biology, *65*, 20–31. https://doi.org/10.1016/j.biocel.2015.05.008

Almany, L., & Seliktar, D. (2005). Biosynthetic hydrogel scaffolds made from fibrinogen and polyethylene glycol for 3D cell cultures. *Biomaterials*, *26*(15), 2467–2477. https://doi.org/10.1016/j.biomaterials.2004.06.047

Anjum, F., Lienemann, P. S., Metzger, S., Biernaskie, J., Kallos, M. S., & Ehrbar, M. (2016). Enzyme responsive GAG-based natural-synthetic hybrid hydrogel for tunable growth factor delivery and stem cell differentiation. *Biomaterials*, *87*, 104–117. https://doi.org/10.1016/j.biomaterials.2016.01.050

Annabi, N., Nichol, J. W., Zhong, X., Ji, C., Koshy, S., Khademhosseini, A., & Dehghani, F. (2010). Controlling the Porosity and Microarchitecture of Hydrogels for Tissue Engineering. *Tissue Engineering Part B: Reviews*, *16*(4), 371–383. https://doi.org/10.1089/ten.teb.2009.0639

Assal, Y., Mie, M., & Kobatake, E. (2013). The promotion of angiogenesis by growth factors integrated with ECM proteins through coiled-coil structures. *Biomaterials*, *34*(13), 3315–3323. https://doi.org/10.1016/j.biomaterials.2013.01.067

Auger, F. A., Gibot, L., & Lacroix, D. (2013). The Pivotal Role of Vascularization in Tissue Engineering. *Annual Review of Biomedical Engineering*, *15*(1), 177–200. https://doi.org/10.1146/annurev-bioeng-071812-152428

Aumailley, M. (2013). The laminin family. *Cell Adhesion and Migration*. https://doi.org/10.4161/cam.22826

Baker, B. M., & Chen, C. S. (2012). Deconstructing the third dimension – how 3D culture microenvironments alter cellular cues. *Journal of Cell Science*, *125*(13), 3015–3024. https://doi.org/10.1242/jcs.079509

Ballester-Beltrán, J., Cantini, M., Lebourg, M., Rico, P., Moratal, D., García, A. J., & Salmerón-Sánchez, M. (2012). Effect of topological cues on material-driven fibronectin fibrillogenesis and cell differentiation. *Journal of Materials Science: Materials in Medicine*, *23*(1), 195–204. https://doi.org/10.1007/s10856-011-4532-z

Ballin, A. C., Cazzaniga, A., & Brandt, F. S. (2013). Long-term efficacy, safety and durability of Juvéderm® XC. *Clinical, Cosmetic and Investigational Dermatology*. https://doi.org/10.2147/CCID.S33568

Bao, X., Zhu, L., Huang, X., Tang, D., He, D., Shi, J., & Xu, G. (2017). 3D biomimetic artificial bone scaffolds with dual-cytokines spatiotemporal delivery for large weight-bearing bone defect repair. *Scientific Reports*, *7*(1), 7814. https://doi.org/10.1038/s41598-017-08412-0

Baskin, J. M., Prescher, J. A., Laughlin, S. T., Agard, N. J., Chang, P. V., Miller, I. A., … Bertozzi, C. R. (2007). Copper-free click chemistry for dynamic in vivo imaging. *Proceedings of the National Academy of Sciences*, *104*(43), 16793–16797. https://doi.org/10.1073/pnas.0707090104

Bates, D. O. (2010). Vascular endothelial growth factors and vascular permeability. *Cardiovascular Research*. https://doi.org/10.1093/cvr/cvq105

Bayless, K. J., Salazar, R., & Davis, G. E. (2000). RGD-dependent vacuolation and lumen formation observed during endothelial cell morphogenesis in three-dimensional fibrin matrices involves the alpha(v)beta(3) and alpha(5)beta(1) integrins. *The American Journal of Pathology*, *156*(5), 1673–1683. https://doi.org/10.1016/S0002-9440(10)65038-9

Benito-Jardón, M., Klapproth, S., Gimeno-Lluch, I., Petzold, T., Bharadwaj, M., Mï¿½ller, D. J., … Costell, M. (2017). The fibronectin synergy site re-enforces cell adhesion and mediates a crosstalk between integrin classes. *ELife*, *6*, 1–24. https://doi.org/10.7554/eLife.22264.001

Bennett, M., Cantini, M., Reboud, J., Cooper, J. M., Roca-Cusachs, P., & Salmeron-Sanchez, M. (2018). Molecular clutch drives cell response to surface viscosity. *Proceedings of the National Academy of Sciences*. https://doi.org/10.1073/pnas.1710653115

Benya, P. D., & Shaffer, J. D. (1982). Dedifferentiated chondrocytes reexpress the differentiated collagen phenotype when cultured in agarose gels. *Cell*, *30*(1), 215–224. https://doi.org/10.1016/0092-8674(82)90027-7

Berginski, M. E., & Gomez, S. M. (2013). The Focal Adhesion Analysis Server: a web tool for analyzing focal adhesion dynamics. *F1000Research*. https://doi.org/10.12688/f1000research.2-68.v1

Berkovitch, Y., Yelin, D., & Seliktar, D. (2015). Photo-patterning PEG-based hydrogels for neuronal engineering. *European Polymer Journal*, *72*, 473–483. https://doi.org/10.1016/j.eurpolymj.2015.07.014

Boontheekul, T., Hill, E. E., Kong, H.-J., & Mooney, D. J. (2007). Regulating Myoblast Phenotype Through Controlled Gel Stiffness and Degradation. *Tissue Engineering*, *13*(7), 1431–1442. https://doi.org/10.1089/ten.2006.0356

Borst, S. E. (2004). The role of TNF-alpha in insulin resistance. *Endocrine*, *23*(2–3), 177–182. https://doi.org/10.1385/ENDO:23:2-3:177

Bott, K., Upton, Z., Schrobback, K., Ehrbar, M., Hubbell, J. A., Lutolf, M. P., & Rizzi, S. C. (2010). The effect of matrix characteristics on fibroblast proliferation in 3D gels. *Biomaterials*, *31*(32), 8454–8464. https://doi.org/10.1016/j.biomaterials.2010.07.046

Bowers, S. L. K., Banerjee, I., & Baudino, T. A. (2010). The extracellular matrix: At the center of it all. *Journal of Molecular and Cellular Cardiology*, *48*(3), 474–482. https://doi.org/10.1016/j.yjmcc.2009.08.024

Brinckmann, J. (2005). Collagens at a glance. *Topics in Current Chemistry*, *247*, 1–6. https://doi.org/10.1007/b103817

Briquez, P. S., Clegg, L. E., Martino, M. M., Gabhann, F. Mac, & Hubbell, J. A. (2016). Design principles for therapeutic angiogenic materials. *Nature Reviews Materials*. https://doi.org/10.1038/natrevmats.2015.6

Brizzi, M. F., Tarone, G., & Defilippi, P. (2012). Extracellular matrix, integrins, and growth factors as tailors of the stem cell niche. *Current Opinion in Cell Biology*, *24*(5), 645–651. https://doi.org/10.1016/j.ceb.2012.07.001

Brown, T. E., & Anseth, K. S. (2017). Spatiotemporal hydrogel biomaterials for regenerative medicine. *Chem. Soc. Rev.*, *46*(21), 6532–6552. https://doi.org/10.1039/C7CS00445A

Byzova, T. V, Goldman, C. K., Pampori, N., Thomas, K. a, Bett, A., Shattil, S. J., & Plow, E. F. (2000). A mechanism for modulation of cellular responses to VEGF: activation of the integrins. *Molecular Cell*, *6*(4), 851–860. https://doi.org/http://dx.doi.org/10.1016/S1097-2765(05)00076-6

Cai, Y., López-Ruiz, E., Wengel, J., Creemers, L. B., & Howard, K. A. (2017). A hyaluronic acid-based hydrogel enabling CD44-mediated chondrocyte binding and gapmer oligonucleotide release for modulation of gene expression in osteoarthritis. *Journal of Controlled Release*, *253*, 153–159. https://doi.org/10.1016/j.jconrel.2017.03.004

Caliari, S. R., & Burdick, J. A. (2016). A practical guide to hydrogels for cell

culture. *Nature Methods*, *13*(5), 405–414. https://doi.org/10.1038/nmeth.3839

Caliari, S. R., Vega, S. L., Kwon, M., Soulas, E. M., & Burdick, J. A. (2016). Dimensionality and spreading influence MSC YAP/TAZ signaling in hydrogel environments. *Biomaterials*, *103*, 314–323. https://doi.org/10.1016/j.biomaterials.2016.06.061

Califano, J. P., & Reinhart-King, C. A. (2008). A Balance of Substrate Mechanics and Matrix Chemistry Regulates Endothelial Cell Network Assembly. *Cellular and Molecular Bioengineering*, *1*(2–3), 122–132. https://doi.org/10.1007/s12195-008-0022-x

Cao, R., Bråkenhielm, E., Pawliuk, R., Wariaro, D., Post, M. J., Wahlberg, E., … Cao, Y. (2003). Angiogenic synergism, vascular stability and improvement of hind-limb ischemia by a combination of PDGF-BB and FGF-2. *Nature Medicine*, *9*(5), 604–613. https://doi.org/10.1038/nm848

Carmeliet, P. (2003). Angiogenesis in Health and Disease : Therapeutic Opportunities. *Nature Medicine*, *09*(6), 653–660. https://doi.org/10.1038/nm0603-653

Carmeliet, P., & Jain, R. K. (2011). Molecular mechanisms and clinical applications of angiogenesis. *Nature*, *473*(7347), 298–307. https://doi.org/10.1038/nature10144

Cezar, C. A., Roche, E. T., Vandenburgh, H. H., Duda, G. N., Walsh, C. J., & Mooney, D. J. (2016). Biologic-free mechanically induced muscle regeneration. *Proceedings of the National Academy of Sciences*, *113*(6), 1534–1539. https://doi.org/10.1073/pnas.1517517113

Charras, G., & Sahai, E. (2014). Physical influences of the extracellular environment on cell migration. *Nature Reviews Molecular Cell Biology*, *15*(12), 813–824. https://doi.org/10.1038/nrm3897

Chaubaroux, C., Perrin-Schmitt, F., Senger, B., Vidal, L., Voegel, J.-C., Schaaf, P., … Hemmerlé, J. (2015). Cell Alignment Driven by Mechanically Induced Collagen Fiber Alignment in Collagen/Alginate Coatings. *Tissue Engineering Part C: Methods*, *21*(9), 881–888. https://doi.org/10.1089/ten.tec.2014.0479

Chaudhuri, O., Gu, L., Darnell, M., Klumpers, D., Bencherif, S. A., Weaver, J. C.,

… Mooney, D. J. (2015). Substrate stress relaxation regulates cell spreading. *Nature Communications*, *6*, 1–7. https://doi.org/10.1038/ncomms7365

Chaudhuri, O., Gu, L., Klumpers, D., Darnell, M., Bencherif, S. A., Weaver, J. C., … Mooney, D. J. (2016). Hydrogels with tunable stress relaxation regulate stem cell fate and activity. *Nature Materials*, *15*(3), 326–334. https://doi.org/10.1038/nmat4489

Chavez, A., Smith, M., & Mehta, D. (2011). New Insights into the Regulation of Vascular Permeability. *International Review of Cell and Molecular Biology*. https://doi.org/10.1016/B978-0-12-386037-8.00001-6

Chen, T. T., Luque, A., Lee, S., Anderson, S. M., Segura, T., & Iruela-Arispe, M. L. (2010). Anchorage of VEGF to the extracellular matrix conveys differential signaling responses to endothelial cells. *Journal of Cell Biology*. https://doi.org/10.1083/jcb.200906044

Chen, W. Y. J., & Abatangelo, G. (1999). Functions of hyaluronan in wound repair. *Wound Repair and Regeneration*, *7*(2), 79–89. https://doi.org/10.1046/j.1524-475X.1999.00079.x

Chen, X., Xun, K., Chen, L., & Wang, Y. (2009). TNF-α, a potent lipid metabolism regulator. *Cell Biochemistry and Function*. https://doi.org/10.1002/cbf.1596

Chung, H., Multhaupt, H. A. B., Oh, E. S., & Couchman, J. R. (2016). Minireview: Syndecans and their crucial roles during tissue regeneration. *FEBS Letters*, *590*(15), 2408–2417. https://doi.org/10.1002/1873-3468.12280

Cipitria, A., & Salmeron-Sanchez, M. (2017). Mechanotransduction and Growth Factor Signalling to Engineer Cellular Microenvironments. *Advanced Healthcare Materials*. https://doi.org/10.1002/adhm.201700052

Claesson-Welsh, L. (2015). Vascular permeability—the essentials. *Upsala Journal of Medical Sciences*. https://doi.org/10.3109/03009734.2015.1064501

Colognato, H., & Yurchenco, P. D. (2000). Form and function: The laminin family of heterotrimers. *Developmental Dynamics*. https://doi.org/10.1002/(SICI)1097-0177(200006)218:2<213::AID-DVDY1>3.0.CO;2-R

Comoglio, P. M., Boccaccio, C., & Trusolino, L. (2003). Interactions between growth factor receptors and adhesion molecules: Breaking the rules. *Current Opinion in Cell Biology*, *15*(5), 565–571. https://doi.org/10.1016/S0955-

0674(03)00096-6

Cosgrove, B. D., Mui, K. L., Driscoll, T. P., Caliari, S. R., Mehta, K. D., Assoian, R. K., … Mauck, R. L. (2016). N-cadherin adhesive interactions modulate matrix mechanosensing and fate commitment of mesenchymal stem cells. *Nature Materials*, *15*(12), 1297–1306. https://doi.org/10.1038/nmat4725

Coultas, L., Chawengsaksophak, K., & Rossant, J. (2005). Endothelial cells and VEGF in vascular development. *Nature*, *438*(7070), 937–945. https://doi.org/10.1038/nature04479

Cruz-Acuña, R., Quirós, M., Farkas, A. E., Dedhia, P. H., Huang, S., Siuda, D., … García, A. J. (2017). Synthetic hydrogels for human intestinal organoid generation and colonic wound repair. *Nature Cell Biology*, *19*(11), 1326–1335. https://doi.org/10.1038/ncb3632

Dalby, M. J., Gadegaard, N., & Oreffo, R. O. C. (2014). Harnessing nanotopography and integrin-matrix interactions to influence stem cell fate. *Nature Materials*, *13*(6), 558–569. https://doi.org/10.1038/nmat3980

Dalby, M. J., García, A. J., & Salmeron-Sanchez, M. (2018). Receptor control in mesenchymal stem cell engineering. *Nature Reviews Materials*. https://doi.org/10.1038/natrevmats.2017.91

Deforest, C. A., Polizzotti, B. D., & Anseth, K. S. (2009). Sequential click reactions for synthesizing and patterning three-dimensional cell microenvironments. *Nature Materials*, *8*(8), 659–664. https://doi.org/10.1038/nmat2473

Dejana, E. (2004). Endothelial cell-cell junctions: Happy together. *Nature Reviews Molecular Cell Biology*, *5*(4), 261–270. https://doi.org/10.1038/nrm1357

Denisin, A. K., & Pruitt, B. L. (2016). Tuning the Range of Polyacrylamide Gel Stiffness for Mechanobiology Applications. *ACS Applied Materials and Interfaces*, *8*(34), 21893–21902. https://doi.org/10.1021/acsami.5b09344

Deryugina, E. I., & Quigley, J. P. (2008). Chapter 2 Chick Embryo Chorioallantoic Membrane Models to Quantify Angiogenesis Induced by Inflammatory and Tumor Cells or Purified Effector Molecules. *Methods in Enzymology*, *444*(08), 21–41. https://doi.org/10.1016/S0076-6879(08)02802-4

DeVolder, R., & Kong, H.-J. (2012). Hydrogels for in vivo-like three-dimensional cellular studies. *Wiley Interdisciplinary Reviews. Systems Biology and*

Medicine, *4*(4), 351–365. https://doi.org/10.1002/wsbm.1174

Dewhirst, M. W., Cao, Y., & Moeller, B. (2008). Cycling hypoxia and free radicals regulate angiogenesis and radiotherapy response. *Nature Reviews Cancer*, *8*(6), 425–437. https://doi.org/10.1038/nrc2397

Dikovsky, D., Bianco-Peled, H., & Seliktar, D. (2006). The effect of structural alterations of PEG-fibrinogen hydrogel scaffolds on 3-D cellular morphology and cellular migration. *Biomaterials*, *27*(8), 1496–1506. https://doi.org/10.1016/j.biomaterials.2005.09.038

Discher, D. E. (2005). Tissue Cells Feel and Respond to the Stiffness of Their Substrate. *Science*, *310*(5751), 1139–1143. https://doi.org/10.1126/science.1116995

Doyle, A. D., Carvajal, N., Jin, A., Matsumoto, K., & Yamada, K. M. (2015). Local 3D matrix microenvironment regulates cell migration through spatiotemporal dynamics of contractility-dependent adhesions. *Nature Communications*, *6*, 1–15. https://doi.org/10.1038/ncomms9720

Du, X., Wang, J., Diao, W., Wang, L., Long, J., & Zhou, H. (2014). A genetically modified protein-based hydrogel for 3D culture of AD293 cells. *PLoS ONE*, *9*(9). https://doi.org/10.1371/journal.pone.0107949

Dupont, S., Morsut, L., Aragona, M., Enzo, E., Giulitti, S., Cordenonsi, M., … Piccolo, S. (2011). Role of YAP/TAZ in mechanotransduction. *Nature*. https://doi.org/10.1038/nature10137

Eble, J. a, & Niland, S. (2009). The extracellular matrix of blood vessels. *Current Pharmaceutical Design*, *15*, 1385–1400. https://doi.org/10.2174/138161209787846757

Eilken, H. M., Diéguez-Hurtado, R., Schmidt, I., Nakayama, M., Jeong, H. W., Arf, H., … Adams, R. H. (2017). Pericytes regulate VEGF-induced endothelial sprouting through VEGFR1. *Nature Communications*, *8*(1). https://doi.org/10.1038/s41467-017-01738-3

El-Rashidy, A. A., Roether, J. A., Harhaus, L., Kneser, U., & Boccaccini, A. R. (2017). Regenerating bone with bioactive glass scaffolds: A review of in vivo studies in bone defect models. *Acta Biomaterialia*, *62*, 1–28. https://doi.org/10.1016/j.actbio.2017.08.030

Elbert, D. L., Pratt, A. B., Lutolf, M. P., Halstenberg, S., & Hubbell, J. A. (2001).

Protein delivery from materials formed by self-selective conjugate addition reactions. *Journal of Controlled Release*, *76*(1–2), 11–25. https://doi.org/10.1016/S0168-3659(01)00398-4

Elosegui-Artola, A., Bazellières, E., Allen, M. D., Andreu, I., Oria, R., Sunyer, R., … Roca-Cusachs, P. (2014). Rigidity sensing and adaptation through regulation of integrin types. *Nature Materials*. https://doi.org/10.1038/nmat3960

Elosegui-Artola, A., Oria, R., Chen, Y., Kosmalska, A., Pérez-González, C., Castro, N., … Roca-Cusachs, P. (2016). Mechanical regulation of a molecular clutch defines force transmission and transduction in response to matrix rigidity. *Nature Cell Biology*, *18*(5), 540–548. https://doi.org/10.1038/ncb3336

Engelmayr, G. C., Cheng, M., Bettinger, C. J., Borenstein, J. T., Langer, R., & Freed, L. E. (2008). Accordion-like honeycombs for tissue engineering of cardiac anisotropy. *Nature Materials*, *7*(12), 1003–1010. https://doi.org/10.1038/nmat2316

Engler, A., Bacakova, L., Newman, C., Hategan, A., Griffin, M., & Discher, D. (2004). Substrate Compliance versus Ligand Density in Cell on Gel Responses. *Biophysical Journal*. https://doi.org/10.1016/S0006-3495(04)74140-5

Engler, A. J., Sen, S., Sweeney, H. L., & Discher, D. E. (2006). Matrix Elasticity Directs Stem Cell Lineage Specification. *Cell*, *126*(4), 677–689. https://doi.org/10.1016/j.cell.2006.06.044

Esche, C., Stellato, C., & Beck, L. A. (2005). Chemokines: Key players in innate and adaptive immunity. *Journal of Investigative Dermatology*, *125*(4), 615–628. https://doi.org/10.1111/j.0022-202X.2005.23841.x

Esko, J. D., Kimata, K., & Lindahl, U. (2009). Proteoglycans and Sulfated Glycosaminoglycans. In *Essentials of Glycobiology* (pp. 229–248). https://doi.org/10:0-87969-559-5

Ezashi, T., Das, P., & Roberts, R. M. (2005). Low O2 tensions and the prevention of differentiation of HES cells. *Nature Methods*, *2*(5), 325. https://doi.org/10.1038/nmeth0505-325

Fairbanks, B. D., Schwartz, M. P., Halevi, A. E., Nuttelman, C. R., Bowman, C. N., & Anseth, K. S. (2009). A versatile synthetic extracellular matrix mimic via thiol-norbornene photopolymerization. *Advanced Materials*.

https://doi.org/10.1002/adma.200901808

Fanning, A. S., Jameson, B. J., Lynne, a, Anderson, J. M., Jesaitis, L. a, & Melvin, J. (1998). CELL BIOLOGY AND METABOLISM : The Tight Junction Protein ZO-1 Establishes a Link between the Transmembrane Protein Occludin and the Actin Cytoskeleton The Tight Junction Protein ZO-1 Establishes a Link between the Transmembrane Protein Occludin and the Ac, *273*(45), 29745–29753. https://doi.org/10.1074/jbc.273.45.29745

Félétou, M. (2011). *The Endothelium Part 1: Multiple Functions of the Endothelial Cells—Focus on Endothelium-Derived Vasoactive Mediators*. *The Endothelium: Part 1: Multiple Functions of the Endothelial Cells—Focus on Endothelium-Derived Vasoactive Mediators*. https://doi.org/10.4199/C00031ED1V01Y201105ISP019

Feng, J.-F., Liu, J., Zhang, X.-Z., Zhang, L., Jiang, J.-Y., Nolta, J., & Zhao, M. (2012). Guided Migration of Neural Stem Cells Derived from Human Embryonic Stem Cells by an Electric Field. *Stem Cells*, *30*(2), 349–355. https://doi.org/10.1002/stem.779

Feng, Q., Zhu, M., Wei, K., & Bian, L. (2014). Cell-mediated degradation regulates human mesenchymal stem cell chondrogenesis and hypertrophy in MMP-sensitive hyaluronic acid hydrogels. *PLoS ONE*, *9*(6), 1–7. https://doi.org/10.1371/journal.pone.0099587

Ferrara, N., Gerber, H. P., & LeCouter, J. (2003). The biology of VEGF and its receptors. *Nature Medicine*, *9*(6), 669–676. https://doi.org/10.1038/nm0603-669

Ferrara, N., & Kerbel, R. S. (2005). Angiogenesis as a therapeutic target. *Nature*, *438*(7070), 967–974. https://doi.org/10.1038/nature04483

Ferreira, L. S., Gerecht, S., Fuller, J., Shieh, H. F., Vunjak-Novakovic, G., & Langer, R. (2007). Bioactive hydrogel scaffolds for controllable vascular differentiation of human embryonic stem cells. *Biomaterials*, *28*(17), 2706–2717. https://doi.org/10.1016/j.biomaterials.2007.01.021

Fischbach, C., Kong, H. J., Hsiong, S. X., Evangelista, M. B., Yuen, W., & Mooney, D. J. (2009). Cancer cell angiogenic capability is regulated by 3D culture and integrin engagement. *Proceedings of the National Academy of Sciences of the United States of America*, *106*(2), 399–404. https://doi.org/10.1073/pnas.0808932106

Fischer-Cripps, A. C. (2011). Nanoindentation, 21–37. https://doi.org/10.1007/978-1-4419-9872-9

Folkman, J., & D'Amore, P. A. (1996). Blood vessel formation: What is its molecular basis? *Cell*, *87*(7), 1153–1155. https://doi.org/10.1016/S0092-8674(00)81810-3

Fontaine, S. D., Reid, R., Robinson, L., Ashley, G. W., & Santi, D. V. (2015). Long-term stabilization of maleimide-thiol conjugates. *Bioconjugate Chemistry*, *26*(1), 145–152. https://doi.org/10.1021/bc5005262

Fontana, A., Spolaore, B., Mero, A., & Veronese, F. M. (2008). Site-specific modification and PEGylation of pharmaceutical proteins mediated by transglutaminase. *Advanced Drug Delivery Reviews*. https://doi.org/10.1016/j.addr.2007.06.015

Forristal, C. E., Wright, K. L., Hanley, N. A., Oreffo, R. O. C., & Houghton, F. D. (2010). Hypoxia inducible factors regulate pluripotency and proliferation in human embryonic stem cells cultured at reduced oxygen tensions. *Reproduction*, *139*(1), 85–97. https://doi.org/10.1530/REP-09-0300

Francisco, A. T., Hwang, P. Y., Jeong, C. G., Jing, L., Chen, J., & Setton, L. A. (2014). Photocrosslinkable laminin-functionalized polyethylene glycol hydrogel for intervertebral disc regeneration. *Acta Biomaterialia*, *10*(3), 1102–1111. https://doi.org/10.1016/j.actbio.2013.11.013

Frantz, C., Stewart, K. M., & Weaver, V. M. (2010). The extracellular matrix at a glance. *Journal of Cell Science*, *123*(24), 4195–4200. https://doi.org/10.1242/jcs.023820

Fu, Y., & Kao, W. J. (2011). In situ forming poly(ethylene glycol)-based hydrogels via thiol-maleimide Michael-type addition. *Journal of Biomedical Materials Research - Part A*, *98 A*(2), 201–211. https://doi.org/10.1002/jbm.a.33106

Garlanda, C., & Dejana, E. (1997). Heterogeneity of endothelial cells: Specific markers. *Arteriosclerosis, Thrombosis, and Vascular Biology*. https://doi.org/10.1161/01.ATV.17.7.1193

Gee, E. P. S., Ingber, D. E., & Stultz, C. M. (2008). Fibronectin unfolding revisited: Modeling cell traction-mediated unfolding of the tenth type-III repeat. *PLoS ONE*. https://doi.org/10.1371/journal.pone.0002373

George, E. L., Georges-Labouesse, E. N., Patel-King, R. S., Rayburn, H., & Hynes, R. O. (1993). Defects in mesoderm, neural tube and vascular development in mouse embryos lacking fibronectin. *Development (Cambridge, England)*. https://doi.org/10.1083/jcb.200107107

Gerber, H. P., Hillan, K. J., Ryan, a M., Kowalski, J., Keller, G. a, Rangell, L., … Ferrara, N. (1999). VEGF is required for growth and survival in neonatal mice. *Development*, *126*(6), 1149–1159.

Gerhardt, H. (2008). VEGF and endothelial guidance in angiogenic sprouting. *Organogenesis*, *4*(4), 241–246. https://doi.org/10.4161/org.4.4.7414

Getz, E. B., Xiao, M., Chakrabarty, T., Cooke, R., & Selvin, P. R. (1999). A Comparison between the Sulfhydryl Reductants Tris (2-carboxyethyl) phosphine and Dithiothreitol for Use in Protein Biochemistry 1. *Analytical Biochemistry*, *273*, 73–80.

Goldshmid, R., & Seliktar, D. (2017). *Hydrogel Modulus Affects Proliferation Rate and Pluripotency of Human Mesenchymal Stem Cells Grown in Three-Dimensional Culture*. *ACS Biomaterials Science and Engineering* (Vol. 3). https://doi.org/10.1021/acsbiomaterials.7b00266

Gong, Z., Szczesny, S. E., Caliari, S. R., Charrier, E. E., Chaudhuri, O., Cao, X., … Shenoy, V. B. (2018). Matching material and cellular timescales maximizes cell spreading on viscoelastic substrates. *Proceedings of the National Academy of Sciences*, 201716620. https://doi.org/10.1073/pnas.1716620115

Gramlich, W. M., Kim, I. L., & Burdick, J. A. (2013). Synthesis and orthogonal photopatterning of hyaluronic acid hydrogels with thiol-norbornene chemistry. *Biomaterials*, *34*(38), 9803–9811. https://doi.org/10.1016/j.biomaterials.2013.08.089

Griffin, D. R., & Kasko, A. M. (2012). Photoselective delivery of model therapeutics from hydrogels. *ACS Macro Letters*, *1*(11), 1330–1334. https://doi.org/10.1021/mz300366s

Gubareva, E. A., Sjöqvist, S., Gilevich, I. V., Sotnichenko, A. S., Kuevda, E. V., Lim, M. L., … Macchiarini, P. (2016). Orthotopic transplantation of a tissue engineered diaphragm in rats. *Biomaterials*, *77*, 320–335. https://doi.org/10.1016/j.biomaterials.2015.11.020

Gupta, S. (2002). Tumor necrosis factor-α-induced apoptosis in T cells from aged

humans: A role of TNFR-I and downstream signaling molecules. *Experimental Gerontology*, *37*(2–3), 293–299. https://doi.org/10.1016/S0531-5565(01)00195-4

Guvendiren, M., & Burdick, J. A. (2013). Engineering synthetic hydrogel microenvironments to instruct stem cells. *Current Opinion in Biotechnology*, *24*(5), 841–846. https://doi.org/10.1016/j.copbio.2013.03.009

H. Gulrez, S. K., Al-Assaf, S., & O, G. (2011). Hydrogels: Methods of Preparation, Characterisation and Applications. *Progress in Molecular and Environmental Bioengineering - From Analysis and Modeling to Technology Applications*. https://doi.org/10.5772/24553

Hahn, M. S., Miller, J. S., & West, J. L. (2006). Three-dimensional biochemical and biomechanical patterning of hydrogels for guiding cell behavior. *Advanced Materials*, *18*(20), 2679–2684. https://doi.org/10.1002/adma.200600647

Hakkinen, K. M., Harunaga, J. S., Doyle, A. D., & Yamada, K. M. (2011). Direct Comparisons of the Morphology, Migration, Cell Adhesions, and Actin Cytoskeleton of Fibroblasts in Four Different Three-Dimensional Extracellular Matrices. *Tissue Engineering Part A*, *17*(5–6), 713–724. https://doi.org/10.1089/ten.tea.2010.0273

Han, J. C., & Han, G. Y. (1994). A procedure for quantitative determination of tris(2- carboxyethyl)phosphine, an odorless reducing agent more stable and effective than dithiothreitol. *Analytical Biochemistry*. https://doi.org/10.1006/abio.1994.1290

Haraguchi, Y., Shimizu, T., Yamato, M., Kikuchi, A., & Okano, T. (2006). Electrical coupling of cardiomyocyte sheets occurs rapidly via functional gap junction formation. *Biomaterials*, *27*(27), 4765–4774. https://doi.org/10.1016/j.biomaterials.2006.04.034

Hascall, V., & Esko, J. D. (2017). Hyaluronan. *Essentials of Glycobiology, 3rd Edition*, *42*, Chapter 16. https://doi.org/10.1101/GLYCOBIOLOGY.3E.016

Hasenberg, T., Mühleder, S., Dotzler, A., Bauer, S., Labuda, K., Holnthoner, W., … Marx, U. (2015). Emulating human microcapillaries in a multi-organ-chip platform. *Journal of Biotechnology*, *216*, 1–10.

https://doi.org/10.1016/j.jbiotec.2015.09.038

Hendriks, J., Riesle, J., & Blitterswijk, C. A. van. (2010). Co-culture in cartilage tissue engineering. *Journal of Tissue Engineering and Regenerative Medicine*, *4*(7), 524–531. https://doi.org/10.1002/term

Her, G. J., Wu, H. C., Chen, M. H., Chen, M. Y., Chang, S. C., & Wang, T. W. (2013). Control of three-dimensional substrate stiffness to manipulate mesenchymal stem cell fate toward neuronal or glial lineages. *Acta Biomaterialia*, *9*(2), 5170–5180. https://doi.org/10.1016/j.actbio.2012.10.012

Hermanson, G. T. (2013a). *PEGylation and Synthetic Polymer Modification*. *Bioconjugate Techniques*. https://doi.org/10.1016/B978-0-12-382239-0.00018-2

Hermanson, G. T. (2013b). The Reactions of Bioconjugation. *Bioconjugate Techniques*, 229–258. https://doi.org/10.1016/B978-0-12-382239-0.00003-0

Hersel, U., Dahmen, C., & Kessler, H. (2003). RGD modified polymers: Biomaterials for stimulated cell adhesion and beyond. *Biomaterials*, *24*(24), 4385–4415. https://doi.org/10.1016/S0142-9612(03)00343-0

Hervé, J. C., & Derangeon, M. (2013). Gap-junction-mediated cell-to-cell communication. *Cell and Tissue Research*, *352*(1), 21–31. https://doi.org/10.1007/s00441-012-1485-6

Hirose, Y., Saijou, E., Sugano, Y., Takeshita, F., Nishimura, S., Nonaka, H., … Miyajima, A. (2012). Inhibition of Stabilin-2 elevates circulating hyaluronic acid levels and prevents tumor metastasis. *Proceedings of the National Academy of Sciences*, *109*(11), 4263–4268. https://doi.org/10.1073/pnas.1117560109

Hirschi, K. K. (2012). Hemogenic endothelium during development and beyond. *Blood*. https://doi.org/10.1182/blood-2011-12-353466

Hochman-Mendez, C., Lacerda de Menezes, J. R., Sholl-Franco, A., & Coelho-Sampaio, T. (2014). Polylaminin recognition by retinal cells. *Journal of Neuroscience Research*, *92*(1), 24–34. https://doi.org/10.1002/jnr.23298

Hoffmann, C., Ohlsen, K., & Hauck, C. R. (2011). Integrin-mediated uptake of fibronectin-binding bacteria. *European Journal of Cell Biology*. https://doi.org/10.1016/j.ejcb.2011.03.001

Hoyle, C. E., & Bowman, C. N. (2010). Thiol-ene click chemistry. *Angewandte Chemie - International Edition*, *49*(9), 1540–1573. https://doi.org/10.1002/anie.200903924

Huber, T. L., Kouskoff, V., Fehling, H. J., Palis, J., & Keller, G. (2004). Haemangioblast commitment is initiated in the primitive streak of the mouse embryo. *Nature*. https://doi.org/10.1038/nature03122

Huebsch, N., Arany, P. R., Mao, A. S., Shvartsman, D., Ali, O. A., Bencherif, S. A., … Mooney, D. J. (2010). Harnessing traction-mediated manipulation of the cell/matrix interface to control stem-cell fate. *Nature Materials*, *9*(6), 518–526. https://doi.org/10.1038/nmat2732

Humphrey, J. D., Dufresne, E. R., & Schwartz, M. A. (2014). Mechanotransduction and extracellular matrix homeostasis. *Nature Reviews Molecular Cell Biology*, *15*(12), 802–812. https://doi.org/10.1038/nrm3896

Hur, S. S., del Alamo, J. C., Park, J. S., Li, Y.-S., Nguyen, H. A., Teng, D., … Chien, S. (2012). Roles of cell confluency and fluid shear in 3-dimensional intracellular forces in endothelial cells. *Proceedings of the National Academy of Sciences*, *109*(28), 11110–11115. https://doi.org/10.1073/pnas.1207326109

Hynes, R. O. (2009). The extracellular matrix: Not just pretty fibrils. *Science*. https://doi.org/10.1126/science.1176009

Impellitteri, N. A., Toepke, M. W., Lan Levengood, S. K., & Murphy, W. L. (2012). Specific VEGF sequestering and release using peptide-functionalized hydrogel microspheres. *Biomaterials*, *33*(12), 3475–3484. https://doi.org/10.1016/j.biomaterials.2012.01.032

Ingham, K. C., Brew, S. A., Huff, S., & Litvinovich, S. V. (1997). Cryptic self-association sites in type III modules of fibronectin. *Journal of Biological Chemistry*. https://doi.org/10.1074/jbc.272.3.1718

Inostroza-Brito, K. E., Collin, E., Siton-Mendelson, O., Smith, K. H., Monge-Marcet, A., Ferreira, D. S., … Mata, A. (2015). Co-Assembly, spatiotemporal control and morphogenesis of a hybrid protein-peptide system. *Nature Chemistry*, *7*(11), 897–904. https://doi.org/10.1038/nchem.2349

Ishak, S. A., Djuansjah, J. R. P., Kadir, M. R. A., & Sukmana, I. (2014).

Angiogenesis in tissue engineering: From concept to the vascularization of scaffold construct. *IOP Conference Series: Materials Science and Engineering*, *58*(1). https://doi.org/10.1088/1757-899X/58/1/012015

Jain, R. K., Au, P., Tam, J., Duda, D. G., & Fukumura, D. (2005). Engineering vascularized tissue. *Nature Biotechnology*, *23*(7), 821–823. https://doi.org/10.1038/nbt0705-821

Jana, S., Cooper, A., & Zhang, M. (2013). Chitosan scaffolds with unidirectional microtubular pores for large skeletal myotube generation. *Advanced Healthcare Materials*, *2*(4), 557–561. https://doi.org/10.1002/adhm.201200177

Jha, A. K., Jackson, W. M., & Healy, K. E. (2014). Controlling osteogenic stem cell differentiation via soft bioinspired hydrogels. *PLoS ONE*, *9*(6), 1–11. https://doi.org/10.1371/journal.pone.0098640

Jha, A. K., Tharp, K. M., Browne, S., Ye, J., Stahl, A., Yeghiazarians, Y., & Healy, K. E. (2016). Matrix metalloproteinase-13 mediated degradation of hyaluronic acid-based matrices orchestrates stem cell engraftment through vascular integration. *Biomaterials*, *89*, 136–147. https://doi.org/10.1016/j.biomaterials.2016.02.023

Jha, A. K., Tharp, K. M., Ye, J., Santiago-Ortiz, J. L., Jackson, W. M., Stahl, A., … Healy, K. E. (2015). Enhanced survival and engraftment of transplanted stem cells using growth factor sequestering hydrogels. *Biomaterials*, *47*, 1–12. https://doi.org/10.1016/j.biomaterials.2014.12.043

Jones, D. R., Marchant, R. E., Von Recum, H., Gupta, A. Sen, & Kottke-Marchant, K. (2015). Photoinitiator-free synthesis of endothelial cell-adhesive and enzymatically degradable hydrogels. *Acta Biomaterialia*, *13*, 52–60. https://doi.org/10.1016/j.actbio.2014.11.012

Juliar, B. A., Keating, M. T., Kong, Y. P., Botvinick, E. L., & Putnam, A. J. (2018). Sprouting angiogenesis induces significant mechanical heterogeneities and ECM stiffening across length scales in fibrin hydrogels. *Biomaterials*, *162*, 99–108. https://doi.org/10.1016/j.biomaterials.2018.02.012

Kadler, K. E., Hill, A., & Canty-Laird, E. G. (2008). Collagen fibrillogenesis: fibronectin, integrins, and minor collagens as organizers and nucleators. *Current Opinion in Cell Biology*. https://doi.org/10.1016/j.ceb.2008.06.008

Kano, M. R. (2005). VEGF-A and FGF-2 synergistically promote neoangiogenesis through enhancement of endogenous PDGF-B-PDGFR signaling. *Journal of Cell Science*, *118*(16), 3759–3768. https://doi.org/10.1242/jcs.02483

Kantlehner, M., Schaffner, P., Finsinger, D., Meyer, J., Jonczyk, A., Diefenbach, B., … Kessler, H. (2000). Surface coating with cyclic RGD peptides stimulates osteoblast adhesion and proliferation as well as bone formation. *Chembiochem : A European Journal of Chemical Biology*. https://doi.org/10.1002/1439-7633(20000818)1:2<107::AID-CBIC107>3.0.CO;2-4

Karnik, S. K. (2003). A critical role for elastin signaling in vascular morphogenesis and disease. *Development*, *130*(2), 411–423. https://doi.org/10.1242/dev.00223

Kerscher, P., Turnbull, I. C., Hodge, A. J., Kim, J., Seliktar, D., Easley, C. J., … Lipke, E. A. (2016). Direct hydrogel encapsulation of pluripotent stem cells enables ontomimetic differentiation and growth of engineered human heart tissues. *Biomaterials*, *83*, 383–395. https://doi.org/10.1016/j.biomaterials.2015.12.011

Keselowsky, B. G., Collard, D. M., & García, A. J. (2003). Surface chemistry modulates fibronectin conformation and directs integrin binding and specificity to control cell adhesion. *Journal of Biomedical Materials Research Part A*. https://doi.org/10.1002/jbm.a.10537

Keselowsky, B. G., Collard, D. M., & García, A. J. (2005). Integrin binding specificity regulates biomaterial surface chemistry effects on cell differentiation. *Proceedings of the National Academy of Sciences of the United States of America*. https://doi.org/10.1073/pnas.0407356102

Keyt, B. A., & Berleau, L. T. (1996). The Carboxyl-terminal Domain(111-165) of Vascular Endothelial Growth Factor Is Critical for Its Mitogenic Potency. *Journal of Biological Chemistry*, *271*(13), 7788–7795. https://doi.org/10.1074/jbc.271.13.7788

Khetan, S., & Burdick, J. (2009a). Cellular Encapsulation in 3D Hydrogels for Tissue Engineering. *Journal of Visualized Experiments*, (32), 3–7. https://doi.org/10.3791/1590

Khetan, S., & Burdick, J. (2009b). Cellular Encapsulation in 3D Hydrogels for Tissue Engineering. *Journal of Visualized Experiments*, (32), 2009. https://doi.org/10.3791/1590

Khetan, S., & Burdick, J. A. (2010). Patterning network structure to spatially control cellular remodeling and stem cell fate within 3-dimensional hydrogels. *Biomaterials*, *31*(32), 8228–8234. https://doi.org/10.1016/j.biomaterials.2010.07.035

Khetan, S., Guvendiren, M., Legant, W. R., Cohen, D. M., Chen, C. S., & Burdick, J. A. (2013a). Degradation-mediated cellular traction directs stem cell fate in covalently crosslinked three-dimensional hydrogels. *Nature Materials*, *12*(5), 458–465. https://doi.org/10.1038/nmat3586

Khetan, S., Guvendiren, M., Legant, W. R., Cohen, D. M., Chen, C. S., & Burdick, J. A. (2013b). Degradation-mediated cellular traction directs stem cell fate in covalently crosslinked three-dimensional hydrogels. *Nature Materials*, *12*(5), 458–465. https://doi.org/10.1038/nmat3586

Khetan, S., Katz, J. S., & Burdick, J. A. (2009). Sequential crosslinking to control cellular spreading in 3-dimensional hydrogels. *Soft Matter*, *5*(8), 1601. https://doi.org/10.1039/b820385g

Kiran, M. S., Viji, R., Kumar, S., Prabhakaran, A., & Sudhakaran, P. R. (2011). Changes in expression of VE-cadherin and MMPs in endothelial cells: Implications for angiogenesis. *Vascular Cell*, *3*(1), 6. https://doi.org/10.1186/2045-824X-3-6

Kloxin, A. M., Kasko, A. M., Salinas, C. N., & Anseth, K. S. (2009). Photodegradable hydrogels for dynamic tuning of physical and chemical properties. *Science*, *324*(5923), 59–63. https://doi.org/10.1126/science.1169494

Kniazeva, E., & Putnam, A. J. (2009). Endothelial cell traction and ECM density influence both capillary morphogenesis and maintenance in 3-D. *American Journal of Physiology-Cell Physiology*, *297*(1), C179–C187. https://doi.org/10.1152/ajpcell.00018.2009

Koch, S., Yao, C., Grieb, G., Prével, P., Noah, E. M., & Steffens, G. C. M. (2006). Enhancing angiogenesis in collagen matrices by covalent incorporation of VEGF. *Journal of Materials Science: Materials in Medicine*, *17*(8), 735–741. https://doi.org/10.1007/s10856-006-9684-x

Kogan, G., Šoltés, L., Stern, R., & Gemeiner, P. (2007). Hyaluronic acid: A natural biopolymer with a broad range of biomedical and industrial applications. *Biotechnology Letters*. https://doi.org/10.1007/s10529-006-9219-z

Koike, N., Fukumura, D., Gralla, O., Au, P., Schechner, J. S., & Jain, R. K. (2004). Creation of long-lasting blood vessels. *Nature*, *428*(6979), 138–139. https://doi.org/10.1038/428138a

Krammer, A., Craig, D., Thomas, W. E., Schulten, K., & Vogel, V. (2002). A structural model for force regulated integrin binding to fibronectin's RGD-synergy site. *Matrix Biology*. https://doi.org/10.1016/S0945-053X(01)00197-4

Krammer, A., Lu, H., Isralewitz, B., Schulten, K., & Vogel, V. (1999). Forced unfolding of the fibronectin type III module reveals a tensile molecular recognition switch. *Proceedings of the National Academy of Sciences*. https://doi.org/10.1073/pnas.96.4.1351

Krsko, P., & Libera, M. (2005). Biointeractive hydrogels. *Materials Today*, *8*(12), 36–44. https://doi.org/10.1016/S1369-7021(05)71223-2

Ku, D. D., Zaleski, J. K., Liu, S., & Brock, T. a. (1993). Vascular endothelial growth factor induces EDRF-dependent relaxation in coronary arteries. *The American Journal of Physiology*, *265*(2 Pt 2), H586-92. Retrieved from http://www.ncbi.nlm.nih.gov/pubmed/8368362

Kuen, Y. L., Alsberg, E., Hsiong, S., Comisar, W., Linderman, J., Ziff, R., & Mooney, D. (2004). Nanoscale adhesion ligand organization regulates osteoblast proliferation and differentiation. *Nano Letters*, *4*(8), 1501–1506. https://doi.org/10.1021/nl0493592

Kwon, M. Y., Vega, S. L., Gramlich, W. M., Kim, M., Mauck, R. L., & Burdick, J. A. (2018). Dose and Timing of N-Cadherin Mimetic Peptides Regulate MSC Chondrogenesis within Hydrogels. *Advanced Healthcare Materials*. https://doi.org/10.1002/adhm.201701199

Kyburz, K. A., & Anseth, K. S. (2015). Synthetic Mimics of the Extracellular Matrix: How Simple is Complex Enough? *Annals of Biomedical Engineering*, *43*(3), 489–500. https://doi.org/10.1007/s10439-015-1297-4

Lai, J. Y. (2014). Relationship between structure and cytocompatibility of divinyl

sulfone cross-linked hyaluronic acid. *Carbohydrate Polymers*, *101*(1), 203–212. https://doi.org/10.1016/j.carbpol.2013.09.060

Lam, J., Truong, N. F., & Segura, T. (2014). Design of cell-matrix interactions in hyaluronic acid hydrogel scaffolds. *Acta Biomaterialia*, *10*(4), 1571–1580. https://doi.org/10.1016/j.actbio.2013.07.025

Laporte, L. De, Rice, J. J., Tortelli, F., & Hubbell, J. A. (2013). Tenascin C Promiscuously Binds Growth Factors via Its Fifth Fibronectin Type III-Like Domain, *8*(4). https://doi.org/10.1371/journal.pone.0062076

Leary, A. G., Ikebuchi, K., Hirai, Y., Wong, G. G., Yang, Y. C., Clark, S. C., & Ogawa, M. (1988). Synergism between interleukin-6 and interleukin-3 in supporting proliferation of human hematopoietic stem cells: comparison with interleukin-1 alpha. *Blood*, *71*(6), 1759–1763. Retrieved from http://www.ncbi.nlm.nih.gov/pubmed/3259443%5Cnhttp://www.bloodjournal.org/content/bloodjournal/71/6/1759.full.pdf

Leckband, D. E., & de Rooij, J. (2014). Cadherin Adhesion and Mechanotransduction. *Annual Review of Cell and Developmental Biology*, *30*(1), 291–315. https://doi.org/10.1146/annurev-cellbio-100913-013212

Lee, H. J., Diaz, M. F., Price, K. M., Ozuna, J. A., Zhang, S., Sevick-Muraca, E. M., … Wenzel, P. L. (2017). Fluid shear stress activates YAP1 to promote cancer cell motility. *Nature Communications*, *8*. https://doi.org/10.1038/ncomms14122

Lee, K., Kaplan, D. L., Lovett, M., Ph, D., Lee, K., Ph, D., … Ph, D. (2009). Vascularization Strategies for Tissue Engineering Vascularization Strategies for Tissue Engineering, *15*(July). https://doi.org/10.1089/ten.TEB.2009.0085

Lee, S. H., Jeong, D., Han, Y.-S., & Baek, M. J. (2015). Pivotal role of vascular endothelial growth factor pathway in tumor angiogenesis. *Annals of Surgical Treatment and Research*, *89*(1), 1. https://doi.org/10.4174/astr.2015.89.1.1

Leiss, M., Beckmann, K., Girós, A., Costell, M., & Fässler, R. (2008). The role of integrin binding sites in fibronectin matrix assembly in vivo. *Current Opinion in Cell Biology*, *20*(5), 502–507. https://doi.org/10.1016/j.ceb.2008.06.001

Leslie-barbick, J. E., Moon, J. J., & West, J. L. (2009). Covalently-Immobilized Vascular Endothelial Growth Factor Promotes Endothelial Cell Tubulogenesis in Poly (ethylene glycol) Diacrylate Hydrogels, *20*(September 2012), 1763–

1779. https://doi.org/10.1163/156856208X386381

Leslie-Barbick, J. E., Moon, J. J., & West, J. L. (2009). Covalently-immobilized vascular endothelial growth factor promotes endothelial cell tubulogenesis in poly(ethylene glycol) diacrylate hydrogels. *Journal of Biomaterials Science, Polymer Edition*, *20*(12), 1763–1779. https://doi.org/10.1163/156856208X386381

Li, L. (2003). The biology of VEGF and its receptors and the mechanisms of anti-tumour activity. *Nature Medicine*, *9*(6), 669–676.

Li, S., Nih, L. R., Bachman, H., Fei, P., Li, Y., Nam, E., … Segura, T. (2017). Hydrogels with precisely controlled integrin activation dictate vascular patterning and permeability. *Nature Materials*, *16*(9), 953–961. https://doi.org/10.1038/nmat4954

Li, W., Zhan, P., De Clercq, E., Lou, H., & Liu, X. (2013). Current drug research on PEGylation with small molecular agents. *Progress in Polymer Science*. https://doi.org/10.1016/j.progpolymsci.2012.07.006

Li, Z., Qu, T., Ding, C., Ma, C., Sun, H., Li, S., & Liu, X. (2015). Injectable gelatin derivative hydrogels with sustained vascular endothelial growth factor release for induced angiogenesis. *Acta Biomaterialia*, *13*, 88–100. https://doi.org/10.1016/j.actbio.2014.11.002

Lin, C., McGough, R., Aswad, B., Block, J., & Terek, R. (2004). Hypoxia induces HIF-1-alpha and VEGF expression in chondrosarcoma cells and chondrocytes. *Journal of Orthopaedic Research*, *22*, 1175–1181. https://doi.org/10.1016/j.orthres.2004.03.002

Lin, L., Marchant, R. E., Zhu, J., & Kottke-Marchant, K. (2014). Extracellular matrix-mimetic poly(ethylene glycol) hydrogels engineered to regulate smooth muscle cell proliferation in 3-D. *Acta Biomaterialia*, *10*(12), 5106–5115. https://doi.org/10.1016/j.actbio.2014.08.025

Llopis-hernández, V., Cantini, M., González-garcía, C., Cheng, Z. A., Yang, J., Tsimbouri, P. M., … Salmerón-sánchez, M. (2016). Material-driven fibronectin assembly for high-efficiency presentation of growth factors, (August), 1–10.

Llopis-Hernández, V., Cantini, M., González-García, C., & Salmerón-Sánchez, M. (2015). Material-based strategies to engineer fibronectin matrices for

regenerative medicine. *International Materials Reviews*, *60*(5), 245–264. https://doi.org/10.1179/1743280414Y.0000000049

Loh, Q. L., & Choong, C. (2013). Three-Dimensional Scaffolds for Tissue Engineering Applications: Role of Porosity and Pore Size. *Tissue Engineering Part B: Reviews*, *19*(6), 485–502. https://doi.org/10.1089/ten.teb.2012.0437

Lugus, J. J., Chung, Y. S., Mills, J. C., Kim, S.-I., Grass, J. A., Kyba, M., … Choi, K. (2007). GATA2 functions at multiple steps in hemangioblast development and differentiation. *Development*. https://doi.org/10.1242/dev.02731

Lutolf, M. P., & Hubbell, J. A. (2003). Synthesis and physicochemical characterization of end-linked poly(ethylene glycol)-co-peptide hydrogels formed by Michael-type addition. *Biomacromolecules*, *4*(3), 713–722. https://doi.org/10.1021/bm025744e

Lutolf, M. P., & Hubbell, J. A. (2005). Synthetic biomaterials as instructive extracellular microenvironments for morphogenesis in tissue engineering. *Nature Biotechnology*, *23*(1), 47–55. https://doi.org/10.1038/nbt1055

Maheshwari, G., Brown, G., Lauffenburger, D. a, Wells, a, & Griffith, L. G. (2000). Cell adhesion and motility depend on nanoscale RGD clustering. *Journal of Cell Science*, *113 (Pt 1*, 1677–1686. https://doi.org/10.1083/jcb.144.5.1019

Markowski, M. C., Brown, A. C., & Barker, T. H. (2012). Directing epithelial to mesenchymal transition through engineered microenvironments displaying orthogonal adhesive and mechanical cues. *Journal of Biomedical Materials Research - Part A*. https://doi.org/10.1002/jbm.a.34068

Martino, M. M., Briquez, P. S., Maruyama, K., & Hubbell, J. A. (2015). Extracellular matrix-inspired growth factor delivery systems for bone regeneration. *Advanced Drug Delivery Reviews*, *94*, 41–52. https://doi.org/10.1016/j.addr.2015.04.007

Martino, M. M., Briquez, P. S., Ranga, A., Lutolf, M. P., & Hubbell, J. A. (2013). Heparin-binding domain of fibrin(ogen) binds growth factors and promotes tissue repair when incorporated within a synthetic matrix. *Proceedings of the National Academy of Sciences*, *110*(12), 4563–4568. https://doi.org/10.1073/pnas.1221602110

Martino, M. M., & Hubbell, J. A. (2010). The 12th-14th type III repeats of fibronectin function as a highly promiscuous growth factor-binding domain.

The FASEB Journal, *24*(12), 4711–4721. https://doi.org/10.1096/fj.09-151282

Martino, M. M., Tortelli, F., Mochizuki, M., Traub, S., Ben-david, D., Kuhn, G. A., … Hubbell, J. A. (2011). Engineering the Growth Factor Microenvironment with Fibronectin Domains to Promote Wound and Bone Tissue Healing, *3*(100), 1–10.

Martino, M. M., Tortelli, F., Mochizuki, M., Traub, S., Ben-David, D., Kuhn, G. A., … Hubbell, J. A. (2011). Engineering the growth factor microenvironment with fibronectin domains to promote wound and bone tissue healing. *Science Translational Medicine*, *3*(100). https://doi.org/10.1126/scitranslmed.3002614

Mascharak, S., Benitez, P. L., Proctor, A. C., Madl, C. M., Hu, K. H., Dewi, R. E., … Heilshorn, S. C. (2017). YAP-dependent mechanotransduction is required for proliferation and migration on native-like substrate topography. *Biomaterials*. https://doi.org/10.1016/j.biomaterials.2016.11.019

Mason, B. N., Starchenko, A., Williams, R. M., Bonassar, L. J., & Reinhart-King, C. A. (2013). Tuning three-dimensional collagen matrix stiffness independently of collagen concentration modulates endothelial cell behavior. *Acta Biomaterialia*, *9*(1), 4635–4644. https://doi.org/10.1016/j.actbio.2012.08.007

Massia, S. P., & Hubbell, J. A. (1991). An RGD spacing of 440 nm is sufficient for integrin αvβ3-mediated fibroblast spreading and 140 nm for focal contact and stress fiber formation. *Journal of Cell Biology*. https://doi.org/10.1083/jcb.114.5.1089

McCall, J. D., & Anseth, K. S. (2012). Thiol-ene photopolymerizations provide a facile method to encapsulate proteins and maintain their bioactivity. *Biomacromolecules*, *13*(8), 2410–2417. https://doi.org/10.1021/bm300671s

Mellott, M. B., Searcy, K., & Pishko, V. (2001). Release of protein from highly cross-linked hydrogels of poly (ethylene glycol) diacrylate fabricated by UV polymerization. *Biomaterials*, *22*, 929–941. https://doi.org/10.1016/S0142-9612(00)00258-1

Mendelson, A., & Frenette, P. S. (2014). Hematopoietic stem cell niche maintenance during homeostasis and regeneration. *Nature Medicine*, *20*(8),

833–846. https://doi.org/10.1038/nm.3647

Menezes, K., Ricardo Lacerda de Menezes, J., Assis Nascimento, M., de Siqueira Santos, R., & Coelho-Sampaio, T. (2010). Polylaminin, a polymeric form of laminin, promotes regeneration after spinal cord injury. *The FASEB Journal*, *24*(11), 4513–4522. https://doi.org/10.1096/fj.10-157628

Miller, A. (2015). Peptide based Hydrogels in the study of Mesenchymal stem cells for the purposes of regenerative medicine.

Mithieux, B. S. M., & Weiss, A. S. (2006). A bstract Elastin is a key extracellular matrix protein that is critical to the elasticity The extracellular matrix imparts structural integrity on the tissues and. *Advances in Protein Chemistry*, *70*(04), 437–461. https://doi.org/10.1016/S0065-3233(04)70013-3

Mitsi, M., Hong, Z., Costello, C. E., & Nugent, M. A. (2006). Heparin-mediated conformational changes in fibronectin expose vascular endothelial growth factor binding sites. *Biochemistry*. https://doi.org/10.1021/bi060974p

Moreno-Jimenez, I., Kanczler, J. M., Hulsart-Billstrom, G. S., Inglis, S., & Oreffo, R. O. C. (2017). The chorioallantoic membrane (CAM) assay for biomaterial testing in tissue engineering: a short term in vivo preclinical model. *Tissue Engineering Part C: Methods*, *00*(00), ten.TEC.2017.0186. https://doi.org/10.1089/ten.TEC.2017.0186

Morita, H. (2005). Heparan Sulfate of Perlecan Is Involved in Glomerular Filtration. *Journal of the American Society of Nephrology*, *16*(6), 1703–1710. https://doi.org/10.1681/ASN.2004050387

Moulisová, V., Gonzalez-García, C., Cantini, M., Rodrigo-Navarro, A., Weaver, J., Costell, M., … Salmerón-Sánchez, M. (2017). Engineered microenvironments for synergistic VEGF – Integrin signalling during vascularization. *Biomaterials*, *126*, 61–74. https://doi.org/10.1016/j.biomaterials.2017.02.024

Mouw, J. K., Ou, G., & Weaver, V. M. (2014). Extracellular matrix assembly: A multiscale deconstruction. *Nature Reviews Molecular Cell Biology*, *15*(12), 771–785. https://doi.org/10.1038/nrm3902

Murphy, W. L., McDevitt, T. C., & Engler, A. J. (2014). Materials as stem cell regulators. *Nature Materials*, *13*(6), 547–557. https://doi.org/10.1038/nmat3937

Nakada, Y., Canseco, D. C., Thet, S., Abdisalaam, S., Asaithamby, A., Santos, C.

X., … Sadek, H. A. (2017). Hypoxia induces heart regeneration in adult mice. *Nature*, *541*(7636), 222–227. https://doi.org/10.1038/nature20173

Nakatsu, M. N., Sainson, R. C. A., Aoto, J. N., Taylor, K. L., Aitkenhead, M., Pérez-del-Pulgar, S., … Hughes, C. C. W. (2003). Angiogenic sprouting and capillary lumen formation modeled by human umbilical vein endothelial cells (HUVEC) in fibrin gels: The role of fibroblasts and Angiopoietin-1. *Microvascular Research*, *66*(2), 102–112. https://doi.org/10.1016/S0026-2862(03)00045-1

Nie, T., Baldwin, A., Yamaguchi, N., & Kiick, K. L. (2007). Production of heparin-functionalized hydrogels for the development of responsive and controlled growth factor delivery systems. *Journal of Controlled Release*, *122*(3), 287–296. https://doi.org/10.1016/j.jconrel.2007.04.019

Nitsche, A., Junghahn, I., Thulke, S., Aumann, J., Radonic, A., Fichtner, I., & Siegert, W. (2003). Interleukin-3 promotes proliferation and differentiation of human hematopoietic stem cells but reduces their repopulation potential in NOD/SCID mice. *Stem Cells*, *21*(2), 236–244. https://doi.org/10.1634/stemcells.21-2-236

Nuttelman, C. R., Mortisen, D. J., Henry, S. M., & Anseth, K. S. (2001). Attachment of fibronectin to poly(vinyl alcohol) hydrogels promotes NIH3T3 cell adhesion, proliferation, and migration. *Journal of Biomedical Materials Research*, *57*(2), 217–223. https://doi.org/10.1002/1097-4636(200111)57:2<217::AID-JBM1161>3.0.CO;2-I

Ott, H. C., Matthiesen, T. S., Goh, S. K., Black, L. D., Kren, S. M., Netoff, T. I., & Taylor, D. A. (2008). Perfusion-decellularized matrix: Using nature's platform to engineer a bioartificial heart. *Nature Medicine*, *14*(2), 213–221. https://doi.org/10.1038/nm1684

Ozcelik, B. (2015). *Degradable hydrogel systems for biomedical applications*. *Biosynthetic Polymers for Medical Applications*. Elsevier Ltd. https://doi.org/10.1016/B978-1-78242-105-4.00007-9

Page-McCaw, A., Ewald, A. J., & Werb, Z. (2007). Matrix metalloproteinases and the regulation of tissue remodelling. *Nature Reviews Molecular Cell Biology*, *8*(3), 221–233. https://doi.org/10.1038/nrm2125

Pankov, R. (2002). Fibronectin at a glance. *Journal of Cell Science*, *115*(20), 3861–

3863. https://doi.org/10.1242/jcs.00059

Parekh, S. H., Chatterjee, K., Lin-Gibson, S., Moore, N. M., Cicerone, M. T., Young, M. F., & Simon, C. G. (2011). Modulus-driven differentiation of marrow stromal cells in 3D scaffolds that is independent of myosin-based cytoskeletal tension. *Biomaterials*, *32*(9), 2256–2264. https://doi.org/10.1016/j.biomaterials.2010.11.065

Park, H., Bhalla, R., Saigal, R., Radisic, M., Watson, N., Langer, R., & Vunjak-Novakovic, G. (2008). Effects of electrical stimulation in C2C12 muscle constructs. *Journal of Tissue Engineering and Regenerative Medicine*, *2*(5), 279–287. https://doi.org/10.1002/term.93

Pasut, G., & Veronese, F. M. (2012). State of the art in PEGylation: The great versatility achieved after forty years of research. *Journal of Controlled Release*. https://doi.org/10.1016/j.jconrel.2011.10.037

Patan, S. (2000). Vasculogenesis and angiogenesis as mechanisms of vascular network formation, growth and remodeling. *Journal of Neuro-Oncology*, *50*(1–2), 1–15. https://doi.org/10.1023/A:1006493130855

Patel, S., Chaffotte, A. F., Amana, B., Goubard, F., & Pauthe, E. (2006). In vitro denaturation-renaturation of fibronectin. Formation of multimers disulfide-linked and shuffling of intramolecular disulfide bonds. *International Journal of Biochemistry and Cell Biology*, *38*(9), 1547–1560. https://doi.org/10.1016/j.biocel.2006.03.005

Patel, S., Chaffotte, A. F., Goubard, F., & Pauthe, E. (2004). Urea-Induced Sequential Unfolding of Fibronectin: A Fluorescence Spectroscopy and Circular Dichroism Study. *Biochemistry*, *43*(6), 1724–1735. https://doi.org/10.1021/bi0347104

Patterson, J., & Hubbell, J. A. (2010). Enhanced proteolytic degradation of molecularly engineered PEG hydrogels in response to MMP-1 and MMP-2. *Biomaterials*, *31*(30), 7836–7845. https://doi.org/10.1016/j.biomaterials.2010.06.061

Patterson, J., Siew, R., Herring, S. W., Lin, A. S. P., Guldberg, R., & Stayton, P. S. (2010). Hyaluronic acid hydrogels with controlled degradation properties for oriented bone regeneration. *Biomaterials*, *31*(26), 6772–6781. https://doi.org/10.1016/j.biomaterials.2010.05.047

Pek, Y. S., Wan, A. C. A., & Ying, J. Y. (2010). The effect of matrix stiffness on mesenchymal stem cell differentiation in a 3D thixotropic gel. *Biomaterials*, *31*(3), 385–391. https://doi.org/10.1016/j.biomaterials.2009.09.057

Pelham, R. J., & Wang, Y. -l. (1997). Cell locomotion and focal adhesions are regulated by substrate flexibility. *Proceedings of the National Academy of Sciences*. https://doi.org/10.1073/pnas.94.25.13661

Peng, K., Tomatsu, I., van den Broek, B., Cui, C., Korobko, A. V., van Noort, J., … Kros, A. (2011). Dextran based photodegradable hydrogels formed via a Michael addition. *Soft Matter*, *7*(10), 4881. https://doi.org/10.1039/c1sm05291h

Peters, E. B., Christoforou, N., Leong, K. W., Truskey, G. A., & West, J. L. (2016). Poly(Ethylene Glycol) Hydrogel Scaffolds Containing Cell-Adhesive and Protease-Sensitive Peptides Support Microvessel Formation by Endothelial Progenitor Cells. *Cellular and Molecular Bioengineering*, *9*(1), 38–54. https://doi.org/10.1007/s12195-015-0423-6

Petersen, O. W., Ronnov-Jessen, L., Howlett, A. R., & Bissell, M. J. (1992). Interaction with basement membrane serves to rapidly distinguish growth and differentiation pattern of normal and malignant human breast epithelial cells. *Proceedings of the National Academy of Sciences*, *89*(19), 9064–9068. https://doi.org/10.1073/pnas.89.19.9064

Petrie, T. A., Capadona, J. R., Reyes, C. D., & García, A. J. (2006). Integrin specificity and enhanced cellular activities associated with surfaces presenting a recombinant fibronectin fragment compared to RGD supports. *Biomaterials*, *27*(31), 5459–5470. https://doi.org/10.1016/j.biomaterials.2006.06.027

Peyton, S. R., Raub, C. B., Keschrumrus, V. P., & Putnam, A. J. (2006). The use of poly(ethylene glycol) hydrogels to investigate the impact of ECM chemistry and mechanics on smooth muscle cells. *Biomaterials*, *27*(28), 4881–4893. https://doi.org/10.1016/j.biomaterials.2006.05.012

Pfister, D., & Morbidelli, M. (2014). Process for protein PEGylation. *Journal of Controlled Release*. https://doi.org/10.1016/j.jconrel.2014.02.002

Phelps, E. A., Enemchukwu, N. O., Fiore, V. F., Sy, J. C., Murthy, N., Sulchek, T.

A., … García, A. J. (2012). Maleimide cross-linked bioactive PEG hydrogel exhibits improved reaction kinetics and cross-linking for cell encapsulation and in situ delivery. *Advanced Materials*, *24*(1), 64–70. https://doi.org/10.1002/adma.201103574

Phelps, E. A., & García, A. J. (2010). Engineering more than a cell: Vascularization strategies in tissue engineering. *Current Opinion in Biotechnology*, *21*(5), 704–709. https://doi.org/10.1016/j.copbio.2010.06.005

Phelps, E. A., Landazuri, N., Thule, P. M., Taylor, W. R., & Garcia, A. J. (2010). Bioartificial matrices for therapeutic vascularization. *Proceedings of the National Academy of Sciences*, *107*(8), 3323–3328. https://doi.org/10.1073/pnas.0905447107

Phelps, E. A., Templeman, K. L., Thulé, P. M., & García, A. J. (2015). Engineered VEGF-releasing PEG–MAL hydrogel for pancreatic islet vascularization. *Drug Delivery and Translational Research*. https://doi.org/10.1007/s13346-013-0142-2

Pike, D. B., Cai, S., Pomraning, K. R., Firpo, M. A., Fisher, R. J., Shu, X. Z., … Peattie, R. A. (2006). Heparin-regulated release of growth factors in vitro and angiogenic response in vivo to implanted hyaluronan hydrogels containing VEGF and bFGF. *Biomaterials*, *27*(30), 5242–5251. https://doi.org/10.1016/j.biomaterials.2006.05.018

Pobloth, A. M., Checa, S., Razi, H., Petersen, A., Weaver, J. C., Chmidt-Bleek, K., … Schwabe, P. (2018). Mechanobiologically optimized 3D titanium-mesh scaffolds enhance bone regeneration in critical segmental defects in sheep. *Science Translational Medicine*, *10*(423). https://doi.org/10.1126/scitranslmed.aam8828

Purcell, B. P., Lobb, D., Charati, M. B., Dorsey, S. M., Wade, R. J., Zellars, K. N., … Burdick, J. A. (2014). Injectable and bioresponsive hydrogels for on-demand matrix metalloproteinase inhibition. *Nature Materials*, *13*(6), 653–661. https://doi.org/10.1038/nmat3922

Qi, Y., Jiang, J., Jiang, X., Wang, X., Ji, S., Han, Y., … Shen, B. (2011). PDGF-BB and TGF-ß1 on cross-talk between endothelial and smooth muscle cells in vascular remodeling induced by low shear stress. *Pnas*, *108*, 1908–1913. https://doi.org/10.1073/pnas.1019219108/-/DCSupplemental.www.pnas.org/cgi/doi/10.1073/pnas.1019219108

Qian, Y., Zhao, X., Han, Q., Chen, W., Li, H., & Yuan, W. (2018). An integrated multi-layer 3D-fabrication of PDA/RGD coated graphene loaded PCL nanoscaffold for peripheral nerve restoration. *Nature Communications*, *9*(1). https://doi.org/10.1038/s41467-017-02598-7

Qin, X. H., Wang, X., Rottmar, M., Nelson, B. J., & Maniura-Weber, K. (2018). Near-Infrared Light-Sensitive Polyvinyl Alcohol Hydrogel Photoresist for Spatiotemporal Control of Cell-Instructive 3D Microenvironments. *Advanced Materials*, *30*(10). https://doi.org/10.1002/adma.201705564

Quint, C., Kondo, Y., Manson, R. J., Lawson, J. H., Dardik, A., & Niklason, L. E. (2011). Decellularized tissue-engineered blood vessel as an arterial conduit. *Proceedings of the National Academy of Sciences*, *108*(22), 9214–9219. https://doi.org/10.1073/pnas.1019506108

Raeber, G. P., Lutolf, M. P., & Hubbell, J. A. (2005). Molecularly engineered PEG hydrogels: A novel model system for proteolytically mediated cell migration. *Biophysical Journal*, *89*(2), 1374–1388. https://doi.org/10.1529/biophysj.104.050682

Rao, R. R., Peterson, A. W., Ceccarelli, J., Putnam, A. J., & Stegemann, J. P. (2012). Matrix composition regulates three-dimensional network formation by endothelial cells and mesenchymal stem cells in collagen/fibrin materials. *Angiogenesis*, *15*(2), 253–264. https://doi.org/10.1007/s10456-012-9257-1

Rhodes, J. M., & Simons, M. (2007). The extracellular matrix and blood vessel formation: Not just a scaffold: Angiogenesis Review Series. *Journal of Cellular and Molecular Medicine*, *11*(2), 176–205. https://doi.org/10.1111/j.1582-4934.2007.00031.x

Ribatti, D. (2008). *Chapter 5 Chick Embryo Chorioallantoic Membrane as a Useful Tool to Study Angiogenesis*. *International Review of Cell and Molecular Biology* (Vol. 270). Elsevier Inc. https://doi.org/10.1016/S1937-6448(08)01405-6

Ribatti, D. (2016). The chick embryo chorioallantoic membrane (CAM). A multifaceted experimental model. *Mechanisms of Development*, *141*, 70–77. https://doi.org/10.1016/j.mod.2016.05.003

Ribatti, D., Nico, B., & Crivellato, E. (2011). The role of pericytes in angiogenesis.

International Journal of Developmental Biology, *55*(3), 261–268. https://doi.org/10.1387/ijdb.103167dr

Ricard-Blum, S., & Salza, R. (2014). Matricryptins and matrikines: Biologically active fragments of the extracellular matrix. *Experimental Dermatology*, *23*(7), 457–463. https://doi.org/10.1111/exd.12435

Rice, J. J., Martino, M. M., De Laporte, L., Tortelli, F., Briquez, P. S., & Hubbell, J. A. (2013). Engineering the Regenerative Microenvironment with Biomaterials. *Advanced Healthcare Materials*, *2*(1), 57–71. https://doi.org/10.1002/adhm.201200197

Riching, K. M., Cox, B. L., Salick, M. R., Pehlke, C., Riching, A. S., Ponik, S. M., … Keely, P. J. (2015). 3D collagen alignment limits protrusions to enhance breast cancer cell persistence. *Biophysical Journal*, *107*(11), 2546–2558. https://doi.org/10.1016/j.bpj.2014.10.035

Rioja, A. Y., Tiruvannamalai Annamalai, R., Paris, S., Putnam, A. J., & Stegemann, J. P. (2016). Endothelial sprouting and network formation in collagen- and fibrin-based modular microbeads. *Acta Biomaterialia*, *29*, 33–41. https://doi.org/10.1016/j.actbio.2015.10.022

Rizzi, S. C., Ehrbar, M., Halstenberg, S., Raeber, G. P., Schmoekel, H. G., Hagenmüller, H., … Hubbell, J. A. (2006). Recombinant protein-co-PEG networks as cell-adhesive and proteolytically degradable hydrogel matrixes. Part II: Biofunctional characteristics. *Biomacromolecules*, *7*(11), 3019–3029. https://doi.org/10.1021/bm060504a

Rizzi, S. C., & Hubbell, J. A. (2005). Recombinant Protein- *co* -PEG Networks as Cell-Adhesive and Proteolytically Degradable Hydrogel Matrixes. Part I: Development and Physicochemical Characteristics. *Biomacromolecules*, *6*(3), 1226–1238. https://doi.org/10.1021/bm049614c

Roam, J. L., Yan, Y., Nguyen, P. K., Kinstlinger, I. S., Leuchter, M. K., Hunter, D. A., … Elbert, D. L. (2015). A modular, plasmin-sensitive, clickable poly(ethylene glycol)-heparin-laminin microsphere system for establishing growth factor gradients in nerve guidance conduits. *Biomaterials*, *72*, 112–124. https://doi.org/10.1016/j.biomaterials.2015.08.054

Roberts, W. G., & Palade, G. E. (1995). Increased microvascular permeability and endothelial fenestration induced by vascular endothelial growth factor. *Journal of Cell Science*, *108*, 2369–2379. Retrieved from

http://www.ncbi.nlm.nih.gov/pubmed/7673356

Rose, J. C., Cámara-Torres, M., Rahimi, K., Köhler, J., Möller, M., & De Laporte, L. (2017). Nerve Cells Decide to Orient inside an Injectable Hydrogel with Minimal Structural Guidance. *Nano Letters*, *17*(6), 3782–3791. https://doi.org/10.1021/acs.nanolett.7b01123

Rothdiener, M., Hegemann, M., Uynuk-Ool, T., Walters, B., Papugy, P., Nguyen, P., … Rolauffs, B. (2016). Stretching human mesenchymal stromal cells on stiffness-customized collagen type I generates a smooth muscle marker profile without growth factor addition. *Scientific Reports*, *6*(May), 1–15. https://doi.org/10.1038/srep35840

Roudsari, L. C., Jeffs, S. E., Witt, A. S., Gill, B. J., & West, J. L. (2016). A 3D Poly(ethylene glycol)-based Tumor Angiogenesis Model to Study the Influence of Vascular Cells on Lung Tumor Cell Behavior. *Scientific Reports*, *6*(May), 1–15. https://doi.org/10.1038/srep32726

Rowley, J. A., & Mooney, D. J. (2002). Alginate type and RGD density control myoblast phenotype. *Journal of Biomedical Materials Research*, *60*(2), 217–223. https://doi.org/10.1002/jbm.1287

Roy, D. C., Mooney, N. A., Raeman, C. H., Dalecki, D., & Hocking, D. C. (2013). Fibronectin Matrix Mimetics Promote Full-Thickness Wound Repair in Diabetic Mice. *Tissue Engineering Part A*, *19*(21–22), 2517–2526. https://doi.org/10.1089/ten.tea.2013.0024

Roy, D. C., Wilke-Mounts, S. J., & Hocking, D. C. (2011). Chimeric fibronectin matrix mimetic as a functional growth- and migration-promoting adhesive substrate. *Biomaterials*, *32*(8), 2077–2087. https://doi.org/10.1016/j.biomaterials.2010.11.050

Rufaihah, A. J., & Seliktar, D. (2016). Hydrogels for therapeutic cardiovascular angiogenesis. *Advanced Drug Delivery Reviews*, *96*, 31–39. https://doi.org/10.1016/j.addr.2015.07.003

Saik, J. E., Gould, D. J., Keswani, A. H., Dickinson, M. E., & West, J. L. (2011). Biomimetic hydrogels with immobilized EphrinA1 for therapeutic angiogenesis. *Biomacromolecules*, *12*(7), 2715–2722. https://doi.org/10.1021/bm200492h

Salimath, A. S., & García, A. J. (2016). Biofunctional hydrogels for skeletal muscle constructs. *Journal of Tissue Engineering and Regenerative Medicine*, *10*(11), 967–976. https://doi.org/10.1002/term.1881

Salinas, C. N., & Anseth, K. S. (2008). The influence of the RGD peptide motif and its contextual presentation in PEG gels on human mesenchymal stem cell viability. *Journal of Tissue Engineering and Regenerative Medicine*, *2*(5), 296–304. https://doi.org/10.1002/term.95

Salmerón-Sánchez, M., & Dalby, M. J. (2016). Synergistic growth factor microenvironments. *Chemical Communications*. https://doi.org/10.1039/c6cc06888j

Salmerón-Sánchez, M., Rico, P., Moratal, D., Lee, T. T., Schwarzbauer, J. E., & García, A. J. (2011). Role of material-driven fibronectin fibrillogenesis in cell differentiation. *Biomaterials*, *32*(8), 2099–2105. https://doi.org/10.1016/j.biomaterials.2010.11.057

Sawicka, K. M., Seeliger, M., Musaev, T., Macri, L. K., & Clark, R. A. F. (2015). Fibronectin Interaction and Enhancement of Growth Factors: Importance for Wound Healing. *Advances in Wound Care*, *4*(8), 469–478. https://doi.org/10.1089/wound.2014.0616

Schultz, K. M., Kyburz, K. A., & Anseth, K. S. (2015). Measuring dynamic cell–material interactions and remodeling during 3D human mesenchymal stem cell migration in hydrogels. *Proceedings of the National Academy of Sciences*, *112*(29), E3757–E3764. https://doi.org/10.1073/pnas.1511304112

Schwarzbauer, J. E. (1991). Identification of the fibronectin sequences required for assembly of a fibrillar matrix. *Journal of Cell Biology*. https://doi.org/10.1083/jcb.113.6.1463

Schweller, R. M., Wu, Z. J., Klitzman, B., & West, J. L. (2017). Stiffness of Protease Sensitive and Cell Adhesive PEG Hydrogels Promotes Neovascularization In Vivo. *Annals of Biomedical Engineering*, *45*(6), 1387–1398. https://doi.org/10.1007/s10439-017-1822-8

Seidlits, S. K., Drinnan, C. T., Petersen, R. R., Shear, J. B., Suggs, L. J., & Schmidt, C. E. (2011). Fibronectin-hyaluronic acid composite hydrogels for three-dimensional endothelial cell culture. *Acta Biomaterialia*, *7*(6), 2401–2409. https://doi.org/10.1016/j.actbio.2011.03.024

Serini, G., Valdembri, D., & Bussolino, F. (2006). Integrins and angiogenesis: A sticky business. *Experimental Cell Research*, *312*(5), 651–658. https://doi.org/10.1016/j.yexcr.2005.10.020

Shalaby, F., Janet, R., Yamaguchi, T. P., Gertsenstein, M., Wu, X. F., Breitman, M. L., & Schuh, A. C. (1995). Failure of blood-island formation and vasculogenesis in Flk-1-deficient mice. *Nature*. https://doi.org/10.1038/376062a0

Shankar, K. G., Gostynska, N., Montesi, M., Panseri, S., Sprio, S., Kon, E., … Sandri, M. (2017). Investigation of different cross-linking approaches on 3D gelatin scaffolds for tissue engineering application: A comparative analysis. *International Journal of Biological Macromolecules*, *95*, 1199–1209. https://doi.org/10.1016/j.ijbiomac.2016.11.010

Shaunak, S., Godwin, A., Choi, J. W., Balan, S., Pedone, E., Vijayarangam, D., … Brocchini, S. (2006). Site-specific PEGylation of native disulfide bonds in therapeutic proteins. *Nature Chemical Biology*, *2*(6), 312–313. https://doi.org/10.1038/nchembio786

Shekaran, A., García, J. R., Clark, A. Y., Kavanaugh, T. E., Lin, A. S., Guldberg, R. E., & García, A. J. (2014a). Bone regeneration using an alpha 2 beta 1 integrin-specific hydrogel as a BMP-2 delivery vehicle. *Biomaterials*, *35*(21), 5453–5461. https://doi.org/10.1016/j.biomaterials.2014.03.055

Shekaran, A., García, J. R., Clark, A. Y., Kavanaugh, T. E., Lin, A. S., Guldberg, R. E., & García, A. J. (2014b). Bone regeneration using an alpha 2 beta 1 integrin-specific hydrogel as a BMP-2 delivery vehicle. *Biomaterials*, *35*(21), 5453–5461. https://doi.org/10.1016/j.biomaterials.2014.03.055

Silva, L. P. D., Pirraco, R. P., Santos, T. C., Novoa-Carballal, R., Cerqueira, M. T., Reis, R. L., … Marques, A. P. (2016). Neovascularization Induced by the Hyaluronic Acid-Based Spongy-Like Hydrogels Degradation Products. *ACS Applied Materials and Interfaces*, *8*(49), 33464–33474. https://doi.org/10.1021/acsami.6b11684

Silvestre, J.-S., Lévy, B. I., & Tedgui, A. (2008). Mechanisms of angiogenesis and remodelling of the microvasculature. *Cardiovascular Research*, *78*(2), 201–202. https://doi.org/10.1093/cvr/cvn070

Singh, P., Carraher, C., & Schwarzbauer, J. E. (2010). Assembly of fibronectin extracellular marix. *Annu Rev Cell Dev Biol*, *26*, 397–419. https://doi.org/10.1146/annurev-cellbio-100109-104020

Smith, E. L., Kanczler, J. M., Gothard, D., Roberts, C. A., Wells, J. A., White, L. J., … Oreffo, R. O. C. (2014). Evaluation of skeletal tissue repair, Part 1: Assessment of novel growth-factor-releasing hydrogels in an ex vivo chick femur defect model. *Acta Biomaterialia*, *10*(10), 4186–4196. https://doi.org/10.1016/j.actbio.2014.06.011

Song, H. H. G., Park, K. M., & Gerecht, S. (2014). Hydrogels to model 3D in vitro microenvironment of tumor vascularization. *Advanced Drug Delivery Reviews*, *79*, 19–29. https://doi.org/10.1016/j.addr.2014.06.002

Sottile, J. (2002). Fibronectin Polymerization Regulates the Composition and Stability of Extracellular Matrix Fibrils and Cell-Matrix Adhesions. *Molecular Biology of the Cell*. https://doi.org/10.1091/mbc.E02-01-0048

Stern, R., Asari, A. A., & Sugahara, K. N. (2006). Hyaluronan fragments: An information-rich system. *European Journal of Cell Biology*, *85*(8), 699–715. https://doi.org/10.1016/j.ejcb.2006.05.009

Stevens, K. R., Miller, J. S., Blakely, B. L., Chen, C. S., & Bhatia, S. N. (2015). Degradable hydrogels derived from PEG-diacrylamide for hepatic tissue engineering. *Journal of Biomedical Materials Research - Part A*, *103*(10), 3331–3338. https://doi.org/10.1002/jbm.a.35478

Stock, K., Estrada, M. F., Vidic, S., Gjerde, K., Rudisch, A., Santo, V. E., … Graeser, R. (2016). Capturing tumor complexity in vitro: Comparative analysis of 2D and 3D tumor models for drug discovery. *Scientific Reports*, *6*(February), 1–15. https://doi.org/10.1038/srep28951

Storkebaum, E., & Carmeliet, P. (2004). VEGF: A critical player in neurodegeneration. *Journal of Clinical Investigation*, *113*(1), 14–18. https://doi.org/10.1172/JCI200420682

Stratesteffen, H., Köpf, M., Kreimendahl, F., Blaeser, A., Jockenhoevel, S., & Fischer, H. (2017). GelMA-collagen blends enable drop-on-demand 3D printablility and promote angiogenesis. *Biofabrication*, *9*(4). https://doi.org/10.1088/1758-5090/aa857c

Tae, G., Kim, Y. J., Choi, W. Il, Kim, M., Stayton, P. S., & Hoffman, A. S. (2007).

Formation of a novel heparin-based hydrogel in the presence of heparin-binding biomolecules. *Biomacromolecules*, *8*(6), 1979–1986. https://doi.org/10.1021/bm0701189

Tallawi, M., Rai, R., Boccaccini, A. R., & Aifantis, K. E. (2015). Effect of Substrate Mechanics on Cardiomyocyte Maturation and Growth. *Tissue Engineering Part B: Reviews*, *21*(1), 157–165. https://doi.org/10.1089/ten.teb.2014.0383

Tandon, N., Cannizzaro, C., Chao, P.-H. G., Maidhof, R., Marsano, A., Au, H. T. H., … Vunjak-Novakovic, G. (2009). Electrical stimulation systems for cardiac tissue engineering. *Nature Protocols*, *4*(2), 155–173. https://doi.org/10.1038/nprot.2008.183

Tanihara, M., Suzuki, Y., Yamamoto, E., Noguchi, A., & Mizushima, Y. (2001). Sustained release of basic fibroblast growth factor and angiogenesis in a novel covalently crosslinked gel of heparin and alginate. *Journal of Biomedical Materials Research*, *56*(2), 216–221. https://doi.org/10.1002/1097-4636(200108)56:2<216::AID-JBM1086>3.0.CO;2-N

Taubenberger, A. V., Bray, L. J., Haller, B., Shaposhnykov, A., Binner, M., Freudenberg, U., … Werner, C. (2016). 3D extracellular matrix interactions modulate tumour cell growth, invasion and angiogenesis in engineered tumour microenvironments. *Acta Biomaterialia*, *36*, 73–85. https://doi.org/10.1016/j.actbio.2016.03.017

Tocchio, A., Martello, F., Tamplenizza, M., Rossi, E., Gerges, I., Milani, P., & Lenardi, C. (2015). RGD-mimetic poly(amidoamine) hydrogel for the fabrication of complex cell-laden micro constructs. *Acta Biomaterialia*, *18*, 144–154. https://doi.org/10.1016/j.actbio.2015.02.017

Trappmann, B., Gautrot, J. E., Connelly, J. T., Strange, D. G. T., Li, Y., Oyen, M. L., … Huck, W. T. S. (2012). Extracellular-matrix tethering regulates stem-cell fate. *Nature Materials*, *11*(7), 642–649. https://doi.org/10.1038/nmat3339

Tse, J. R., & Engler, A. J. (2010). Preparation of hydrogel substrates with tunable mechanical properties. *Current Protocols in Cell Biology*. https://doi.org/10.1002/0471143030.cb1016s47

Turner, M. D., Nedjai, B., Hurst, T., & Pennington, D. J. (2014). Cytokines and

chemokines: At the crossroads of cell signalling and inflammatory disease. *Biochimica et Biophysica Acta - Molecular Cell Research*, *1843*(11), 2563–2582. https://doi.org/10.1016/j.bbamcr.2014.05.014

Ucuzian, A. A., Gassman, A. A., East, A. T., & Greisler, H. P. (2010). Molecular mediators of angiogenesis. *Journal of Burn Care and Research*, *31*(1), 158–175. https://doi.org/10.1097/BCR.0b013e3181c7ed82

Utech, M., Bruwer, M., & Nustrat, A. (2006). *Tight Junctions and Cell-Cell Interactions. Methods Mol. Biol. 341*.

Veronese, F. M. (2001). Peptide and protein PEGylation: A review of problems and solutions. *Biomaterials*, *22*(5), 405–417. https://doi.org/10.1016/S0142-9612(00)00193-9

Veronese, F. M., & Mero, a. (2009). Protein PEGylation, basic science and biological applications BT - PEGylated Protein Drugs: Basic Science and Clinical Applications. *PEGylated Protein Drugs: Basic Science and Clinical Applications*, 11–31. https://doi.org/10.1007/978-3-7643-8679-5_2

Wade, R. J., Bassin, E. J., Gramlich, W. M., & Burdick, J. A. (2015). Nanofibrous hydrogels with spatially patterned biochemical signals to control cell behavior. *Advanced Materials*, *27*(8), 1356–1362. https://doi.org/10.1002/adma.201404993

Wang, K., Seo, B. R., Fischbach, C., & Gourdon, D. (2016). Fibronectin Mechanobiology Regulates Tumorigenesis. *Cellular and Molecular Bioengineering*. https://doi.org/10.1007/s12195-015-0417-4

Wang, N., Tytell, J. D., & Ingber, D. E. (2009). Mechanotransduction at a distance: Mechanically coupling the extracellular matrix with the nucleus. *Nature Reviews Molecular Cell Biology*, *10*(1), 75–82. https://doi.org/10.1038/nrm2594

Wang, S., Li, X., Parra, M., Verdin, E., Bassel-Duby, R., & Olson, E. N. (2008). Control of endothelial cell proliferation and migration by VEGF signaling to histone deacetylase 7. *Proceedings of the National Academy of Sciences of the United States of America*, *105*(22), 7738–7743. https://doi.org/10.1073/pnas.0802857105

Wang, W., Guo, L., Yu, Y., Chen, Z., Zhou, R., & Yuan, Z. (2015). Peptide REDV-modified polysaccharide hydrogel with endothelial cell selectivity for the

promotion of angiogenesis. *Journal of Biomedical Materials Research - Part A*, *103*(5), 1703–1712. https://doi.org/10.1002/jbm.a.35306

Wang, X., Freire Valls, A., Schermann, G., Shen, Y., Moya, I. M., Castro, L., … Ruiz de Almodóvar, C. (2017). YAP/TAZ Orchestrate VEGF Signaling during Developmental Angiogenesis. *Developmental Cell*, *42*(5), 462–478.e7. https://doi.org/10.1016/j.devcel.2017.08.002

Wang, X., Yan, C., Ye, K., He, Y., Li, Z., & Ding, J. (2013). Effect of RGD nanospacing on differentiation of stem cells. *Biomaterials*, *34*(12), 2865–2874. https://doi.org/10.1016/j.biomaterials.2013.01.021

Watarai, A., Schirmer, L., Thönes, S., Freudenberg, U., Werner, C., Simon, J. C., & Anderegg, U. (2015). TGFß functionalized starPEG-heparin hydrogels modulate human dermal fibroblast growth and differentiation. *Acta Biomaterialia*, *25*, 65–75. https://doi.org/10.1016/j.actbio.2015.07.036

Weaver, V. M. M., Petersen, O. W. W., Wang, F., Larabell, C. A. A., Briand, P., Damsky, C., & Bissell, M. J. J. (1997). Reversion of the Malignant Phenotype of Human Breast Cells in Three-Dimensional Culture and In Vivo by Integrin Blocking Antibodies. *The Journal of Cell Biology*, *137*(1), 231–245. https://doi.org/10.1083/jcb.137.1.231

Wijelath, E. S., Murray, J., Rahman, S., Patel, Y., Ishida, A., Strand, K., … Sobel, M. (2002). Novel vascular endothelial growth factor binding domains of fibronectin enhance vascular endothelial growth factor biological activity. *Circulation Research*. https://doi.org/10.1161/01.RES.0000026420.22406.79

Wijelath, E. S., Rahman, S., Murray, J., Patel, Y., Savidge, G., & Sobel, M. (2004). Fibronectin promotes VEGF-induced CD34+cell differentiation into endothelial cells. *Journal of Vascular Surgery*. https://doi.org/10.1016/j.jvs.2003.10.042

Wijelath, E. S., Rahman, S., Namekata, M., Murray, J., Nishimura, T., Mostafavi-Pour, Z., … Sobel, M. (2006). Heparin-II domain of fibronectin is a vascular endothelial growth factor-binding domain: Enhancement of VEGF biological activity by a singular growth factor/matrix protein synergism. *Circulation Research*, *99*(8), 853–860. https://doi.org/10.1161/01.RES.0000246849.17887.66

Yamada, K. M., & Even-Ram, S. (2002). Integrin regulation of growth factor receptors. *Nature Cell Biology*, *4*(4). https://doi.org/10.1038/ncb0402-e75

Yamaguchi, Y., Takihara, T., Chambers, R. A., Veraldi, K. L., Larregina, A. T., & Feghali-Bostwick, C. A. (2012). A peptide derived from endostatin ameliorates organ fibrosis. *Science Translational Medicine*, *4*(136). https://doi.org/10.1126/scitranslmed.3003421

Yamamoto, Y., Tsutsumi, Y., Yoshioka, Y., Nishibata, T., Kobayashi, K., Okamoto, T., … Mayumi, T. (2003). Site-specific pegylation of a lysine-deficient TNF-α with full bioactivity. *Nature Biotechnology*, *21*(5), 546–552. https://doi.org/10.1038/nbt812

Yang, K., Basu, A., Wang, M., Chintala, R., Hsieh, M.-C., Liu, S., … Filpula, D. (2003). Tailoring structure-function and pharmacokinetic properties of single-chain Fv proteins by site-specific PEGylation. *Protein Engineering Design and Selection*, *16*(10), 761–770. https://doi.org/10.1093/protein/gzg093

Yao, C., Roderfeld, M., Rath, T., Roeb, E., Bernhagen, J., & Steffens, G. (2006). The impact of proteinase-induced matrix degradation on the release of VEGF from heparinized collagen matrices. *Biomaterials*, *27*(8), 1608–1616. https://doi.org/10.1016/j.biomaterials.2005.08.037

Ye, K., Wang, X., Cao, L., Li, S., Li, Z., Yu, L., & Ding, J. (2015). Matrix Stiffness and Nanoscale Spatial Organization of Cell-Adhesive Ligands Direct Stem Cell Fate. *Nano Letters*, *15*(7), 4720–4729. https://doi.org/10.1021/acs.nanolett.5b01619

Yu, Y., Alkhawaji, A., Ding, Y., & Mei, J. (2016). Decellularized scaffolds in regenerative medicine. *Oncotarget*, *7*(36), 58671–58683. https://doi.org/10.18632/oncotarget.10945

Zhang, C., Desai, R., Perez-Luna, V., & Karuri, N. (2014). PEGylation of lysine residues improves the proteolytic stability of fibronectin while retaining biological activity. *Biotechnology Journal*, *9*(8), 1033–1043. https://doi.org/10.1002/biot.201400115

Zhang, C., Hekmatfar, S., Ramanathan, A., & Karuri, N. W. (2013). PEGylated human plasma fibronectin is proteolytically stable, supports cell adhesion, cell migration, focal adhesion assembly, and fibronectin fibrillogenesis. *Biotechnology Progress*. https://doi.org/10.1002/btpr.1689

Zhang, C., Hekmatfer, S., & Karuri, N. W. (2014). A comparative study of polyethylene glycol hydrogels derivatized with the RGD peptide and the cell-binding domain of fibronectin. *Journal of Biomedical Materials Research - Part A*, *102*(1), 170–179. https://doi.org/10.1002/jbm.a.34687

Zhang, Q., Lu, H., Kawazoe, N., & Chen, G. (2014). Pore size effect of collagen scaffolds on cartilage regeneration. *Acta Biomaterialia*, *10*(5), 2005–2013. https://doi.org/10.1016/j.actbio.2013.12.042

Zhou, M., Smith, A. M., Das, A. K., Hodson, N. W., Collins, R. F., Ulijn, R. V., & Gough, J. E. (2009). Self-assembled peptide-based hydrogels as scaffolds for anchorage-dependent cells. *Biomaterials*, *30*(13), 2523–2530. https://doi.org/10.1016/j.biomaterials.2009.01.010

Zhou, X., Rowe, R. G., Hiraoka, N., George, J. P., Wirtz, D., Mosher, D. F., … Weiss, S. J. (2008). Fibronectin fibrillogenesis regulates three-dimensional neovessel formation. *Genes and Development*. https://doi.org/10.1101/gad.1643308

Zhu, J. (2010). Bioactive modification of poly(ethylene glycol) hydrogels for tissue engineering. *Biomaterials*, *31*(17), 4639–4656. https://doi.org/10.1016/j.biomaterials.2010.02.044

Zhu, J., & Clark, R. A. F. (2014a). Fibronectin at select sites binds multiple growth factors and enhances their activity: Expansion of the collaborative ECM-GF paradigm. *Journal of Investigative Dermatology*, *134*(4), 895–901. https://doi.org/10.1038/jid.2013.484

Zhu, J., & Clark, R. A. F. (2014b). Fibronectin at select sites binds multiple growth factors and enhances their activity: Expansion of the collaborative ECM-GF paradigm. *Journal of Investigative Dermatology*, *134*(4), 895–901. https://doi.org/10.1038/jid.2013.484

Zhu, J., Tang, C., Kottke-Marchant, K., & Marchant, R. E. (2009). Design and synthesis of biomimetic hydrogel scaffolds with controlled organization of cyclic RGD peptides. *Bioconjugate Chemistry*, *20*(2), 333–339. https://doi.org/10.1021/bc800441v

Zisch, A. H. (2003). Cell-demanded release of VEGF from synthetic, biointeractive cell-ingrowth matrices for vascularized tissue growth. *The FASEB Journal*.

https://doi.org/10.1096/fj.02-1041fje

Zollinger, A. J., & Smith, M. L. (2017). Fibronectin, the extracellular glue. *Matrix Biology*, *60–61*, 27–37. https://doi.org/10.1016/j.matbio.2016.07.011

Zustiak, S. P., & Leach, J. B. (2010). Hydrolytically degradable poly(ethylene glycol) hydrogel scaffolds with tunable degradation and mechanical properties. *Biomacromolecules*, *11*(5), 1348–1357. https://doi.org/10.1021/bm100137q